Università degli Studi di Salerno

Dipartimento di Chimica e Biologia "A. Zambelli"

Dottorato di ricerca in Chimica XXXIV ciclo

Complexes of coinage metals stabilized by N-heterocyclic carbenes: catalytic and biological activities

Tutor

Prof. Pasquale Longo

Co-Tutor

Prof. Annaluisa Mariconda

Coordinatore del dottorato

Prof. Claudio Pellecchia

Candidato

Marco Sirignano

Anno Accademico 2021/2022

Università degli Studi di Salerno

Dipartimento di Chimica e Biologia "A. Zambelli"

Dottorato di ricerca in Chimica XXXIV ciclo

Complexes of coinage metals stabilized by N-heterocyclic carbenes: catalytic and biological activities

Tutor

Prof. Pasquale Longo

Co-Tutor

Prof. Annaluisa Mariconda

Coordinatore del dottorato

Prof. Claudio Pellecchia

Candidato

Marco Sirignano

Anno Accademico 2021/2022

A Claudia,

Che sei la Luna in grado di illuminare il buio che non finisce

E di farmi dimenticare di quanto il Mondo sia difficile lì fuori.

Il suo era stato un cammino lungo e pieno di sorprese
Un viaggio fatto di magnifiche rivelazioni, ma
Anche lastricato di ostacoli
Finalmente, però, era arrivato sulla sua personale cima

Si mise con le gambe incrociate e le mani sulle ginocchia
Per ammirare dall'alto l'intera città che si dispiegava davanti ai suoi occhi
Ascoltando con attenzione la pace di quel momento di solitudine
Scoprì però di essere in compagnia

Tutta la gente che aveva incontrato nella vita
Tutte le forme che aveva assunto e le persone che era stato
I mostri che aveva sconfitto
E gli amori che lo avevano protetto erano lì accanto a lui
E da lì in poi visse ~~ferito~~ dottorato e contento.

[Vissero Feriti e Contenti, dott. Giovanni Luca Picariello a.k.a Ghemon]

Abstract

Since the synthesis, the isolation, and the characterization of the first stable N-heterocyclic carbene (NHC) in 1991 by Arduengo and collaborators, this class of ligands has attracted the attention of researchers for the synthesis of metal complexes active in different catalytic processes, and biological applications. The main advantages of NHCs are the facile modulation of the electronic and steric characteristics, the ease of manipulation, and interesting electron-donating properties.

During the last decades, the team I am part of has focused on the synthesis, characterization, and evaluation of catalytic and biological properties of NHC metal complexes. Our interest keeps in the study of the influence of substituents on nitrogen atoms and/or on the backbone might have on the performance of the complex in catalysis and biological environment.

In this doctoral thesis, the catalytic and biological activity of *N*-heterocyclic carbene silver and gold complexes will be examined. The catalytic performance will be evaluated in the A^3 (aldehyde, amine, and alkyne) coupling reaction, to lead propargylamines, and in the hydroamination of phenylacetylene with different arylamines, to produce the corresponding ketoimines. Finally, it will evaluate the antibacterial and the antitumoral activity of these complexes, against different bacterial strains and tumoral cells.

Chapter 1 gives an overview of *N*-heterocyclic carbene, the relative silver and gold complexes, and their biological and catalytic applications.

Chapter 2 reports the obtained results and is organized as follows:

Sections 2.1-2.4 are reported the synthetic strategies and characterization of NHC pro-ligands and the relative silver and gold complexes.

In Section 2.5, we have described the catalytic activity of silver and gold NHC complexes in the A^3-coupling reaction with p-formaldehyde, benzaldehyde, and cyclohexanal.

Section 2.6 reported the results obtained by Au-NHC complex in the hydroamination reaction of phenylacetylene.

Section 2.7 reported the biological activity of silver and gold complexes as potential antimicrobial and tumoral compounds.

Chapter 3 gives an overview of the obtained results in A^3coupling reaction and hydroamination of alkynes, and in the biological field, as antibacterial and antitumoral compounds, by silver and gold NHC, synthesized in this doctoral thesis.

Chapter 4 described the experimental part.

Summary

Chapter 1: Introduction ***1***

1.1 Carbenes **1**

1.2 Carbenes in organometallic chemistry **3**

1.3 *N*-heterocyclic Carbenes **4**

1.3.1 Synthetic strategies for the preparation of *N*-heterocyclic carbenes 6

1.4 Coordination chemistry of *N*-heterocyclic Carbene **8**

1.5 Silver *N*-heterocyclic carbene complexes **10**

1.5.1 The use of silver in medicine 10

1.5.2 Antimicrobial Properties of Ag-NHC complexes 11

1.5.3 Antitumor Properties of Ag-NHC complexes 15

1.5.4 Catalytic Activity of Silver NHC complexes 17

1.6 Gold *N*-heterocyclic carbene complexes **20**

1.6.1 The use of gold in medicine 20

1.6.2 Antimicrobial Properties of Au-NHC complexes 20

1.6.3 Antitumoral Properties of Au-NHC complexes 23

1.6.4 Catalytic Activity of Au-NHC complexes 25

Chapter 2: Results and discussion ***31***

2.1 Synthesis of N-Heterocyclic carbene pro-ligands and silver and gold NHC complexes **31**

2.2 Synthetic strategies for the synthesis of imidazolium salts **34**

2.2.1 Synthesis of pro-ligands P-L1, P-L2 35

2.2.2 Synthesis of pro-ligands P-L3, P-L4 35

2.2.3 Characterization of P-L3, 4,5-diphenyl, *N*-methyl-*N'*-[2-hydroxy-phenyl) ethyl] imidazolium iodide 36

2.2.4 Characterization of P-L4, *N*-methyl-*N'*-[2-(hydroxy-phenyl) ethyl] benzimidazolium iodide 39

2.2.5 Synthesis of pro-ligands P-L5, P-L6 41

2.2.6 Characterization of P-L5, *N*-2-hydroxy ethyl-*N'*-[2-(hydroxy-phenyl) ethyl] imidazolium iodide 42

2.2.7 Characterization of P-L6, 4,5-dichloro-*N*-2-hydroxy ethyl-*N'*-[2-(hydroxy-phenyl) ethyl] imidazolium iodide 44

2.2.8 Synthesis of pro-ligands P-L7 46

2.2.12 Characterization of P-L7, *N*-2-hydroxy ethyl-*N'*-[2-(methoxy-phenyl) ethyl] imidazolium iodide 46

2.2.9 Synthesis of pro-ligands P-L8, P-L9, P-L10, P-L11 48

2.2.10 Characterization of P-L11, 4,5-dichloro *N*-methyl-*N'*-[cyclohexan-2-ol] imidazolium iodide 48

2.2.11 Synthesis of caffeine-based imidazolium salts P-L12, P-L13, P-L14 49

2.2.12 Characterization of P-L12, *N'*-[2-(hydroxy phenyl) ethyl] trimethylxantinium iodide 50

2.2.13 Characterization of P-L13, *N'*-[2-(hydroxy) ethyl] trimethylxantinium iodide 52
2.2.14 Characterization of P-L14, *N'*-[cyclohexan-2-ol] trimethylxanthinium iodide 54

2.3 Synthesis of silver *N*-heterocyclic carbene complexes 56

2.3.1 Characterization of Silver complexes AgL1, AgL2, AgL3, AgL4, AgL5, AgL6, AgL7 58
2.3.2 Characterization of Silver complexes AgL7' 67
2.3.3 Characterization of Silver complexes AgL8, AgL9, AgL10, AgL11 68
2.3.4 Characterization of caffeine-based silver NHC complexes AgL12, AgL13, AgL14 70
2.3.5 Characterization of Silver complexes AgL1-OAc, AgL2-OAc, AgL7-OAc 74

2.4 Synthesis of gold(I) *N*-heterocyclic carbene complexes 78

2.4.1 Characterization of Gold complexes AuL1-L11 80
2.4.2 Characterization of caffeine-based gold NHC complexes AuL12-AuL13-AuL14 92

2.5 A^3coupling reaction catalysed by Ag and Au(I) *N*-heterocyclic carbene complexes 97

2.5.1 Synthesis of propargylamine through A^3-coupling reaction 97
2.5.2 Catalytic Performance of Ag and Au NHC complexes 99
2.5.3 Kinetic studies on A^3coupling reaction catalyzed by AuL2 and its halo and (pseudo)halo-derivates 109
2.5.4 Conclusion 119

2.6 Hydroamination of alkynes catalyzed by Au(I) *N*-heterocyclic carbene complexes 121

2.6.1. Hydroamination reaction 121
2.6.2 Aim of the project 122
2.6.3 Screening of the Gold (I) complexes as Catalyst in the Hydroamination of Phenylacetylene with Aniline 122
2.6.4 Screening of the Solvent for the Hydroamination of Phenylacetylene with Aniline, promoted by AuL2. 124
2.6.5 Hydroamination of alkyne with different arylamine. 125
2.6.7 Conclusions 126

2.7 Biological activity 127

2.7.1 Antimicrobial activity of silver and gold N-heterocyclic carbene complexes 128
2.7.1 Antitumoral activity of silver and gold N-heterocyclic carbene complexes 130
2.7.3 Conclusion 136

Chapter 3: Conclusion and Perspective 137

Chapter 4: Experimental part 138

4.1 General Procedure 138

4.2 Synthesis of imidazolium salts 138

4.2.1 General procedure for Synthesis of N-Heterocyclic carbene Proligands P-L1-6, P-L8-11 138
4.2.2 Synthesis of *N*-methyl, *N'*-(2-Hydroxy-2-phenyl ethyl) imidazolium iodide (P-L1) 139
4.2.3 Synthesis of 4,5-dichloro-*N*-methyl, N'-(2-Hydroxy-2-phenyl ethyl) imidazolium iodide (P-L2) 139

4.2.4 Synthesis of 4,5-diphenyl-*N*-methyl, N'-(2-Hydroxy-2-phenyl ethyl) imidazolium iodide (P-L3) 139
4.2.5 Synthesis of *N*-methyl, *N*'-(2-Hydroxy-2-phenyl ethyl) benzimidazolium iodide (P-L4) 139
4.2.6 Synthesis of *N*-[2-Hydroxyethyl], *N*'-(2-Hydroxy-2-phenyl ethyl) imidazolium iodide (P-L5) 140
4.2.7 Synthesis of 4,5-dichloro *N*-[2-Hydroxyethyl], *N*'-(2-Hydroxy-2-phenyl ethyl) imidazolium iodide (P-L6) 140
4.2.8 Synthesis of *N*-methyl, *N*'-(2-methoxy-2-phenyl) ethyl) imidazolium iodide (P-L7) 141
4.2.9 Synthesis of *N*-methyl, *N*'-(cyclopentane-2-ol) imidazolium iodide (P-L8) 141
4.2.10 Synthesis of 4,5-dichloro *N*-methyl, *N*'-(cyclopentane-2-ol) imidazolium iodide (P-L9) 141
4.2.11 Synthesis of *N*-methyl, *N*'-(cyclohexane-2-ol) imidazolium iodide (P-L10) 141
4.2.12 Synthesis of 4,5-dichloro-*N*-methyl, *N*'-(cyclohexane-2-ol) imidazolium iodide (P-L10) 141
4.2.13 General procedure for the synthesis of xanthinium *N*-Heterocyclic carbene Proligands P-L12-14 142
4.2.14 Synthesis of *N'*-[2-(hydroxy-phenyl) ethyl] trimethyl xanthinium iodide (P-L12) 142
4.2.15 Synthesis of *N'*-[2-(hydroxy) ethyl] trimethyl xanthinium iodide (P-L13) 143
4.2.16 Synthesis of *N'*-[cyclohexan-2-ol] trimethyl xanthinium iodide (P-L14) 143

4.3 Synthesis of *N*-heterocyclic carbene silver complexes 144

4.3.1 General procedure for the synthesis of *N*-Heterocyclic silver carbene complexes AgL1-L6, AgL8-L11 144
4.3.2 Synthesis of Iodo [*N*-(methyl)-*N'*(2-hydroxy phenyl)ethyl-imidazolyden]silver(I) (AgL1) 144
4.3.3 Synthesis of Iodo 4,5-dichloro-[*N*-(methyl)-*N'*(2-hydroxy phenyl)ethyl-imidazolyden]silver(I) (AgL2) 144
4.3.4 Synthesis of Iodo 4,5-diphenyl-[*N*-(methyl)-*N'*(2-hydroxy phenyl)ethyl-imidazolyden]silver(I) (AgL3) 144
4.3.5 Synthesis of Iodo-[*N*-(methyl)-*N'*(2-hydroxy phenyl)ethyl-benzimidazolyden]silver(I) (AgL4) 144
4.3.6 Synthesis of Iodo-[*N*-(2-hydroxyethyl)-*N'*(2-hydroxy phenyl)ethyl-imidazolyden]silver(I) (AgL5) 145
4.3.7 Synthesis of Iodo-4,5-dichloro-[*N*-(2-hydroxyethyl)-*N'*(2-hydroxy phenyl)ethyl-imidazolyden]silver(I) (AgL6) 145
4.3.8 Synthesis of Iodo [*N*-(methyl)-*N'*(2-methoxy phenyl)ethyl-imidazolyden]silver(I) (AgL7) 146
4.3.9 Synthesis of Iodo [*N*-(methyl)-*N'*(sodium alcholate-2-phenyll)ethyl-imidazolyden]silver(I) (AgL7') 146
4.3.10 Synthesis of Iodo [*N*-(methyl)-*N'*(cyclopent-2-ol)-imidazolyden] silver(I) (AgL8) 146
4.3.11 Synthesis of Iodo 4,5-dichloro-[*N*-(methyl)-*N'*(cyclopent-2-ol)-imidazolyden] silver(I) (AgL9) 146
4.3.12 Synthesis of Iodo [*N*-(methyl)-*N'*(cyclopent-2-ol)-imidazolyden] silver(I) (AgL10) 146
4.3.13 Synthesis of Iodo 4,5-dichloro-[*N*-(methyl)-*N'*(cyclopent-2-ol)-imidazolyden] silver(I) (AgL11) 146
4.3.14 General procedure for the synthesis of caffeine-based *N*-Heterocyclic carbene silver complexes AgL12-L14 147
4.3.15 Synthesis of acetate-[*N'*(2-hydroxy phenyl)ethyl-trimethylxanthium] silver(I) (AgL12) 147
4.3.16 Synthesis of acetate-[*N'*(2-hydroxy ethyl)-trimethylxanthium] silver(I) (AgL13) 147
4.3.17 Synthesis of acetate-[*N'*(cyclohexan-2-ol)-trimethylxanthium] silver(I) (AgL14) 148
4.3.18 General Procedure for the synthesis of NHC silver acetate complexes 148
4.3.19 Synthesis of acetate [*N*-(methyl)-*N'*(2-hydroxy phenyl)ethyl-imidazolyden]silver(I) (AgL1-OAc) 148
4.3.20 Synthesis of acetate [4,5-dichloro-*N*-(methyl)-*N'*(2-hydroxy phenyl)ethyl-imidazolyden]silver(I) (AgL2-OAc) 149
4.3.21 Synthesis of acetate [*N*-(methyl)-*N'*(2-methoxy phenyl)ethyl-imidazolyden]silver(I) (AgL7-OAc) 149

4.4 Synthesis of gold(I) *N*-heterocyclic carbene complexes AuL1-L11 149

4.4.1 Synthesis of chloro [*N*-(methyl)-*N'*(2-hydroxy phenyl)ethyl-imidazolyden]gold(I) (AuL1) 149

4.4.2 Synthesis of chloro 4,5-dichloro-[*N*-(methyl)-*N'*(2-hydroxy phenyl)ethyl-imidazolyden]gold(I) (AuL2) 149

4.4.3 Synthesis of chloro 4,5-diphenyl-[*N*-(methyl)-*N'*(2-hydroxy phenyl)ethyl-imidazolyden]gold(I) (AuL3) 150

4.4.4 Synthesis of chloro [*N*-(methyl)-*N'*(2-hydroxy phenyl)ethyl-benzimidazolyden]gold(I) (AuL4) 150

4.4.5 Synthesis of chloro [*N*-(2-hydroxy ethyl)-*N'*(2-hydroxy phenyl)ethyl-imidazolyden]gold(I) (AuL5) 151

4.4.6 Synthesis of chloro, 4,5-dichloro-[*N*-(2-hydroxy ethyl)-*N'*(2-hydroxy phenyl)ethyl-imidazolyden]gold(I) (AuL6) 151

4.4.7 Synthesis of chloro,[*N*-(methyl)-*N'*(2-methooxy phenyl)ethyl-imidazolyden]gold(I) (AuL7) 151

4.4.8 Synthesis of chloro, 4,5-[*N*-(methyl)-*N'*(2-sodium alcoholate phenyl)ethyl-imidazolyden]gold(I) (AuL7') 152

4.4.9 Synthesis of chloro [*N*-(methyl)-*N'*(cyclopentane-2-ol)-imidazolyden]gold(I) (AuL8) 153

4.4.10 Synthesis of chloro4,5-dichloro[*N*-(methyl)-*N'*(cyclopentane-2-ol)-imidazolyden] gold(I) (AuL9) 153

4.4.11 Synthesis of chloro, [*N*-(methyl)-*N'*(cyclohexane-2-ol)-imidazolyden]gold(I) (AuL10) 153

4.4.12 Synthesis of chloro,4,5-dichloro[*N*-(methyl)-*N'*(cyclohexane-2-ol)-imidazolyden]gold(I) (AuL11) 153

4.4.13 General procedure for the synthesis of caffeine-based gold *N*-Heterocyclic carbene complexes AuL12-L14 153

4.4.14 Synthesis of chloro -[*N'*(2-hydroxy phenyl)ethyl-trimethylxanthium] gold(I) (AuL12) 153

4.4.15 Synthesis of chloro -[*N'*(2-hydroxy)ethyl-trimethylxanthium] gold(I) (AuL13) 154

4.4.16 Synthesis of chloro -[*N'*(ciclohexane-2-ol)-trimethylxanthium] gold(I) (AuL14) 154

4.4.17 Synthesis of acetato 4,5-dichloro-[*N*-(methyl)-*N'*(2-hydroxy phenyl)ethyl-imidazolyden]gold(I) (AuL2-OAc) 155

4.4.18 Synthesis of bromo 4,5-dichloro-[N-(methyl)-N'(2-hydroxy phenyl)ethyl-imidazolyden]gold(I) (AuL2-Br) 155

4.4.19 Synthesis of iodo 4,5-dichloro-[N-(methyl)-N'(2-hydroxy phenyl)ethyl-imidazolyden]gold(I) (AuL2-I 155

4.4.20 Synthesis of hexafluorophosphate 4,5-dichloro-[*N*-(methyl)-*N'*(2-hydroxy phenyl)ethyl-imidazolyden]gold(I) (AuL2-PF_6) 156

4.4.21 Synthesis of phenylacetylide 4,5-dichloro-[*N*-(methyl)-*N'*(2-hydroxy phenyl)ethyl-imidazolyden]gold(I) (AuL2CCPh) 156

4.5 General Procedure for A^3 (aldehyde, amine, alkyne) coupling reaction promoted by M-NHC complexes 157

N-(3-phenyl-2-propynyl) piperidine 157

1-(1-cyclohexyl-3-phenyl-2propynyl) 157

N-(1,3-diphenyl-2-propynyl)piperdine 157

4.6 General Procedure for hydroamination reaction promoted by Au-NHC complex 157

(E)-*N*-(4-nitrophenyl) -1-phenylethan-1-imine (4f) 158

(E)-*N*-(2,6-difluorophenyl)-1-phenylethan-1-imine (4f) 158

4.7 Antibacterial Activity 158

4.8 Antitumoral Activity **158**

Permissions ***159***

References ***160***

Chapter 1: Introduction

1.1 Carbenes

The carbenes are a class of compounds having a divalent, uncharged carbon atom with six electrons on its valence shell. Introduced in 1950 in organic chemistry as an intermediate in different transformations, and in organometallic chemistry by Fischer in 1964, carbenes have become one of the most important topics in chemistry, due to their chemical and physical properties [1,2].

Their geometry is related to the two possible hybridizations of the carbon atom (sp, linear geometry or sp^2, bent geometry). In the linear geometry, carbene carbon has two degenerate orbitals, named p_x and p_y. The sp hybridization is a rarer case, most of it has a bent geometry based on an sp^2 hybridization. The energy of p-orbital, also called p_π, does not change in both hybridization states. The new sp^2 orbital is more stable than the original p orbital, by the assuming s character.

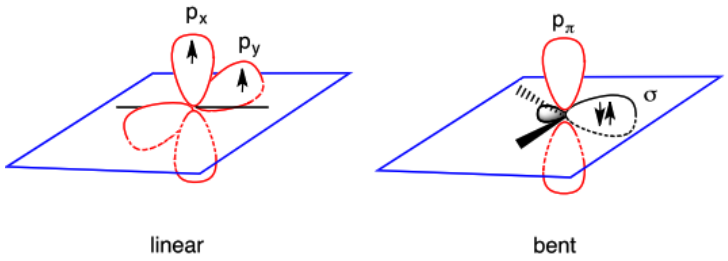

Figure 1 Linear and bent geometry of carbene carbon atom

The arrangement of nonbonding electrons determines the reactivity and properties of carbenes [3]. As shown in **Figure2**, four different electronic configurations can be described. The two nonbonding electrons can occupy the two orbitals with parallel spin orientation, leading to a triplet state ($\sigma^1p_\pi^1$,$^3B_1$ state). Otherwise, for the singlet ground state, the nonbonding electrons can occupy the same orbital (σ or p_π). The σ^2 configuration is usually more stable than p_π^2. Lastly, it can be defined as an excited singlet state with $\sigma^1p_\pi^1$configuration, where the two electrons occupy two different orbitals with anti-parallel spin ($^1B_1$ state). Thus, due to the presence of a filled and vacant orbital, singlet carbenes could have an amphiphilic behavior.

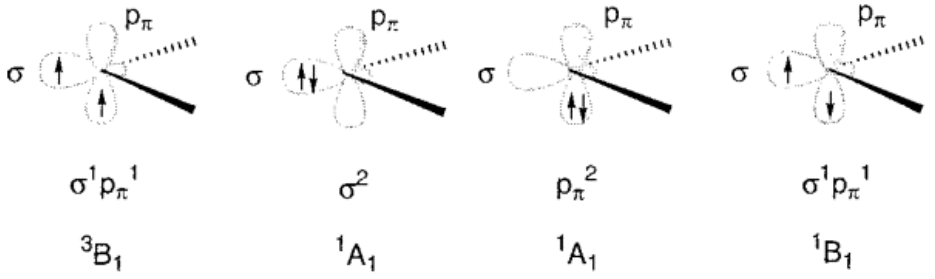

Figure 2 Possible electronic configuration of the carbene carbon atom. Reprinted with permission Bourissou, D.; Guerret, O.; Gabbaï, F.P.; Bertrand, G. Stable Carbenes. Chem. Rev. ***2000****, 100, 39–92, [1] Copyright 2000, American Chemical Society.*

The multiplicity of carbene carbon atom is strictly related to the difference of energy among σ and p_π orbitals. Large energetic separation of these orbitals favors the singlet ground state; Hoffman established through quantum chemical computation that a difference of about 2eV is necessary to stabilize the singlet ground state[4]. The triplet ground state is favored if the difference between σ and p_π is less than 1.5 eV [4].

Substituents on carbon atom influence the multiplicity of the carbene ground state. These influences can be easily summarized in electronic and steric effects. It was observed that σ-withdrawing substituents stabilize singlet ground state through the increasing of s-character of nonbonding orbital, leaving p_π orbital unchanged. Instead, σ-donating substituents favor the triplet state because they cause the decrease of the energetic gap among σ and p_π orbitals[5–7]. Beyond inductive electronic effects, the carbene ground state is influenced by mesomeric effects[4-8]. π-donor substituents (such as -Cl, -Br, $-NR_2$, $-PR_2$,-OR), induce a strongly bent singlet ground state; the interaction of the π electrons with p_π orbital of the carbene carbon atom increases the energy gap among σ-p_π. Most carbenes with π-acceptor substituent (for example Li, BeH, BH_2) on carbon atom are in linear singlet ground state, by the formation of two-electron three-center π-system[9,10]. The combination of two types of substituents induces quasi-linear geometry at carbene.

Bulky substituents stabilize the triplet carbene because they force the carbon atom of the carbene to assume a large bond angle, which stabilizes the triplet state. Diadamantyl- and di(*tert*-butyl)- carbenes have bond angles respectively of 152° and 143°, they are triplets, whereas di-methylcarbene is singlet carbene with bent geometry.

Free carbenes are thermodynamically and kinetically unstable. Due to their instability, carbenes are used in coordination chemistry for the synthesis of metal complexes, having a metal=carbon double bond[11]. Two types of carbene complexes with different properties have been distinguished: Fischer[12] and Shrock[13] type.

1.2 Carbenes in organometallic chemistry

In 1925, the first carbene metal complex was reported in the literature by Chugaev and his co-workers[14]. As shown in **Figure 3**, they synthesized new platinum (II) complex by the reaction of methyl isocyanide, a platinum (II) salt and hydrazine.

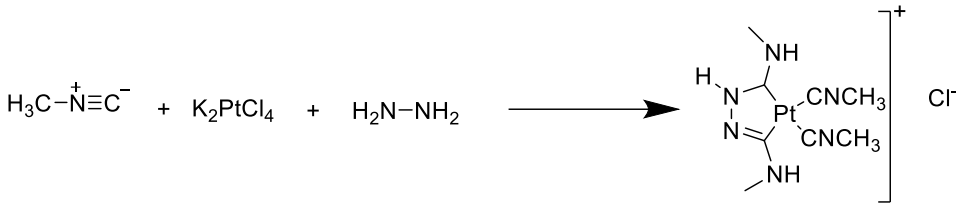

Figure 3 The synthesis of Chugaev complex

Unfortunately, the structure of this complex was determined only in 1970 by NMR spectroscopy and X-ray crystal diffraction[15]. Despite this, the methodologies published by Chugaev are important because they are still used for the synthesis of interesting platinum[16] and palladium complexes[17].

The first structure of metal carbene complex was reported by Fischer in 1964 [12]. Fischer et al. reported the synthesis and the characterization of methoxyphenylmethylene tungsten (0) pentacarbonyl.

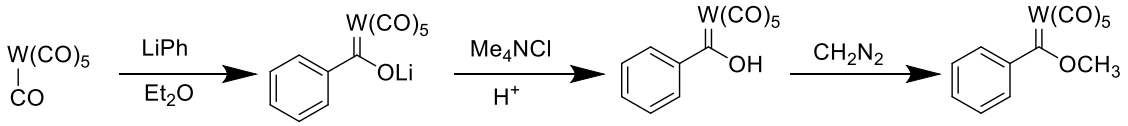

Figure 4 Synthesis of the Fischer carbene complex

Fischer carbene complexes have a low-valent metal center, π-acceptor ancillary ligand and they are stabilized by carbene having heteroatom substituents on the carbon atom. The main feature of these complexes is the partial double bond resulting from a σ-donation of the carbene to the metal and a simultaneous π-back donation of the metal to carbene.

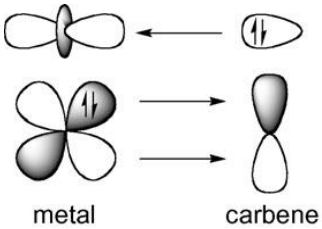

Figure 5 Metal-Fischer Carbene bonding. Reprinted with permission de Frémont, P.; Marion, N.; Nolan, S.P. Carbenes: Synthesis, Properties, and Organometallic Chemistry. Coord. Chem. Rev. ***2009****, 253, 862–892, Copyright 2008, Elsevier B.V.*

The interaction between the metal center and Fischer carbene is shown in **Figure 5** [18]. These complexes are electrophilic, they are susceptible to nucleophilic attacks on the carbon atom.

Ten years later, Schrock published the synthesis and characterization of a new tantalum carbene complex, with a high oxidation state(d^0), by the reaction of α-hydrogen abstraction[13].

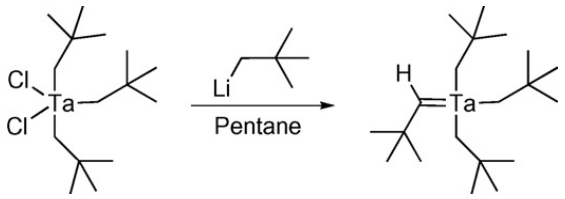

Figure 6 Synthesis of the first Schrock Carbene Complex Reprinted with permission de Frémont, P.; Marion, N.; Nolan, S.P. Carbenes: Synthesis, Properties, and Organometallic Chemistry. Coord. Chem. Rev. ***2009****, 253, 862–892, Copyright 2008, Elsevier B.V.*

As seen in section 1.1, dialkylcarbene has small energetic gap between σ-p_π orbital, and they have a triplet ground-state. They form a true double metal-carbon bond, which arises by homogenous electron coupling. Unlike Fischer carbene complexes, Schrock-type complexes are nucleophilic and are capable to react with electrophilic species, in such manner of Wittig's reaction[19].

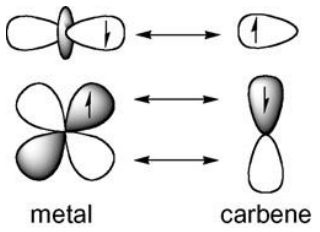

Figure 7 Metal- Schrock Carbene bond Reprinted with permission de Frémont, P.; Marion, N.; Nolan, S.P. Carbenes: Synthesis, Properties, and Organometallic Chemistry. Coord. Chem. Rev. ***2009****, 253, 862–892, Copyright 2008, Elsevier B.V.*

In the last twenty years a new class of carbene ligands has become a hot topic in organometallic, organic chemistry, and in material science. These ligands are *N*-heterocyclic carbenes, also known as Arduengo carbenes[20].

1.3 *N*-heterocyclic Carbenes

In the 1960s, Wanzlick conducted the first studies about *N*-heterocyclic carbenes (NHCs). He supposed that diaminocarbenes were stable and he was fascinated to isolate them. He postulated that by α-elimination of chloroform from 1,3-diphenyl-2-trichloromethylimidazolidine was possible to isolate the resulting diamino carbene, but he obtained only the dimer (entetramine)a s shown in **Figure 8**[21].

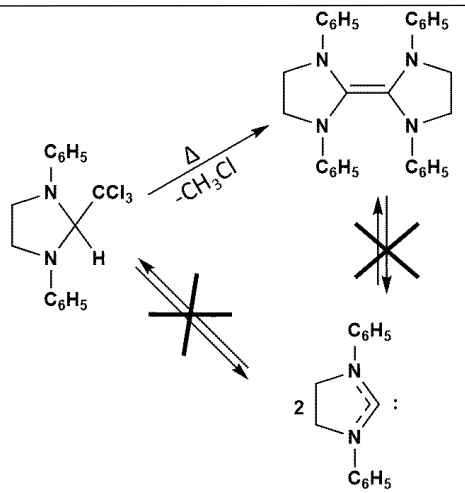

Figure 8 Wanzlick's tentative to isolate diaminocarbene

A few years later, Wanzlick and Öfele independently reported the synthesis of two NHC-metal complexes, by treatment of imidazolium salt with base, and consequent coordination to the metal center[22,23].

The real innovation in the carbene's chemistry has happened in 1991, when Arduengo and his collaborators reported the synthesis and the characterization, by X-ray analysis of the first stable N-heterocyclic carbene, 1,3-bis(adamantyl)imidazole-2-ylidene [20]. The first stable diaminocarbene was obtained by the deprotonation of *N, N'* diadamantyl imidazolium salt with sodium hydride and a catalytic amount of DMSO. The X-ray analysis of crystals had shown indisputably the isolation of the first stable NHC.

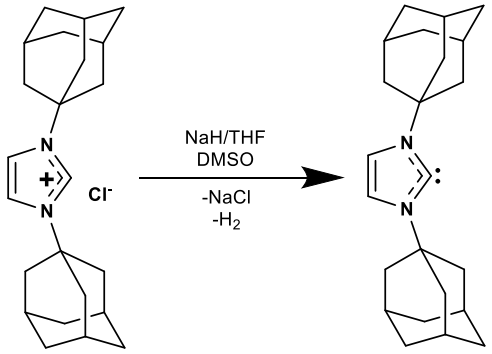

Figure 9 Synthesis of the first stable NHC carbene

The stability of bulky substituted NHC is attributable to steric and electronic effects.

The electronic stabilization provided by the nitrogen atoms, however, is a much more important factor. The presence of bulky substituents, such as the adamantyl group, disfavors the dimerization, by kinetic stabilization. However, electronic stabilization plays the most important role. The presence of adjacent σ-withdrawing nitrogen atoms promotes the inductive stabilization of carbene carbon atom, by lowering of the energy of the occupied σ orbital. Furthermore, the π-donating nitrogen atoms donate electronic density to the empty p_π carbene orbital [24]. The singlet ground state is stabilized by mesomeric interaction

because the energy gap between σ-p_π orbitals, is further increased. In **Figure 10** are summarized the inductive and mesomeric effects of nitrogen atoms.

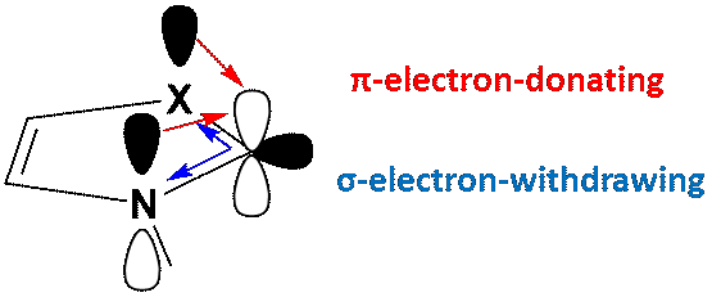

Figure 10 The electronic effects in NHCs

The reactivity of *N*-heterocyclic carbene is strictly influenced by the electronic ground state; the presence of lone pair, on the carbon atom, consent them to coordinate, by σ-donation, diverse metallic and non-metallic species. The resulting compounds are characterized by extraordinary thermodynamic stability, and are used as a catalyst in different types of reactions (*e.g.*: C-C cross-coupling [25], olefin metathesis [26], carbonylative coupling [27], ring-opening polymerization[28] and other interesting transformations [29]). A second important characteristic, of these ancillary ligands, is the facile modulation of steric and electronic features; slight modifications on nitrogen substituents, backbone, and size ring could have an important impact on their coordination capacity. The facile variation of steric and electronic parameters has allowed the preparation of libraries of these compounds. Since the first synthesis of Arduengo, many different *N*-heterocyclic carbenes have been synthesized and characterized. In the following section are discussed the synthetic methodologies are used for their synthesis.

1.3.1 Synthetic strategies for the preparation of *N*-heterocyclic carbenes

N-heterocyclic carbenes are synthesized by deprotonation of imidazolium salts [20] or by reductive desulfurization of imidazolin-2-thiones [30]. The two main synthetic procedures are shown in **Figure 11**.

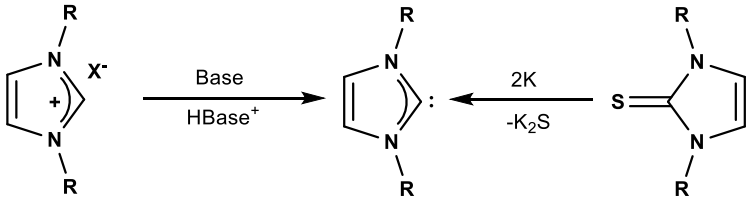

Figure 11 The two most important procedures used for the synthesis of imidazolin-2-ylidenes

Imidazolium salts are prepared following two different routes: 1) nucleophilic addition to the nitrogen atom of imidazole or 2) using a one-pot multicomponent reaction. The direct alkylation of imidazole is conducted with the addition of alkyl halides, after the deprotonation of the nitrogen atom. The second addition of alkyl halide leads to the imidazolium salt. The main limitation of this methodology is the exclusive use of primary

alkyl substituents. As shown in **Figure 12**, the direct alkylation is possible to conduct in a single step to achieve a symmetric imidazolium salt, or in two steps, for the introduction of different substituents on the nitrogen atoms.

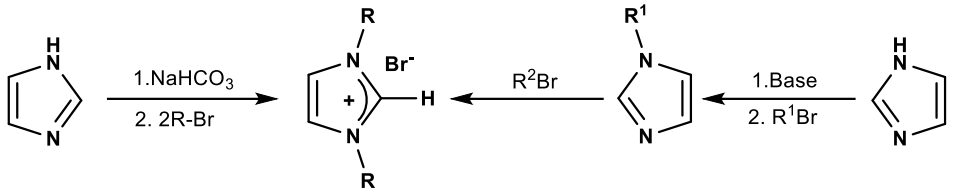

Figure 12 Direct alkylation of imidazole to lead the imidazolium salts

Otherwise, the multicomponent reaction between glyoxal, two equivalents of primary amine and formaldehyde in acid conditions consent the synthesis of varied symmetrically *N, N'*-substituted imidazolium salts. Further, the reaction can be conducted in two steps with the isolation of the diimine (Schiff base), and successive cyclic condensation with paraformaldehyde [31].

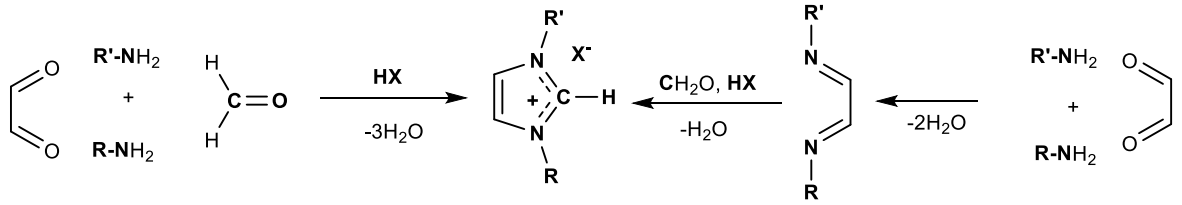

Figure 13 Multicomponent reaction for the synthesis of imidazolium salts

The combination of multicomponent reaction and *N*-alkylation leads the synthesis of unsymmetrically *N, N'* substituted imidazolium salts. A first cyclization, conducted with one equivalent of primary amine, produces *N'*alkylated imidazole. After, the addition of alkyl halide gives the unsymmetrically substituted derivate[32].

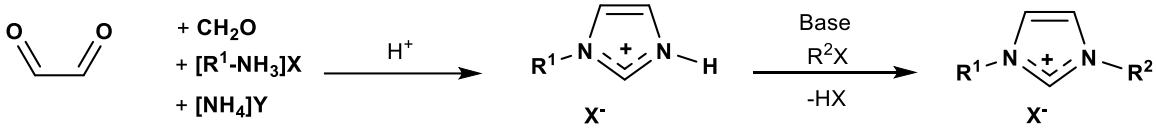

Figure 14 The synthesis of unsymmetrically N, N' substituted imidazolium salt by the combination of one-pot reaction and N'alkylation

As indicated in **Figure 11**, NHCs are obtained by reductive desulfurization of imidazoline-2-thiones [30]. The reductive reaction is conducted in very harsh conditions (in excess of potassium in boiling THF), even though, the yields are practically quantitative. For this reason, is noteworthy to mention the synthesis of cyclic thioureas. Kuhn and co-workers have published in 1993 an interesting synthetic procedure for the production of cyclic thioureas by the condensation of α-hydroxyketones and thioureas derivates[33].

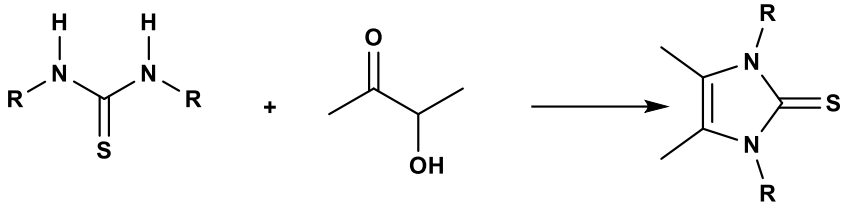

Figure 15 Synthesis of cyclic thioureas derivates

The most important application of *N*-heterocyclic carbenes is as ancillary ligands for transition metals. As seen above, these transition metal compounds have shown catalytic properties in different reactions [25–29]. Moreover, in the last years, NHC-Metal complexes have found applications as metal drugs in pharmacology [34–36] and as organometallic materials[35,37].

1.4 Coordination chemistry of *N*-heterocyclic Carbene

The motivations for the growing interest on NHC are attributable to facile fine-tuning of steric and electronic properties of these ancillary ligands, their capacity to stabilize a great variety of oxidation states of transition metals, and the application of these complexes in different fields of organometallic chemistry[38]. The stability of these complexes is attributable to a strong metal-carbon bond, by σ-donation of sp^2-lone pair of the carbene carbon atom to an empty orbital of transition metal., while the π-back donation is negligible [39]. The difference between NHC and Fischer/Schrock carbene is underlined by the experimental possibility of rotation of the metal-carbon bond.

N-heterocyclic carbenes generally have more σ-electron-donatory properties than phosphines, in fact, infrared spectroscopy studies of different Ni(0) carbonyl complexes, bearing an NHC in *trans*-position, revealed lower vibrational frequencies (ν_{CO}) than basic phosphine complexes [40]. This characteristic is reflected in a major thermodynamically stability and shorter length of the carbene carbon atom and the metal center. The success of the 2nd generation Grubb's catalyst is due to the electronic differences between NHC and phosphines; the σ-donation by N-heterocyclic carbene ligand induces the dissociation of the *trans*-oriented phosphine[41]. The full comprehension of the nature of the NHC-M bond was studied by Nolan [42] and Cavallo[43].

Different procedures are developed for the synthesis of *N*-heterocyclic carbene complexes. They can be summarized in the following routes (**Figure 16**):

1. The reaction between a free carbene with an appropriate metal source (Free carbene route);
2. *Trans*-metalation reaction with silver NHC complex (*trans*-metalation route);
3. Reaction among imidazolium salt, transition metal, and a weak base (weak base route).

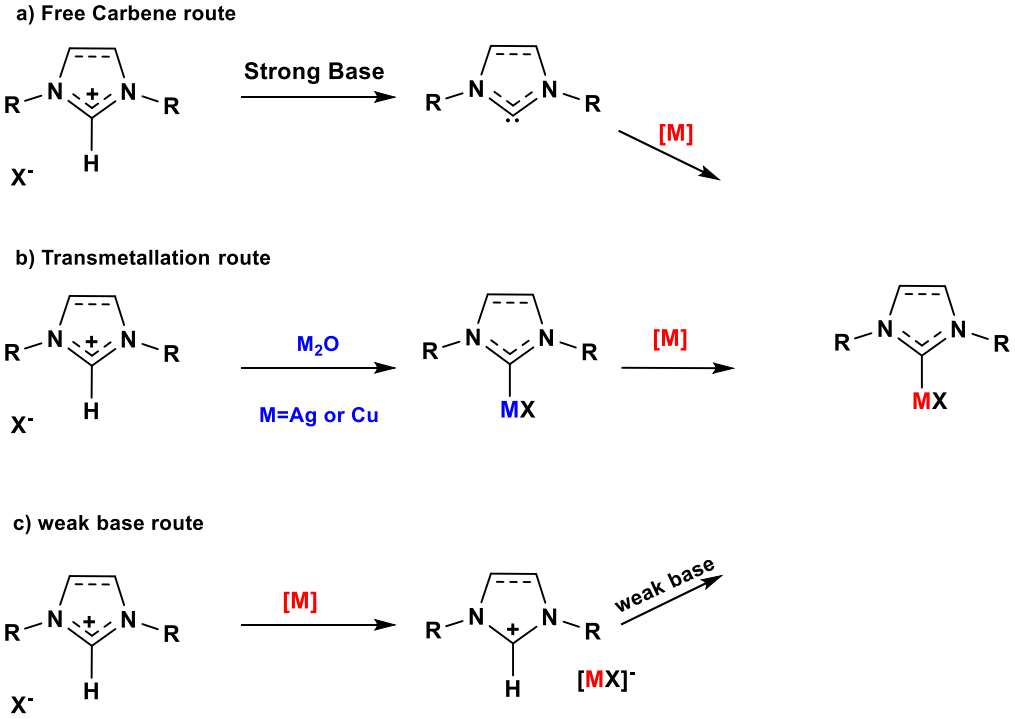

Figure 16 Synthetic procedure for the synthesis of M-NHC complexes

1. *Free carbene route*

   The first synthesized NHC metal complexes were obtained by Wanzlick[22] and Ofele [23] developing this procedure. This methodology includes two steps; in the first, the imidazolium salt is deprotonated by a strong base in anhydrous condition, while in the second step, the transition metal precursor is added to the free-carbene solution.

2. *Trans-metalation route*

   The *trans*-metalation reaction is also carried out in two steps. In the first, the azolium salt is deprotonated by silver or copper oxide, with the purpose to achieve the Ag- or Cu-NHC complexes [44]. The second step involves the transfer to a different transition metal. The advantages of the *trans*-metalation route are the use of air-stable reactants, and the formation of water as by-products, in the first step. However, the limitations of this route are the use of toxic solvents and the application of high temperatures.

3. *Weak base route*

   The research group of Nolan [45] and Gimeno[46], 2013, reported the synthesis of gold and silver NHC complexes in a one-pot manner using a weak base (K_2CO_3). This synthetic route can be used in aerobic conditions, with a greener solvent such as acetone and ethyl acetate, and are not necessary hazardous bases. Recently, this synthetic strategy has been developed for the synthesis of other transition metal complexes [47].

The development of different synthetic pathways, in addition to the intrinsic properties of NHC ligands, has allowed the application in different fields of chemistry. In the literature the study of pharmacological and catalytic properties of silver and gold(I) N-heterocyclic complexes are reported.

1.5 Silver *N*-heterocyclic carbene complexes

1.5.1 The use of silver in medicine

Since ancient times, silver and its compounds had a great impact on civilization, in fact, they were used as antibacterial agents in the purification of water and wine, and additionally, Hippocrates observed their therapeutic properties [48,49]. During the 17th and 18th centuries, before the discovery of penicillin and antibiotics, silver nitrate was largely used as an antibacterial compound. Silver compounds are still used for the treatment of ulcers, and burns and the prevention of bacterial infections [50].

Despite they having been used for a long-time, their mechanism of cytotoxic action against *Gram-positive* and *Gram-negative* bacteria is not yet well established. Several studies have associated the mechanism of action with bacterial morphological changes produced by silver cation (Ag^+) its interaction with condensed DNA molecules and inhibition of the respiratory chain. Silver cations can react with different nitrogen-, and sulfur-containing biomolecules due to their soft Lewis acidity.

Generally, silver is considered non-toxic metal for humans, but its extensive use can have undesirable effects. It was observed that the prolonged use of silver compounds causes an irreversible pigmentation of the skin, called Argyria, and of eyes, knowns as Argyrosis, attributable to the production and storage in the dermis and the eyes of silver precipitate such as silver sulfide. Furthermore, the high concentration of chloride in the cell leads, in a short time, to the precipitation of silver salt and the loss of its effectiveness, unless the silver cations are bound to biomolecules. Today, silver sulfadiazine is used for the treatment of topical burns due to its low dissociation rate and consequent gradual release of silver cations.

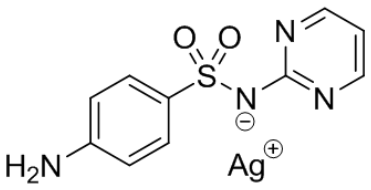

Figure 17 Silver Sulfadiazine

The discovery of antibiotics-resistant bacteria has prompted the scientific community to synthesize new stable silver compounds and to study their antibacterial effects. During these years, new ligands were synthesized which allowed the stabilization of silver cations.

Among the various classes of ligands, NHCs are the best candidates for these scopes. In fact, in the last decades, a lot of NHCs and the corresponding silver complexes were synthesized for medicinal applications.

1.5.2 Antimicrobial Properties of Ag-NHC complexes

The first exploration of the antibacterial effects of silver *N*-heterocyclic carbene complexes was reported by Young's research group [51]. They synthesized and characterized two AgNHC complexes and tested their activities towards three different bacteria (*E. coli*, *P. aeruginosa,* and *S. aureus*). The antibacterial activity was evaluated by determining the MIC (Minimum Inhibitory Concentration: the lowest concentration, of a compound that inhibits the growth of bacterial population) and compared with that of $AgNO_3$. The authors have associated the better cytotoxic activity of the complexes with their slow release of silver cations, attributable to a partially covalent bond among Ag-C.

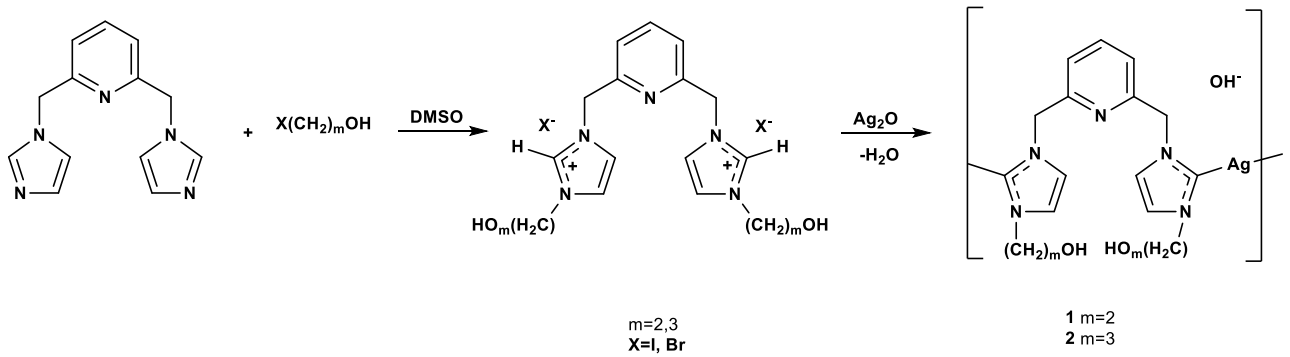

Figure 18 Synthesis of Young's Ag(I)-NHC.

The same research group had reported the synthesis of another water-soluble silver NHC complex; the synthetic procedure is reported in **Figure 18**. The reaction of 2,6-bis(imidazolemethyl)pyridine with 1,3-dichloroacetone has produced the *gem*-diol imidazolium salts. The corresponding silver complex was synthesized by the reaction of imidazolium salt and Ag_2O. The formation of the complex was supported by spectroscopic NMR analysis(^1H and ^{13}C) and X-ray analysis[52]. The complex was incorporated into Tecophilic®, a medicinal-grade polymer by electrospinning. The polymeric matrix is hydrophilic, it can absorb 150% of its dry weight in water. This feature is significant for optimal wound healing. First, if the silver complex-loaded polymeric matrix, is applied to the wound site, the water allows the gradual release of silver cation, while secondly, the hydrophilic polymeric matrix can accelerate recovery maintaining a moist environment. The authors evaluated the activity of encapsulated silver complex against *E. coli*, *P. aeruginosa,* and *S. aureus*. The action of the system was compared with $AgNO_3$. The polymer matrix embedded with complex has shown a better cytotoxic activity, even with lower silver concentration. Also, the most attractive feature is the prolonged bacteriostatic action for a

long time. The long-time prolonged activity of the AgNHC/polymer system was attributable to the slow release of the silver cations from the polymeric matrix.

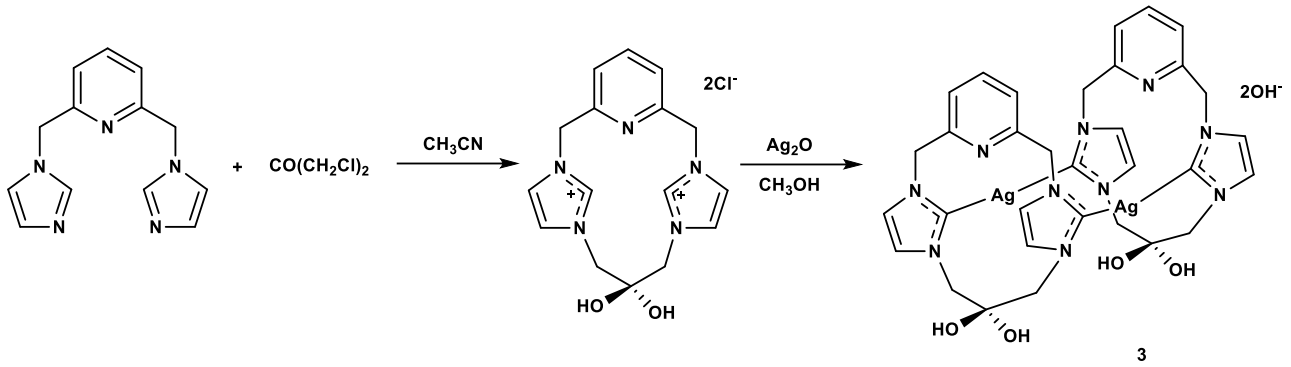

Figure 19 Synthesis gem-diol N-heterocyclic carbene silver complex.

A not negligible property of the use of AgNHC complex is the intrinsic toxicity of the imidazolium salt. The authors have evaluated the toxicity of *gem*-diol imidazolium salt. It was determined a lethal dose (LD_{50}) of 100mg/Kg in rats, where LD_{50} is the concentration that causes the death of 50% of the sample population. This observation had forwarded the research group to use less toxic NHC precursors.

In 2006, it was reported the synthesis of caffeine-based NHC silver complex, having acetate as counterion [53]. The NHC pro-ligand was obtained by the reaction of caffeine with iodomethane in DMF. The silver compounds were obtained by the deprotonation of caffeine salts with two equivalents of silver acetate. The caffeine-based silver complex was tested with different pathogens (bacteria and fungi). The MIC values of the silver complex towards bacterial cell lines fell in the range of 1-10 μg/mL.

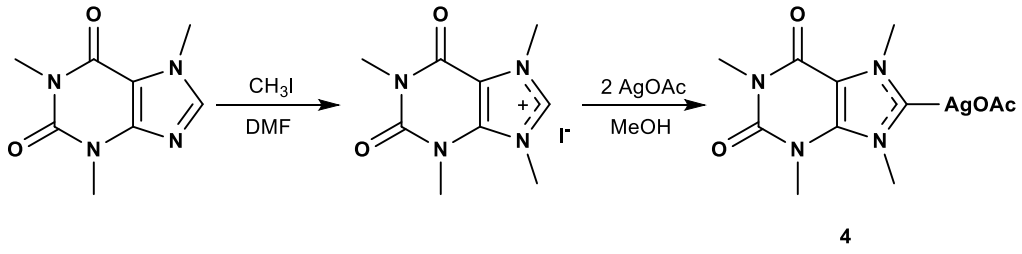

Figure 20 synthesis of caffeine-based silver NHC complex

The Young's research group synthesized a series of imidazolium NHC silver acetate complexes. The stability in D_2O by NMR of these complexes was monitored. The analysis of the date suggests that the presence of σ-electron withdrawing substituents on the backbone, induces a stabilization of the corresponding complex.

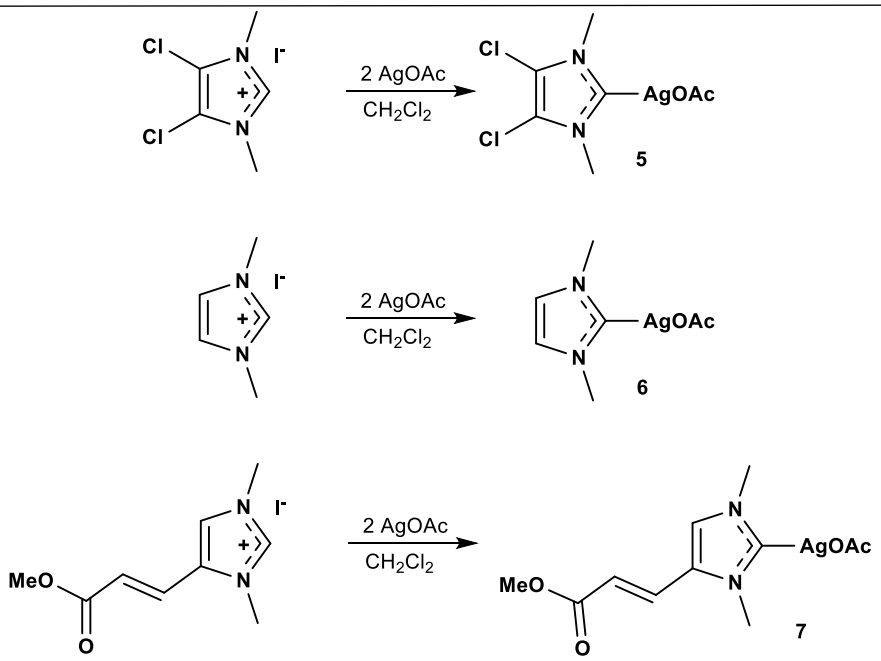

Figure 21 Synthetic route of acetate Ag-NHC complexes

The presence of chlorine atoms on the backbone, leads to the carbon atom of the carbene with lower electron density, therefore less reactive in aqueous media. The stability of the silver complex plays a crucial role in the delivery of metal cations. Based on this observation, NHC bearing chlorine atoms on the backbone, with hydrophilic and hydrophobic *N*-substituents, were synthesized and tested with different pathogens. [54,55].

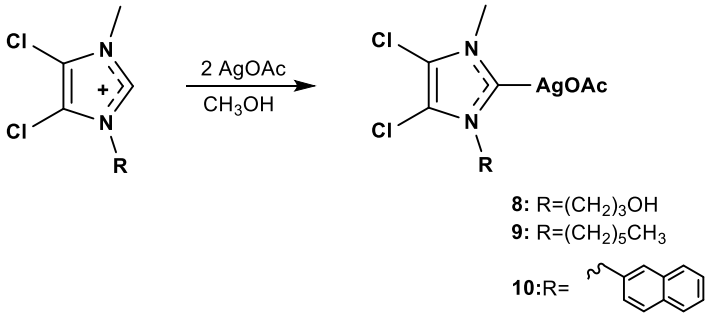

Figure 22 NHC Ag complexes derived by 4,5-dichloro imidazole

The obtained results were very promising, in fact, the complexes exhibited low MIC and MBC (minimum bactericidal concentration) values. MBC is the lowest concentration of a compound to kill, under specific conditions and for a fixed period, the bacterial culture. The complexes showed high activity against *B. Pseudomallei* (MIC: 4-6 μg/mL; MBC: 6-10 μg/mL) and *B. mallei* (1-4μg/mL; 6μg/mL).

Tacke and co-workers have given a great contribution to expanding the library of silver-NHC complexes. In **Figure 23** are reported complex synthesized by Tacke's research group[56–60].

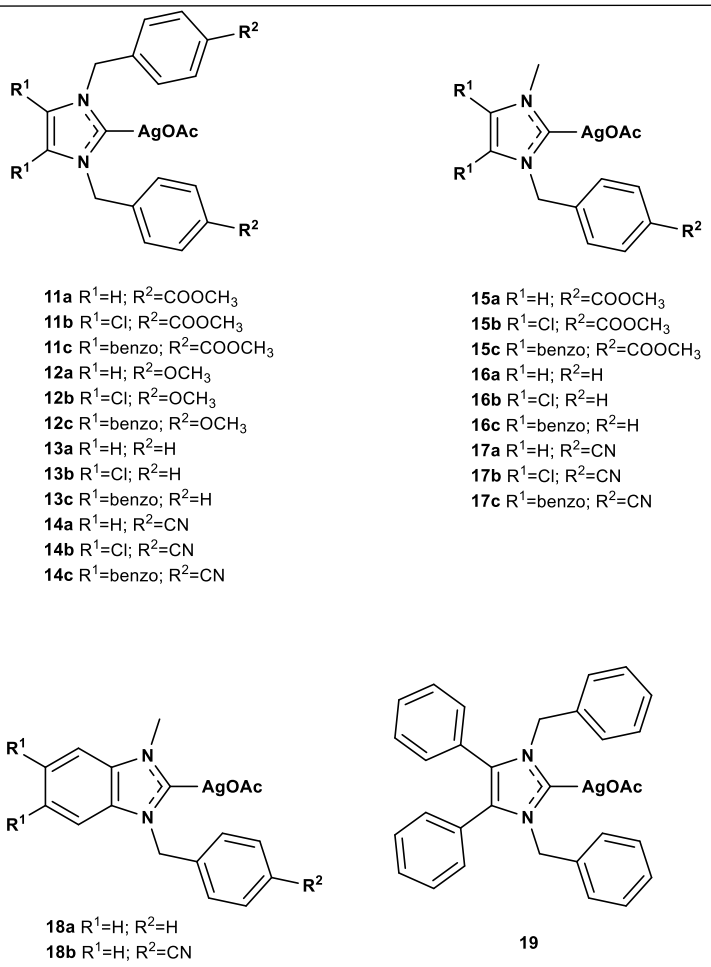

Figure 23 Silver complexes synthesized by Tacke's groups

All the shown complexes, bearing an acetate ion, were tested against *E. coli*, *S. aureus*, measuring the halo of inhibition (Kirby-Baur diffusion method). The authors of the papers have tested the imidazolium salts, silver acetate, and dimethylsulfoxide (DMSO) as controls. For the complexes that showed a modest antibacterial activity, it was measured a 4mm of clearance at the highest concentration used, whereas for the most active complexes it was measured a halo of inhibition of 12mm. For all tested complexes, the activity of silver NHC complexes is better than respective imidazolium salts.

Still today, *N*-heterocyclic carbene silver complexes arouse interest for their antibacterial activity. The literature is enriched by papers and reviews, where are reported the modulation of steric and electronic properties of silver NHC complexes, and their antibacterial properties [34,54,61,62].

As seen in this section, silver compounds are largely studied as anti-infective agents against different pathogens. Initially, unlike other metals (*e.g.:* platinum, gold, ruthenium), the antiproliferative activity of silver compounds was not extensively investigated.

However, the growing number of cancer pathologies has encouraged the development of new metal bioactive molecules with few or no side effects. Starting from the antitumoral

activity showed by non-NHC silver compounds[63,64], the antiproliferative activity of silver NHC compounds has also begun to be evaluated.

1.5.3 Antitumor Properties of Ag-NHC complexes

The cytotoxicity against tumor cell lines, shown by other NHC-metal complexes [65,66], encouraged Young's research group to test the anticancer activity of complexes **5** and **10** [67]. These complexes were tested against three different tumor cell lines, OVACAR-3 (ovarian), MB-157 (breast), and HeLa (cervical), and their *in vitro* efficacy was evaluated by MTT assay.

The MMT assay is used for the evaluation of cell viability. The test is based on the reduction of yellow-colored tetrazolium salt (3-(4,5-dimethylthiazol-2-yl)-2,5-diphenyltetrazolium bromide) to purple-colored formazan crystal, by living cells. The forming crystals are solubilized in Sodium dodecyl sulfate (SDS), and the absorbance of solutions is measured at the wavelength of 570nm by spectrophotometer. The number of living cells is proportional to the concentration of formazan. The reaction is shown in **Figure 24**.

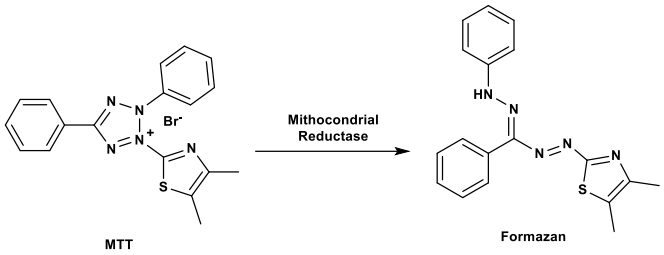

Figure 24 MTT assay reaction

It was observed that imidazolium salts were ineffective against all three tested cell lines, whereas silver NHC complexes have shown comparable activity to *cis*-platin. For the complexes were calculated by MTT assay, the Half-Maximal Inhibitor concentrations (IC_{50}). The results were reassumed in **Table 1**.

Table 1 IC_{50} of AgNHC complexes against OVACAR-3, MB157, HeLa cell lines

AgNHC complex	IC_{50}(μM)		
	OVCAR-3	**MB157**	**HeLa**
5	35	8	>200
9	30	20	>200
10	20	10	>200
cis-platin	12	25	25

The interesting results in preliminary studies by Young's silver NHC complexes had triggered an increase of interest in this research field; in fact, other groups reported the anticancer activity of new and existing silver-NHC complexes. The research group of Tacke reported the *in vitro* activity against Caki-1(renal cancer cell line), and MCF-7 cell lines. The complexes **13a, 15a, 16a, 17c** had shown IC_{50} values lower 10μM [56–60,68]. Whereas the

complexes **20, 21,** and **22** were examined the cytotoxic activity against 6 different tumorigenic cell lines(KB-oral carcinoma, HL60- promyelocytic leukemia, HL60R-resistant HL60, MCF-7-breast, MCF-7R- resistant MCF-7 and T47D- breast cancer)[69]. IC_{50} values of compounds, against MCF-7, varied from 0.03 ±0.01 μM to 0.42 ±0.01 μM. These IC_{50} values were lower than *cis*-platin (10.4±0.1μM).

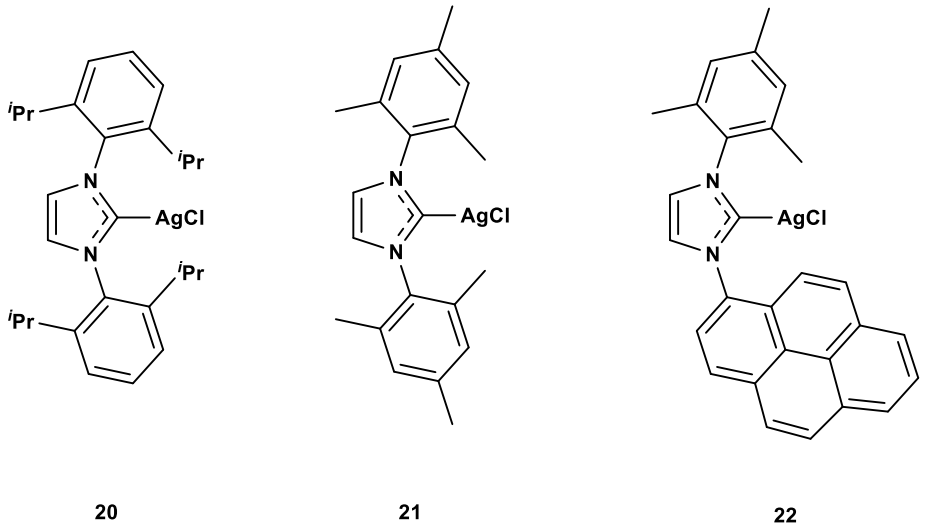

20 **21** **22**

Figure 25 N- hydrophobic substituted Silver NHC complexes tested for anticancer activity

Recently, Yasar and co-workers have reported the synthesis, characterization, and cytotoxic activity of water-soluble sulfonated NHC silver complexes[70].

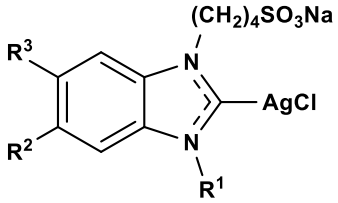

23a R^1=2-methylbenzyl, R^2=R^3=H
23b R^1=2,3,4,5,6-pentamethylbenzyl, R^2=R^3=CH_3
23c R^1=ethylmorpholine, R^2=R^3=H
23d R^1=4-*tert*-butylbenzyl, R^2=R^3=CH_3
23e R^1=3,5-dimethylbenzyl, R^2=R^3=CH_3

Figure 26 Sulphonated NHC-Ag Complexes

These complexes were tested against HeLa, HT29 (human adenocarcinoma), and L929 (mouse fibroblast) cell lines. All the complexes have shown a better cytotoxic activity (lower IC_{50} value) than *cis*-platin. Complex **23b** has shown the best antitumoral activity than the other silver complexes; these results were correlated to better σ-donating properties, that stabilize the metal center. Furthermore, the authors investigated the mechanism of action of these complexes; for all complexes DNA fragmentation was not observed, advising a different mechanism.

The discovery of the cytotoxic activity of silver NHC complexes has focused attention on its use, through an appropriate drug delivery system, for the treatment of cancer. Ag-NHC compounds were encapsulated in an appropriate polymeric system, to improve the activity. Several silver N-heterocyclic carbene complexes have been encapsulated in a diblock copolymer of poly-(lactic-co-glycol acid) and poly(ethylene glycol) (PLGA-PEG). The choice of this polymer is due to its biodegradability by hydrolysis of the ester functionalities of the PLGA portion [71,72].

As already seen, the silver NHC complexes have been largely studied as anticancer and antibacterial compounds. Furthermore, they were used as efficient carbene transfer agents for the synthesis of different metal complexes[44]. Furthermore, in recent years, they have been investigated also for the catalytic activity.

1.5.4 Catalytic Activity of Silver NHC complexes

In 2005, Fernandez and co-workers described the enantioselective diboration of styrene using a chiral NHC silver complex[73]. Unfortunately, the diol was obtained with low yield and low enantioselectivity.

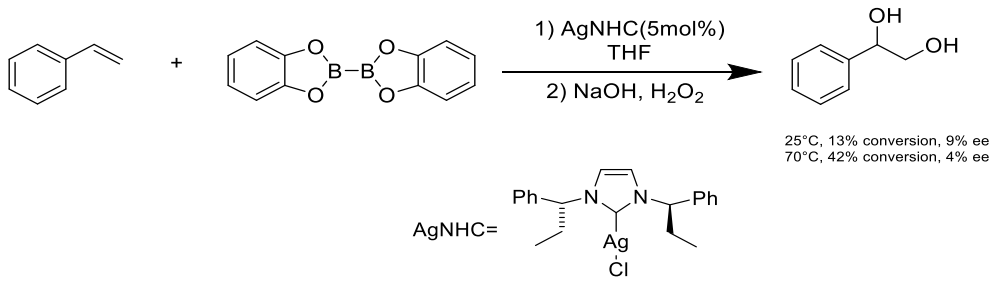

Figure 27 Hydroboration of styrene promoted by silver complex

Following the studies of Fernadez, the silver NHC complexes were tested in different reactions such as 1,3-dipolar cycloaddition of azomethine ylides with *tert*-butyl acrylate [74], in the cyclopropanation reactions among phenyldiazoacetate and styrene [75] in the Sonogashira coupling of phenylacetylene and 4-iodoacetophenone [76].

Silver salts and complexes were tested in reaction using alkyne with imine or carbonyl compounds. The resulting molecules have a plethora of applications for other transformations. The addition of alkyne moiety to an electrophilic substrate (*e.g.:* imine) is also known as the A^3-coupling reaction. It is a condensation among aldehyde, amine, and terminal alkyne, and it has been considered a convenient route to produce propargylamines[77,78].

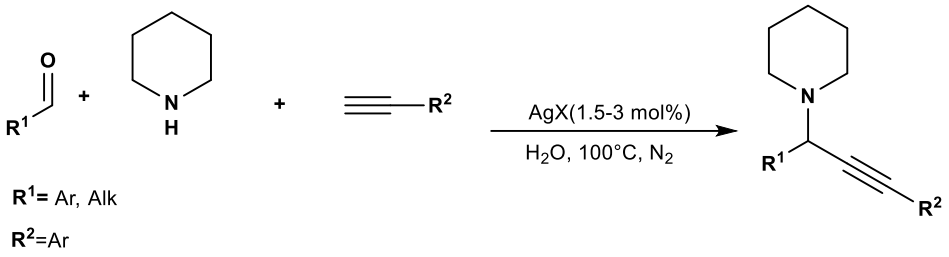

Figure 28 General reaction of A³-coupling reaction catalyzed by Ag(I) salts

In 2003, Li et al. reported the first example of an A³-coupling reaction catalyzed by silver salts[79]. In this innovative work, silver salts, such as AgI, demonstrated the ability to catalyze the addition of alkyne to secondary amine and aldehyde in water at 100°C and under nitrogen atmosphere. The suggested mechanism for obtaining propargylamine involves the formation of the silver acetylide, through the deprotonation of the alkyne, and the subsequent nucleophilic addition to the imine obtained by the reaction of an aldehyde with a secondary amine.

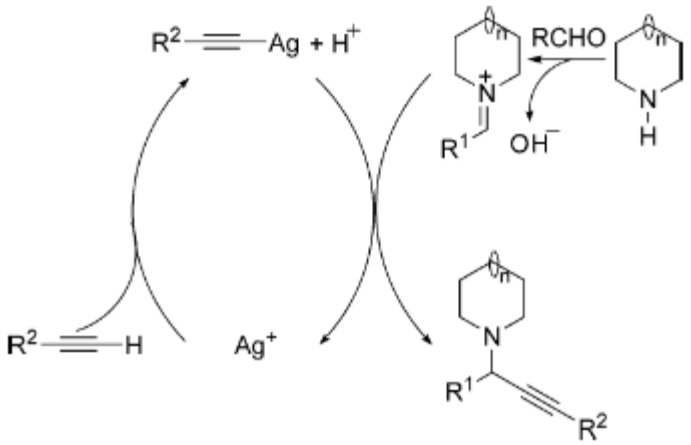

Scheme 1 Proposed mechanism for A³ coupling reaction catalyzed by Ag complexes. Reprinted with permission Wei, C.; Li, Z.; Li, C.-J. The First Silver-Catalyzed Three-Component Coupling of Aldehyde, Alkyne, and Amine. Org. Lett. ***2003****, 5, 4473–4475,*[79]*. 2003, Copyright 2003 American Chemical Society*

After Li's pioneering work, silver N-heterocyclic carbene complexes were studied as catalysts for the A³-coupling reaction. The first reported application of Ag-NHC was submitted by Wang in 2008 [80]. He reported the catalytic activity of Ag-NHC complexes supported on polystyrene, in neat conditions under nitrogen atmosphere. The catalytic system showed interesting catalytic activity with aliphatic and aromatic aldehydes and various cyclic secondary amines. In addition, the PS-NHC-Ag systems were recyclable 12 times, without a decrease in their catalytic activity.

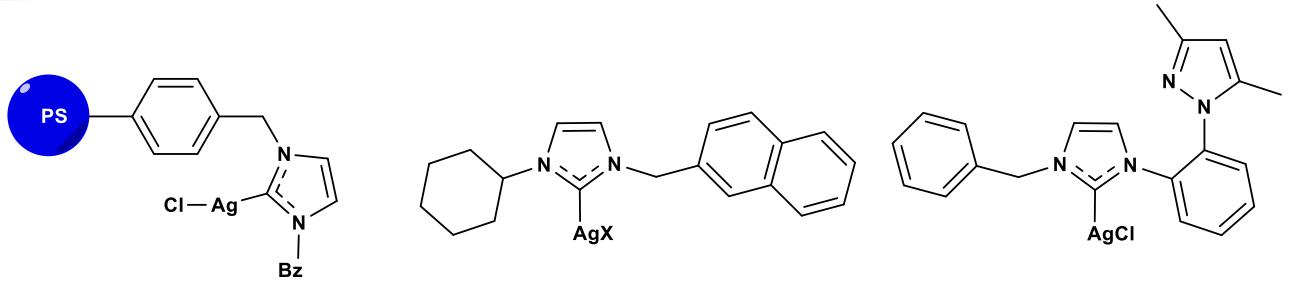

25 Wang | 26 Zou | 27 Tang

Figure 29 Many examples of AgNHC active in A³-coupling reaction

Zou reported in 2011, an interesting study on the A³-coupling reaction of 3-phenylproprionaldehyde, phenylacetylene, and piperidine in dioxane at 100°C in air[81]. It was observed that the catalytic activity of silver NHC complexes was influenced by the nature of the anion, it was observed the following trend Cl>Br>>I (The results are displayed in **Table 2, entries 1-10**).

Table 2 Catalytic Activity of complex 26 in A3 coupling reaction [a]

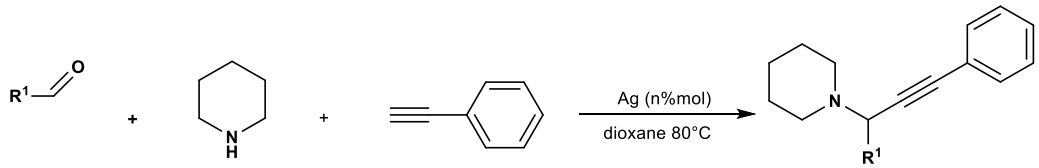

Entry	Catalyst	n	R^1	Temperature (°C)	Time (h)	Yield [b] (%)
1	26	3	$PhCH_2CH_2$	100	2	99
2	26	3	$PhCH_2CH_2$	50	12	81
3	26	3	$PhCH_2CH_2$	r.t	72	69
4	26	3	$PhCH_2CH_2$	100	12	31 [c]
5	26	3	$4\text{-}ClC_6H_4$	100	12	77
6	26	3	Piperonyl	100	12	49
7	AgCl	3	$PhCH_2CH_2$	100	2	80
8	AgBr	3	$PhCH_2CH_2$	100	2	64
9	AgI	3	$PhCH_2CH_2$	100	2	49
10	Ag_2O	3	$PhCH_2CH_2$	100	2	78
11	27	3	H	80	2	55
12	27	3	Ph	80	12	13
13	27	2	Cy	80	8	50
14	27	3	Cy	80	8	95

[a] Reaction conditions: 1 mmol aldehyde, 1.2 mmol piperidine, 1.5 mmol phenylacetylene, 3 mol % Ag catalyst, [b] Isolated yield [c]Run in water

Based on the observation of Zou's research group, Tang and collaborates synthesized new silver NHC complexes derived from 1-[2-(pyrazol-1-yl)phenyl]imidazole, that showed an interesting catalytic activity at 80°C under argon atmosphere[82] (**entries 11-14**, **Table 2**).

1.6 Gold *N*-heterocyclic carbene complexes

1.6.1 The use of gold in medicine

The pharmaceutical properties of gold were known since antiquity; the first application of gold dates back to 2500 BC by the Chinese [83,84]. The modern use of gold in medicine was approved with the demonstration of bacteriostatic properties of $K[Au(CN)_2]$ against tubercle bacillus, by Robert Koch in 1890 [85]. This discovery featured the start of chrysotherapy[86,87].

Later, different gold salts were used for the treatment of juvenile arthritis, discoid lupus erythematosus, and psoriatic arthritis, but the introduction of auranofin, for the treatment of rheumatoid arthritis, represented the start of a new era of chrysotherapy.

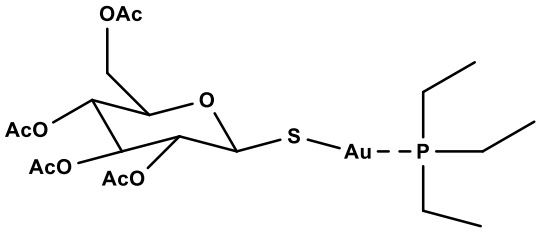

Figure 30 Structure of Auranofin

In the last decades, after the introduction of auranofin, numerous research groups began the study of gold compounds in different medicinal applications such as anticancer, antimalaria, and the treatment of HIV[88]. In this context, *N*-heterocyclic carbene gold complexes were synthesized, characterized, and tested as antibacterial and antitumor agents, as an alternative to more toxic phosphine-based complexes[89].

1.6.2 Antimicrobial Properties of Au-NHC complexes

As seen in section 1.5.2, silver compounds are largely studied for their antibacterial activity. Their application is limited due to the toxicity attributable to the interaction of silver Ag^+ ions with blood cysteine, and for the presence of chloride anion that can limit the action of these compounds. Gold NHC complexes have shown an interesting alternative due to their higher stability than silver analogs.

In 2005, Cetinkaya reported for the first time, the antibacterial activity of different NHC gold complexes, shown in **Figure 31** [90].

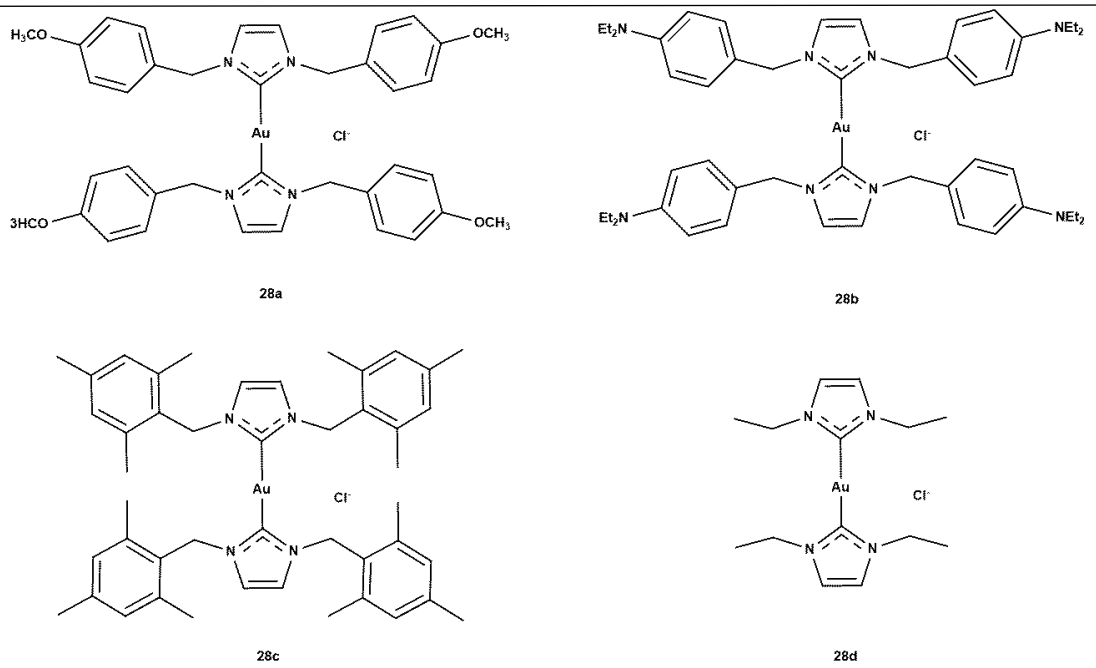

Figure 31 First AuNHC complexes tested as antibacterial compounds

The complexes were tested against Gram-positive and Gram-negative bacteria, and their activity was compared with Ampicillin, a β-lactam antibiotic belonging to the penicillin group. All compounds had shown antimicrobial activity, in particular, the complex **28a** had shown an antibacterial activity comparable to Ampicillin, as shown in **Table 3**.

Table 3 MIC of the complex 28b compared to ampicillin

Bacteria	**28a**	**28b**	**28c**	**28d**	**Ampicillin**
E. coli	1600	3.12	200	400	3.12
S. aureus	3.12	>1600	200	50	3.12
Enteroc. faecalis	3.12	>1600	>1600	>1600	1.56
P. auruginosa	3.12	>1600	>1600	>1600	25

The presence of the methoxy group in the para position of the phenyl ring, bonded to the nitrogen atom, increased the antibacterial activity. Furthermore, it was no observed antibacterial activity for the complex with N-alkyl substituents.

Later, Ghosh and collaborates tested the complex **29** (Figure 32) against B. Subtilis (Gram +) and E. coli (Gram-). It was observed the total inhibition of Gram+ bacteria. The silver analogs demonstrated a similar antibacterial activity, but the gold complex showed the best activity, presumably due to their high stability concerning sulfur-containing groups. The authors have conducted an incubation test, and they observed that the gold complex was able to inhibit the cell division (cytokinesis) of the bacteria [66].

Ozdemir's research group reported the synthesis and the antibacterial activity of a series of *N*-aryl substituted NHC gold complexes, derived from benzimidazole (**complexes 30a-c. Figure 32**)[91].

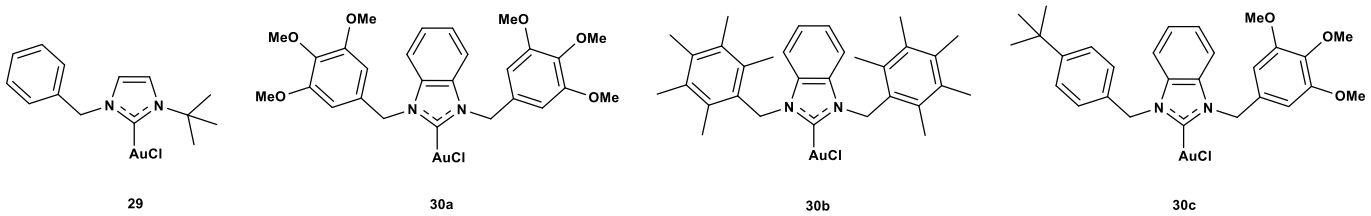

Figure 32 Neutral gold NHC complexes by Ghosh and Ozdemir

They investigated the NHCgold complexes against Gram+/- pathogens (*S. aureus, Enteroc. Faecalis, E. coli, P. aureginosa*). All the complexes were active antibacterial; furthermore, the authors underlined the importance of the steric and electronic parameters on the NHC ligand for improving the antibacterial activity.

Very recently, different NHC and caffeine-based gold complexes were prepared and tested against *Helicobacter pylori in vitro*. All the complexes have displayed an interesting antibacterial activity, particularly *tert*-butyl (**31c, 32c**) and caffeine-derivates(**33a-b**) have inhibited bacterial growth at a very low concentration (2μM). Another noteworthy observation is the lower cytotoxicity of these complexes (20.7-58.0μM) than Auranofin (3.0μM) toward HEK-293 T cells (human embryonic kidney cells)[92].

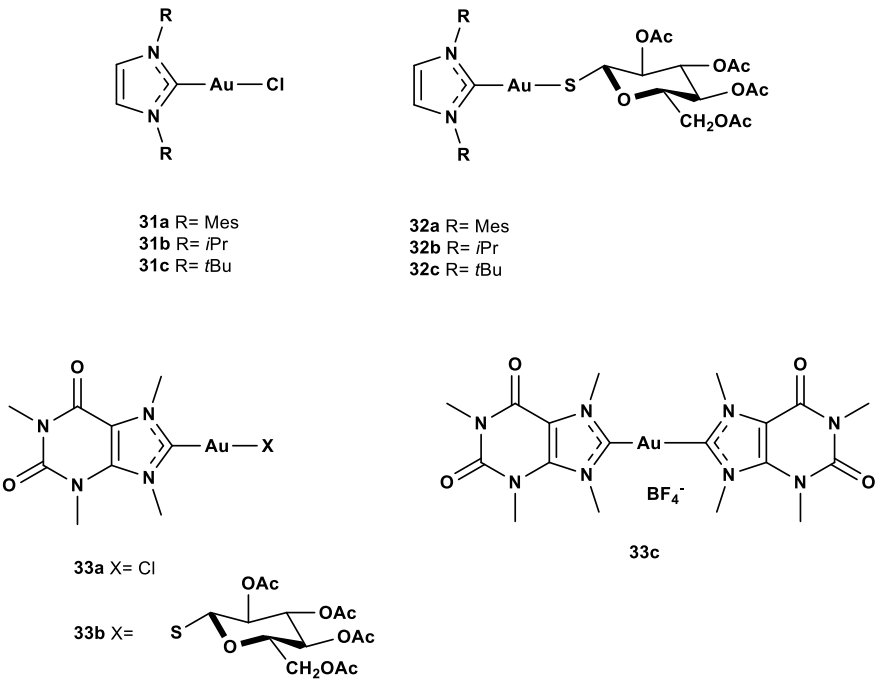

Figure 33 NHC and caffeine gold complexes with antiproliferative activity

In addition to antibacterial action on various bacterial and pathogens strains [92], Auranofin showed an interesting antitumoral activity. The discovery of cytotoxic activity by gold

compounds has brought the synthesis, characterization, and evaluation of the cytotoxic activity of many new gold NHC complexes [93].

1.6.3 Antitumoral Properties of Au-NHC complexes

Despite the discovery of many chemotherapeutic agents having cytotoxic activity such as *cis*-platin and its analogs [94], cancer and tumoral diseases are still common, and nowadays, they remain difficult to treat. The side effects (*e.g.*: nausea, nephrotoxicity, neuropathy, ototoxicity, etc.) attributable to the platinum-based compounds, have stimulated the study of new organic and metalorganic compounds as a new antitumoral agent with few side effects. Recently, the gold organometallic compounds have caught the interest.

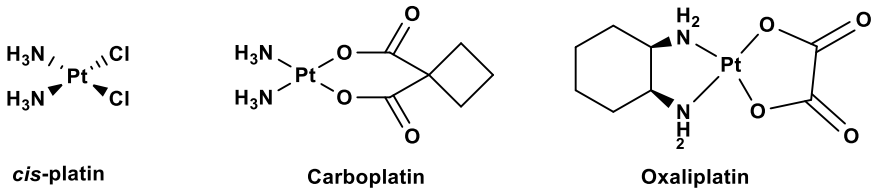

Figure 34 Platinum-based chemotherapeutic compounds

In literature are reported different gold NHC complexes with antiproliferative activity. The cytotoxic activity shown by phosphine-based gold complexes has brought the group of Berners-Price to shift attention to NHC analogs, which have similar electronic properties[63,95,96]. The first study on NHC gold complexes reported in the literature was published by Berner-Price et al.[65]. They have reported the synthesis and the antitumor activity of lipophilic gold NHC complexes (**34a-c**, **Figure 35**). These complexes have shown an interesting cytotoxic activity, against thioredoxin reductase (TrxR), a ubiquitous selenoenzyme, that plays a crucial role against the oxidative stress of cells. In a tumorigenic cell, the TrxR is over-expressed, and it has become the target of new drugs[97].

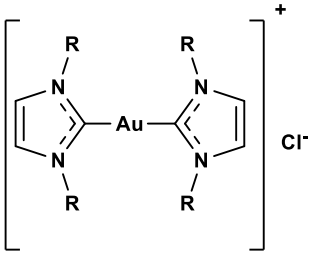

34a R=Et
34b R= ^{i}Pr
34c R= ^{n}Pr

Figure 35 Series of lipophilic NHC-Au complexes with selective antitumor activity

Furthermore, these complexes are selective cytotoxic compounds, because they induce the apotheosis of tumorigenic breast cancer cells, but not that of healthy cells[98]. The selectivity of these complexes was attributable to the binding of Au(I) metal center to selenocysteine, and subsequent substitution of the ligand.

Based on the observed selectivity of Au towards the selenocysteine site of TrxR, Messori and co-workers have reported the interaction between the synthesized C-terminal portion of TrxR, made up of twelve amino acids, and three benzimidazole-derived NHC gold complexes[99]. The mass spectrum analysis (ESI-MS) has confirmed the high strength ability of gold to selenium atoms.

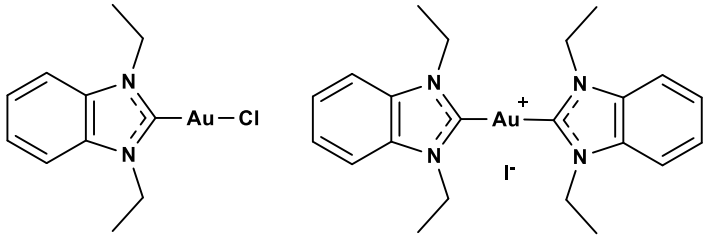

35a 35b

Figure 36 High active gold NHC complexes against selenocysteine site of TrxR

Later, Wölfl and co-workers determined the biological activity of these complexes against four cell lines of pancreatic ductal adenocarcinoma (PDAC) by MTT assay. The compound **35b** has displayed very low inhibition concentration; they ranged between 60 nM to 280 nM[100].

Isab synthesized a series of selenium-coordinated gold NHC complexes against HCT15 (colon), A549, and MCF7 tumorigenic cell lines, showing less activity than *cis*-platin. The authors have attributed the low activity to the high strength of the Au-Se bond[101].

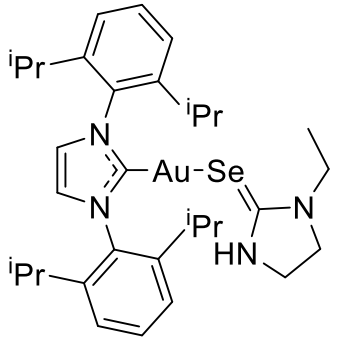

36

Figure 37 Example of Gold-NHC selenone complex

Casini et al. have reported a series of Au(I) N-heterocyclic carbene complexes derived from caffeine and tested their cytotoxicity with different cell lines. The complex **33c** displayed a better cytotoxic activity than *cis*-platin against A2780/R cell lines (ovarian) (IC_{50} 15.6 *vs* 35μM). The caffeine-based complex was not cytotoxic against the non-cancerous cells (IC_{50}>100μM)[102].

In 2017, Casini has given another important contribution to Au(I)NHC field, reporting the synthesis of a series of hydrophilic Au(I)NHC complexes, and evaluating their activity

against human ovarian cell lines. Sulphonated NHC Au(I) complexes(**37a-c, Figure 38**) were not active against human ovarian cancer cell lines, while the hydroxylated NHC gold complexes(**38a-c**, **Figure 38**) have displayed a cytotoxic activity[103].

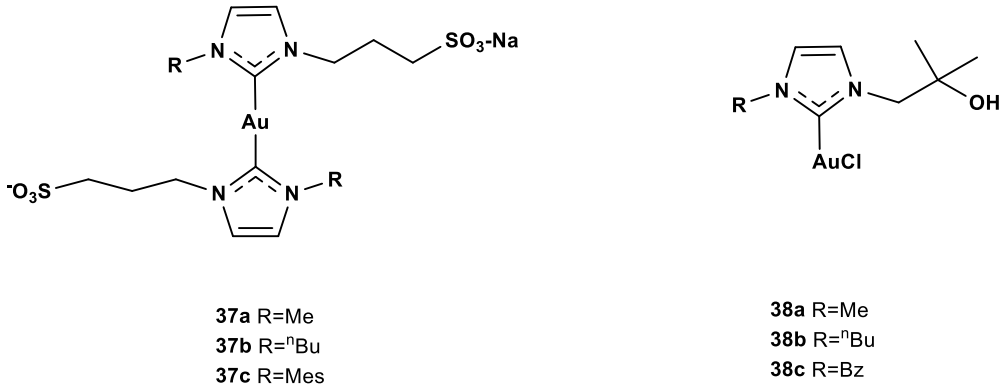

37a R=Me
37b R=^{n}Bu
37c R=Mes

38a R=Me
38b R=^{n}Bu
38c R=Bz

Figure 38 Sulphonated and Hydroxylated Gold(I) NHC complexes reported by Casini et. al

The history of humans has been strongly influenced by gold, omitting its application in currency and jewels. Gold has found applications in many different fields such as aerospace, material science, and medicine, as antibacterial and antitumoral. Despite its use since ancient times in these different fields, gold has found application in homogeneous catalysis, only in the last two decades[104–106].

The application of gold salts, such as AuCl, $AuCl_3$, and $NaAuCl_4$, has been started as a curiosity in diverse organic transformations. It was observed that gold compounds could active multiple carbon-carbon bonds, due to their π-affinity[104,105]. The primary limitation of the use of these salts was the formation of colloidal compounds, with a consequential loss of catalytic activity. Steric and electronic stabilization is required to improve the catalytic activity.

The synthesis of the first stable NHC had an important impact on organometallic chemistry, as well as in that gold chemistry. During the last twenty years, gold NHC complexes have displayed interesting catalytic properties.[107].

1.6.4 Catalytic Activity of Au-NHC complexes

The first application in homogeneous catalysis of NHC-Au(I) complexes was published by Herrman and co-workers in 2003[108]. They studied the nucleophilic addition of water to 3-hexyne, to lead the corresponding ketones, in presence of Lewis acid as $B(C_6F_5)_3$, as co-catalyst.

The reaction of hydration of alkyne is an example of an atom economy and environmentally friendly synthetic strategy. The role of the gold catalyst consists of promoting the addition of a nucleophilic molecule of water to electron-rich π-system of alkyne.

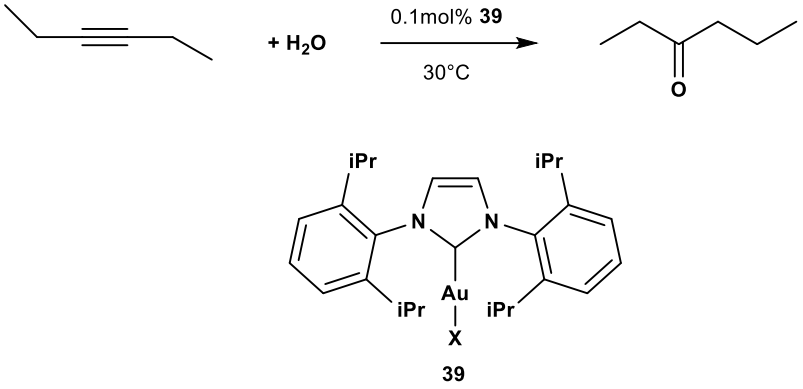

Figure 39 The first catalytic application of Au(I)NHC complex

For these reasons the hydration of alkynes catalyzed by AuNHC complexes is still largely studied [109–113]. Gatto *et al*. reported the synthesis, characterization, and evaluation of the catalytic activity of a series of gold N-heterocyclic carbene complexes with different anions, in the reaction of addition of water to 3-hexyne (**Figure 39**). By the analysis of the results, shown in **Table 4**, the complexes having OTf^-, NTf_2^- as counterion have displayed impressive catalytic activity. Complexes bearing the following counterion $BArF^-$, BF_4^-, SbF_6^-, ClO_4^-, OTs^- and TFA^- have not catalyzed the addition of water to alkyne moiety, due to poor basic properties or low coordination ability, while the complexes bearing OTf^-, NTf_2 ions have given the complete conversion in the hydration reaction of 3-hexyne. Since the obtained results, the authors of the paper proposed the catalytic pathway, illustrated in **Scheme2**, and have underlined the role of the counterion in the reaction.

Table 4 Results obtained by Gatto et. al

Run	X^-	Conversion (%)	Time (h)
1	BF_4^-	<1	24
2	SbF_6^-	<1	24
3	ClO_4^-	<1	24
4	OTf^-	>99%	16
5	NTf_2^-	>99%	16
6	OTs^-	<1	24
7	TFA^-	<1	24
8	$BArF^-$	<1	24

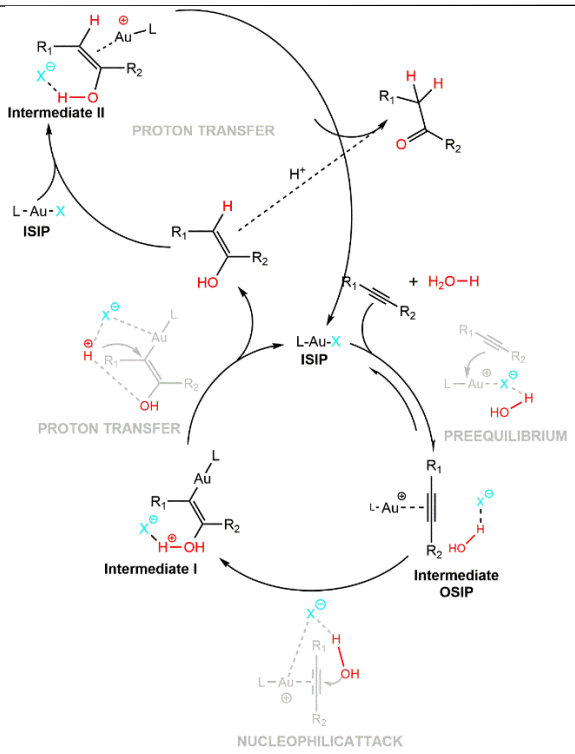

Scheme 2 The proposed mechanism by Gatto et. al. Reprinted with permission from Gatto, M.; Belanzoni, P.; Belpassi, L.; Biasiolo, L.; Del Zotto, A.; Tarantelli, F.; Zuccaccia, D. Solvent-, Silver-, and Acid-Free NHC-Au-X Catalyzed Hydration of Alkynes. The Pivotal Role of the Counterion. ACS Catal. ***2016****, 6, 7363–7376,*[110]*. Copyright 2016, American Chemical Society*

The authors proposed a mechanism in which during the nucleophilic attack, the anion plays two fundamental roles, firstly blocks the water molecule in the right position to allow the addition to the alkyne, leading to the **Intermediate I**, while the second time, it promotes the two transfers of protons, which produce the enol derivatives, and finally the ketone.

Gold *N*-heterocyclic carbene complexes catalyse also the hydroamination reaction of alkynes to produce imines or enamines. In the same manner as hydration reaction, the gold pre-catalyst must be activated by a halide scavenger, such as a silver salt [114,115].

Katari and co-workers reported a study based on density functional theory (DFT) to try to shed light on the mechanism of the hydroamination reaction of terminal alkyne [116]. In **Scheme 3**, it is reported the mechanism proposed by the authors.

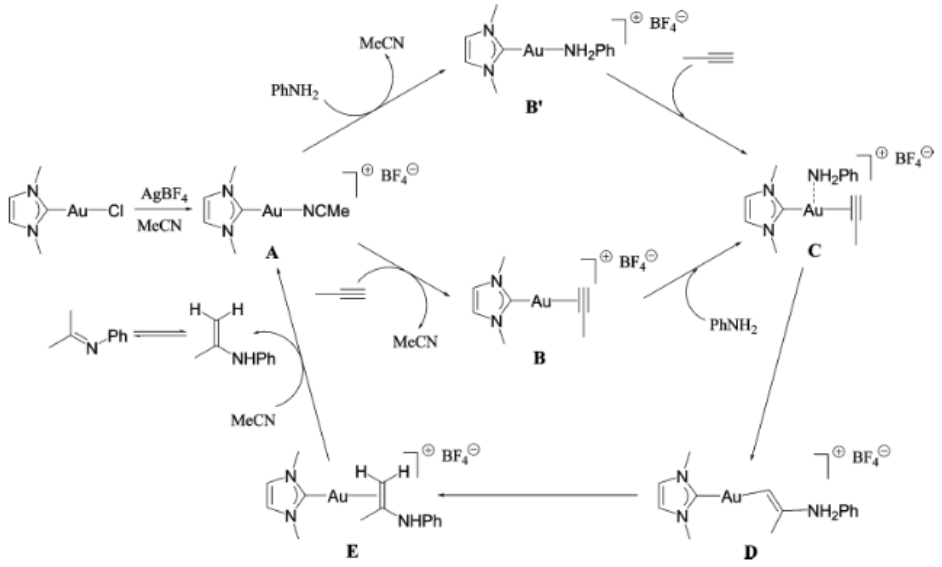

Scheme 3 The hydroamination mechanism proposed by Katari et. al. Reprinted with permission from Katari, M.; Rao, M.N.; Rajaraman, G.; Ghosh, P. Computational Insight into a Gold(I) N-Heterocyclic Carbene Mediated Alkyne Hydroamination Reaction. Inorg. Chem. ***2012****, 51, 5593–5604,* [116]. *Copyright 2012, American Chemical Society.*

In this mechanistic study, the authors used propyne ($CH_3C{\equiv}CH$) and aniline ($PhNH_2$) as representative reagents, whereas, for simplicity, the 1,3-dimethylimidazol-2-ylidene was used as the NHC ligand. As shown in Scheme 3, the hydroamination reaction takes place through activation of the pre-catalyst, by the reaction of Au(NHC)Cl and silver salt ($AgBF_4$), to lead the intermediate **A**, having a molecule of solvent (CH_3CN)coordinated. The formation of specie A was proposed because previously the formation of an analogs specie with mass spectrometry analysis (ESI) was observed [117]. The intermediate A could evolve into two different pathways, with the substitution of a solvent molecule through amine or alkyne, and the consequential formation of adduct **C**. From the energy analysis, the amine coordination pathway is 7 kcal/mol more advantageous than the alkyne one (formation of B'). The authors have attributed this difference to the π acidity of alkyne, which caused a reduction of π-back-donation and an elongation of the Au-$C_{(NHC)}$ bond. The reaction proceeds with the nucleophilic addition of an amine to the alkyne, and a possible tautomerization leads the catalytic active specie and the imine.

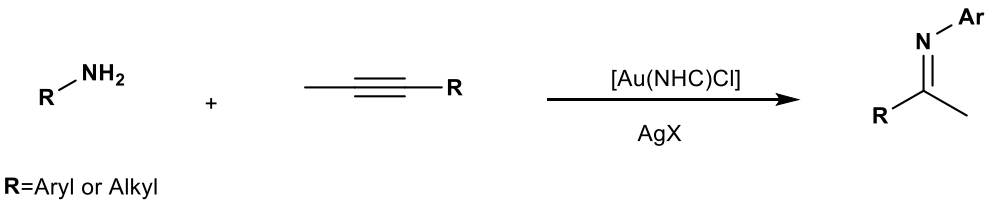

Figure 40 Example of hydroamination reaction catalyzed by AuNHC complex

Recently, Baron and co-workers have reported the catalytic activity of dinuclear gold(I) complexes with two bridged NHC ligands, of the general formula $Au_2Br_2(NHC)_2$. All the dinuclear complexes are illustrated in **Figure 41**[118].

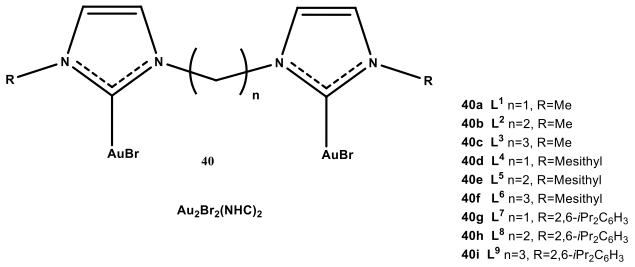

Figure 41 Dinuclear gold(I) NHC complexes of Baron

These complexes, with 2% mol of $AgSbF_6$ as cocatalyst, were tested in the hydroamination reaction of phenylacetylene with 2,4,6-trimethylaniline in neat conditions, for 4 hours. The results are reported in **Table 5**. The complexes bearing *N*-Methyl substituted NHC ligands have shown the best catalytic activity; for these catalysts, the total conversion of amine is observed. Was observed the formation of acetophenone as a by-product. The authors have attributed the formation of ketone by the hydrolysis of imine or the ability of the gold complex to catalyze the addition of the water to the alkyne.

Table 5 Results in the reaction of hydroamination of 2,4,6-trimethylaniline

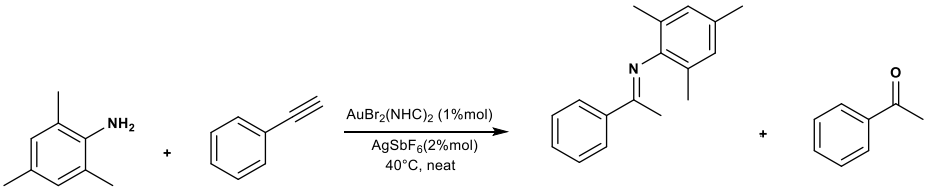

Run	$Au_2Br_2(NHC)_2$	Yield imine (%)	Yield ketone (%)
1	40a	93	7
2	40b	94	6
3	40c	94	6
4	40d	64	3
5	40e	75	9
6	40f	72	10
7	40g	73	2
8	40h	75	2
9	40i	70	6

[a]Reaction conditions: 1 mmol amine, 1 mmol phenylacetylene, 1 mol % Au catalyst, 2 mol% $AgSbF_6$, 40 °C, 4 h.

One of the first catalytic applications of gold compounds was reported by Li and co-workers [119]; they demonstrated that Au (I/III) salts were able to catalyze the A^3 coupling reaction among aldehyde, amine, and terminal alkyne, in water with low catalyst loading (1 mol%).

Furthermore, the gold complexes have displayed better yields with an aromatic aldehyde in contrast to silver catalysts[79]. The mechanism for this type of reaction was the same proposed for the silver compounds **(Scheme1),** involving the C_{alkyne}-H activation. In the same manner for silver catalysis, for many golds, *N*-heterocyclic carbene complexes were evaluated their catalytical activity in this type of reaction. Price *et. al.* reported the screening of the activities of gold NHC complexes in condensation among benzaldehyde, amine, and phenylacetylene with different solvents[120].

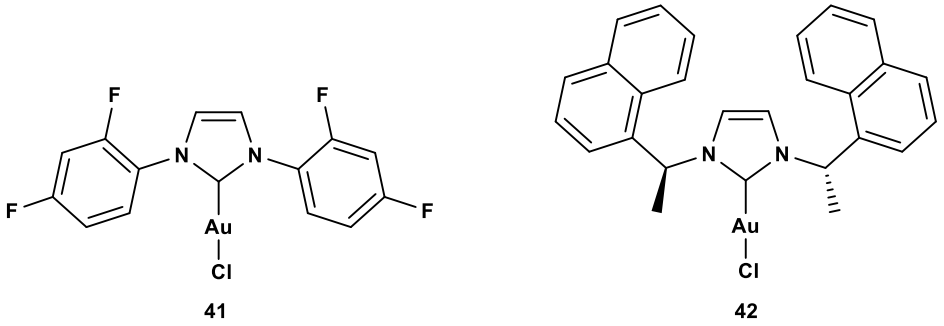

Figure 42 Gold(I)NHC screened in A³-coupling reaction by Price et.al

Table 6 Solvent and catalyst's activity in the A³ coupling reaction

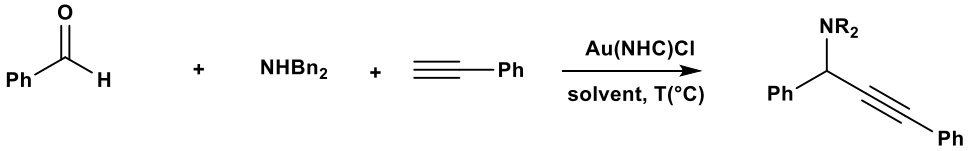

Entry	Catalyst	Solvent	T(°C)	Reaction Time(h)	Conversion (%)
1	41	H_2O	40	24	9
2	41	$CHCl_3$	60	24	65
3	41	CF_3CH_2OH	60	24	88
4	42	H_2O	40	72	10
5	42	$CHCl_3$	60	24	22
6	42	$CHCl_3$	60	72	31
7	42	$CHCl_3$	60	168	62
8	42	CF_3CH_2OH	40	24	96
9	42	CH_3OH	40	24	39

[a] Reaction conditions: 1 mmol aldehyde, 1.1 amine, 1.5 phenylacetylene, 1%mol, 2mL solvent, 24 h.
The conversions were determined by NMR analysis

For two complexes, an improvement in aldehyde conversion was observed when trifluoroethanol was used as solvent. The highest conversion in CF_3CH_2OH was attributable to its elevated polarity. That could consent to the initial formation of iminium ion and the promotion of the subsequent nucleophilic addition of gold acetylene complex. However, the authors did not observe any asymmetric induction using chiral gold complexes[121].

Chapter 2: Results and discussion

2.1 Synthesis of N-Heterocyclic carbene pro-ligands and silver and gold NHC complexes

The growing interest in the various fields of organometallic chemistry and the interesting results achieved in catalysis and pharmaceutical applications have convinced numerous research groups to be interested in the synthesis, characterization, and evaluation of chemical-physical properties of new organometallic compounds and their possible applications. Thus, during the last 30 years, N-heterocyclic carbene (NHC) ligands have caught the attention of researchers. As reported in Chapter One, the silver, and gold(I) NHC complexes have shown interesting properties in catalysis and biological applications, as both antitumoral and antibacterial compounds. For these reasons, we have synthesized, characterized by nuclear magnetic resonance (^{1}H, ^{13}C-NMR) spectroscopy and mass spectrometry imidazolium salts (NHC pro-ligands, **Figure 43**), and the respective Ag (I) and Au (I) complexes (**Figures 44-45**). The imidazolium salts and their silver and gold complexes are obtained in a racemic mixture. In this chapter, we will discuss the synthesis, the characterization of imidazolium salts, and their relative silver and gold NHC complexes.

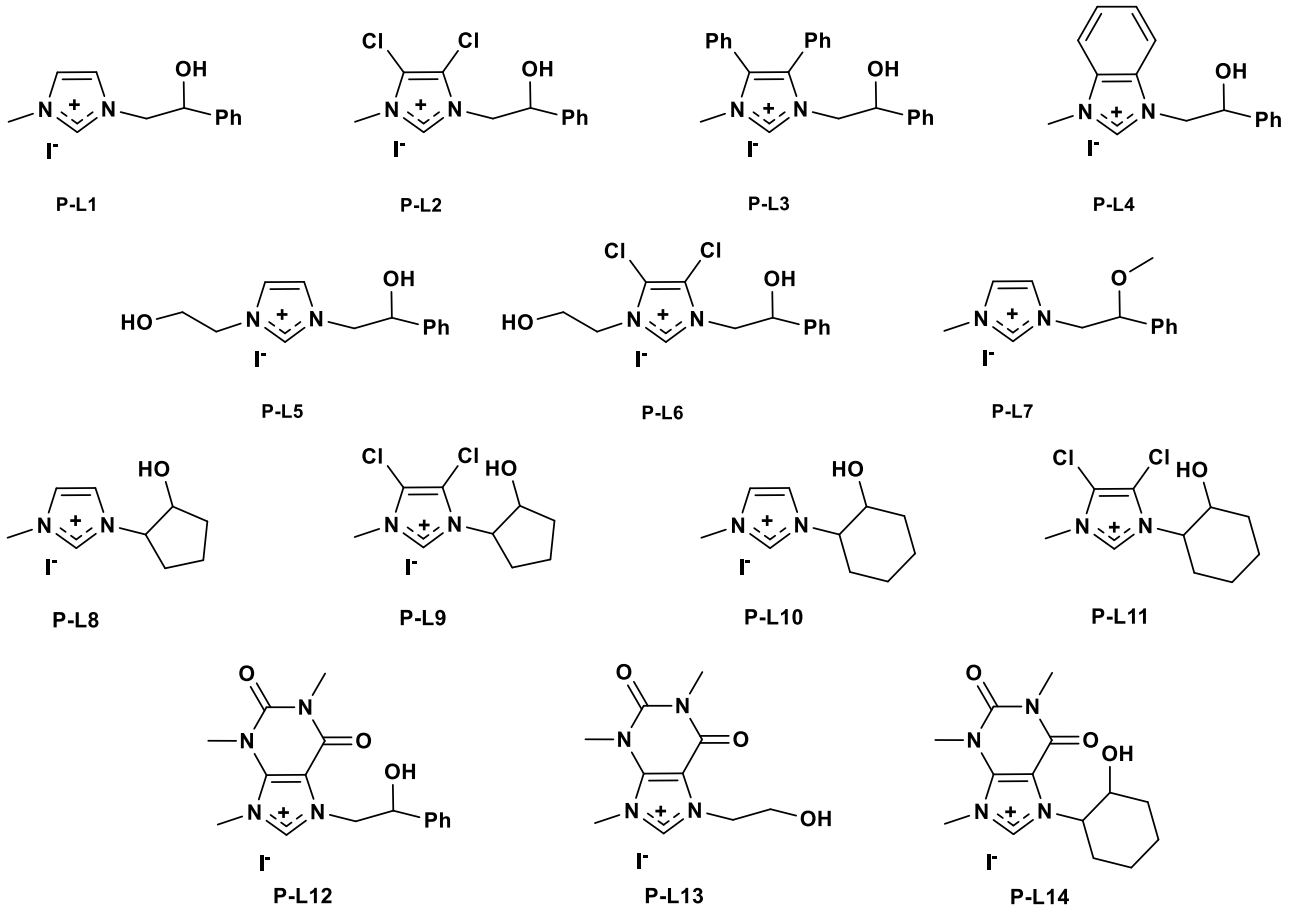

Figure 43 Structure of Imidazolium salts (NHC pro-ligands)

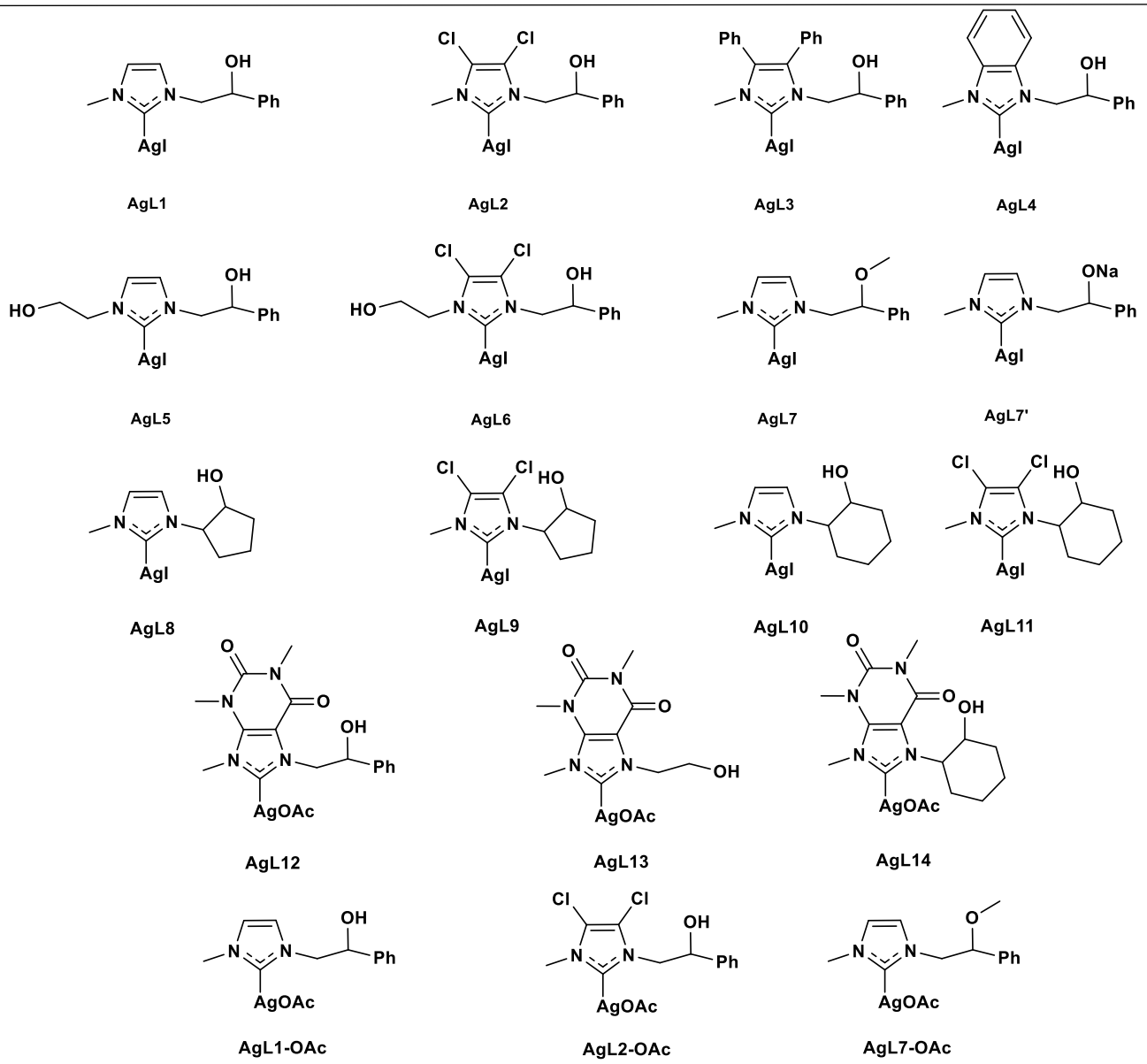

Figure 44 Structure of silver NHC complexes

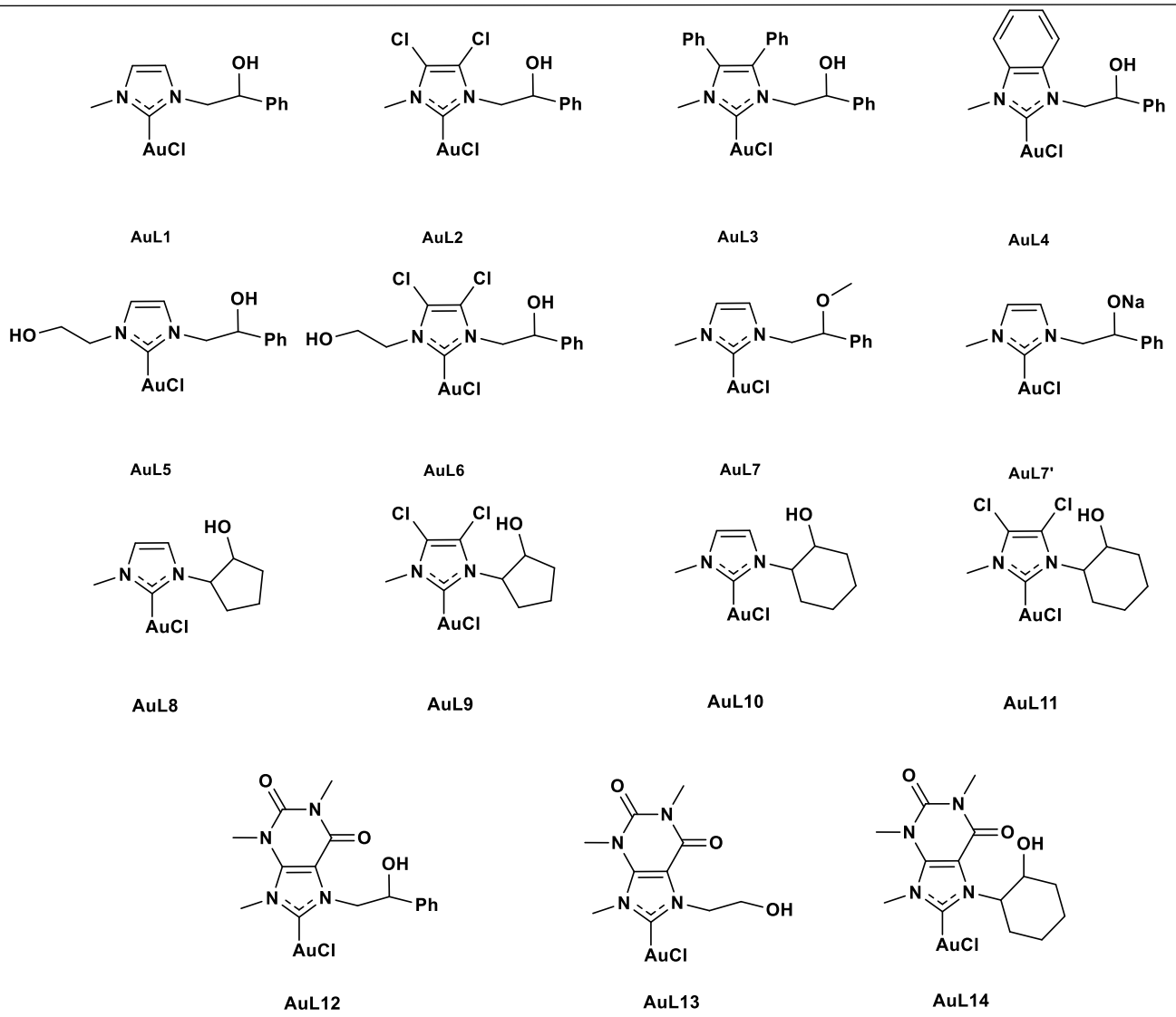

Figure 45 Structure of gold(I) NHC complexes

The success of NHCs in organometallic chemistry is attributable to several factors such as the easy modulation of steric and electronic properties with easy-to-access synthetic strategies of pro-ligand which can give metal complexes. All synthesized NHC pro-ligands, and subsequently, silver and gold complexes are characterized by different groups on two nitrogen atoms, *i.e.*: methyl, and 2-hydroxy alkyl substituents, to enhance the stability of the complexes, for catalytic purposes, and the hydrophilicity for biological applications.

2.2 Synthetic strategies for the synthesis of imidazolium salts

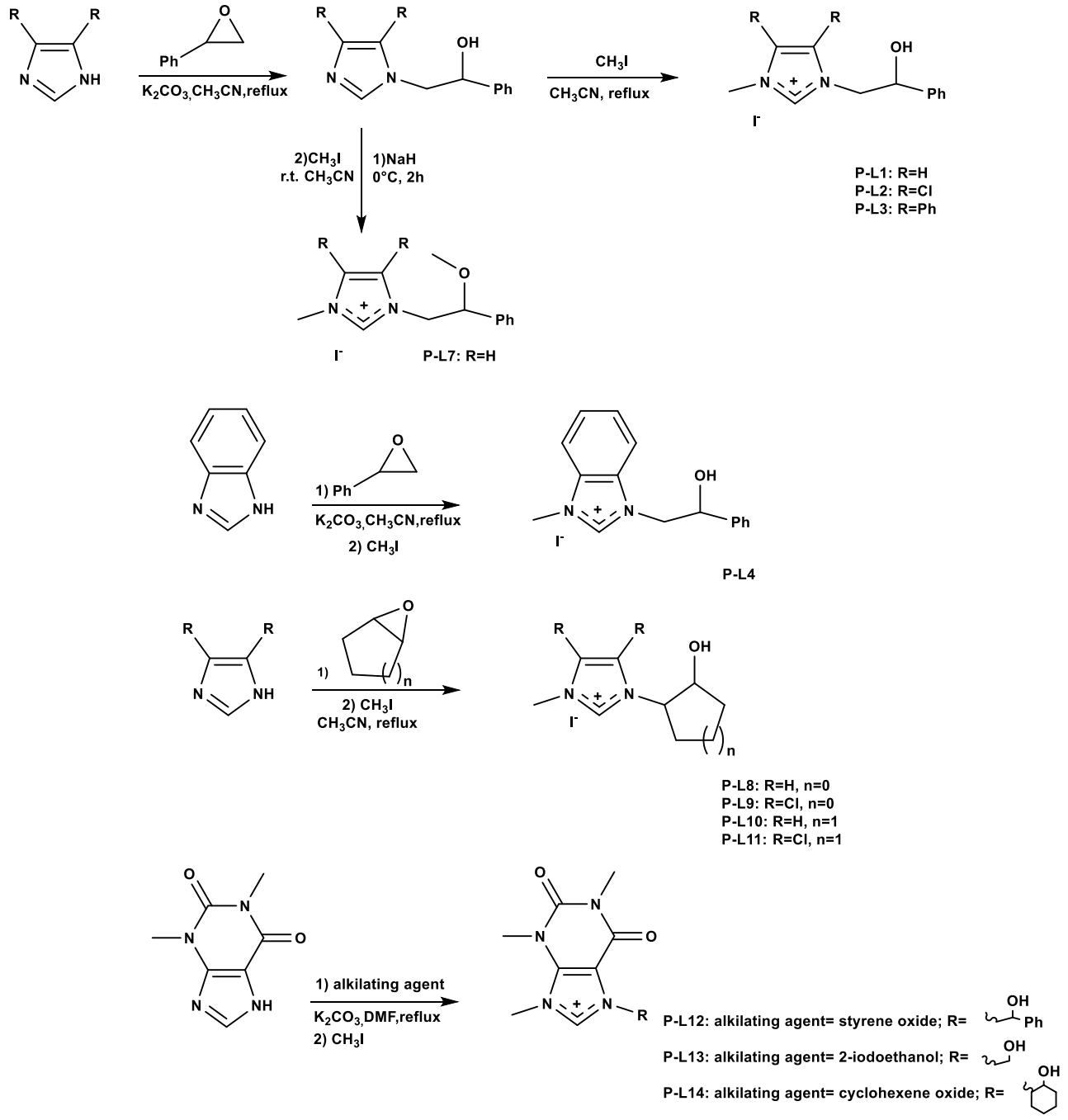

Figure 46 Synthetic strategies used to produce NHC precursors

The synthesis of pro-ligands (P-L1-14) is reported in **Figure 46**. They were synthesized following the published literature procedures [122–125] and appropriately modified by us [126–130], via the reaction of imidazole ring with epoxy alkylating reactant (styrene oxide, cyclohexene oxide, cyclopentene oxide). In this reaction, the epoxy ring was opened by the nucleophilic attack of imidazole by the nitrogen atom. The monoalkylated compound of 4,5-dichloro imidazole, 4-5 diphenyl imidazole, and benzimidazole were not isolated, and they were subsequently alkylated with iodomethane (P-L2-4) or 2-iodoethanol (P-L5, P-L6). The

pro-ligand 7 was obtained by the reaction of isolated alkylated imidazole with sodium hydride (NaH) and an excess of iodomethane, following the synthetic strategy [131] slightly modified by us [132]. All the synthesized salts were characterized by the ^{1}H-NMR, ^{13}C-NMR analysis, and mass spectrometry, and the signals were fully attributed. The formation of the NHC precursor is justified by the shift of singlet signal attributable to hydrogen (NC**H**N) to downfield, by the appearance of multiplet signals attributable to the opening of the epoxy ring. The mass spectrum of the NHC precursor have shown a peak attributable to the cationic portion of the salt.

2.2.1 Synthesis of pro-ligands P-L1, P-L2

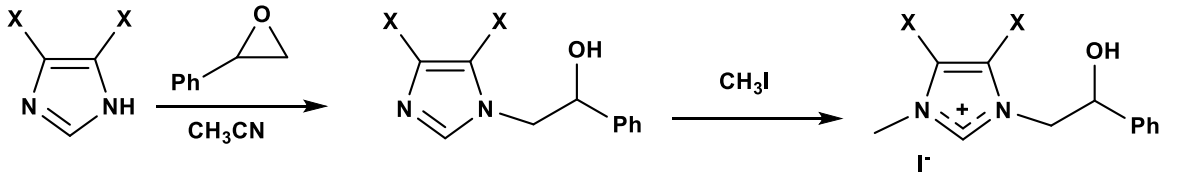

P-L1 X=H
P-L2 X=Cl

The complete characterization of complexes P-L1 and P-L2 is reported in the literature by us [128,130].

2.2.2 Synthesis of pro-ligands P-L3, P-L4

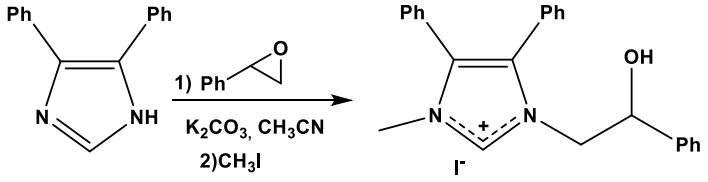

P-L3

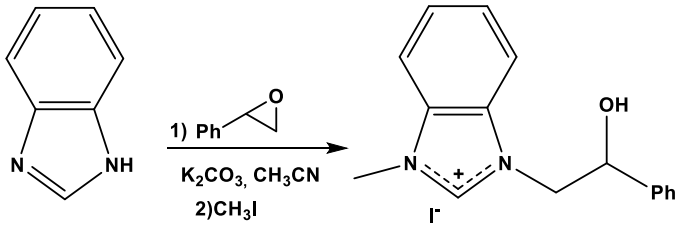

P-L4

The proligands P-L3 e P-L4 have been synthesized using the literature procedure published by Tacke and collaborators[58]. In first time, a mild base (K_2CO_3) was added to the solution of the corresponding imidazole (4,5-diphenylimidazole for P-L3, benzimidazole for P-L4) to deprotonate the sp^3-hybridized nitrogen atom of the reactant. The reaction mixture was stirred for two hours, to allow the deprotonation. Subsequently, in the reaction mixture, was added the alkylating agent (styrene oxide), and the resulting reaction mixture was stirred

for twenty-four hours. As seen in the previous section (2.1.2), the epoxy ring is opened by the nucleophilic nitrogen atom, to lead to the monoalkylated compound. Then, iodomethane was added, and the reaction mixture was stirred for a further six hours, at refluxing temperature. The imidazolium salts were recovered by filtration after precipitation in acetone. The salts were characterized by ^{1}H-NMR, ^{13}C-NMR analysis, and mass spectrometry. All the spectra show the expected signals which were assigned as reported. The acid protons of pro-ligands resonate respectively at 9.5$_0$ ppm, for P-L3 and 9.7$_7$ ppm for P-L4. The mass spectra show a single peak attributable to the carbocationic portion of the salts.

2.2.3 Characterization of P-L3, 4,5-diphenyl, *N*-methyl-*N'*-[2-hydroxy-phenyl) ethyl] imidazolium iodide

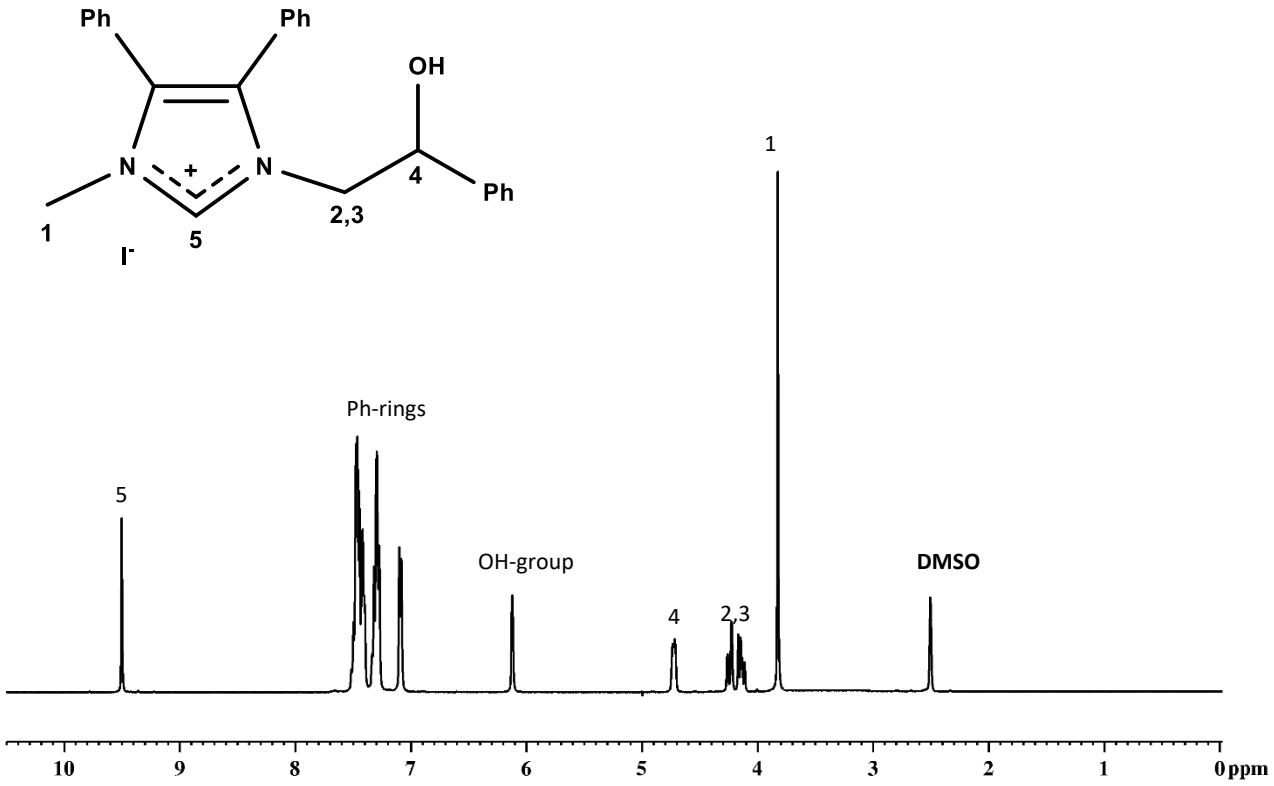

^{1}H-NMR (400MHz, DMSO-d$_6$): δ 9.5$_0$ (s, 1H, NC***H***N);7.4$_6$-7.1$_1$ (m, 15H, ***Ph rings***); 6.1$_2$(s, 1H, O***H***); 4.7$_2$(m, 1H, OC***H***); 4.2$_6$-4.1$_1$(m, 2H, NC***H***$_2$); 3.8$_4$(s,3H, NC***H***$_3$).

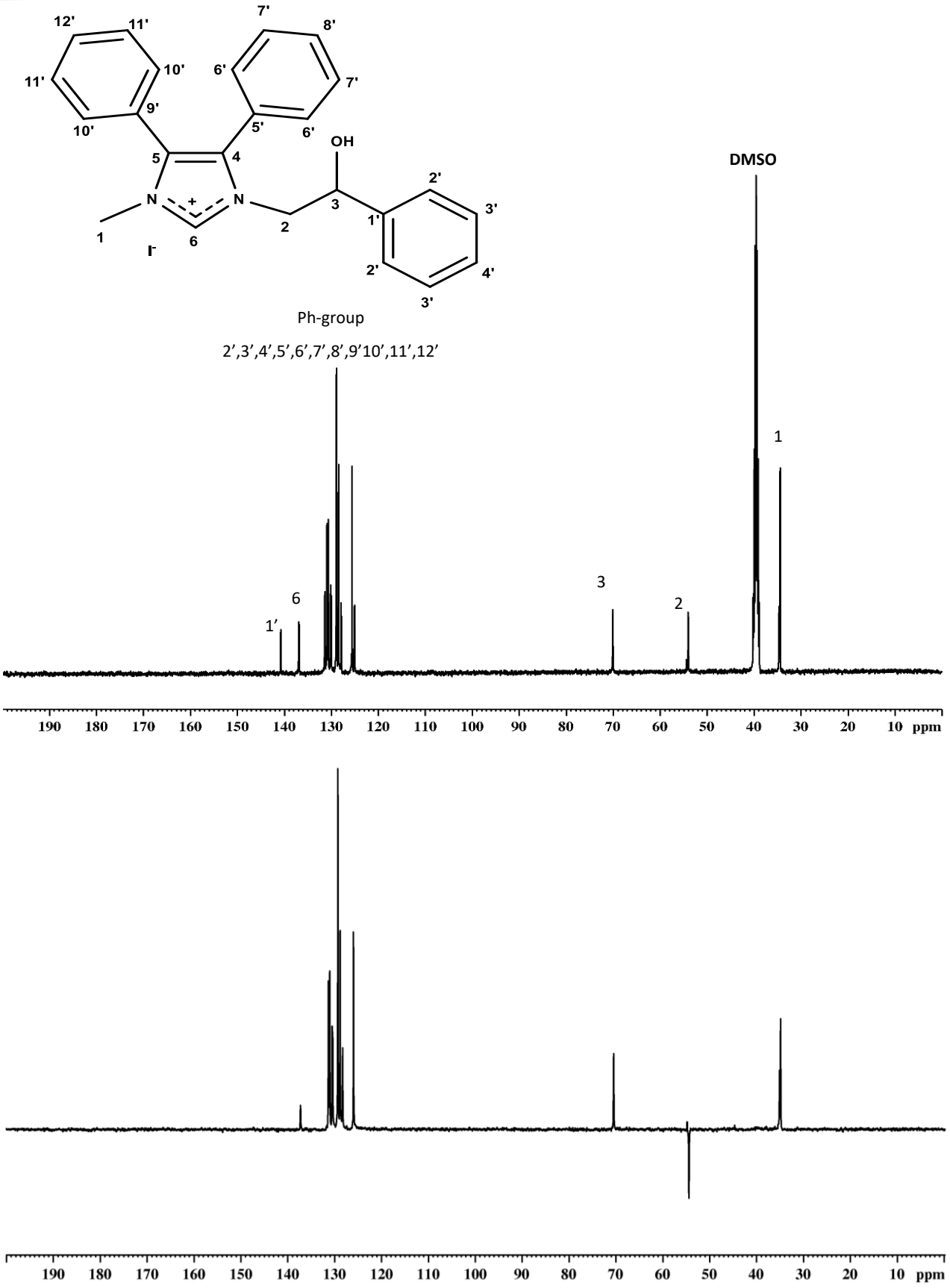
12'
11'
7'
8'
11'
10'
6'
7'
9'
10'
5'
6'
OH
5
4
2'
N
+
N
3
3'
1'
1
2
6
I-
2'
4'
3'
Ph-group
2',3',4',5',6',7',8',9'10',11',12'
DMSO
1
3
6
2
1'
190 180 170 160 150 140 130 120 110 100 90 80 70 60 50 40 30 20 10 ppm
190 180 170 160 150 140 130 120 110 100 90 80 70 60 50 40 30 20 10 ppm

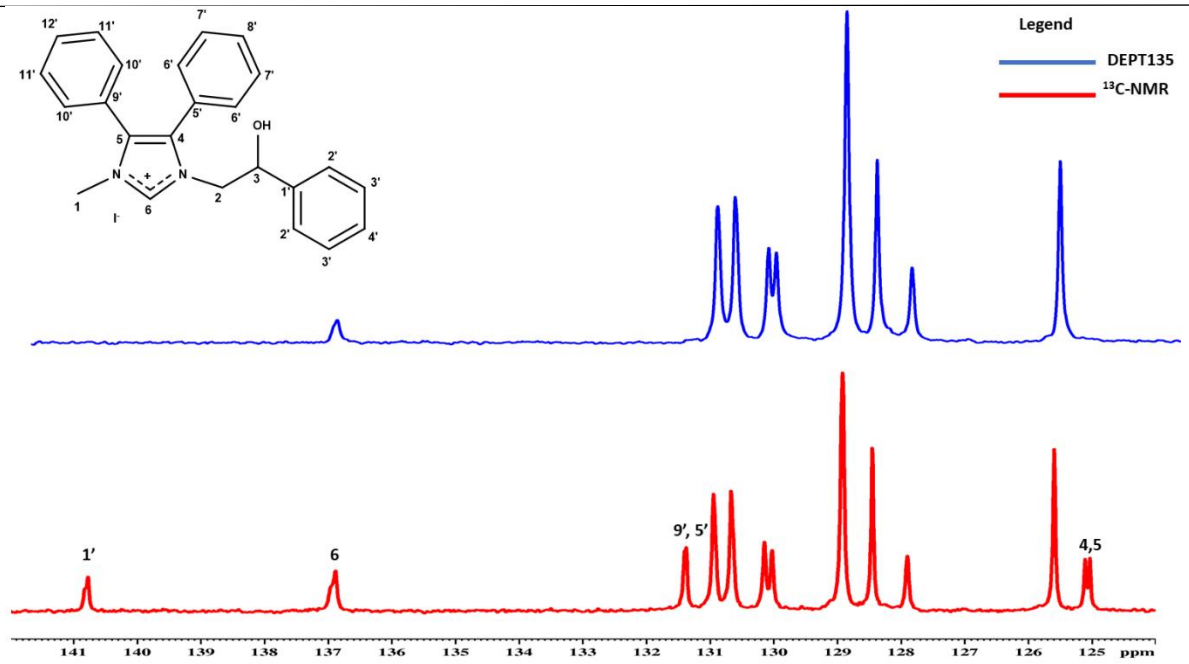

^{13}C-NMR (100 MHz, DMSO-d_6): δ 140.7$_7$ *(ipso aromatic carbon* (1'), **Ph-ring**), 136.8$_8$ (N**C**N), 131.3$_7$-125.5$_9$, (*aromatic carbons*, **Ph ring**), 125.5$_9$-125.0$_3$ (*backbone carbons*, N**C**Ph=**C**PhN),70.0$_6$(O**C**H), 54.0$_2$(N**C**H$_2$), 34.4$_7$(N**C**H$_3$)

MALDI-ToF (m/z): 355.18080 attributable to cationic portion of the imidazolium salt $[C_{24}H_{23}N_2O]^+$

2.2.4 Characterization of P-L4, *N*-methyl-*N′*-[2-(hydroxy-phenyl) ethyl] benzimidazolium iodide

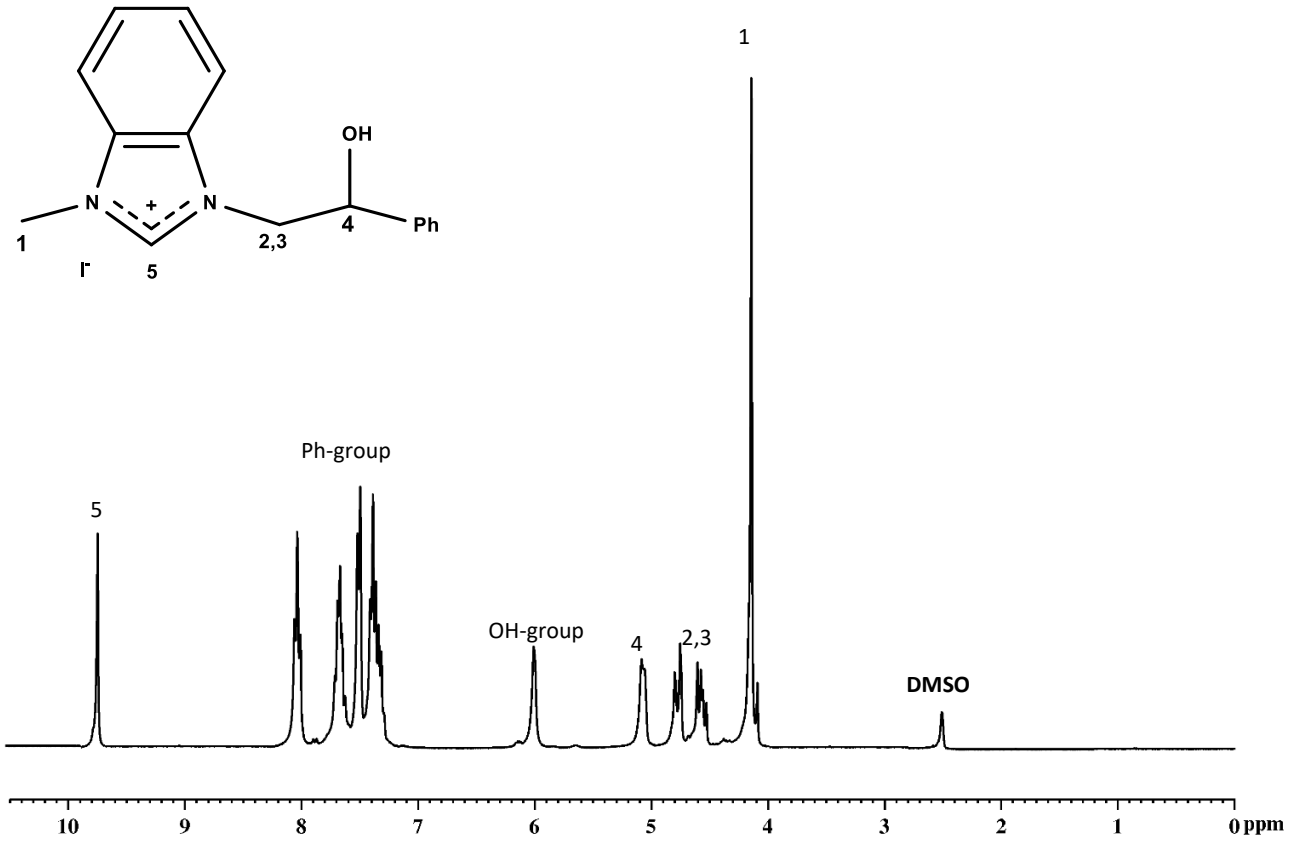

^{1}H-NMR (400MHz, DMSO-d$_6$): δ 9.7$_7$ (s, 1H, NC***H***N);8.0$_6$-7.3$_1$ (m, 9H, ***Ph ring***); 5.9$_9$(d, 1H, O***H***); 5.1$_0$-5.0$_7$ (dd, 1H, OC***H***); 4.6$_1$-4.5$_2$(m, 2H, NC***H***$_2$); 4.1$_4$(s,3H, NC***H***$_3$).

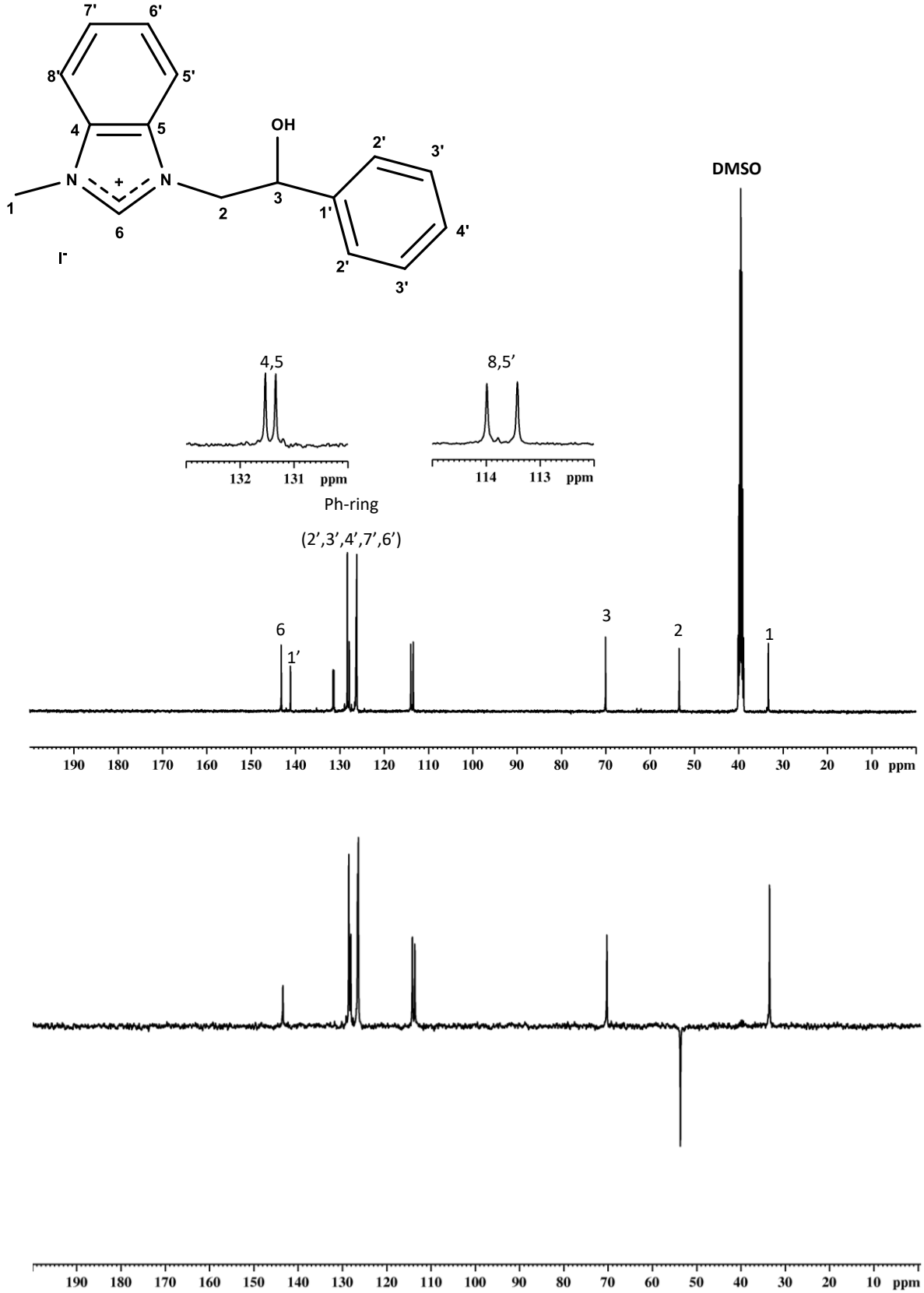

^{13}C-NMR (100 MHz, DMSO-d_6): δ 144.0$_6$ (N***C***N) 141.9$_0$ (*ipso aromatic carbon* (1'), **Ph-ring**), 131.6$_0$-131.3$_6$ (*backbone carbons*, N***C*=*C***N), 128.3$_7$-113.1$_1$, (*aromatic carbons*, **Ph rings**), 70.0$_6$(O***C***H), 54.0$_2$(N***C***H$_2$), 34.4$_7$(N***C***H$_3$)

MALDI-ToF (m/z): 253.13474 Da attributable to cationic portion of the imidazolium salt $[C_{16}H_{17}N_2O]^+$

2.2.5 Synthesis of pro-ligands P-L5, P-L6

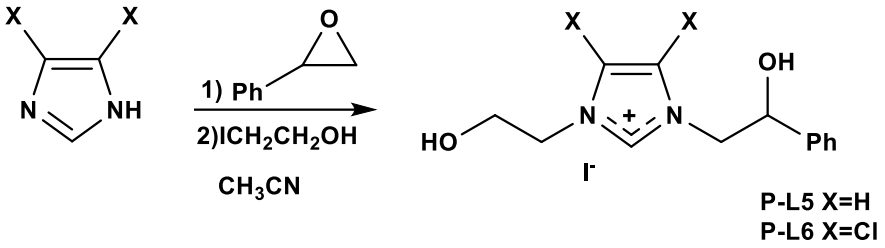

The pro-ligands P-L5 and P-L6 were synthesized according to the procedure reported in references [133,134] and modified by us [129,130,135,136]. After the first alkylation of the imidazole ring with styrene oxide, the monoalkylated product has been reacted with 2-iodoethanol for 8 hours, in acetonitrile at refluxing temperature, under an inert atmosphere. The imidazolium salts were recovered by precipitation with acetone, and they were characterized by NMR analysis and mass spectrometry. The spectra show all the expected signals. As seen above, the formation of the imidazolium salts is justified by the appearance of the down-field singlet, corresponding to the hydrogen atom bonded to the carbon atom, in the ^{1}H-NMR spectrum. The imidazolium protons resonate at 9.1_2 ppm for P-L5, while 9.5_1 ppm for the analogous ligand with chlorine atoms on its backbone (P-L6). The mass spectra show for both ligands a peak attributable to their cationic portion.

2.2.6 Characterization of P-L5, *N*-2-hydroxy ethyl-*N′*-[2-(hydroxy-phenyl) ethyl] imidazolium iodide

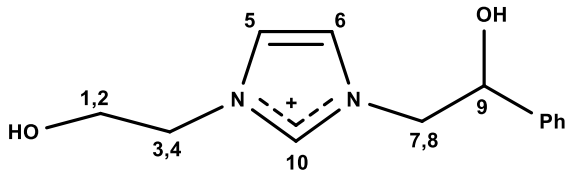

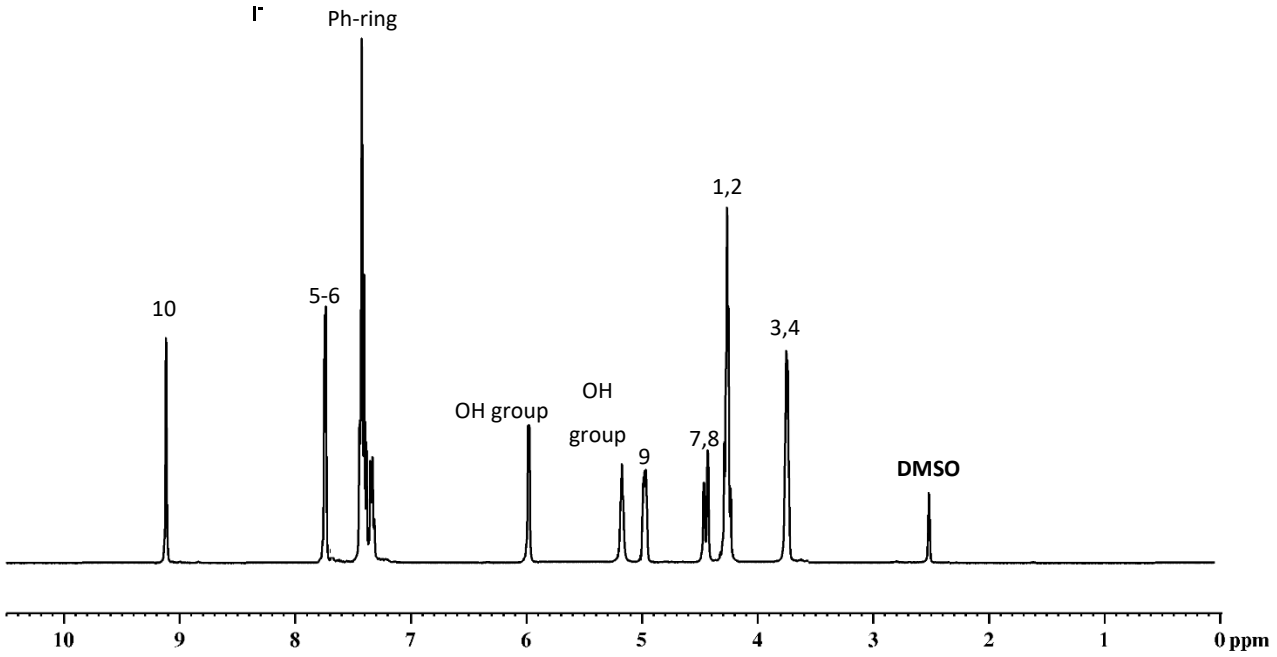

^{1}H-NMR (400MHz, DMSO-d_6): δ 9.1$_2$ (s, 1H, NC***H***N);7.7$_5$-7.3$_5$ (m, 7H, ***Ph rings***); 5.9$_9$(s, 1H, O***H***); 5.1$_7$ (s, 1H, O***H***) 4.9$_7$(m, 1H, OC***H***); 4.4$_6$-4.2$_5$(m, 4H, NC***H***$_2$CH$_2$OH, NC***H***$_2$CHOH); 3.7$_5$(s,2H, NCH$_2$C***H***$_2$OH).

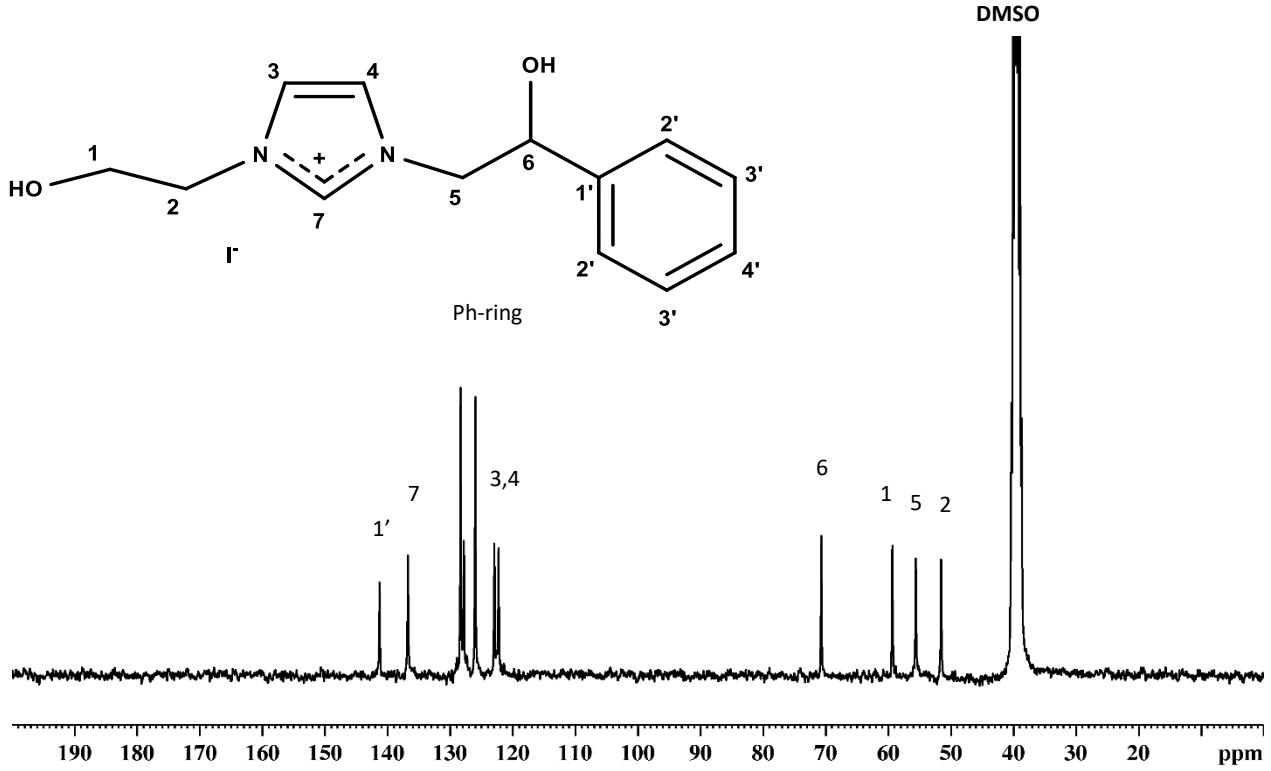

^{13}C-NMR (100 MHz, DMSO-d_6): δ 141.28 (*ipso* carbon of ***Ph ring***), 136.75 (N***C***HN), 128.34, 127.82, 125.99 (aromatic carbon, ***Ph ring***), 122.95, 122.28 (backbone carbons), 70.70 (***C***HOH), 59.36 (***C***H_2OH), 55.60 (N***C***H_2CHOH), 51.56 (N***C***H_2CH_2OH).

MALDI-ToF (m/z): 233.12898 attributable to cationic portion of the imidazolium salt $[C_{13}H_{17}N_2O_2]^+$

2.2.7 Characterization of P-L6, 4,5-dichloro-*N*-2-hydroxy ethyl-*N′*-[2-(hydroxy-phenyl) ethyl] imidazolium iodide

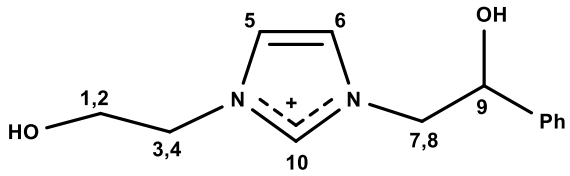

I^-

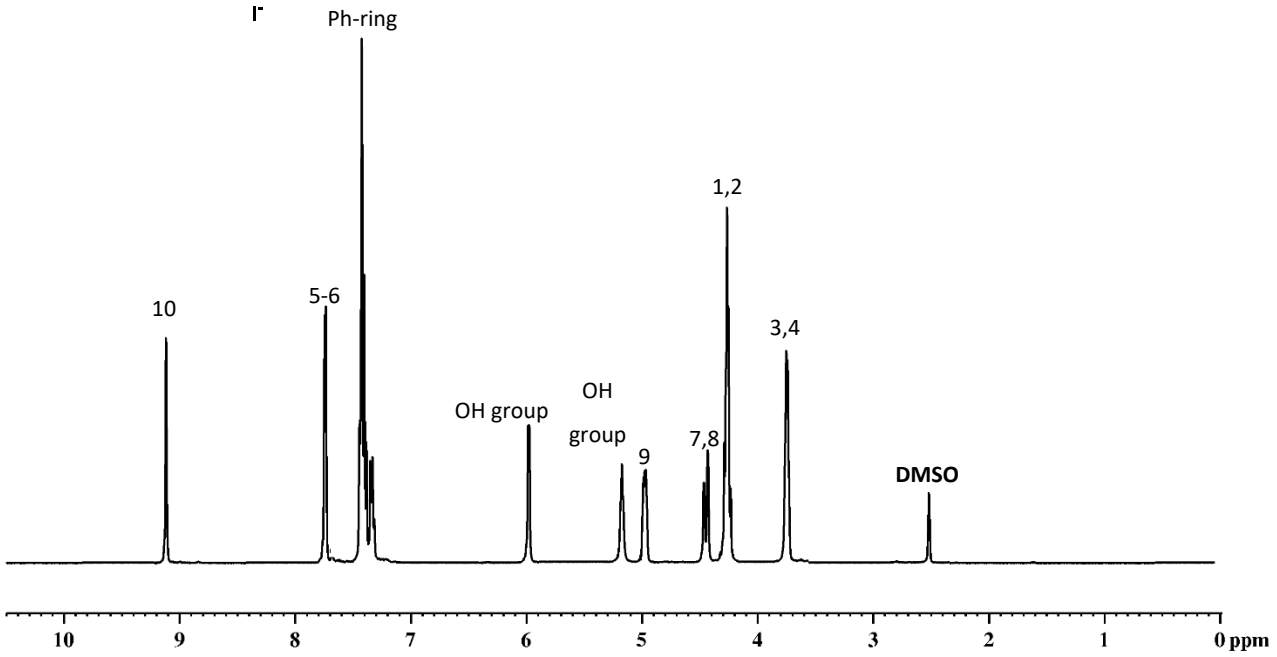

^{1}H-NMR (400MHz, DMSO-d_6): δ 9.5$_1$ (s, 1H, NC***H***N);7.4$_0$-7.3$_3$ (m, 5H, ***Ph rings***); 6.0$_5$(s, 1H, O***H***); 5.1$_8$ (s, 1H, O***H***) 4.9$_9$(m, 1H, OC***H***); 4.4$_9$-4.3$_4$(m, 4H, NC***H***$_2$CH$_2$OH, NC***H***$_2$CHOH); 3.7$_7$(s,2H, NCH$_2$C***H***$_2$OH).

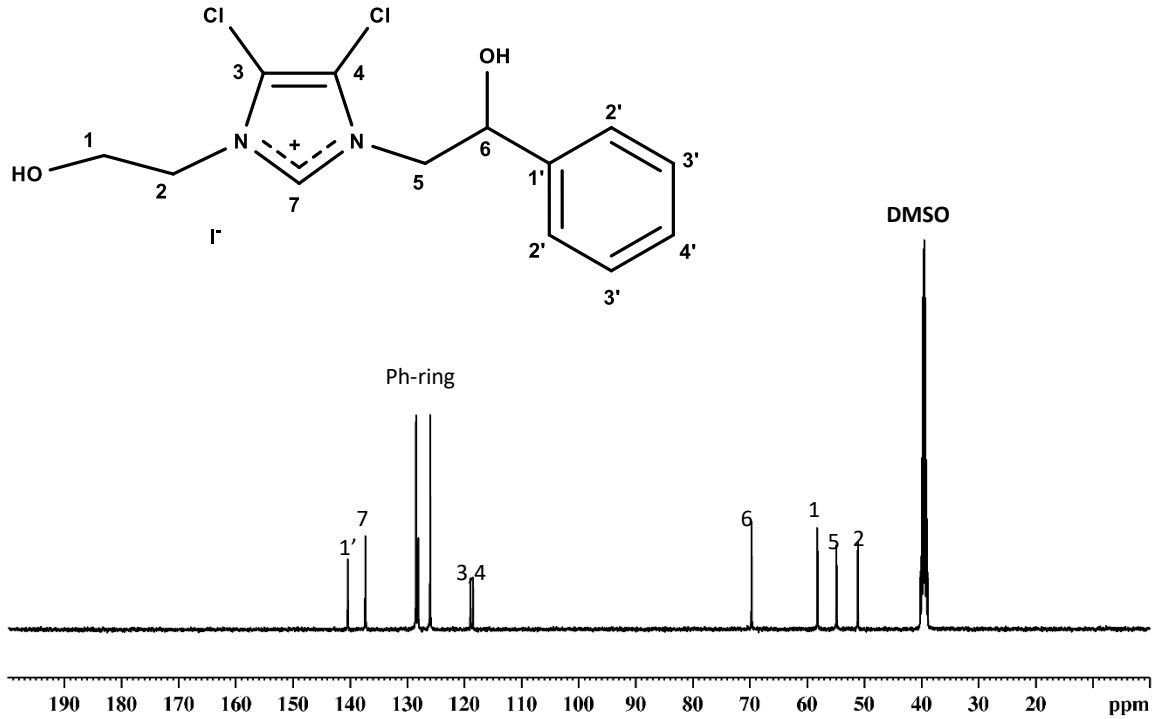

^{13}C-NMR (100 MHz, DMSO-d$_6$): δ 140.4$_4$ (*ipso* carbon of ***Ph ring***), 137.3$_9$ (N***C***HN), 128.4$_4$, 128.1$_0$, 125.9$_6$ (aromatic carbon, ***Ph ring***), 118.9$_1$, 118.4$_7$ (backbone carbons), 69.8$_0$ (***C***HOH), 58.1$_8$ (***C***H$_2$OH), 54.8$_5$ (N***C***H$_2$CHOH), 51.0$_6$ (N***C***H$_2$CH$_2$OH).

MALDI-ToF (m/z): 301.05142 Da attributable to cationic portion of the imidazolium salt $[C_{13}H_{15}Cl_2N_2O_2]^+$

2.2.8 Synthesis of pro-ligands P-L7

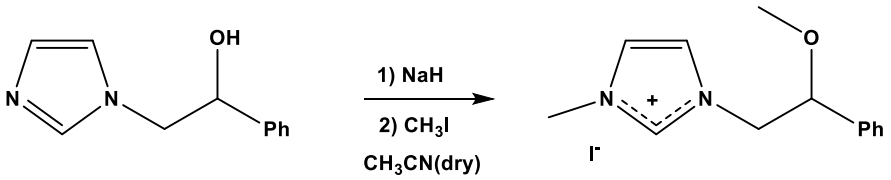

The NHC precursor P-L7 was obtained following the literature procedure [131] modified by us [132]. The mono alkylated imidazole was stirred, under a nitrogen atmosphere, with sodium hydride (NaH) in dry acetonitrile. The reaction mixture was stirred for 2 hours at 4°C. Later, an excess of iodomethane (CH_3I) was added to alkylate either nitrogen and oxygen atoms. The resulting mixture was stirred for 24h at room temperature, then filtered to obtain the imidazolium salt. The presence of the singlet signal at 9.09 ppm attributable to the acid hydrogen and the appearance of the signal attributable to protons of the methyl group on oxygen atom at 3.13 ppm, confirmed the formation of the pro-ligand. Furthermore, the mass spectrum of the salt shows a peak attributable to the positive portion of the salt.

2.2.12 Characterization of P-L7, *N*-2-hydroxy ethyl-*N'*-[2-(methoxy-phenyl) ethyl] imidazolium iodide

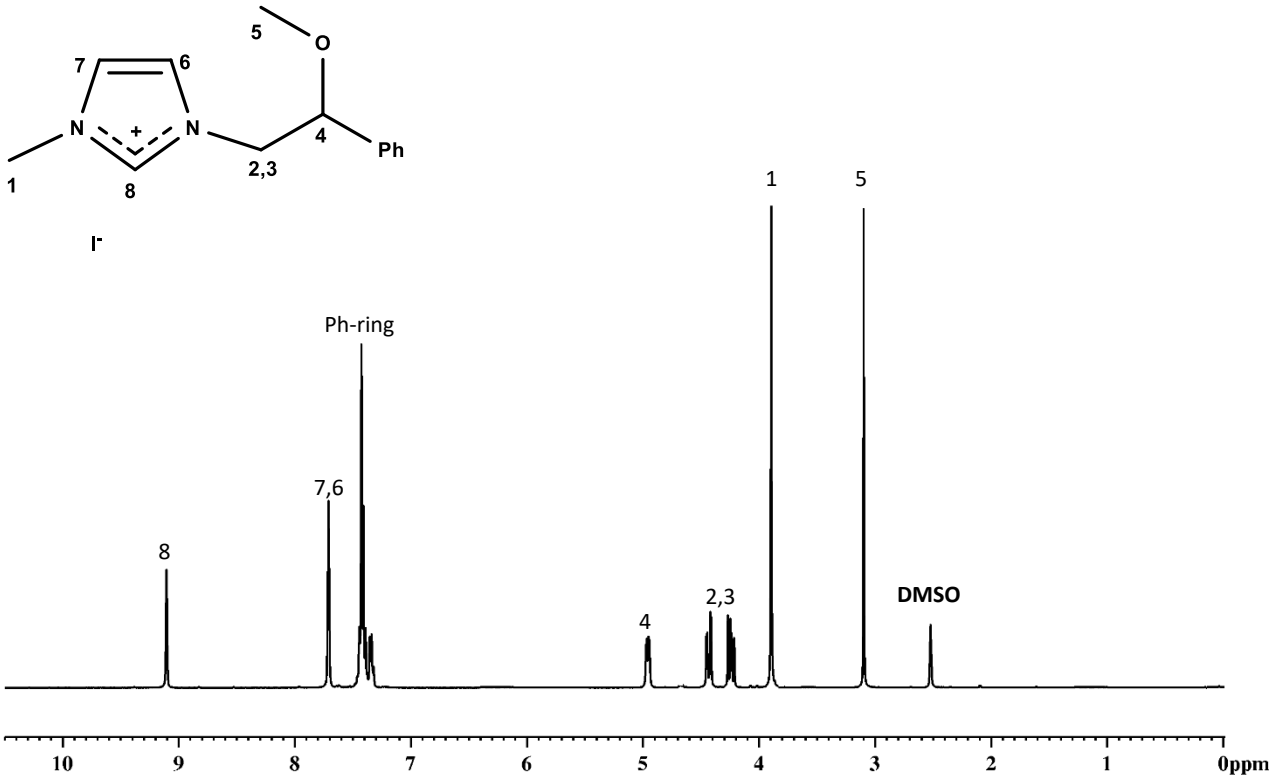

^{1}H-NMR (400MHz, DMSO-d_6): δ 9.09 (s, 1H, NC***H***N);7.70 (s, 2H, NC***H***C***H***N) 7.44-7.37 (m, 5H, ***Ph rings***); 4.65 (m, 1H, OC***H***); 4.45-4.21(m, 2H, NC***H***$_2$); 3.88(s,3H, NC***H***$_3$) 3.13 (s, 3H, OC**H**$_3$).

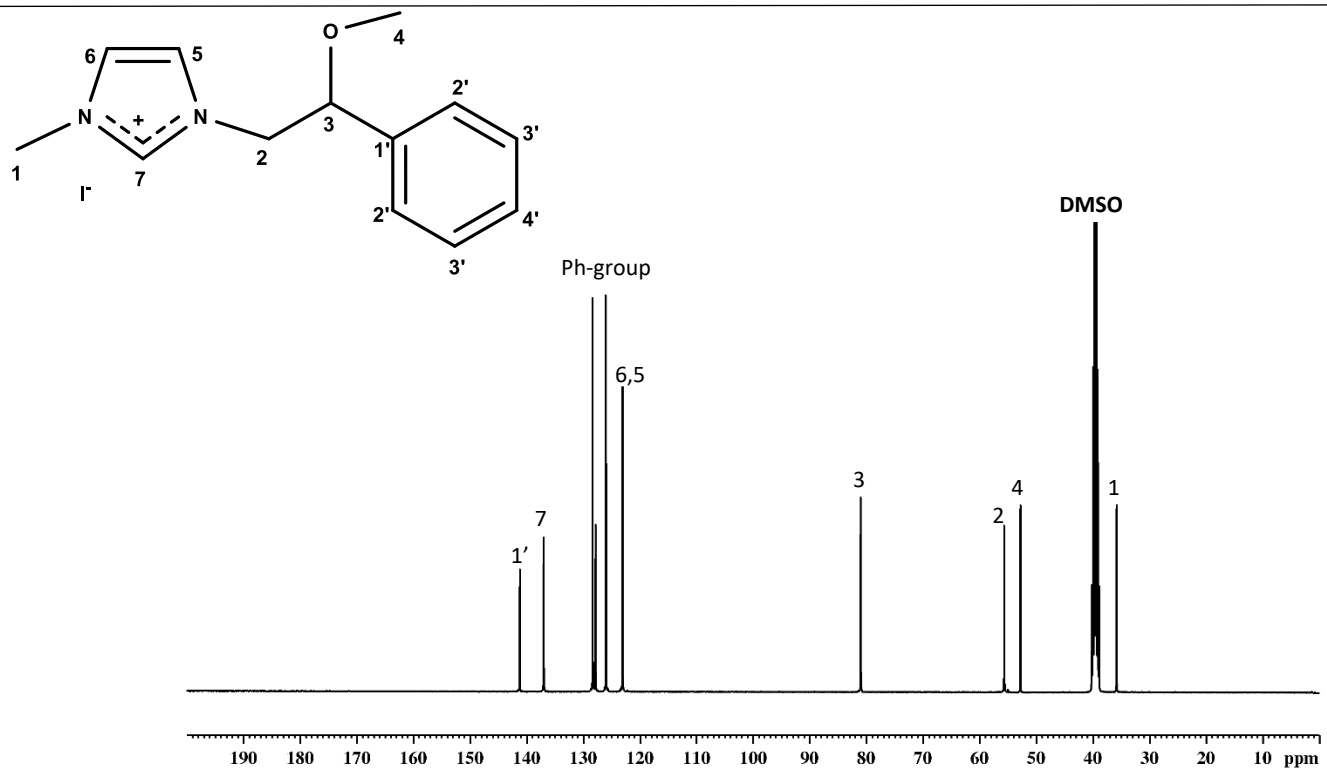

^{13}C-NMR (100 MHz, DMSO-d_6): δ 137.3$_2$ (*ipso aromatic carbon*, **Ph-ring**), 136.9$_4$ (N***C***N), 128.7$_2$, 128.6$_4$, 126.8$_1$ (*aromatic carbons*, **Ph ring**), 123.3$_3$(*backbone carbons*, N***C***H=***C***HN),80.4$_6$(O***C***H), 56.4$_6$(N***C***H$_2$), 54.0$_6$(N***C***H$_3$), 35.9$_7$(N***C***H$_3$)

MALDI-ToF (m/z): 217.1342 Da attributable to cationic portion of the imidazolium salt $[C_{13}H_{17}N_2O]^+$

2.2.9 Synthesis of pro-ligands P-L8, P-L9, P-L10, P-L11

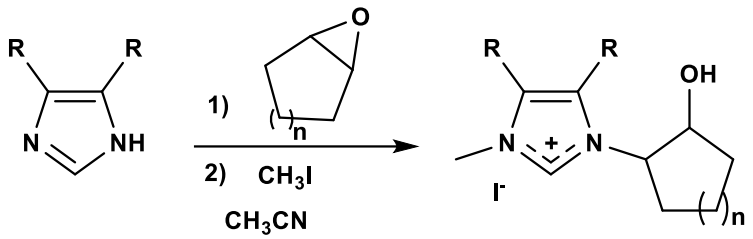

P-L8: R=H, n=0
P-L9: R=Cl, n=0
P-L10: R=H, n=1
P-L11: R=Cl, n=1

P-L8-11 are synthesized following the published procedure [126,129], using cyclopentene oxide or cyclohexene oxide as the alkylating agent. The formation of the imidazolium salt is supported by the NMR spectroscopy analysis and mass spectrometry. In the ^{1}H-NMR spectrum, the appearance of signals attributable to the opening of the epoxy ring supports the formation of the pro-ligand. The complete characterization of P-L8, P-L9, and P-L10 is reported in the literature[126,129], while in the next section, we have reported the characterization of P-L11.

2.2.10 Characterization of P-L11, 4,5-dichloro *N*-methyl-*N'*-[cyclohexan-2-ol] imidazolium iodide

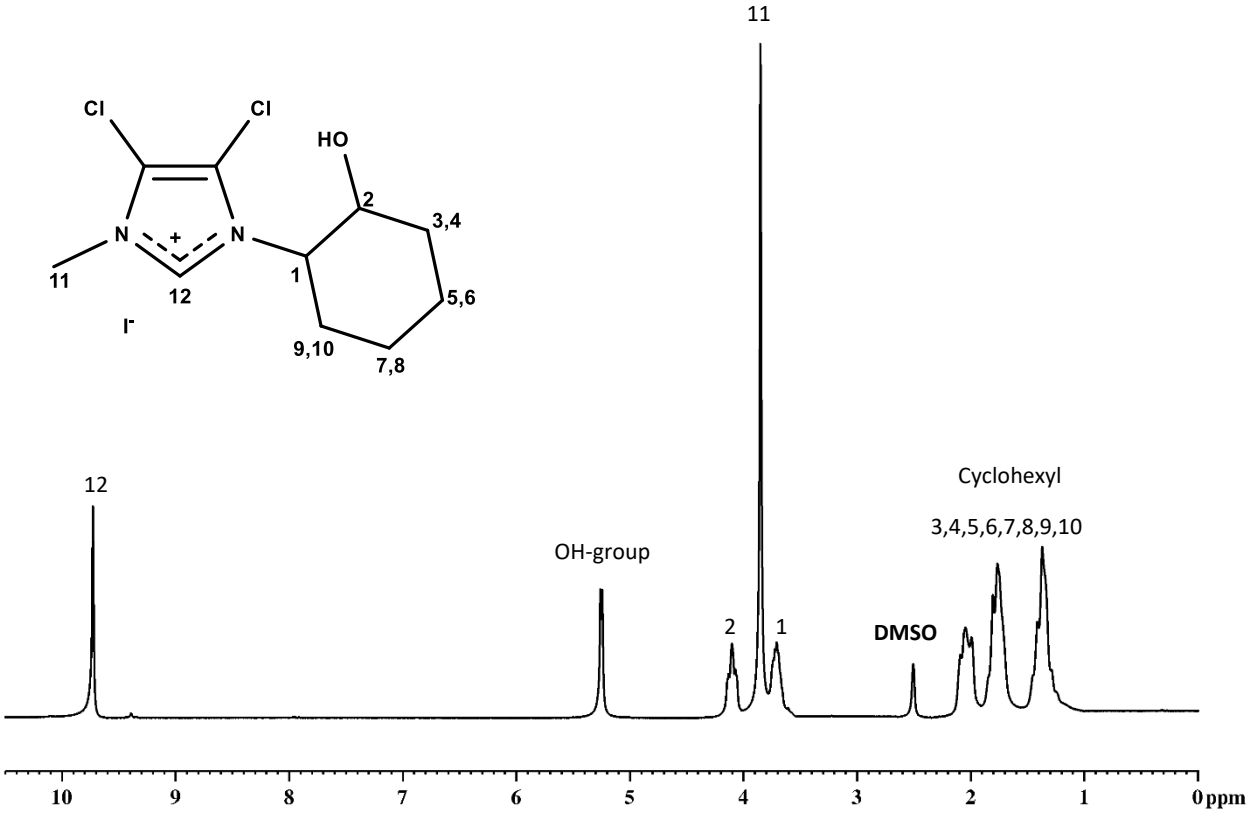

^{1}H-NMR (400MHz, DMSO-d$_6$): δ 9.7$_2$ (s, 1H, NC***H***N); 5.2$_5$ (m, 1H, O***H***); 4.1$_2$-4.0$_7$(m, 1H, OC***H***); 3.8$_4$(s,3H, NC***H***$_3$) 3.7$_4$-3.7$_0$ (m, 1H, NC***H***); 2.0$_8$ 1.3$_6$(s, 8H, Cyclohexyl).

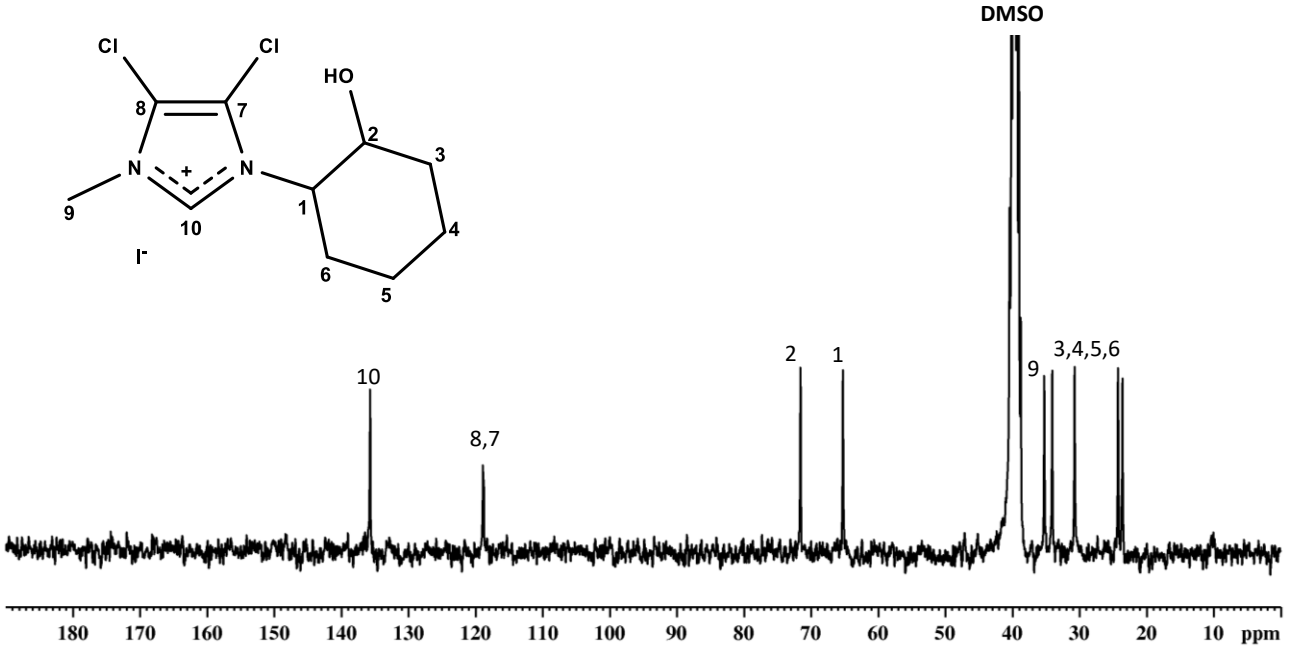

^{13}C-NMR (100 MHz, DMSO-d_6): δ 135.6$_7$ (N***C***N), 118.8$_6$(*backbone carbons*, N***C***Cl=***C***ClN),71.5$_3$(O***C***H), 65.2$_0$(N***C***H), 35.2$_0$(N***C***H$_3$), 34.0$_2$-23.5$_5$(Cyclohexyl group)

MALDI-ToF (m/z): 249.05614 Da attributable to the cationic portion of the imidazolium salt $[C_{10}H_{15}Cl_2N_2O]^+$

2.2.11 Synthesis of caffeine-based imidazolium salts P-L12, P-L13, P-L14

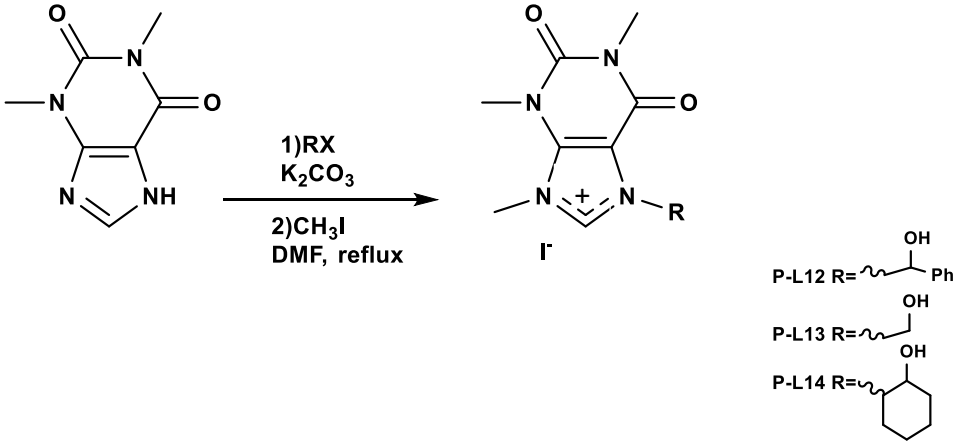

Caffeine-based imidazolium salts have been prepared using the procedure published in the literature [54,102,125,137]and slightly modified by us. Under an inert atmosphere, theophylline was alkylated with an epoxide (styrene oxide P-L12 or cyclohexene oxide P-L14) or alkyl halide (2-iodoethanol, P-L13), in DMF at refluxing temperature, for twelve hours using a mild base (K_2CO_3). Subsequently, the monoalkylated theophyllines were alkylated with iodomethane in six hours, even though the low reactivity of the sp^2 nitrogen

atom. The pro-ligands have been isolated and characterized by NMR (^{1}H, ^{13}C) and mass spectrometry.

2.2.12 Characterization of P-L12, *N'*-[2-(hydroxy phenyl) ethyl] trimethylxantinium iodide

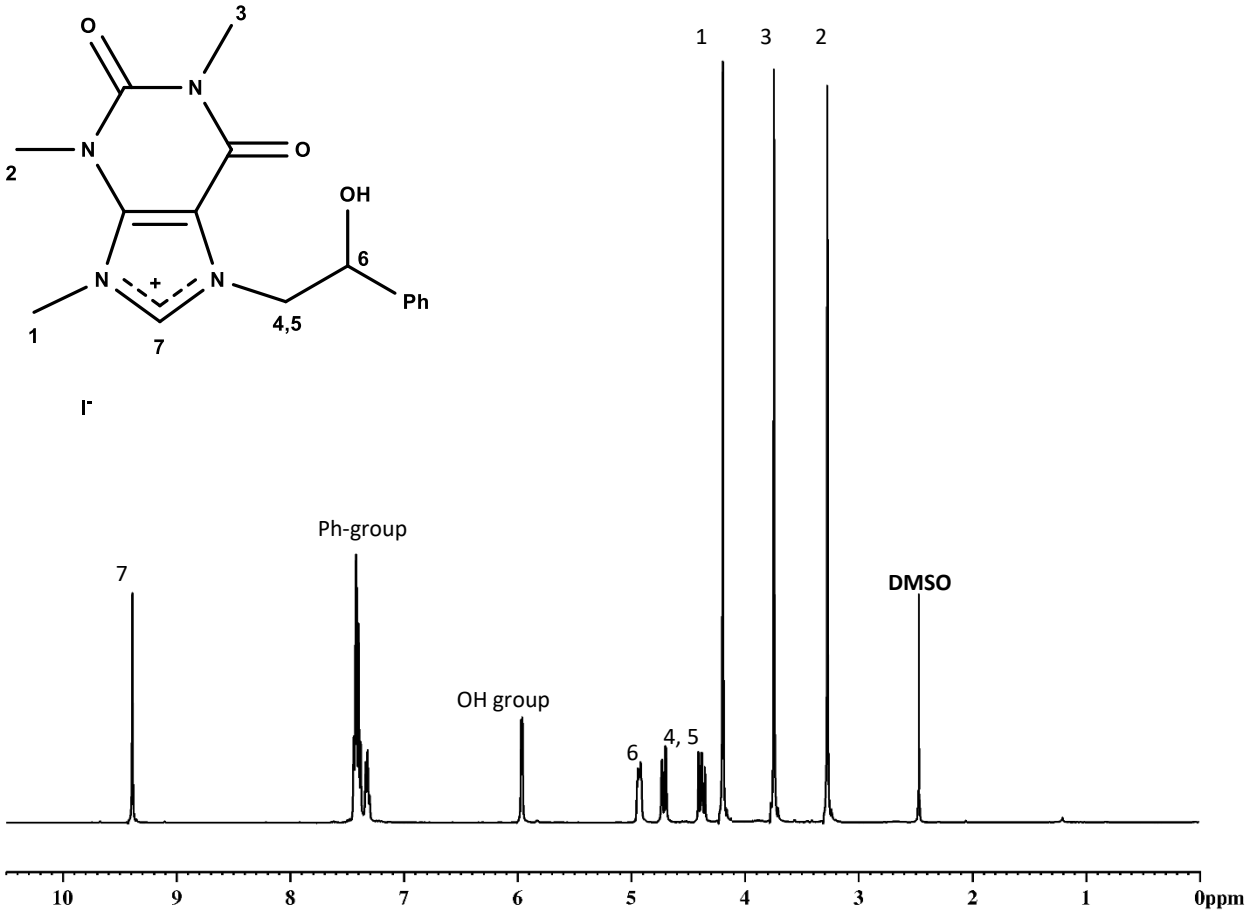

^{1}H-NMR (400 MHz DMSO-d_6): δ 9.3$_9$ (s, 1H, NC***H***N), 7.4$_4$-7.3$_0$ (m,5H, ***Ph-group***), 5.9$_6$ (s,1H, O***H***), 4.7$_3$(s,1H, C***H***OH), 4.6$_9$-4.4$_0$ (m,2H, NC***H***$_2$), 4.3$_5$ (s,3H, NC***H***$_3$ imidazolium ring), 3.7$_4$ (s,3H, NC***H***$_3$), 3.2$_7$ (s,3H, NC***H***$_3$).

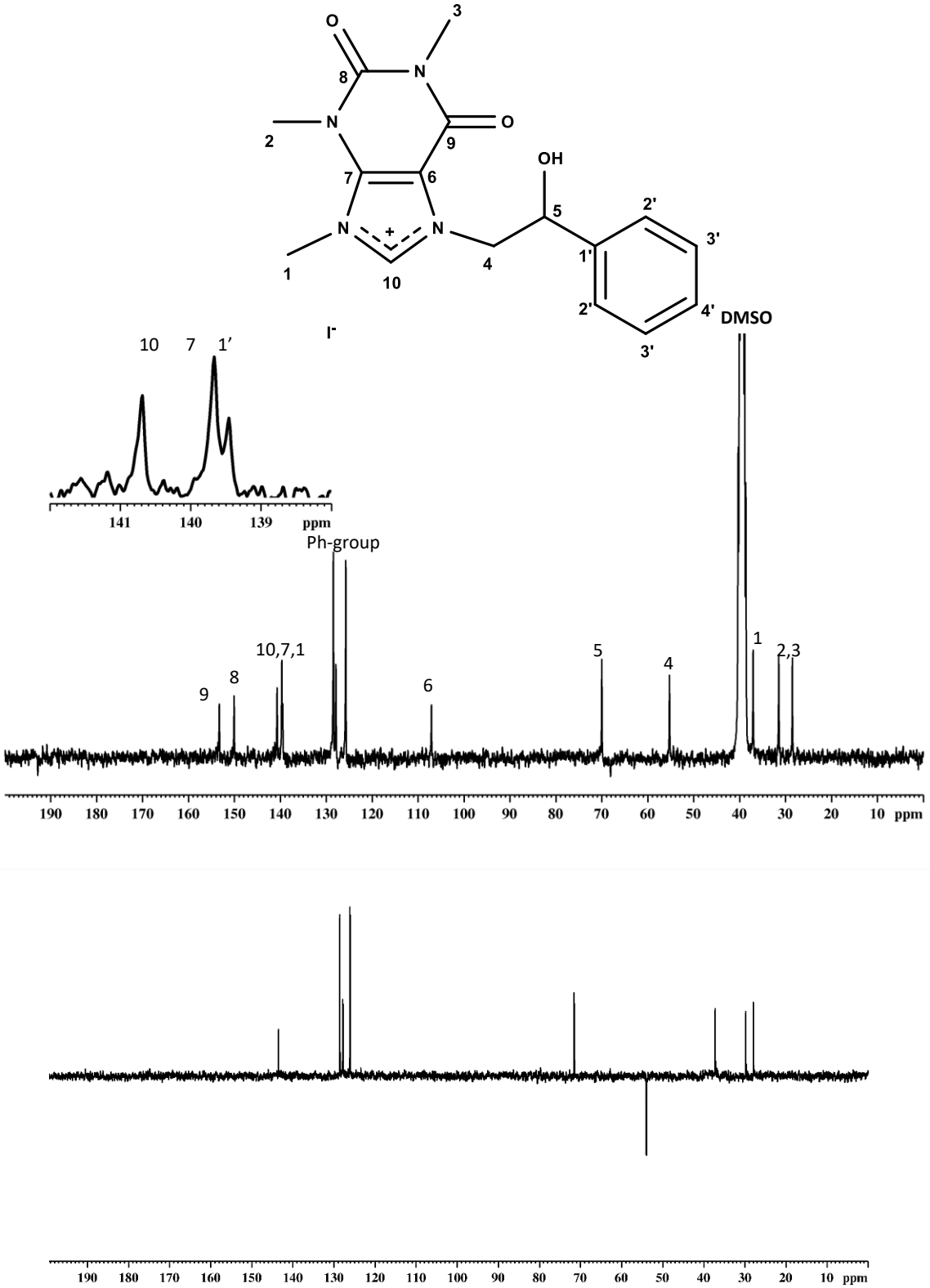

^{13}C-NMR (400MHz DMSO-d_6): δ 153.4$_3$-150.1$_9$(***C***=O), 140.9$_3$(N***C***HN), 139.9$_3$(*backbone carbons*, ***C***=C), 139.5$_5$(*ipso aromatic carbon*, **Ph-ring**), 128.6$_6$, 128.2$_1$, 125.8$_7$(*aromatic carbons*, **Ph ring**), 107.1$_2$ (*backbone carbons*, C=***C***), 70.3$_0$ (***C***HOH), 55.4$_5$(N***C***H$_2$), 36.9$_3$(N***C***H$_3$ imidazolium *ring*), 31.4$_6$, 28.5$_6$(N***C***H$_3$)

MALDI-ToF (m/z): 315.14753 Da attributable to the cationic portion of xantinium salt $[C_{16}H_{19}N_4O_3]^+$

2.2.13 Characterization of P-L13, *N'*-[2-(hydroxy) ethyl] trimethylxantinium iodide

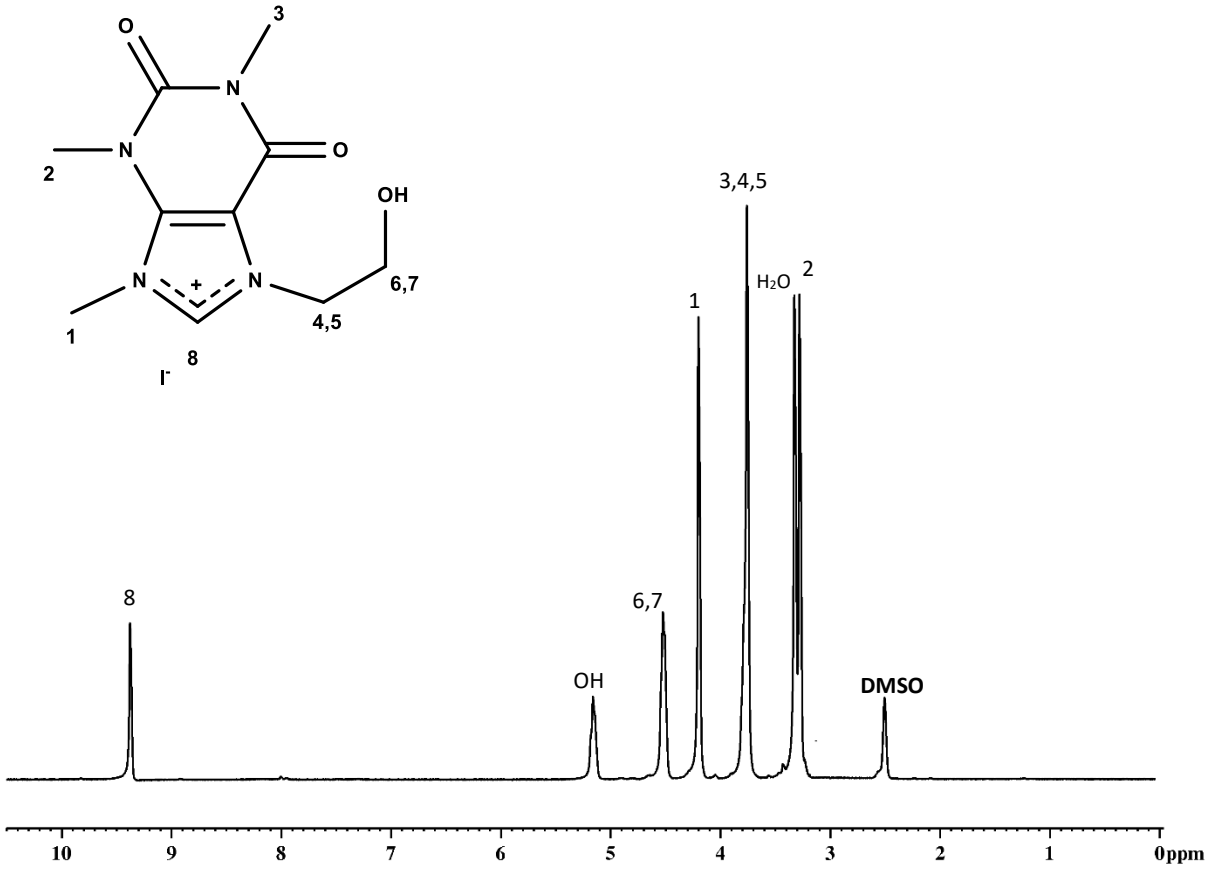

^{1}H-NMR (400 MHz DMSO-d_6): δ 9.3$_7$ (s, 1H, NC***H***N), 5.1$_6$ (s,1H, O***H***), 4.5$_2$-4.5$_0$ (m,2H, C***H***$_2$OH), 4.1$_9$ (s,3H, NC***H***$_3$ imidazolium ring), 3.7$_5$ (b,5H, NC***H***$_2$, N***C*****H**$_3$), 3.2$_7$ (s,3H, NC***H***$_3$).

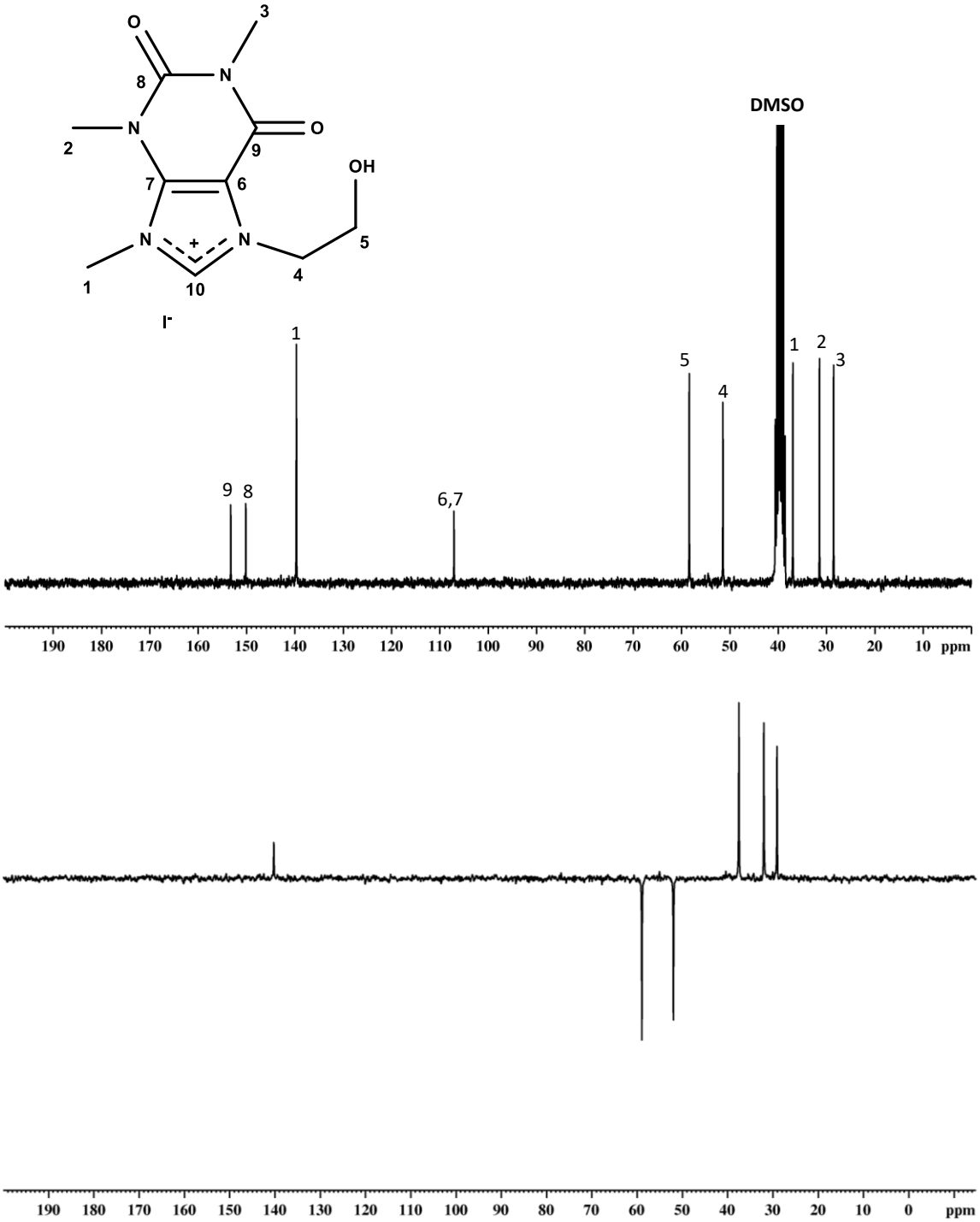

^{13}C-NMR (400MHz DMSO-d_6): δ 153.2$_3$-150.1$_2$(***C***=O), 139.6$_3$(N***C***HN), 107.0$_3$(*backbone carbons*, ***C***=***C***) 58.35 (***C***H$_2$OH), 51.3$_9$(N***C***H$_2$), 36.9$_1$(N***C***H$_3$ imidazolium *ring*), 31.4$_0$, 28.4$_9$(N***C***H$_3$)

MALDI-ToF(m/z):239.11513 Da attributable to the cationic part of imidazolium pro-ligand[$C_{10}H_{15}N_4O_3$]$^+$

2.2.14 Characterization of P-L14, *N'*-[cyclohexan-2-ol] trimethylxanthinium iodide

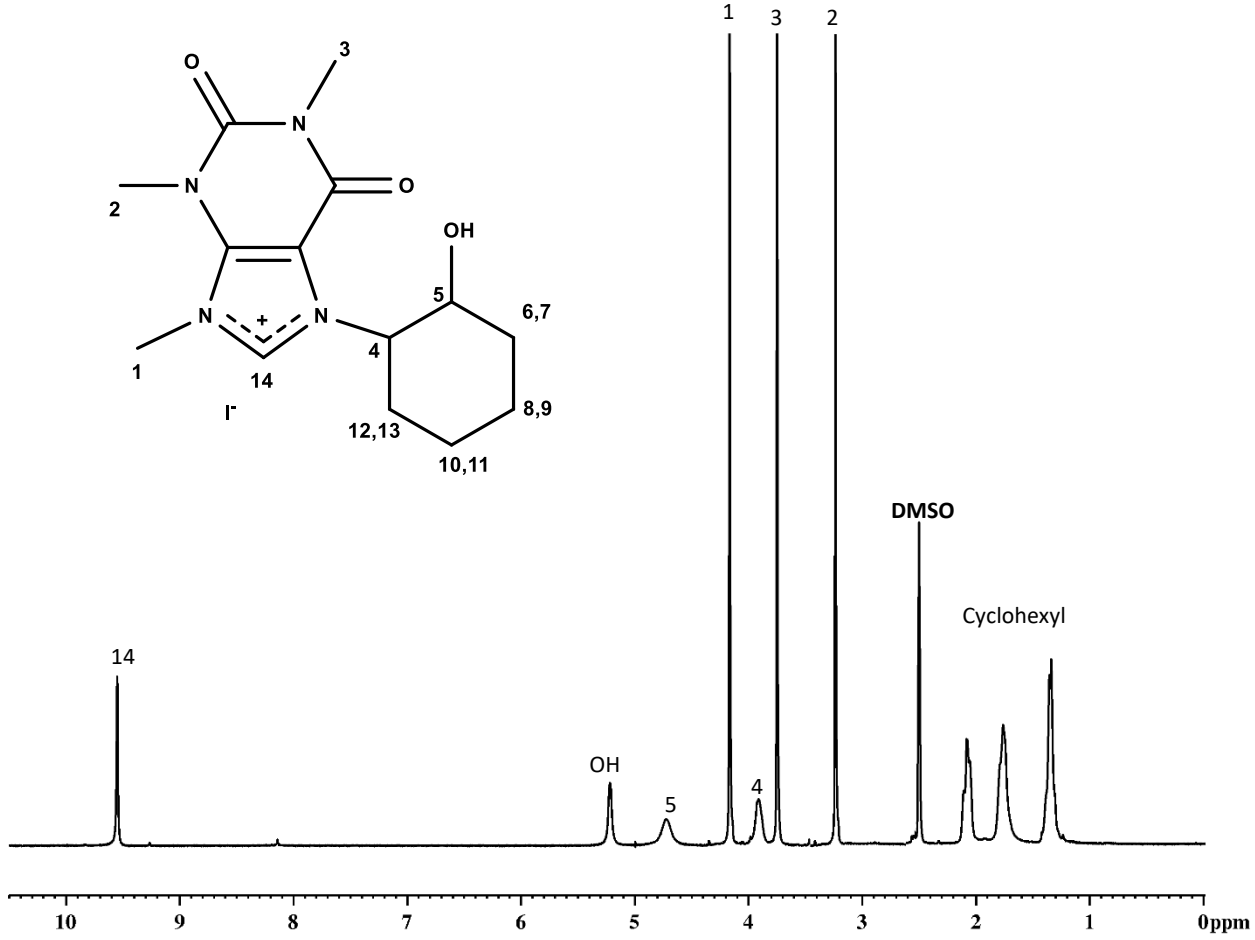

^{1}H-NMR (400 MHz DMSO-d_6): δ 9.5$_4$ (s, 1H, NC***H***N), 5.2$_6$ (s,1H, O***H***), 4.7$_8$-4.7$_0$ (m,1H, C***H***OH), 4.1$_6$ (s,3H, NC***H***$_3$ imidazolium ring), 3.9$_1$-3.9$_0$ (b,1H, NC***H***), 3.7$_5$(s,3H, N***CH***$_3$), 3.2$_8$ (s,3H, NC***H***$_3$), 2.1$_0$-17$_5$(m, 8H, ***Cyclohexyl***)

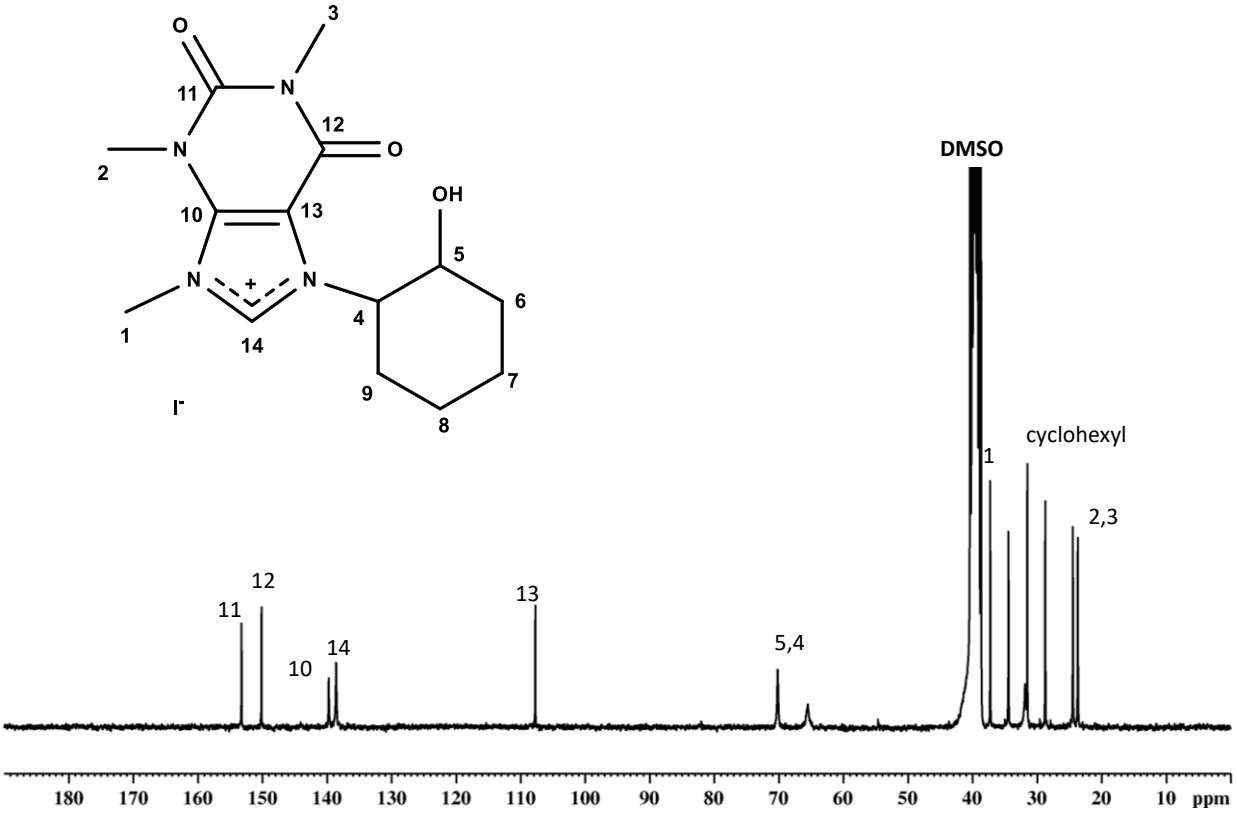

^{13}C-NMR (400MHz DMSO-d_6): δ 153.2$_0$-150.1$_2$(***C***=O), 139.6$_9$ (*backbone carbons*, ***C***=C) 138.5$_5$(N***C***HN), 107.7$_0$(*backbone carbons*, C=***C***) 70.1$_6$ (***C***HOH), 65.4$_7$(N***C***H), 37.24(N***C***H$_3$ *imidazolium ring*), 34.4$_1$-28.7$_2$, (***cyclohexyl carbons***) 24.4$_4$-23.6$_7$(N***C***H$_3$)

MALDI-ToF(m/z):293.16137 Da attributable to the cationic part of imidazolium pro-ligand[$C_{14}H_{21}N_4O_3$]$^+$

2.3 Synthesis of silver *N*-heterocyclic carbene complexes

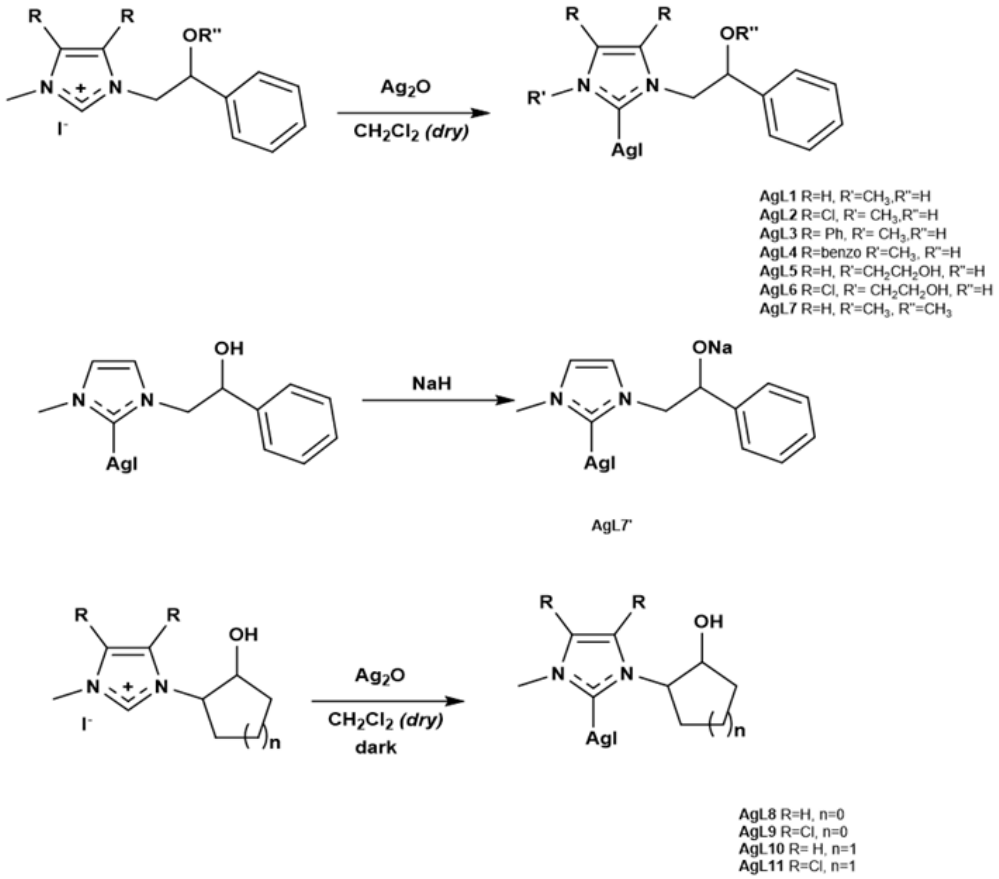

Figure 47 Synthesis of imidazolium-based silver NHC complexes

The silver NHC complexes have been synthesized by the reaction of the imidazolium salt with silver oxide, in dry dichloromethane, under nitrogen atmosphere. Silver oxide gives the deprotonation of the pro-ligand and the consequent coordination to the metal center[44]. The silver oxide route is one of the most used synthetic strategies to produce Ag-NHC complexes for several reasons. Firstly, the reaction can be carried out at room temperature, without the use of an inert atmosphere and a base. Furthermore, silver oxide deprotonates the imidazolium salt, and various solvents (CH_2Cl_2, DMF, CH_3OH, CH_3CN, etc) can be used[138].

All the synthesized complexes have been characterized by nuclear magnetic resonance spectroscopy (^1H, ^{13}C) and mass spectrometry. The ^1H and ^{13}C NMR spectra have shown all the expectable signals. The disappearance of the downfield signal assigned to imidazolium hydrogen, in ^1H-spectra, and the downfield shift of the signal assigned to carbenic carbon, in ^{13}C-NMR analysis, have justified the formation of the silver complex. The mass spectrometry spectra show more signals attributable to a bis carbene structure $[Ag(NHC)_2]^+$. The multiplicity of signals is due to the nearly equal abundance of silver isotopes (^{107} Ag, ^{109}

Ag) and in the case of AgL2, AgL6, AgL9, AgL11 also to the presence of chlorine atoms on the backbone of NHC ligands (^{35}Cl, ^{37}Cl).

The complex AgL7' was synthesized by the reaction of the complex AgL1 with sodium hydride under inert atmosphere, to consent to the deprotonation of the hydroxyl group of carbene ligand.

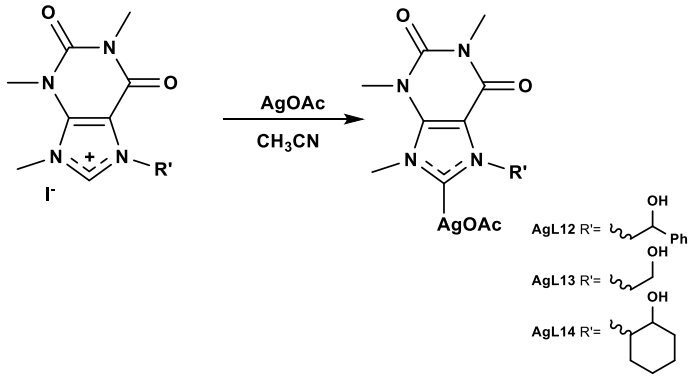

Figure 48 Synthesis of Xanthium based silver complexes

Silver xanthinium complexes have been synthesized by the reaction of imidazolium salt with silver acetate (AgOAc) at room temperature in dry acetonitrile, following the literature procedures [53,55,125,139]. The silver complexes have been synthesized by NMR and mass spectrometry analysis. In the ^{1}H-NMR spectrum, the appearance of the signal assigned to methyl of acetate group and the disappearance of the signal of acid proton of the pro-ligand confirm the formation of the silver complex. Furthermore, the presence of the sharp peak attributable to the carbene carbon atom supported the formation of the silver complexes.

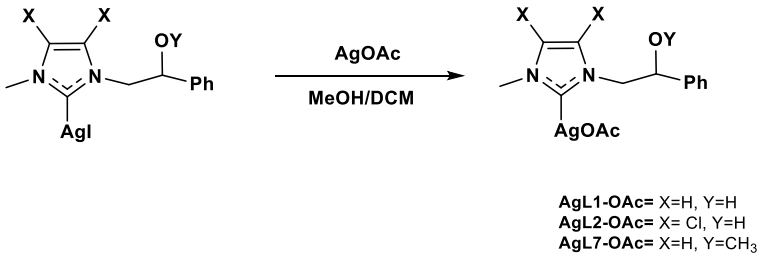

Figure 49 Synthesis of acetate NHC silver complexes

The silver acetate NHC complexes were synthesized following the slightly modified procedure published [140], by the metathesis reaction of iodo silver NHC complex with silver acetate. The driving force of the reaction is the formation of insoluble silver iodide. The formation of the acetate complexes has been confirmed by ^{1}H-NMR spectroscopy with the appearance of singlet signal attributable to the protons of the methyl group of acetate anion, and by ^{13}C-NMR by the appearance of down-field signal attributable to carbonyl carbon and the resonance attributable to methyl carbon.

2.3.1 Characterization of Silver complexes AgL1, AgL2, AgL3, AgL4, AgL5, AgL6, AgL7

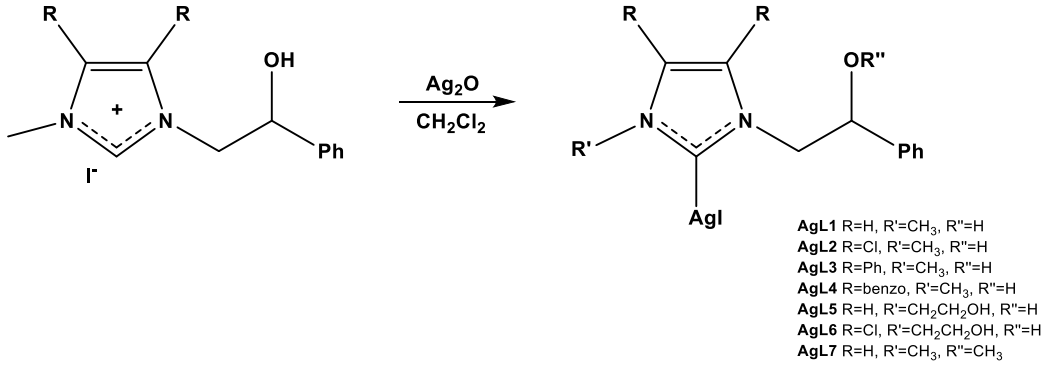

The complete characterization of complexes AgL1, AgL2 is reported in literature by us[126,130].

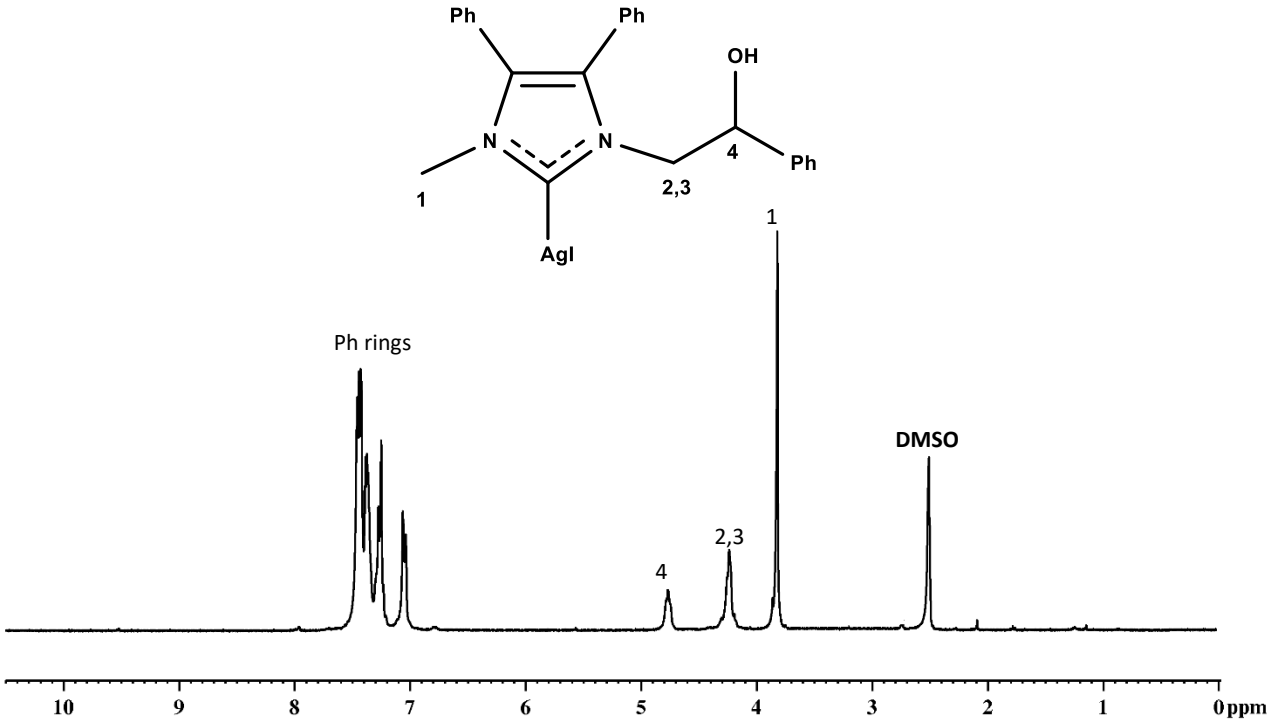

^{1}H-NMR (400MHz, DMSO-d$_6$): δ 7.4$_6$-7.0$_4$ (m, 15H, ***Ph rings***) 4.7$_6$(m, 1H, OC***H***); 4.2$_4$-4.1$_4$(m, 2H, NC***H***$_2$); 3.8$_2$(s,3H, NC***H***$_3$).

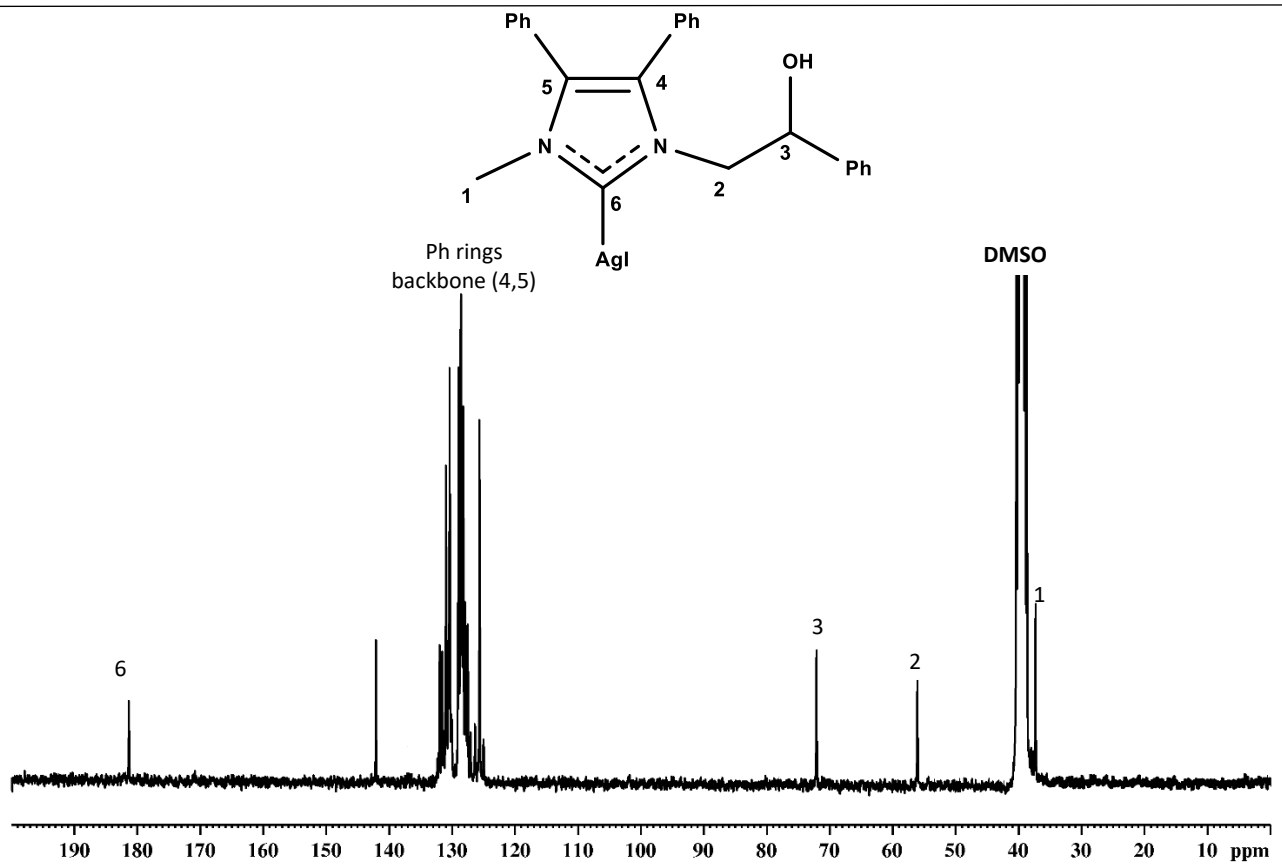

^{13}C-NMR (100 MHz, DMSO-d_6): δ 181.3$_8$ (N**C**N), 142.1$_7$ *(ipso aromatic carbon* (1′), **Ph-ring**), 131.9$_7$-125.5$_9$, (*aromatic carbons*, **Ph ring,** *backbone*), 72.1$_6$(O**C**H), 56.0$_2$(N**C**H$_2$), 37.3$_7$(N**C**H$_3$)

MALDI-ToF (m/z): 817.26229 Da attributable to a structure a bis-carbene structure $[C_{48}H_{44}AgN_4O_2]^+$

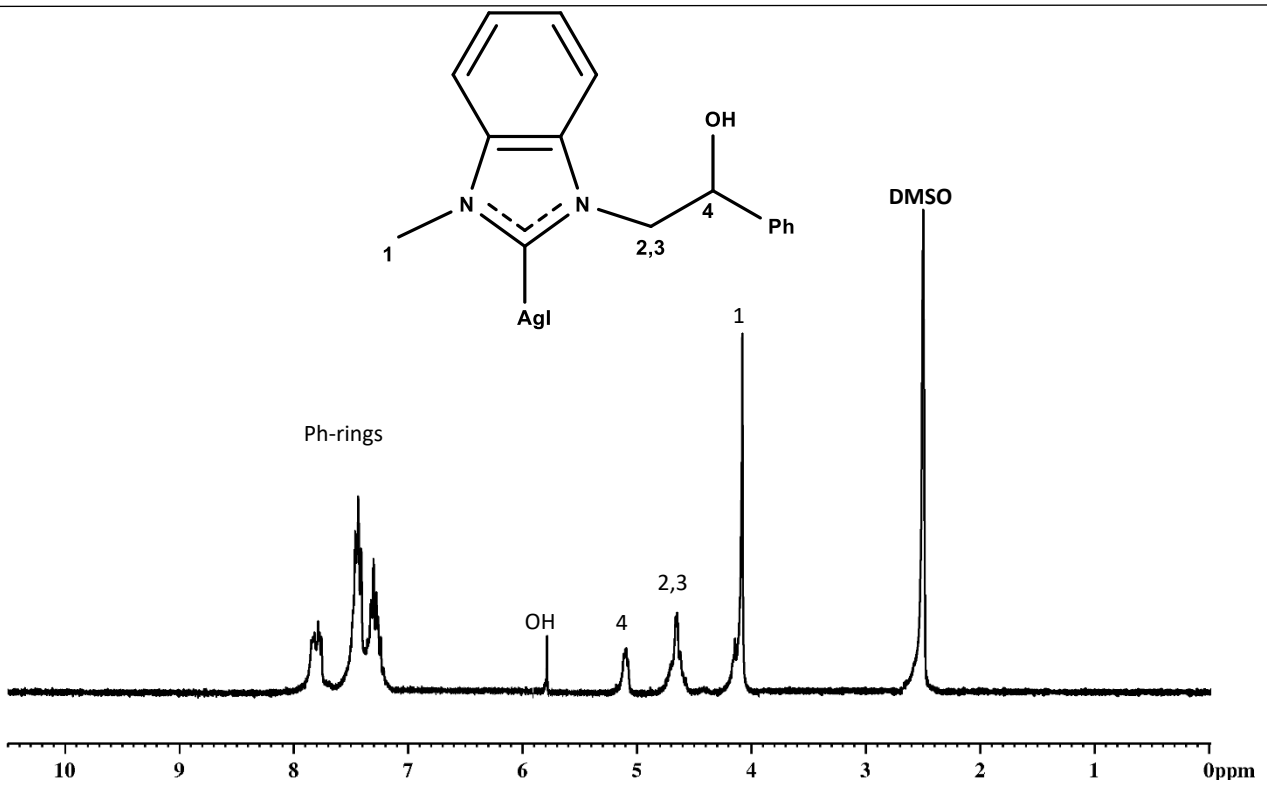

^{1}H-NMR (400MHz, DMSO-d_6): δ 7.8$_2$-7.2$_4$ (m, 9H, ***Ph ring***); 5.8$_6$(s, 1H, O***H***); 5.0$_9$-5.0$_7$ (dd, 1H, OC***H***); 4.6$_9$-4.6$_2$(m, 2H, NC$\boldsymbol{H}_2$); 4.0$_4$(s,3H, NC$\boldsymbol{H}_3$).

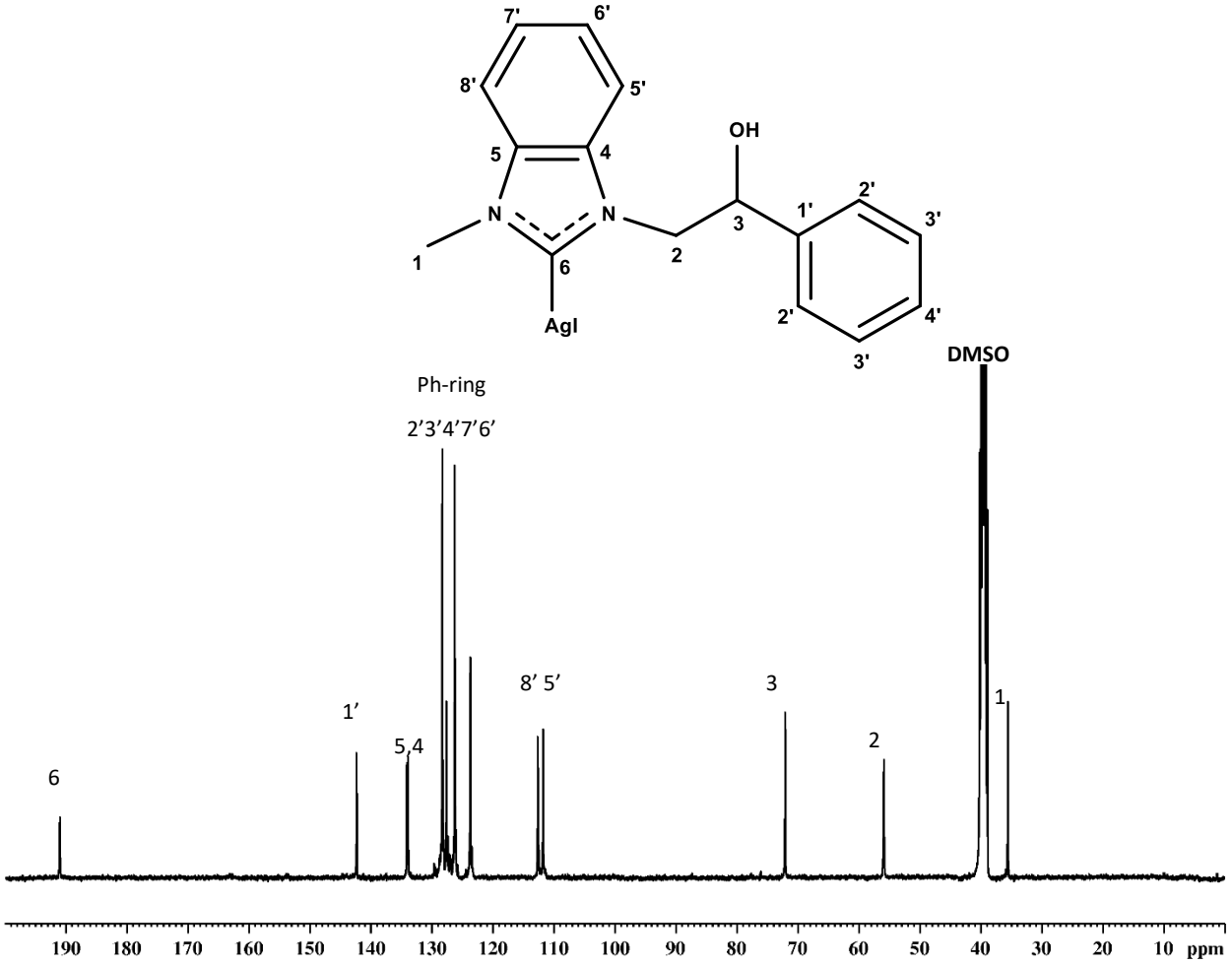

^{13}C-NMR (100 MHz, DMSO-d_6): δ 190.9$_1$ (N***C***N) 142.2$_7$ *(ipso aromatic carbon* (1'), **Ph-ring**), 134.4$_0$-133.8$_2$ (*backbone carbons*, N***C*=*C***N), 128.2$_1$-111.7$_0$, (*aromatic carbons*, **Ph rings**), 72.0$_6$(O***C***H), 55.8$_2$(N***C***H$_2$), 35.5$_0$(N***C***H$_3$)

MALDI-ToF (m/z): 517.26179 Da attributable to a structure a bis-carbene structure $[C_{26}H_{25}AgN_4O]^+$

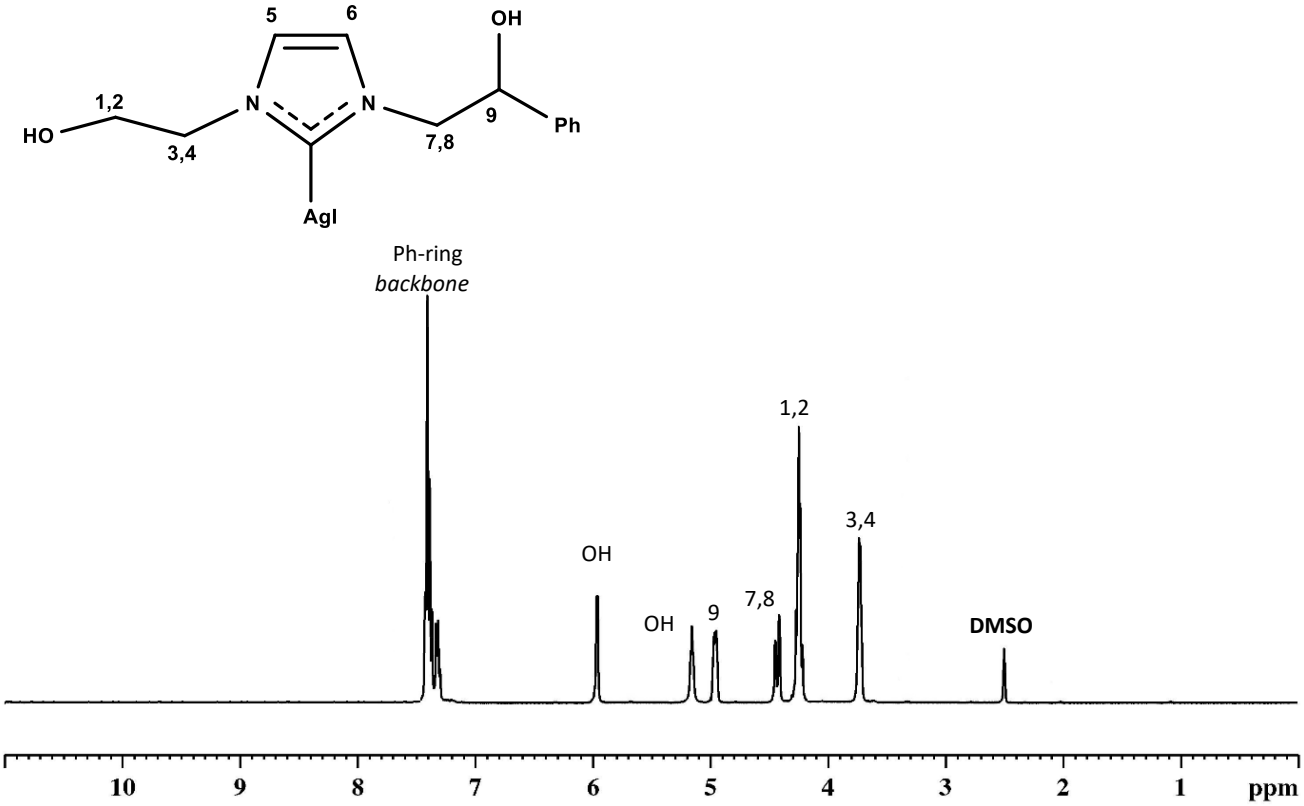

^{1}H NMR (400MHz, DMSO-d_6): δ 7.3$_8$-7.3$_1$ (m, 7H, ***Ph rings***); 5.8$_8$(s, 1H, O***H***); 5.0$_7$ (s, 1H, O***H***) 4.9$_9$(m, 1H, OC***H***); 4.3$_6$-4.2$_7$(m, 4H, NC***H***$_2$CH$_2$OH, NC***H***$_2$CHOH); 3.7$_3$(s,2H, NCH$_2$C***H***$_2$OH).

The formation of the silver complex is supported by the presence of a doublet assignable to $C_{carbene}$ Ag, in the ^{13}C-NMR spectrum. This type of signal is resulting from the coupling constant of C_{NHC}Ag, with two isotopes of silver (^{107}Ag 51.839% and^{109}Ag 48.161%) with nuclear spin ½ (NMR active). In literature for AgNHC complexes, three different patterns of resonances are reported for carbene carbon atom; i) doublet of doublets due to the NMR active silver isotope (^{107}Ag, ^{109}Ag); ii) no splitting pattern (sharp or broad singlet signal); iii) no observation of any signals[141].

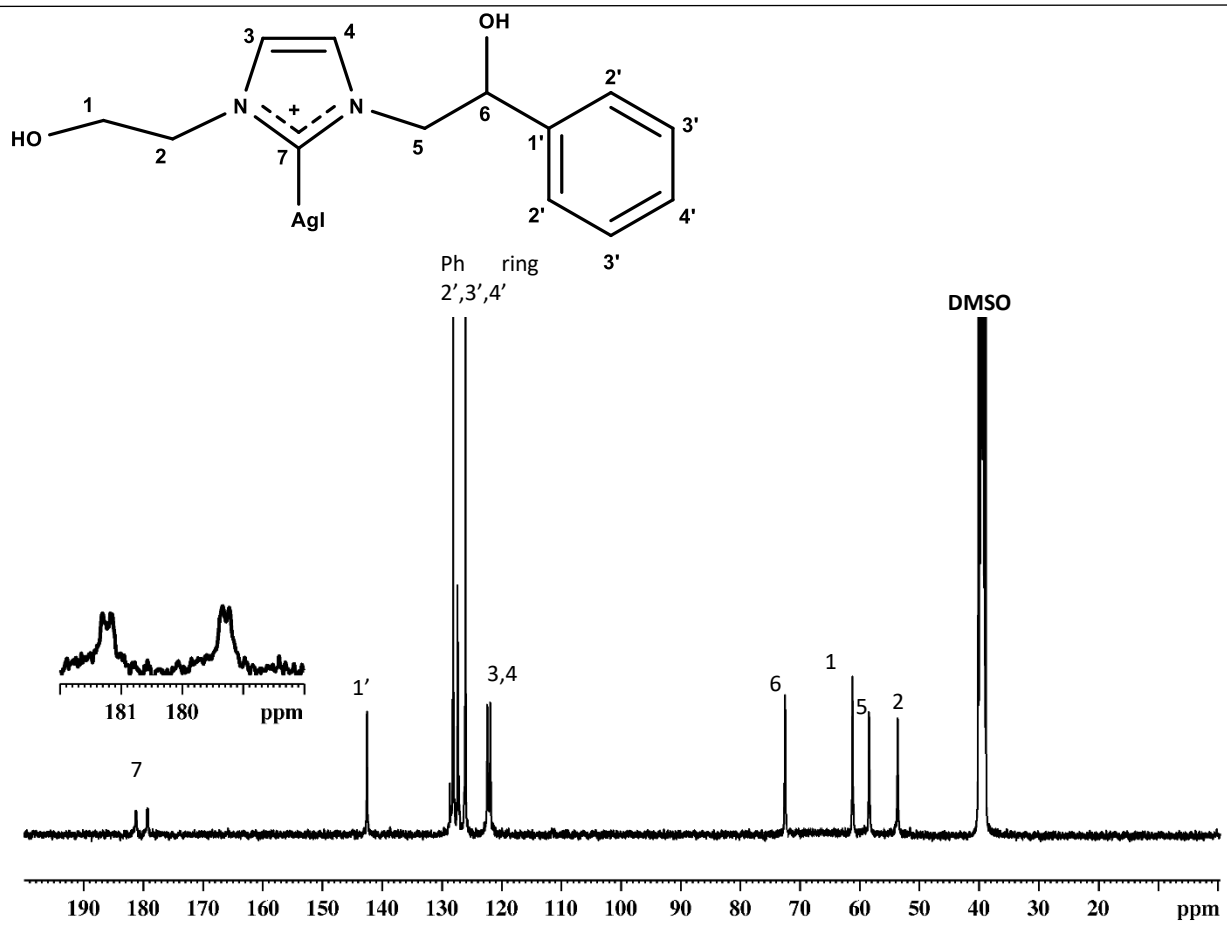

^{13}C-NMR (100 MHz, DMSO-d_6): δ 181.2$_8$ 179.2$_8$ (N***C***N), 142.5$_3$ (*ipso* carbon of ***Ph ring***), 128.1$_0$, 127.1$_0$, 126.0$_6$ (aromatic carbon, ***Ph ring***), 122.4$_0$, 121.8$_5$ (*backbone carbons*), 72.4$_6$ (***C***HOH), 61.1$_9$ (***C***H$_2$OH), 58.4$_0$ (N***C***H$_2$CHOH), 53.6$_2$ (N***C***H$_2$CH$_2$OH).

ESI-MS (CH$_3$CN m/z): 573.14690 Da attributable to $[C_{26}H_{32}AgN_4O_4]^+$

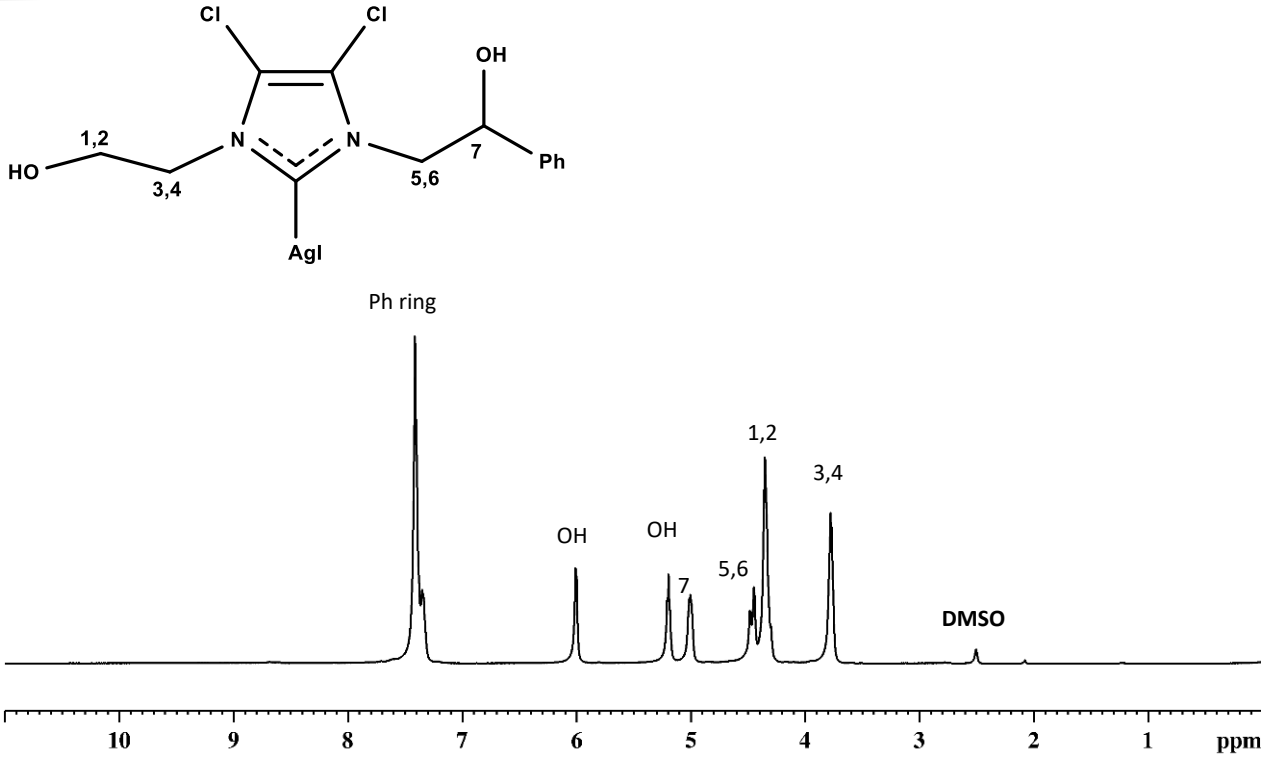

^{1}H-NMR (400MHz, DMSO-d_6): δ 7.3$_8$-7.2$_7$ (m, 5H, ***Ph ring***); 5.8$_9$(s, 1H, O***H***); 5.0$_7$ (s, 1H, O***H***) 4.9$_9$(m, 1H, OC***H***); 4.3$_3$-4.2$_7$(m, 4H, NCH$_2$C***H***$_2$OH, NC***H***$_2$CHOH); 3.7$_4$(s,2H, NC***H***$_2$CH$_2$OH).

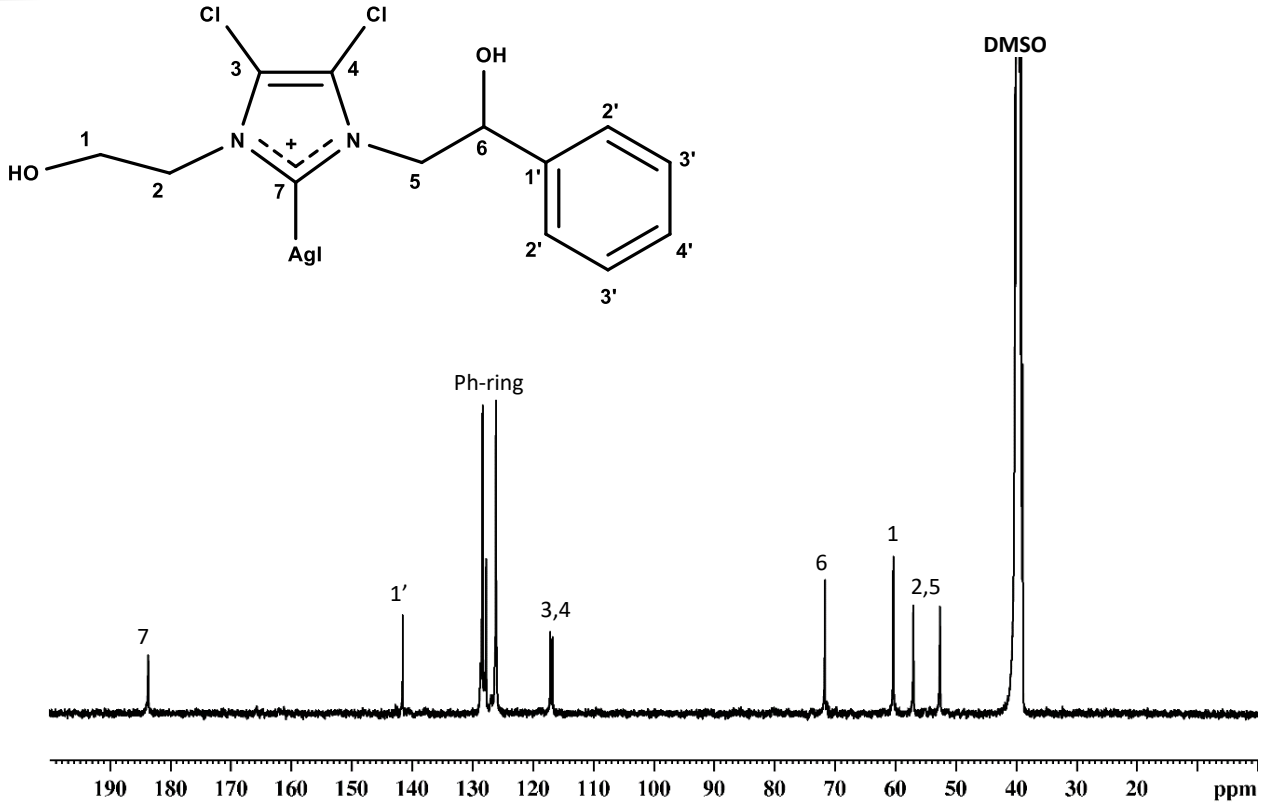

^{13}C-NMR (100 MHz, DMSO-d$_6$): δ 181.3$_0$ (N***C***N), 141.5$_1$ (*ipso* carbon of ***Ph ring***), 128.3$_1$, 127.7$_2$, 126.0$_8$ (aromatic carbon, ***Ph ring***), 117.1$_0$, 116.7$_5$ (*backbone carbons*), 71.6$_3$ (***C***HOH), 60.2$_9$ (***C***H$_2$OH), 56.9$_9$ (N***C***H$_2$CHOH), 52.5$_7$ (N***C***H$_2$CH$_2$OH).

ESI-MS (CH$_3$CN m/z): 707.99716 Da attributable to [C$_{26}$H$_{28}$Cl$_4$AgN$_4$O$_4$]$^+$

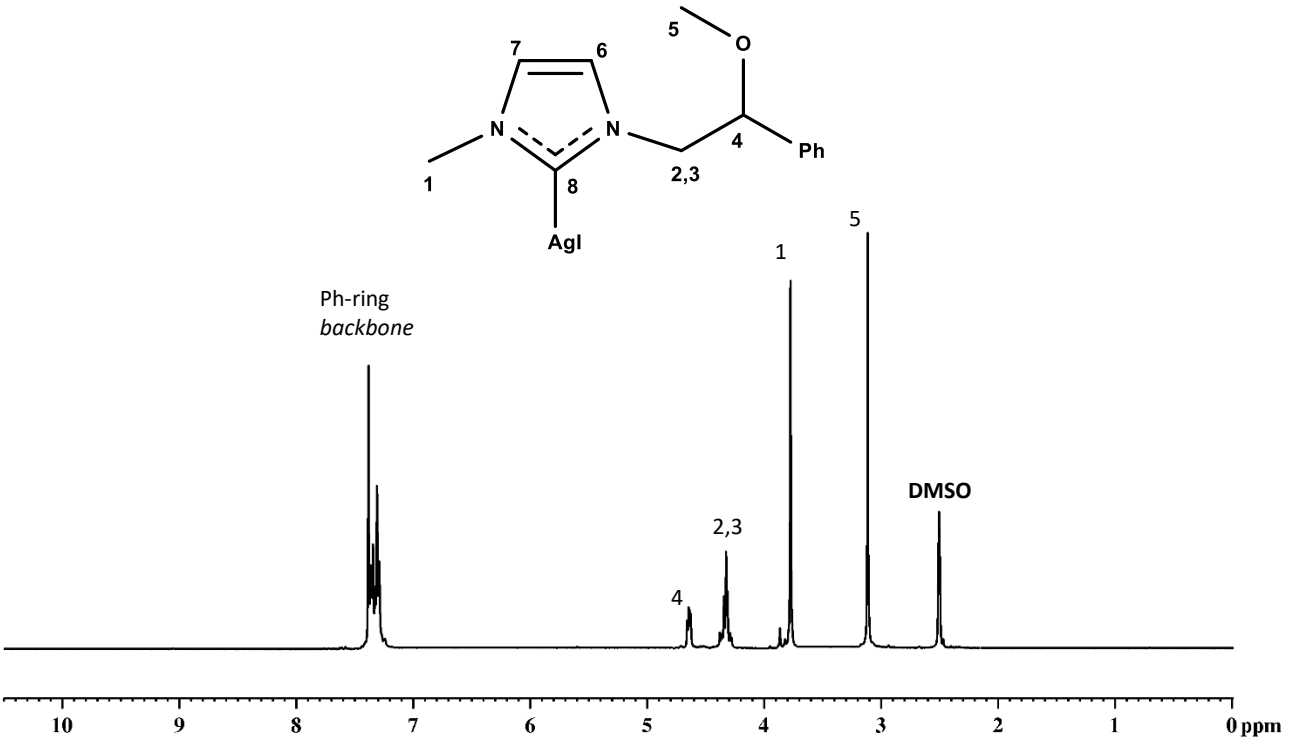

^{1}H-NMR (400MHz, DMSO-d_6): δ 7.3$_4$-7.2$_6$ (m, 7H, ***Ph ring, backbone***), 4.6$_0$(m, 1H, OC***H***), 4.3$_0$-4.2$_7$(m, 2H, NC***H***$_2$), 3.7$_4$(s,3H, NC***H***$_3$), 3.0$_7$(s,3H, OC***H***$_3$).

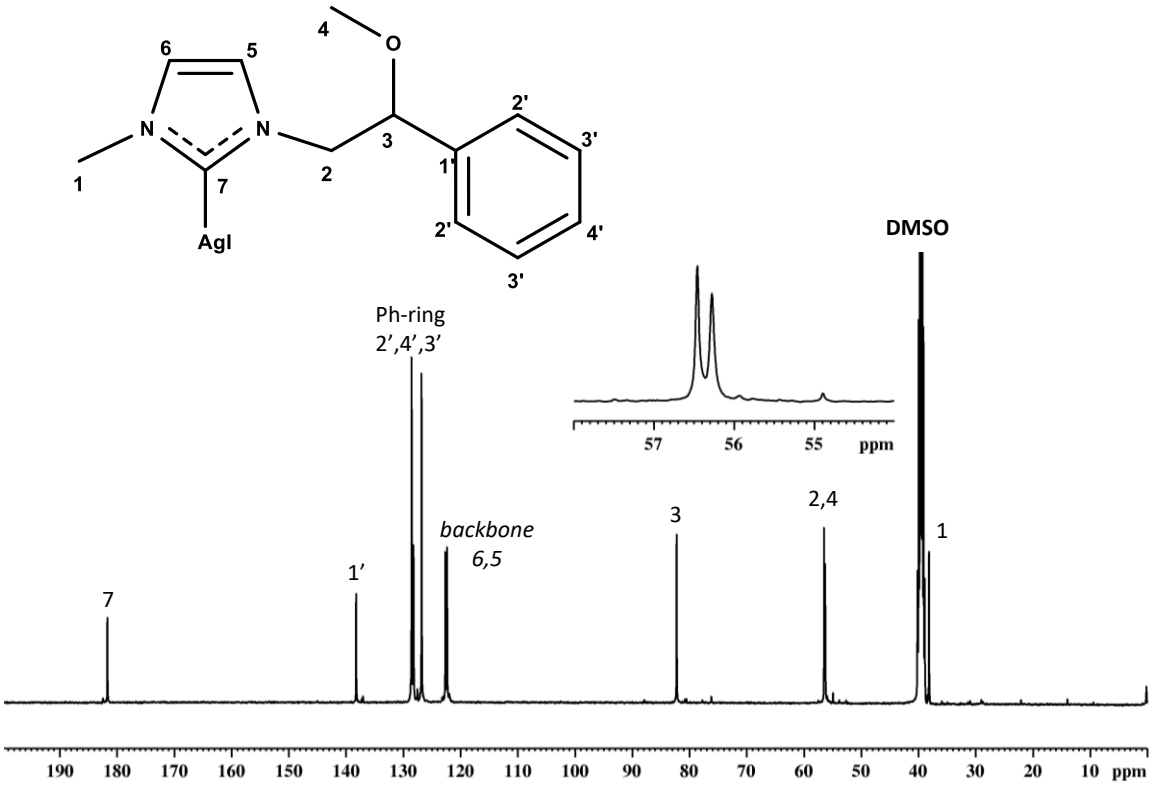

^{13}C-NMR (100 MHz, DMSO-d_6): δ 181.6$_0$ (N***C***N), 138.2$_1$ (*ipso* carbon of ***Ph ring***), 128.5$_1$, 128.2$_2$, 126.8$_8$ (aromatic carbon, ***Ph ring***), 122.6$_0$, 122.3$_5$ (*backbone carbons*), 82.2$_3$ (***C***HO), 56.4$_9$ (N***C***H$_2$), 52.2$_7$ (O***C***H$_3$), 38.1$_6$(N***C***H$_3$).

MALDI-ToF (m/z): 539.1567 Da attributable to $[C_{26}H_{32}AgN_4O_2]^+$

2.3.2 Characterization of Silver complexes AgL7′

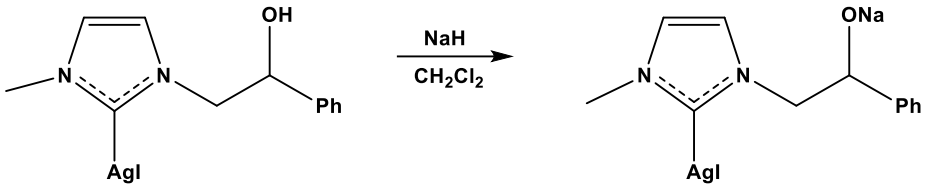

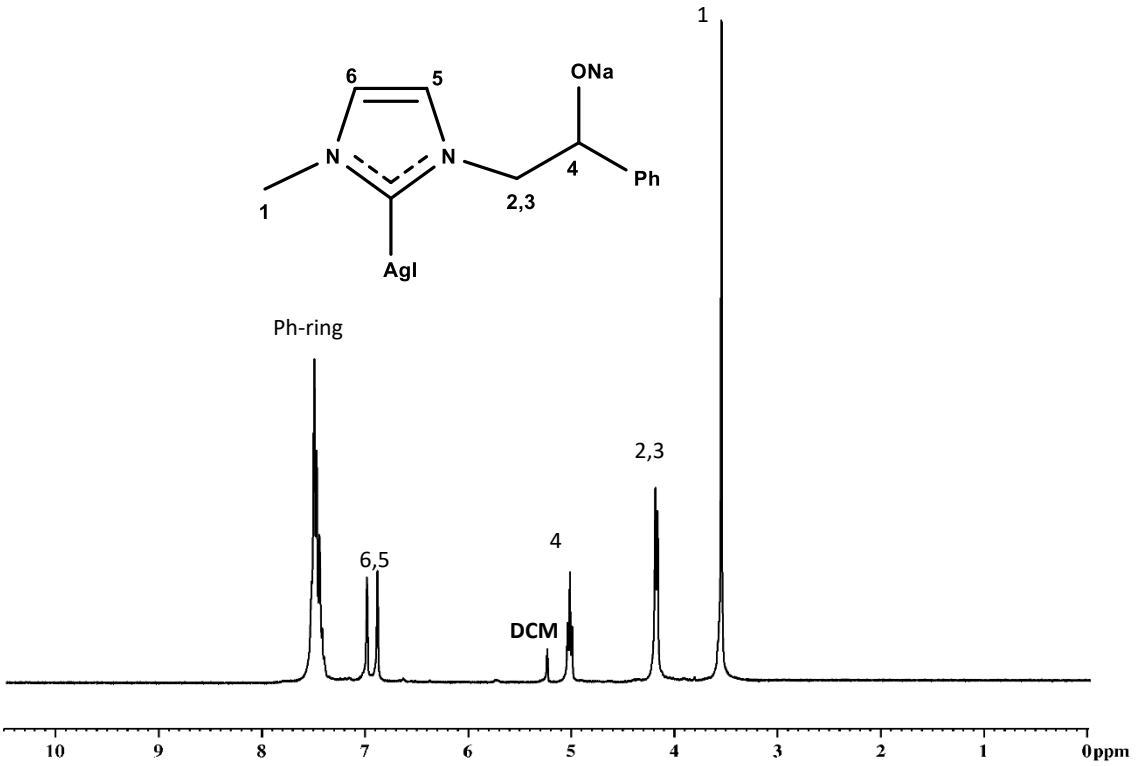

^{1}H-NMR (400MHz, CD_2Cl_2-d_2): δ 7.3$_6$-7.3$_3$ (m, 5H, ***Ph ring***), 6.8$_9$-6.7$_9$ (s, 2H, ***backbone***), 5.1$_3$(t, 1H, -OC***H***), 4.4$_0$-4.3$_0$(m, 2H, NC***H***$_2$), 3.8$_6$(s,3H, NC***H***$_3$).

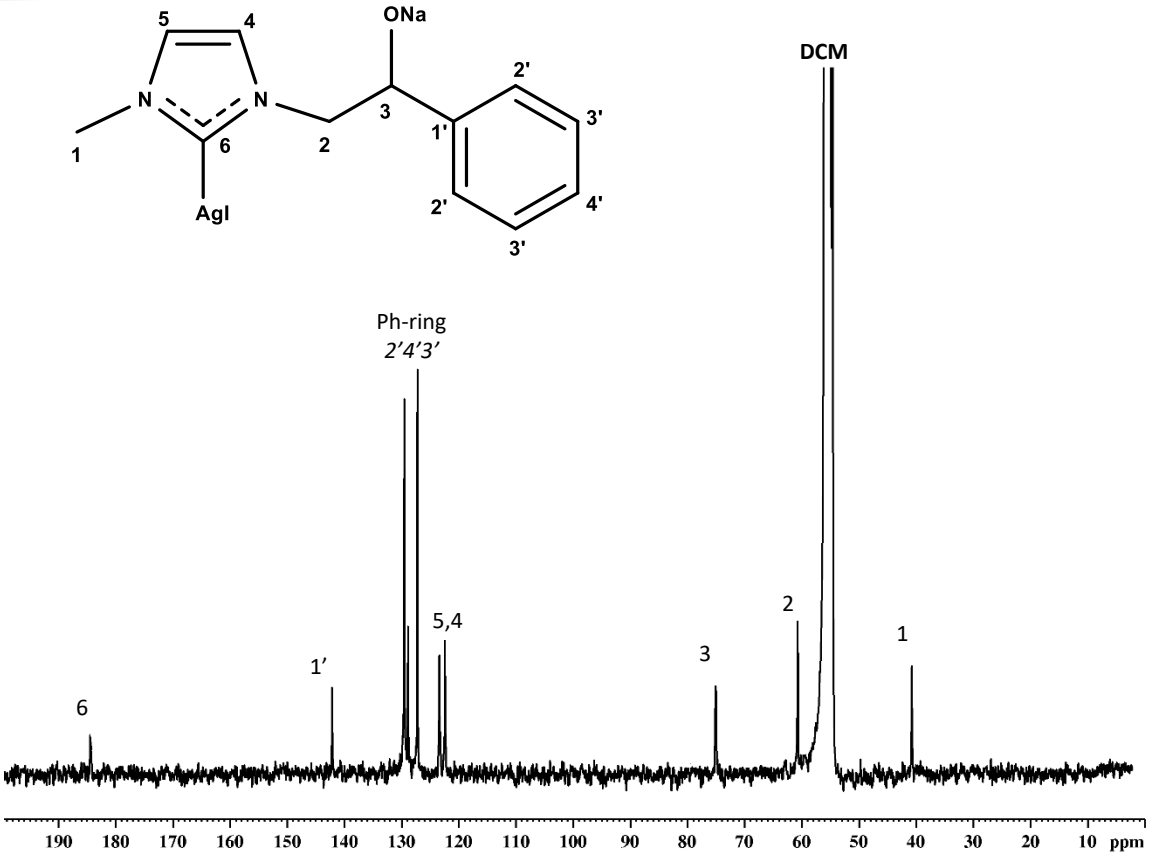

^{13}C-NMR (100 MHz, CD_2Cl_2-d_2): δ 184.6$_0$ (N***C***N), 141.8$_1$ (*ipso* carbon of ***Ph ring***), 129.1$_1$, 128.4$_2$, 126.7$_8$ (aromatic carbon, ***Ph ring***), 123.4$_0$, 122.8$_5$ (*backbone carbons*), 78.1$_3$ (***C***HO$^-$), 59.4$_9$ (N***C***H$_2$), 39.2$_6$(N***C***H$_3$).

ESI-MS (CH_2Cl_2, m/z): 528.0035 Da attributable to $[C_{22}H_{22}AgN_4O_2Na_2]^+$

2.3.3 Characterization of Silver complexes AgL8, AgL9, AgL10, AgL11

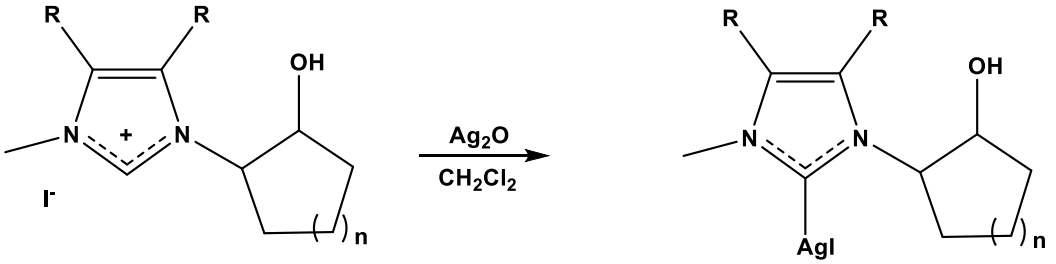

AgL8 R=H, n=0
AgL9 R=Cl, n=0
AgL10 R=H, n=1
AgL11 R=Cl, n=1

The complete characterization of complexes AgL8, AgL9, and AgL10 is reported in the literature by us [126,129].

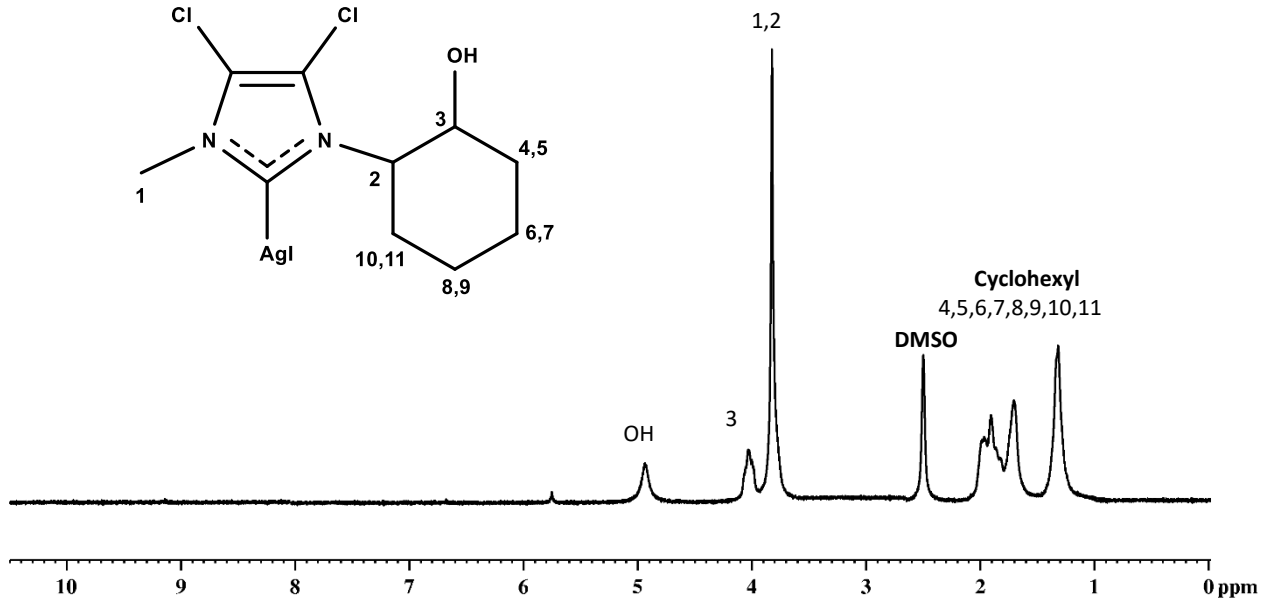

^{1}H-NMR (400MHz, DMSO-d_6): δ 4.9$_3$(b, 1H, O***H***), 4.0$_7$-3.9$_2$(m, 1H, HOC***H***), 3.8$_6$(s,4H, NC***H***, NC***H***$_3$), 1.9$_6$-1.3$_1$(***Cyclohexyl*** group).

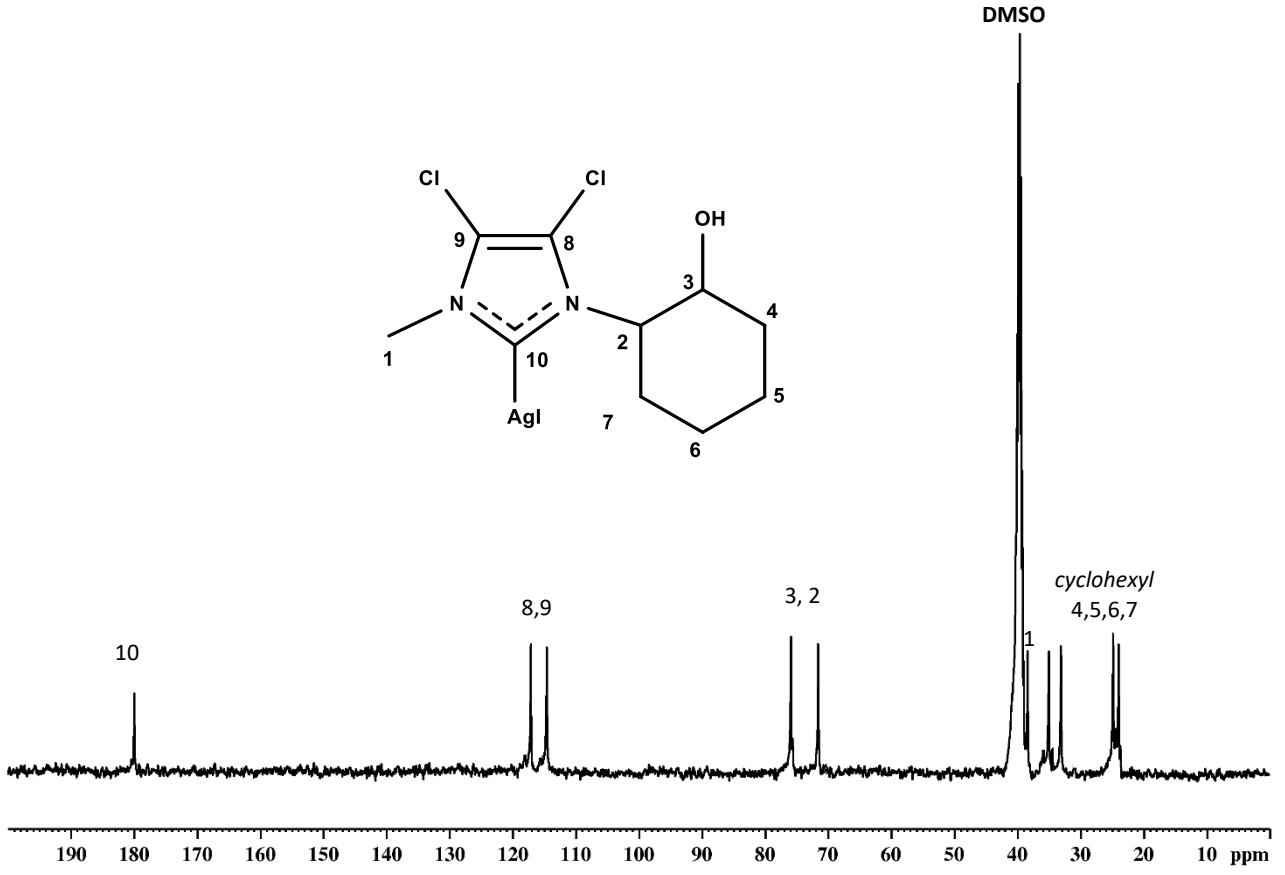

^{13}C-NMR (100 MHz, DMSO d_6): δ 182.9$_0$ (N***C***N), 118.6$_5$, 117.2$_5$ (*backbone carbons*), 76.1$_3$ (***C***HOH), 70.3$_9$ (N***C***H), 38.7$_6$(N***C***H$_3$), 35.0$_1$-23.9$_3$ (***Cyclohexyl carbons***).

ESI-MS (CH_2Cl_2, m/z): 603.0017 Da attributable to $[C_{20}H_{28}AgCl_4N_4O_2]^+$

2.3.4 Characterization of caffeine-based silver NHC complexes AgL12, AgL13, AgL14

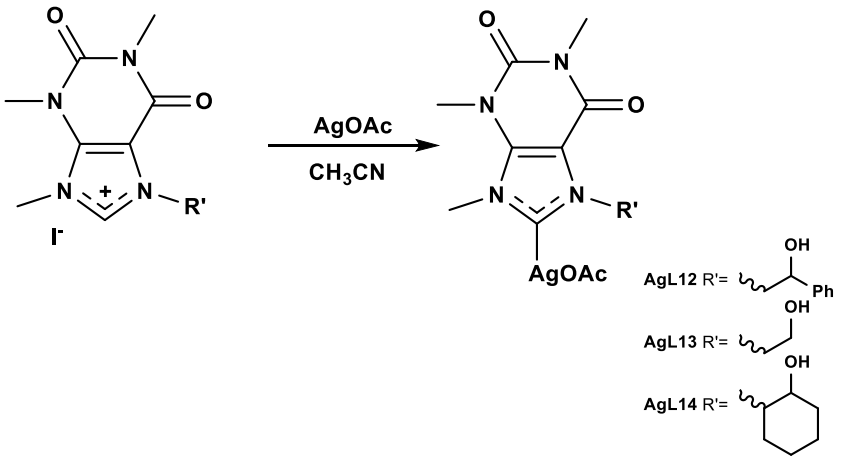

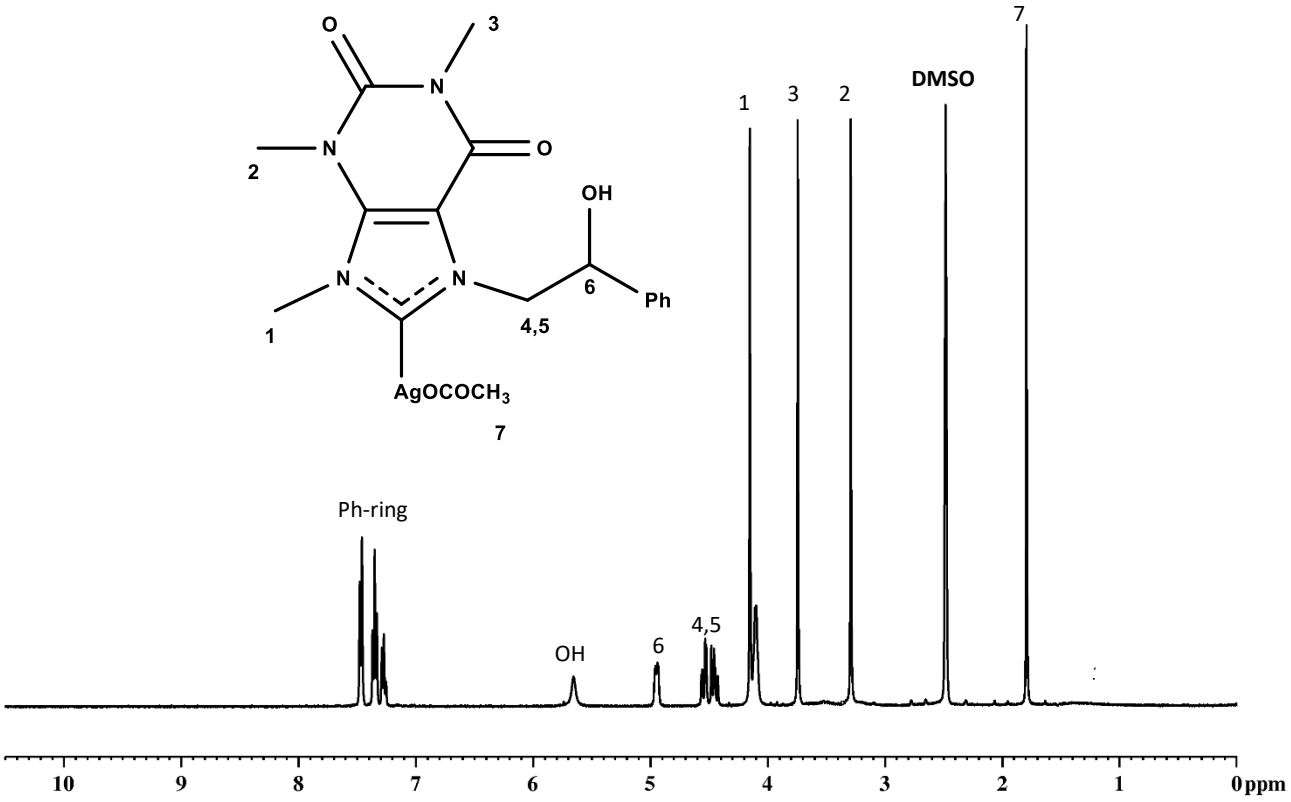

^{1}H-NMR (400 MHz DMSO-d$_6$): δ 7.4$_7$-7.2$_6$ (m,5H, ***Ph-group***), 5.6$_6$ (s,1H, O***H***), 4.9$_3$(m,1H, C***H***OH), 4.5$_6$-4.4$_2$ (m,2H, NC***H***$_2$), 4.1$_5$ (s,3H, NC***H***$_3$ imidazolium ring), 3.7$_4$ (s,3H, NC***H***$_3$), 3.2$_7$ (s,3H, NC***H***$_3$) 1.7$_9$(s, 3H COC***H***$_3$).

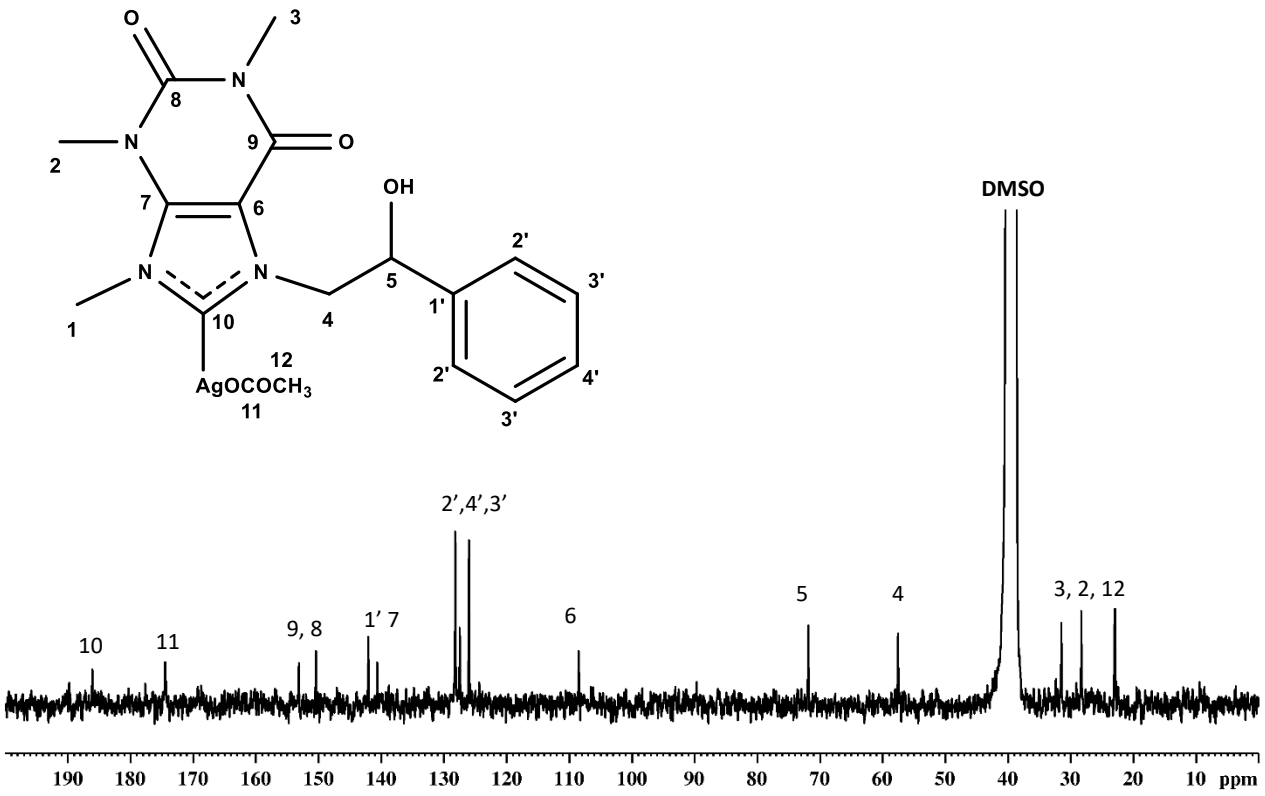

^{13}C-NMR (400MHz DMSO-d_6): δ 186.3$_6$(N***C***N), 174.5$_1$ (CH$_3$***C***=O), 153.3$_3$-150.3$_9$ (***C***=O *purine ring*), 142.4$_5$(*ipso aromatic carbon*, **Ph-ring**), 140.6$_3$(*backbone carbon*, ***C***=C), 128.2$_6$, 128.1$_1$, 125.7$_7$(*aromatic carbons*, **Ph ring**), 108.8$_2$ (*backbone carbon*, C=***C***), 72.1$_0$ (***C***HOH), 57.1$_5$(N***C***H$_2$), 31.4$_8$, 28.3$_6$ (N***C***H$_{3\ \text{purine ring}}$), 22.9$_6$(O=C***C***H$_3$)

ESI-Ms (CH$_2$Cl$_2$ m/z): 705.44325 Da attributable to [C$_{30}$H$_{30}$AgN$_8$O$_6$]$^+$

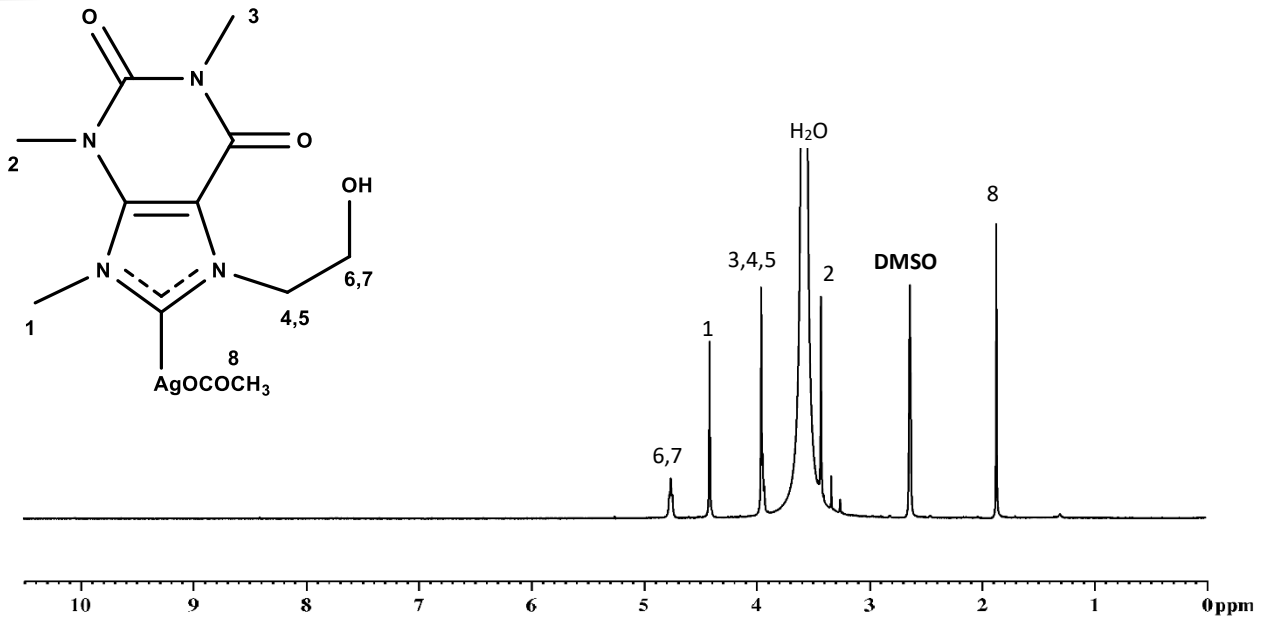

^{1}H-NMR (400 MHz DMSO-d$_6$): δ 4.5$_3$-4.5$_0$ (m,2H, C***H***$_2$OH), 4.1$_9$ (s,3H, NC***H***$_3$ imidazolium ring), 3.7$_6$-3.7$_3$ (b,5H, NC***H***$_2$, NC***H***$_3$), 3.2$_1$ (s,3H, NC***H***$_3$), 1.77(s, 3H, O=CC***H***$_3$).

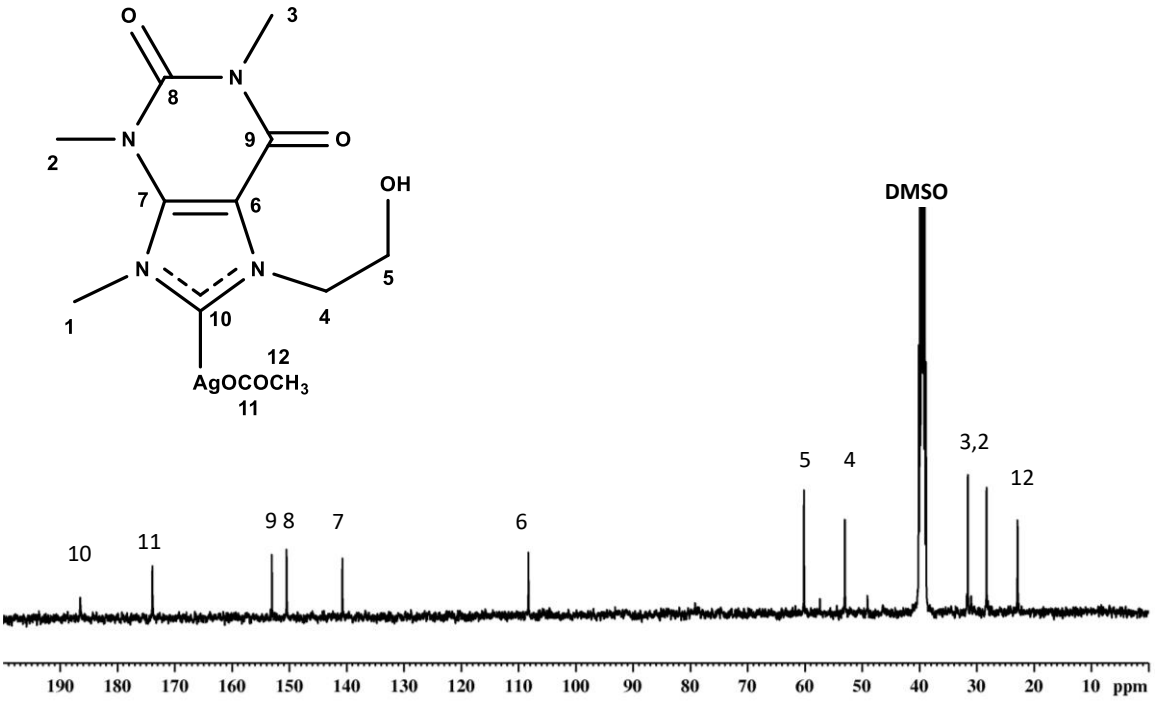

^{13}C-NMR (400MHz DMSO-d$_6$): δ 186.5$_8$(N***C***N); 173.9$_0$ (O=***C***CH3); 153.0$_3$-150.4$_2$(***C***=O *purine ring*); 140.7$_2$ (*backbone carbon* ***C***=C); 108.2$_3$(*backbone carbon*, C=***C***) 60.1$_2$ (***C***H$_2$OH), 52.9$_9$(N***C***H$_2$), 31.5$_1$ 28.2$_4$(N***C***H$_3$ imidazolium *ring*), 31.4$_0$, 28.4$_9$ (N***C***H$_3$ *purine ring*) 22.8$_2$(O=C***C***H$_3$)

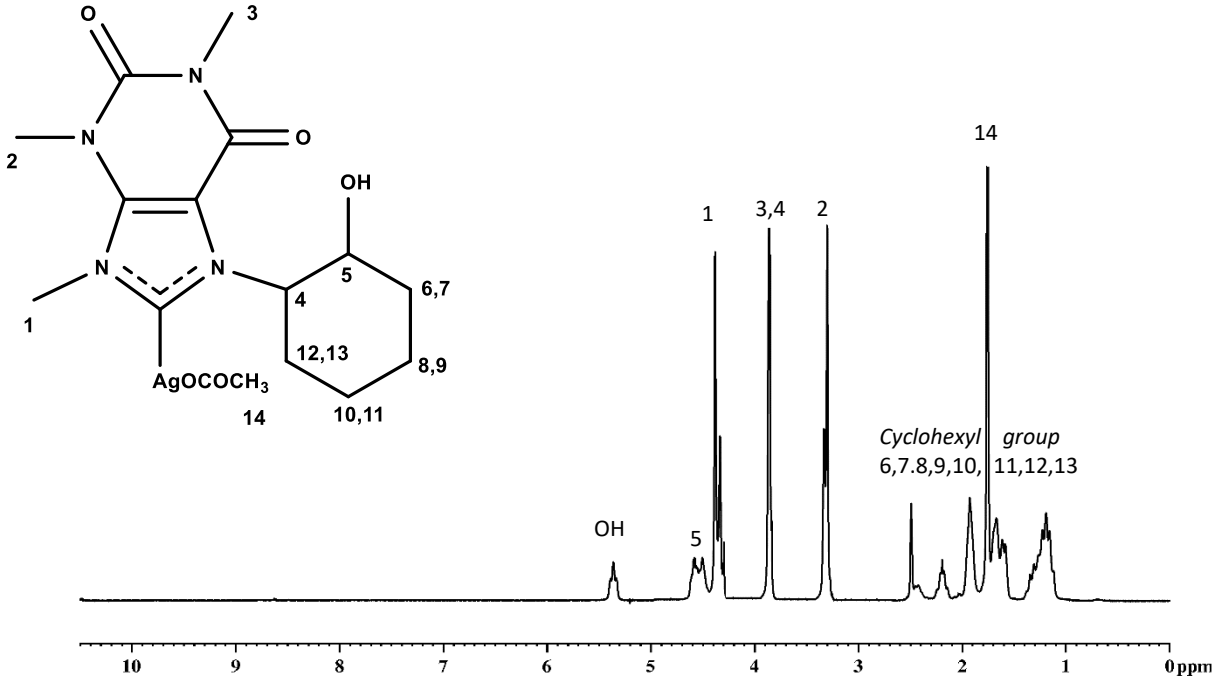

^{1}H-NMR (400 MHz DMSO-d$_6$): δ 5.1$_6$ (s,1H, O***H***), 4.4$_3$-4.3$_5$ (m,1H, C***H***OH), 4.2$_6$ (s,3H, NC***H***$_3$ imidazolium ring), 3.7$_6$(s,4H, NC***H***, N***CH***$_3$), 3.2$_5$ (s,3H, NC***H***$_3$), 2.1$_0$-17$_5$(m, 11H, O=CC***H***$_3$, ***Cyclohexyl***)

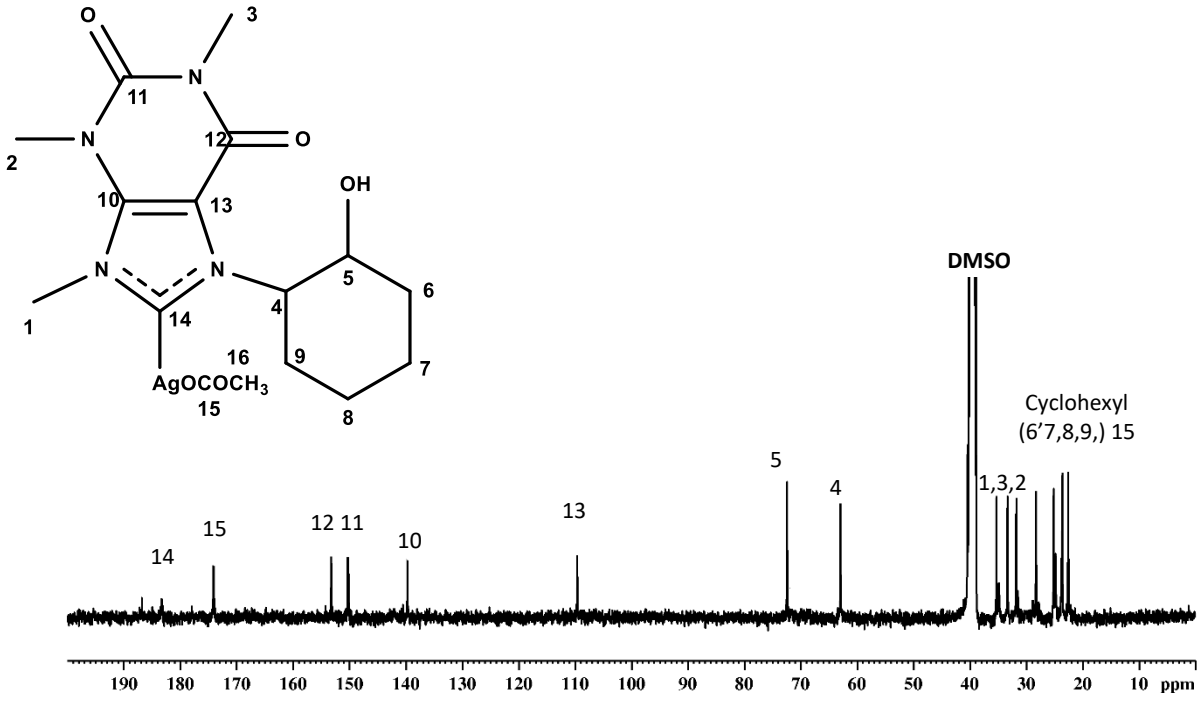

^{13}C-NMR (100 MHz, DMSO-d$_6$): δ 183.8$_5$(N***C***N), 170.4$_0$ (CH$_3$***C***=O), 153.2$_3$-150.2$_2$(***C***=O *purine ring*) 139.67 (*backbone carbon* ***C***=C),109.5$_7$ (*backbone carbon* C=***C***),72.3$_3$(O***C***H), 62.9$_0$(N***C***H), 37.8$_0$(N***C***H$_3$), 33.4$_0$, 28.4$_9$ (N***C***H$_3$ *purine ring*) 34.0$_2$-23.5$_5$(***Cyclohexyl group***) 22.8$_2$(O=C***C***H$_3$)

2.3.5 Characterization of Silver complexes AgL1-OAc, AgL2-OAc, AgL7-OAc

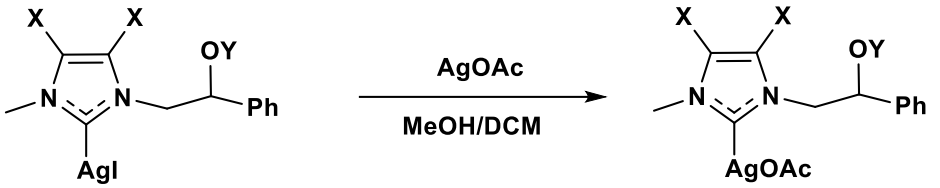

AgL1-OAc= X=H, Y=H
AgL2-OAc= X= Cl, Y=H
AgL7-OAc= X=H, Y=CH_3

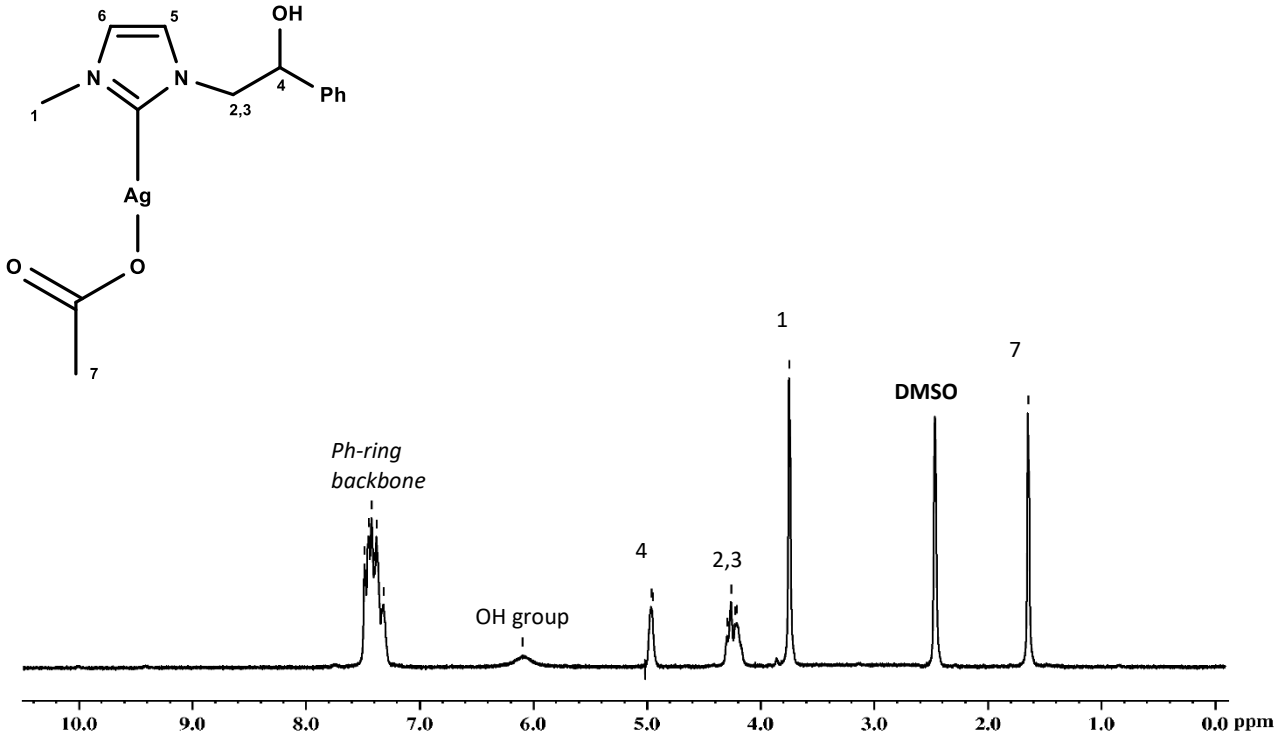

^{1}H-NMR (400 MHz DMSO-d_6): δ 7.4$_1$-7.2$_4$ (m, 7H, ***Ph ring***), 6.0$_5$(b, 1H, ***OH group***) 4.9$_4$-4.9$_3$ (m,1H, C***H***OH), 4.2$_9$ – 4.2$_1$ (m,2H, NC***H***$_2$), 3.7$_5$(s,3H, N***CH***$_3$), 1.7$_0$(s, 3H, OCOC***H***$_3$,)

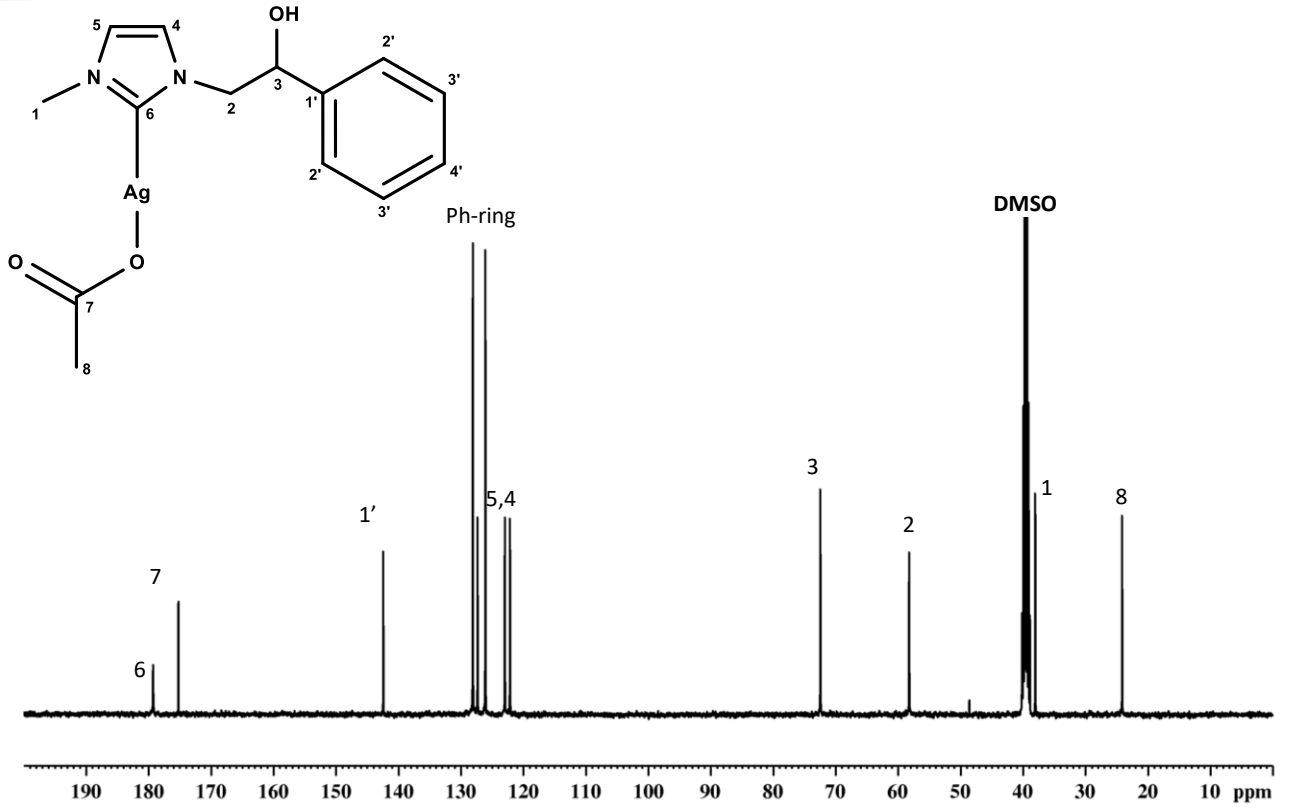

^{13}C-NMR (100 MHz, DMSO-d$_6$): δ 179.2$_8$ (N***C***N), 175.2$_5$ (O***C***OCH$_3$) 142.4$_3$ *(ipso aromatic carbon* (1′), **Ph-ring**), 128.1$_0$-126.0$_9$, (*aromatic carbons*, **Ph ring**), 122.96-122.13 (*backbone carbon* ***C*=*C***) 72.4$_3$(O***C***H), 58.2$_2$(N***C***H$_2$), 38.0$_2$ (N***C***H$_3$), 24.11 (OCO***C***H$_3$)

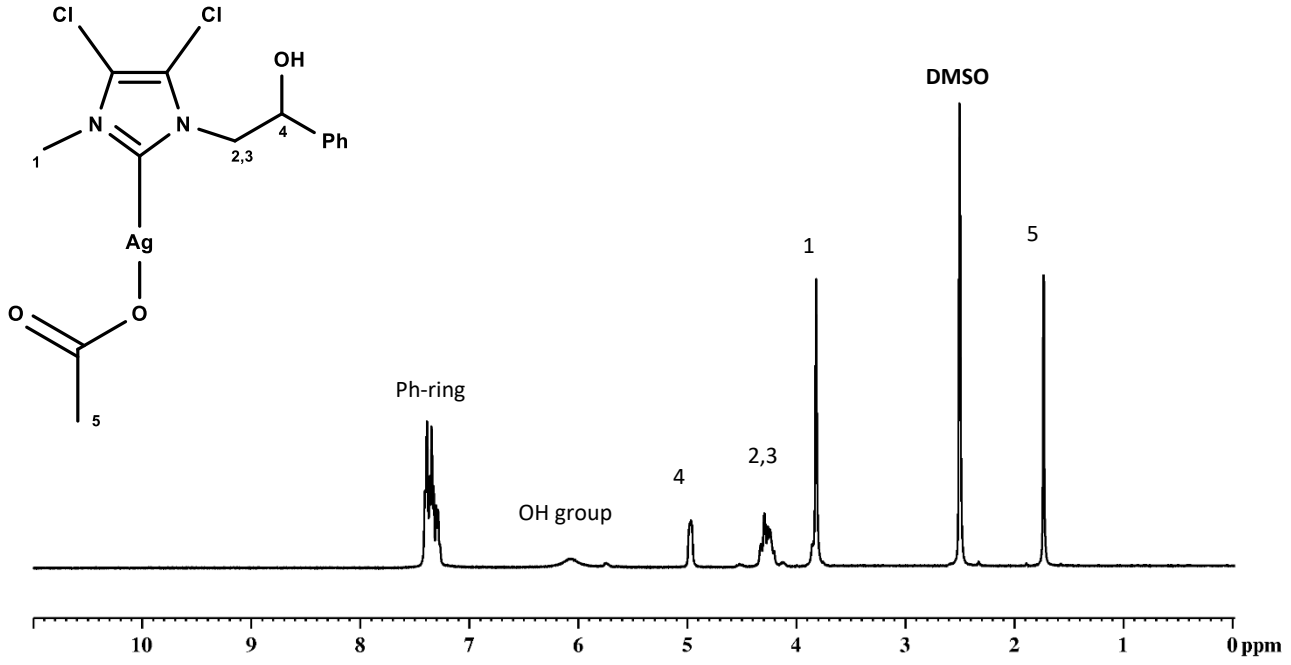

^{1}H-NMR (400 MHz DMSO-d$_6$): δ 7.4$_0$-7.28 (m, 5H, ***Ph ring***), 6.0$_5$(b, 1H, ***OH group***) 4.9$_6$-4.9$_3$ (m,1H, C***H***OH), 4.3$_2$ – 4.2$_3$ (m,2H, NC***H***$_2$), 3.8$_1$(s,3H, N***CH***$_3$), 1.7$_3$(s, 3H, COC***H***$_3$,).

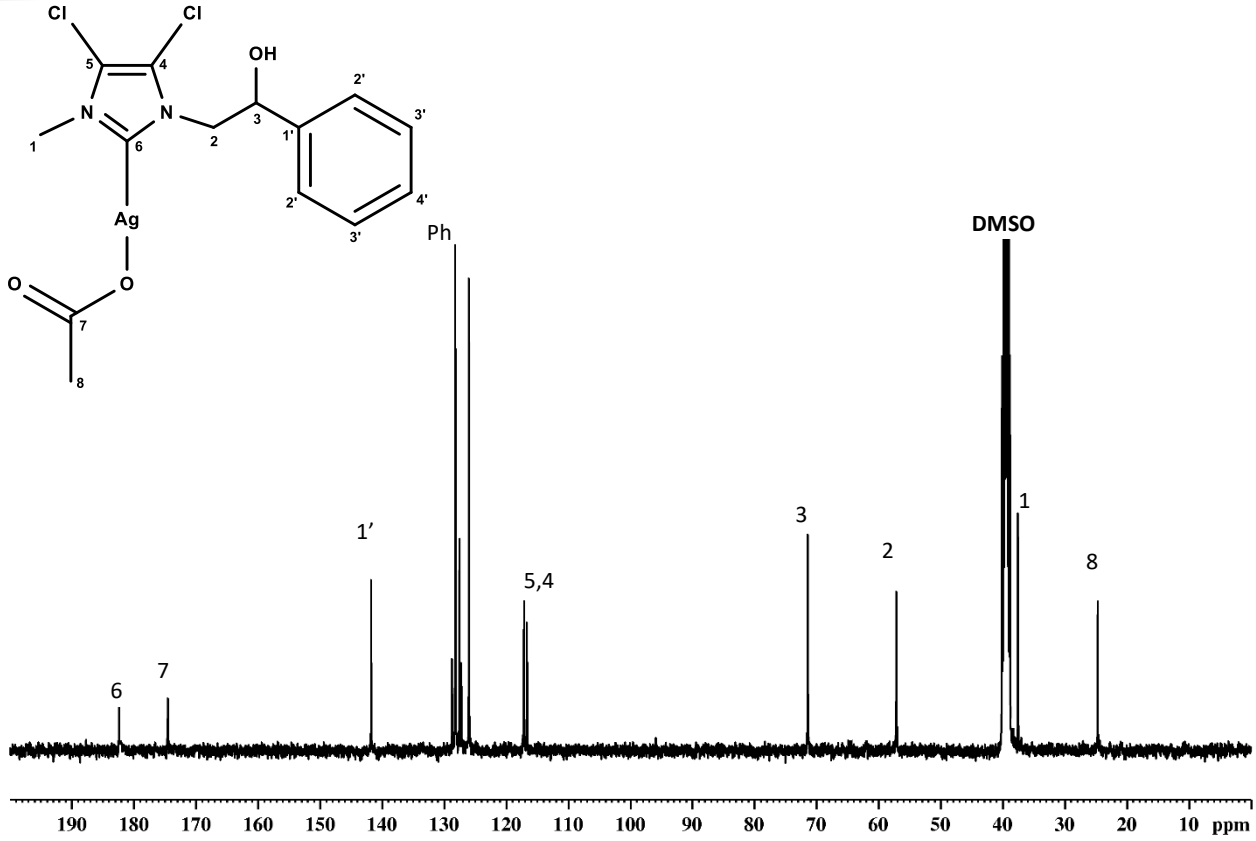

^{13}C-NMR (100 MHz, DMSO-d_6): δ 182.2$_6$ (N***C***N), 174.5$_3$ (O***C***OCH$_3$) 141.79 *(ipso aromatic carbon* (1'), **Ph-ring**), 128.2$_0$-126.0$_3$, (*aromatic carbons*, **Ph ring**), 117.1$_5$-116.6$_7$ (*backbone carbon* ***C*=*C***) 71.4$_4$(O***C***H), 57.1$_6$(N***C***H$_2$), 37.5$_7$ (N***C***H$_3$), 24.7$_1$ (OCO***C***H$_3$)

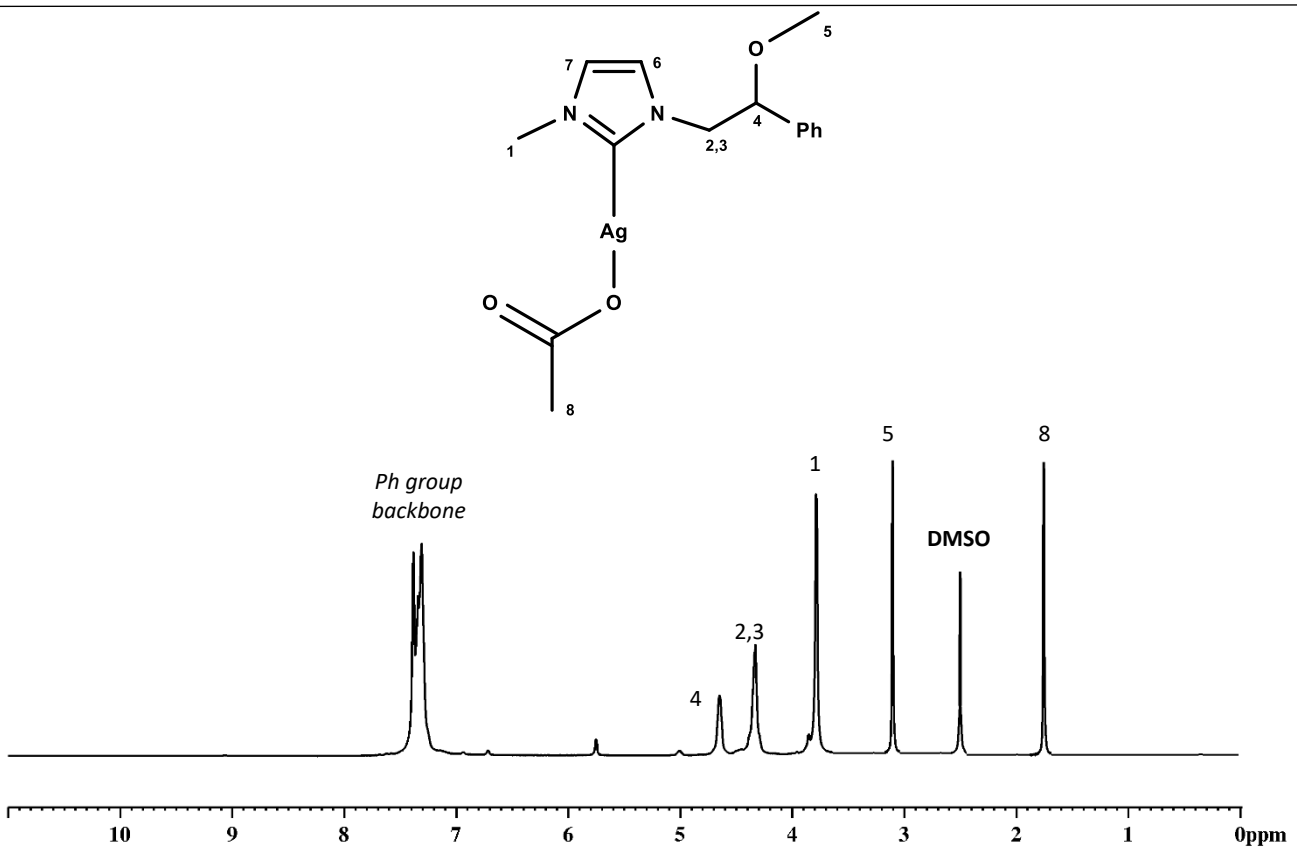

^{1}H NMR (400MHz, DMSO-d_6): δ 7.3$_4$-7.2$_6$ (m, 7H, ***Ph ring, backbone***), 4.6$_0$(m, 1H, OC***H***), 4.3$_0$-4.2$_7$(m, 2H, NC***H***$_2$), 3.7$_4$(s,3H, NC***H***$_3$), 3.0$_7$(s,3H, OC***H***$_3$).1.7$_5$ (s, 3H, COC***H***$_3$,).

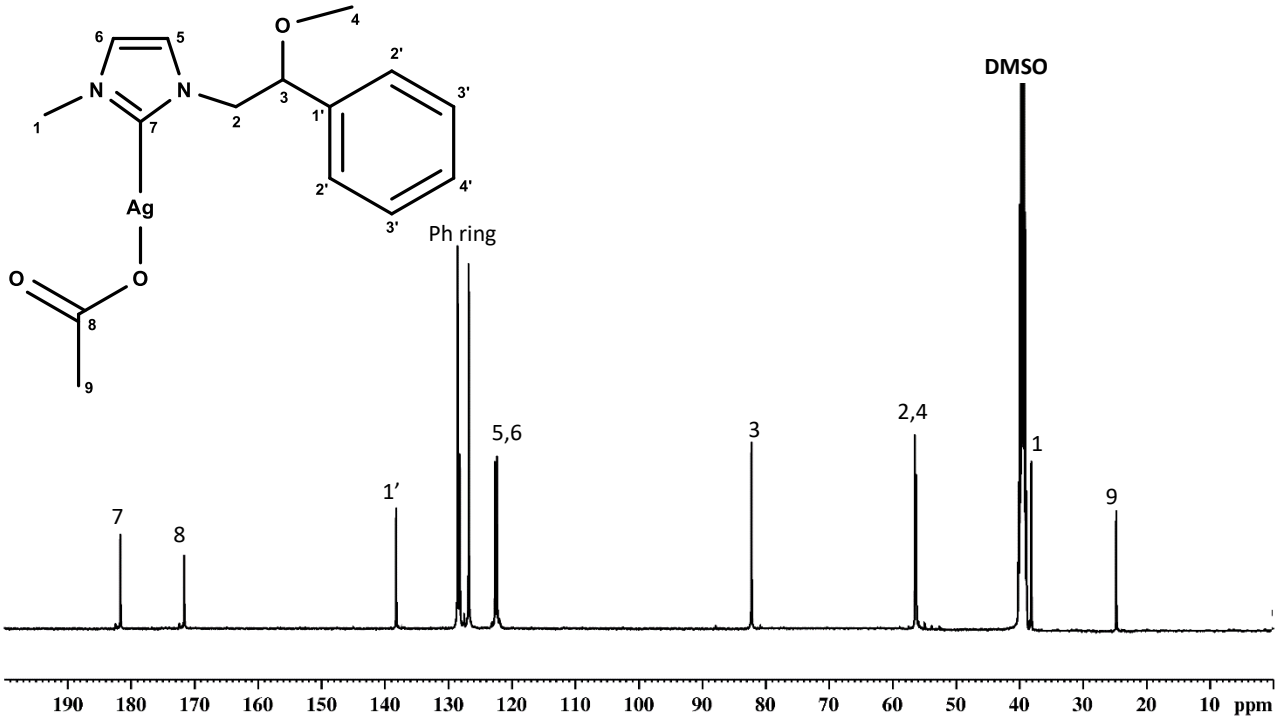

^{13}C-NMR (100 MHz, DMSO-d_6): δ 182.7$_5$ (N***C***N), 173.4$_3$ (O***C***OCH$_3$) 137.2$_1$ (*ipso* carbon of ***Ph ring***), 128.7$_2$, -126.6$_8$ (aromatic carbon, ***Ph ring***), 122.6$_0$, 122.3$_5$ (*backbone carbons* ***C=C***), 83.3$_2$ (***C***HO), 56.7$_9$ (N***C***H$_2$), 54.2$_7$ (O***C***H$_3$), 38.2$_6$(N***C***H$_3$) 24.1$_1$ (OCO***C***H$_3$).

2.4 Synthesis of gold(I) *N*-heterocyclic carbene complexes

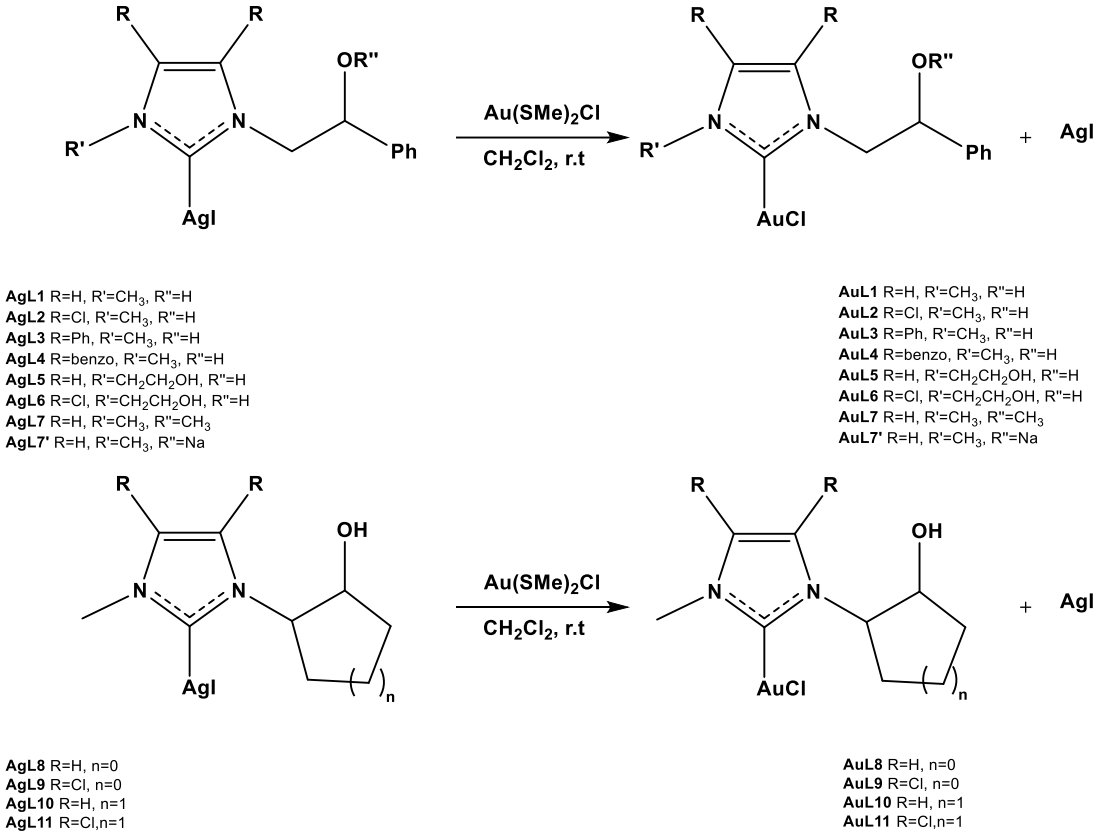

Figure 50 Synthesis of AuNHC complexes

Gold NHC complexes have been synthesized following the *trans*-metalation route, by the reaction of silver NHC complexes with chloro gold(I) dimethylsulfide [Au(SMe_2)Cl]. The driving forces of the reaction are the formation of a less labile carbene gold bond and the formation of insoluble silver iodide[44]. The obtained complexes were analyzed by spectroscopic techniques (^1H, ^{13}C NMR) and mass spectrometry. The NMR spectra have shown all expectable signals and they are reported in the next sections. The formation of gold complexes was confirmed by the 'shift' to up-field of the signals of carbene carbon atom in gold complexes, in comparison with silver analogs.

The mass spectrometry spectra showed more peaks attributable to a bis carbene structure $[Au(NHC)_2]^+$. However, for complexes **AuL2** and **AuL7** it was possible the determination of structure by X-ray diffraction. The X-ray analysis has revealed a linear monocarbene structure. Thus, both AuNHC and AgNHC complexes can highlight an equilibrium between mono-carbene neutral specie [M(NHC)X] and bis-carbene ionic structure $[M(NHC)2]^+[MX2]^-$.

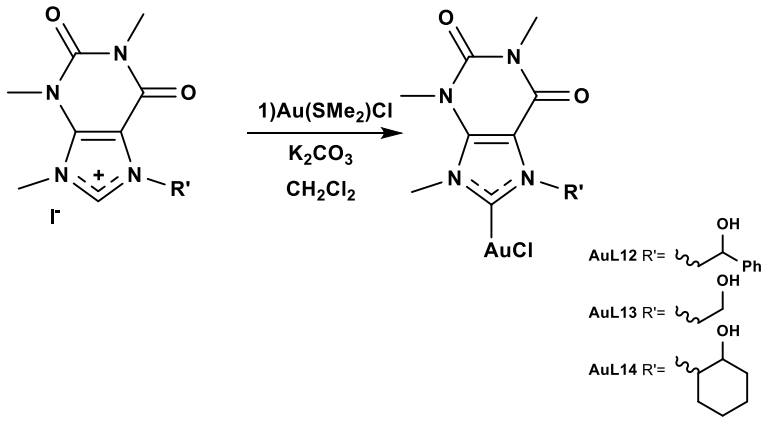

Figure 51 Synthesis of Xanthium gold NHC complexes

Gold xanthinium complexes have synthesized following the mild base route [45,46], by the reaction of imidazolium salt, $Au(SMe_2)Cl$, and potassium carbonate (K_2CO_3). The complexes were characterized by NMR and mass spectrometry. The disappearance of the signal of imidazolium proton in ^{1}H-NMR spectra, and the presence of a sharp signal attributable to carbene carbon have supported the formation of the complexes.

2.4.1 Characterization of Gold complexes AuL1-L11

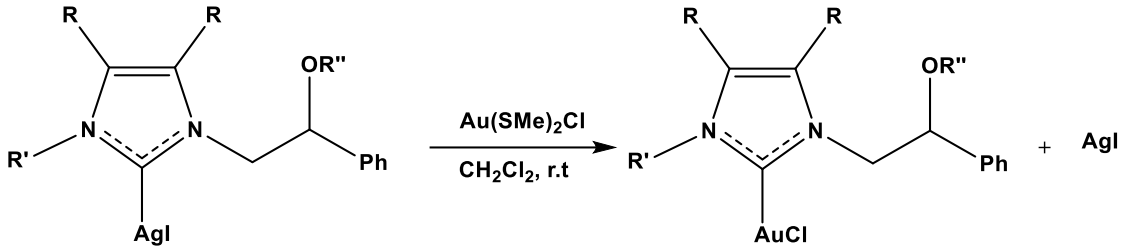

AgL1 R=H, R'=CH_3, R''=H
AgL2 R=Cl, R'=CH_3, R''=H
AgL3 R=Ph, R'=CH_3, R''=H
AgL4 R=benzo, R'=CH_3, R''=H
AgL5 R=H, R'=CH_2CH_2OH, R''=H
AgL6 R=Cl, R'=CH_2CH_2OH, R''=H
AgL7 R=H, R'=CH_3, R''=CH_3
AgL7' R=H, R'=CH_3, R''=Na

AuL1 R=H, R'=CH_3, R''=H
AuL2 R=Cl, R'=CH_3, R''=H
AuL3 R=Ph, R'=CH_3, R''=H
AuL4 R=benzo, R'=CH_3, R''=H
AuL5 R=H, R'=CH_2CH_2OH, R''=H
AuL6 R=Cl, R'=CH_2CH_2OH, R''=H
AuL7 R=H, R'=CH_3, R''=CH_3
AuL7' R=H, R'=CH_3, R''=Na

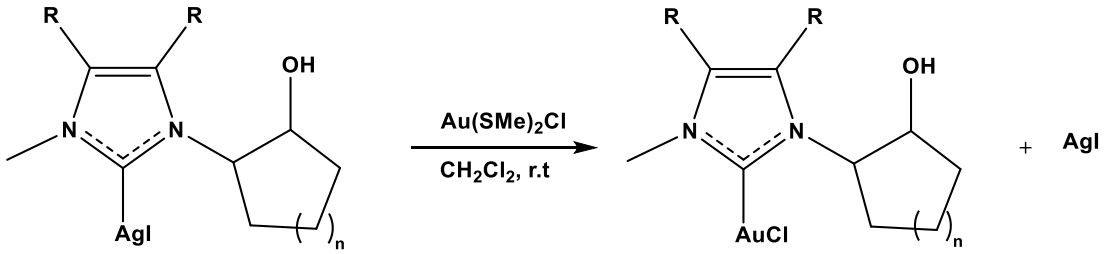

AgL8 R=H, n=0
AgL9 R=Cl, n=0
AgL10 R=H, n=1
AgL11 R=Cl,n=1

AuL8 R=H, n=0
AuL9 R=Cl, n=0
AuL10 R=H, n=1
AuL11 R=Cl,n=1

The complete characterization of **AuL1** and **AuL2** is reported in the literature, published by the research group in which I carried out my Ph.D. thesis work [128,130]. The molecular structure of complex **AuL2** has been determined by Prof. Alessandra Crispini of the University of Calabria.

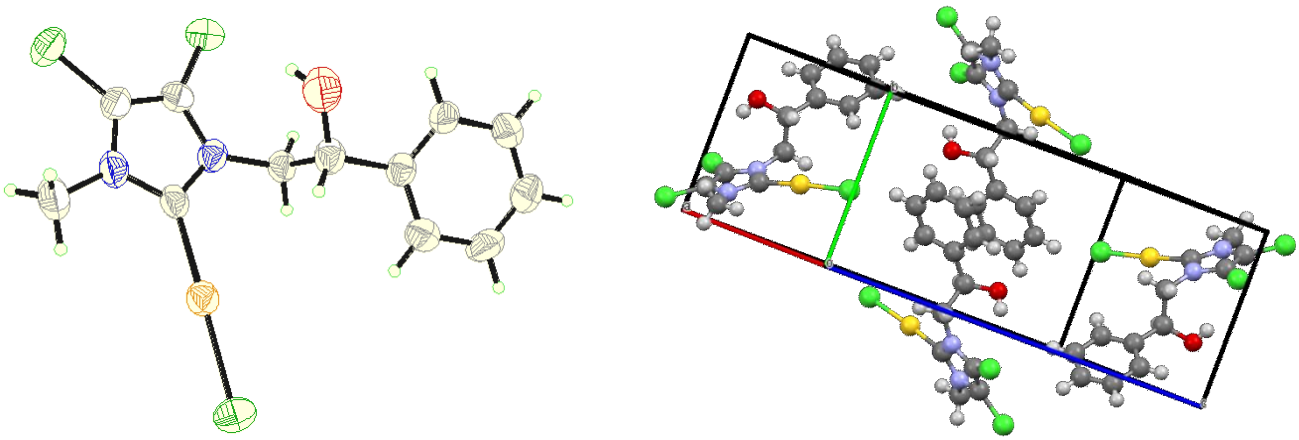

Figure 52 ORTEP and Crystal packing of complex AuL2

Parameters	**Complex AuL2**
Empirical formula	$C_{12}H_{12}AuCl_3N_2O$
Formula weight	503.6
Crystal system	monoclinic
Space group	P $2_1/c$
T(K)	296
radiation	Mo Kα(0.71073)
a(Å)	13.1137(14)
b(Å)	7.5187(7)
c(Å)	16.3437(17)
α(deg)	90
β(deg)	108.986(5)
γ(deg)	90
V($Å^3$)	1523.8(3)
Z	2
ρ (g cm^{-1})	2.195
μ(mm^{-1})	10.172
$\theta range$(°)	2.613- 26.872
Reflections collected	22336
Unique data	3276
Observed reflections	2807

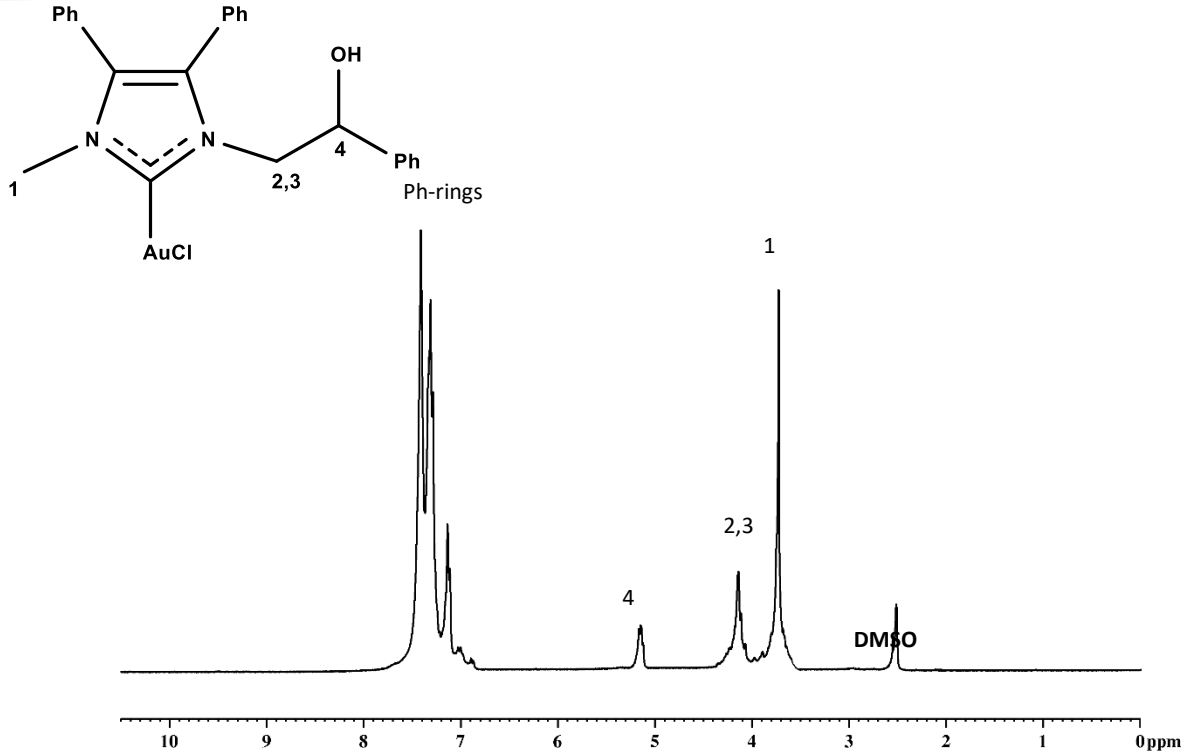

^{1}H NMR (400MHz, DMSO-d$_6$): δ 7.3$_6$-7.1$_4$ (m, 15H, ***Ph rings***) 5.1$_3$(m, 1H, OC***H***); 4.1$_7$-4.0$_6$(m, 2H, NC***H***$_2$); 3.7$_2$(s,3H, NC***H***$_3$).

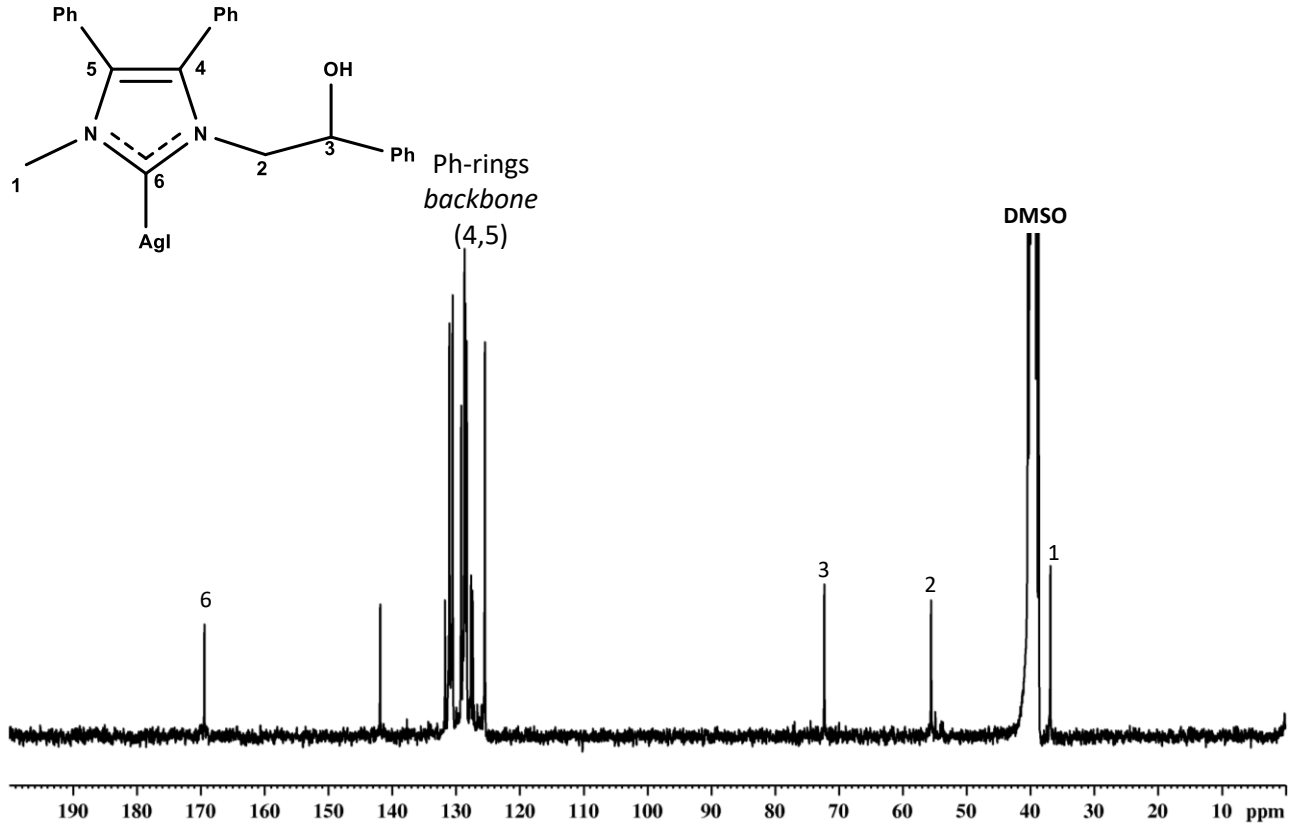

^{13}C-NMR (100 MHz, DMSO-d$_6$): δ 169.4$_6$ (N***C***N), 141.8$_4$ (*ipso aromatic carbon*, **Ph-ring**), 131.7$_0$-125.4$_9$, (*aromatic carbons*, **Ph ring,** *backbone*), 72.3$_0$(O***C***H), 55.5$_7$(N***C***H$_2$), 36.9$_1$(N***C***H$_3$)

MALDI-ToF (m/z): 905.31858 Da attributable to a structure a bis-carbene structure $[C_{48}H_{44}AuN_4O_2]^+$

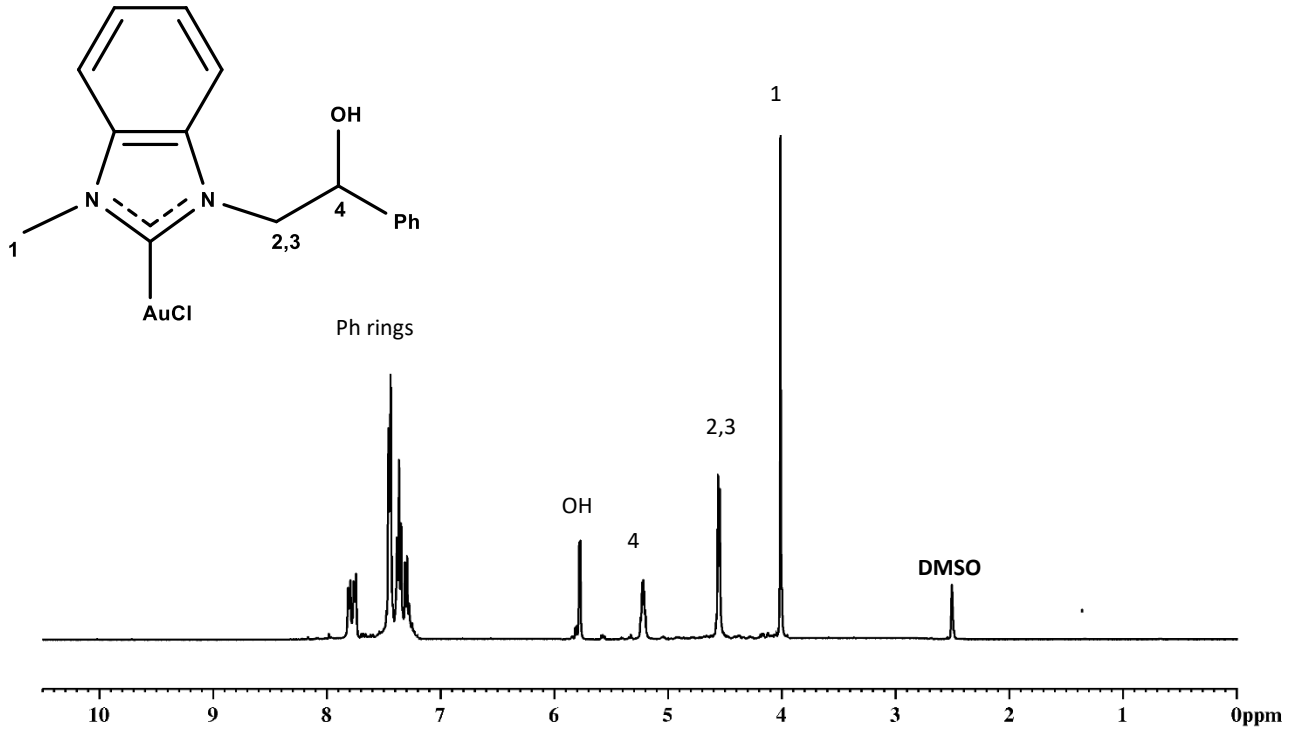

^{1}H-NMR (400MHz, DMSO-d_6): δ 7.8$_0$-7.2$_8$ (m, 9H, ***Ph ring***); 5.7$_6$(s, 1H, O***H***); 5.2$_2$-5.2$_1$ (dd, 1H, OC***H***); 4.6$_9$-4.5$_4$ - 4.5$_0$(m, 2H, NCH_2); 4.0$_0$(s,3H, NCH_3).

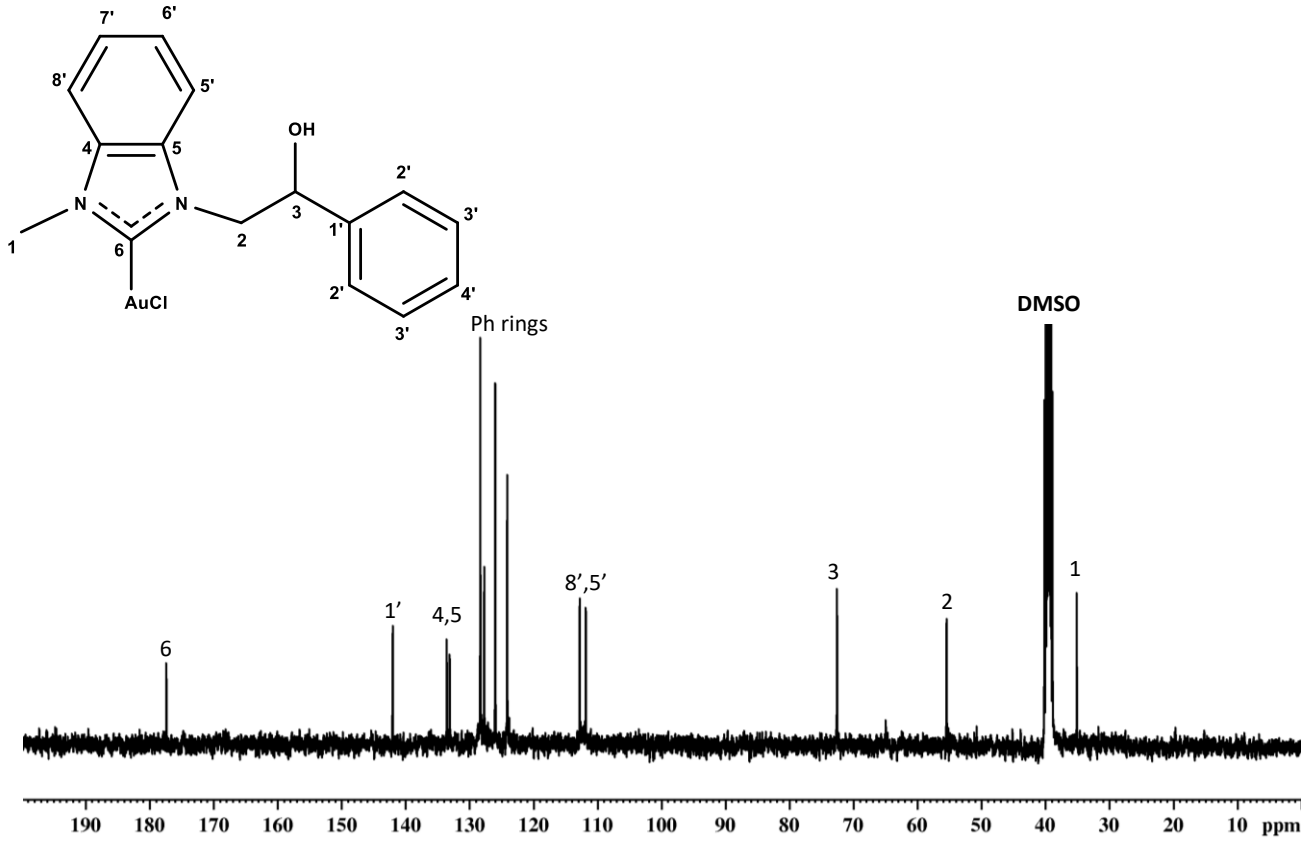

^{13}C-NMR (100 MHz, DMSO-d_6): δ 177.4$_1$ (N***C***N) 141.9$_7$ (*ipso aromatic carbon*, **Ph-ring**), 133.5$_5$-133.1$_0$ (*backbone carbons*, N***C*=*C***N), 128.3-111.8$_2$, (*aromatic carbons*, **Ph rings**), 72.5$_6$(O***C***H), 55.4$_2$(N***C***H$_2$), 35.0$_0$(N***C***H$_3$)

MALDI-ToF (m/z): 701.22194 Da attributable to a structure a bis-carbene structure $[C_{32}H_{32}AuN_4O_2]^+$

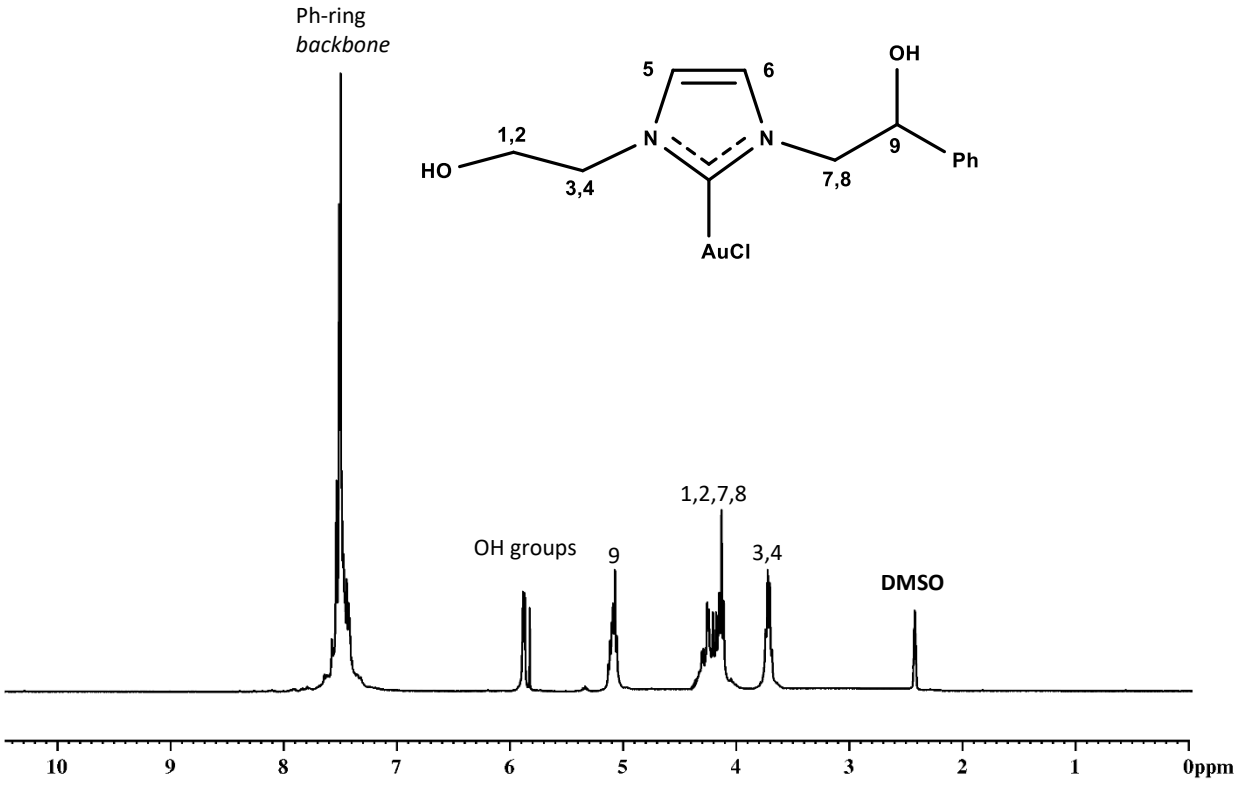

^{1}H-NMR (400MHz, DMSO-d_6): δ 7.3$_8$-7.3$_1$ (m, 7H, ***Ph rings***); 5.8$_8$(s, 1H, O***H***); 5.0$_7$ (s, 1H, O***H***) 4.9$_9$(m, 1H, OC***H***); 4.3$_6$-4.2$_7$(m, 4H, NCH$_2$C***H***$_2$OH, NC***H***$_2$CHOH); 3.7$_3$(s,2H, NC***H***$_2$CH$_2$OH).

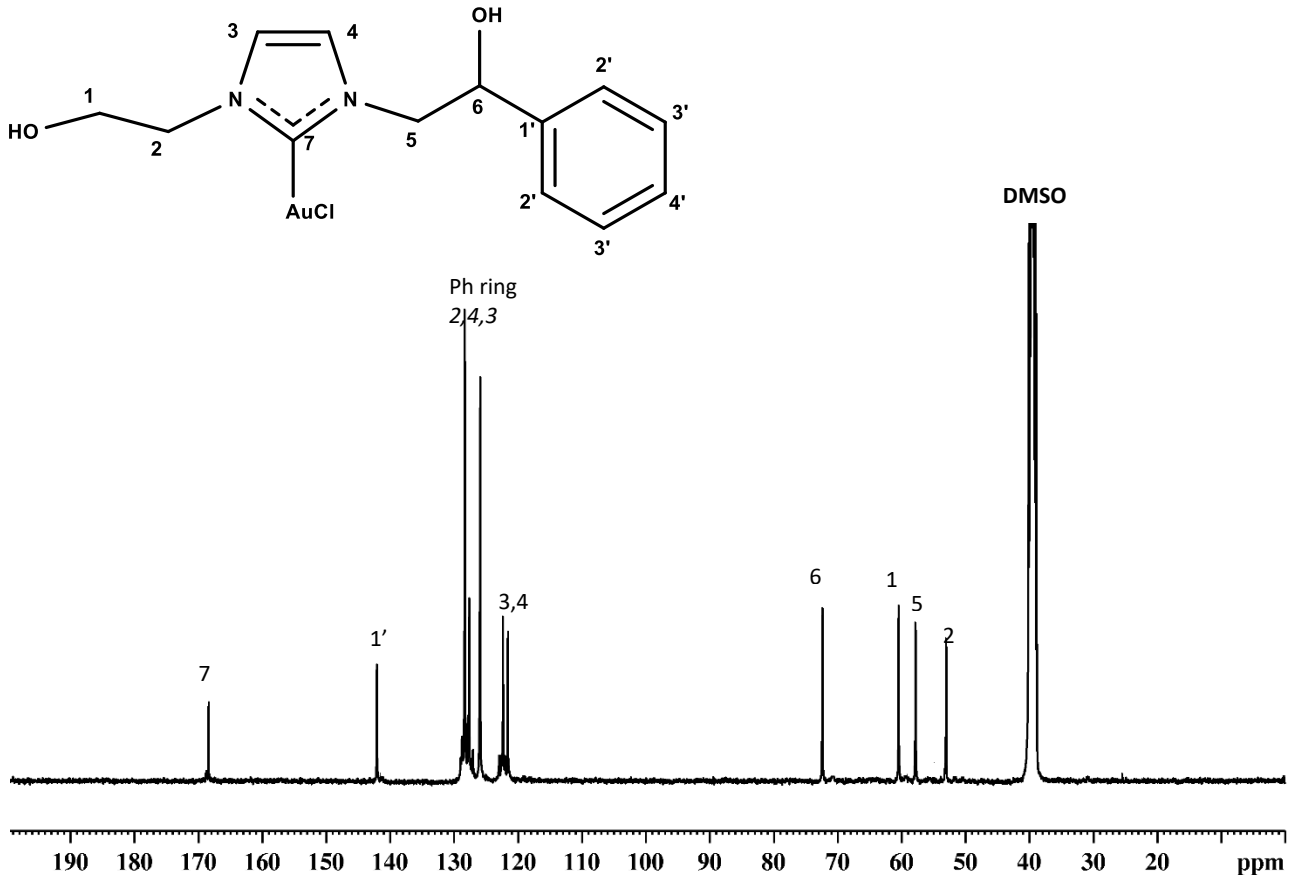

^{13}C-NMR (100 MHz, DMSO-d_6): δ 168.3$_7$(N***C***N), 142.0$_7$ (*ipso* carbon of ***Ph ring***), 128.3$_0$, 127.7$_9$, 127.6$_1$ (aromatic carbon, ***Ph ring***), 122.3$_0$, 121.5$_5$ (*backbone carbons*), 72.3$_6$ (***C***HOH), 60.4$_4$ (***C***H$_2$OH), 57.7$_9$ (N***C***H$_2$CHOH), 53.0$_0$ (N***C***H$_2$CH$_2$OH).

ESI-MS (CH$_3$CN m/z): 661.20838 Da attributable to $[C_{26}H_{32}AuN_4O_4]^+$

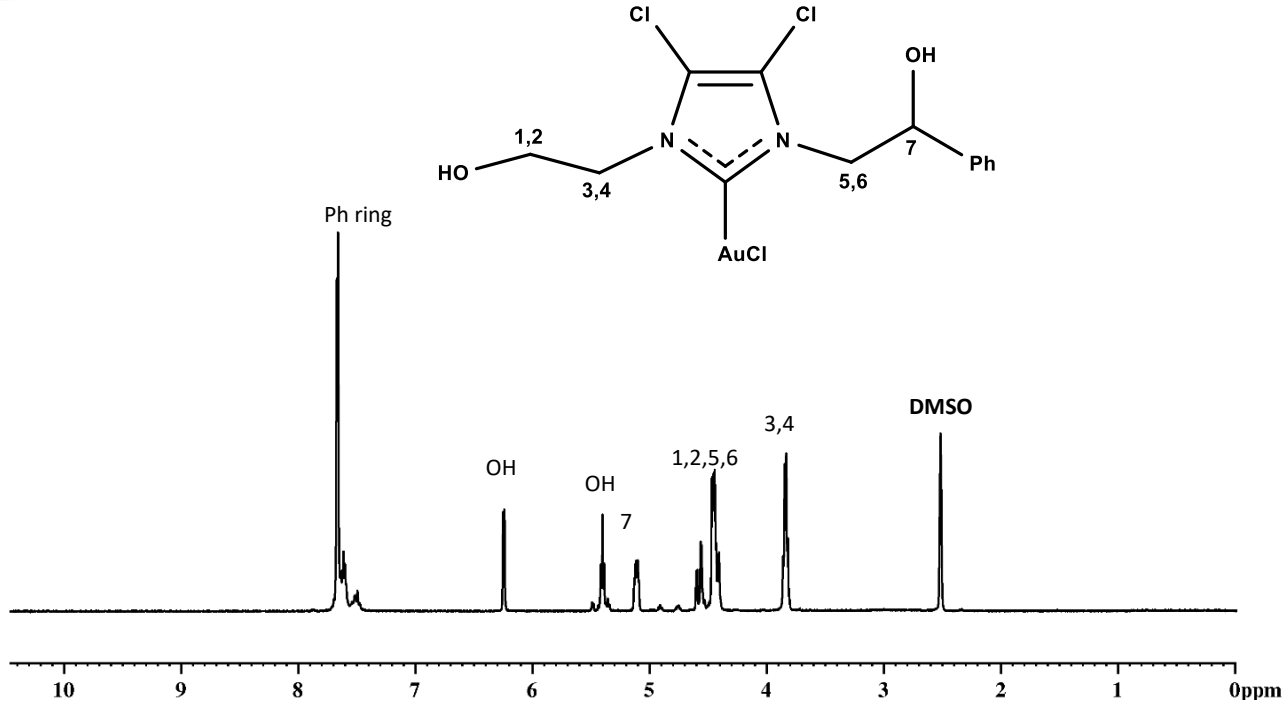

^{1}H-NMR (400MHz, DMSO-d$_6$): δ 7.3$_8$-7.2$_7$ (m, 5H, ***Ph ring***); 5.8$_9$(s, 1H, O***H***); 5.0$_7$ (s, 1H, O***H***) 4.9$_9$(m, 1H, OC***H***); 4.3$_3$-4.2$_7$(m, 4H, NCH$_2$C***H***$_2$OH, NC***H***$_2$CHOH); 3.7$_4$(s,2H, NC***H***$_2$CH$_2$OH).

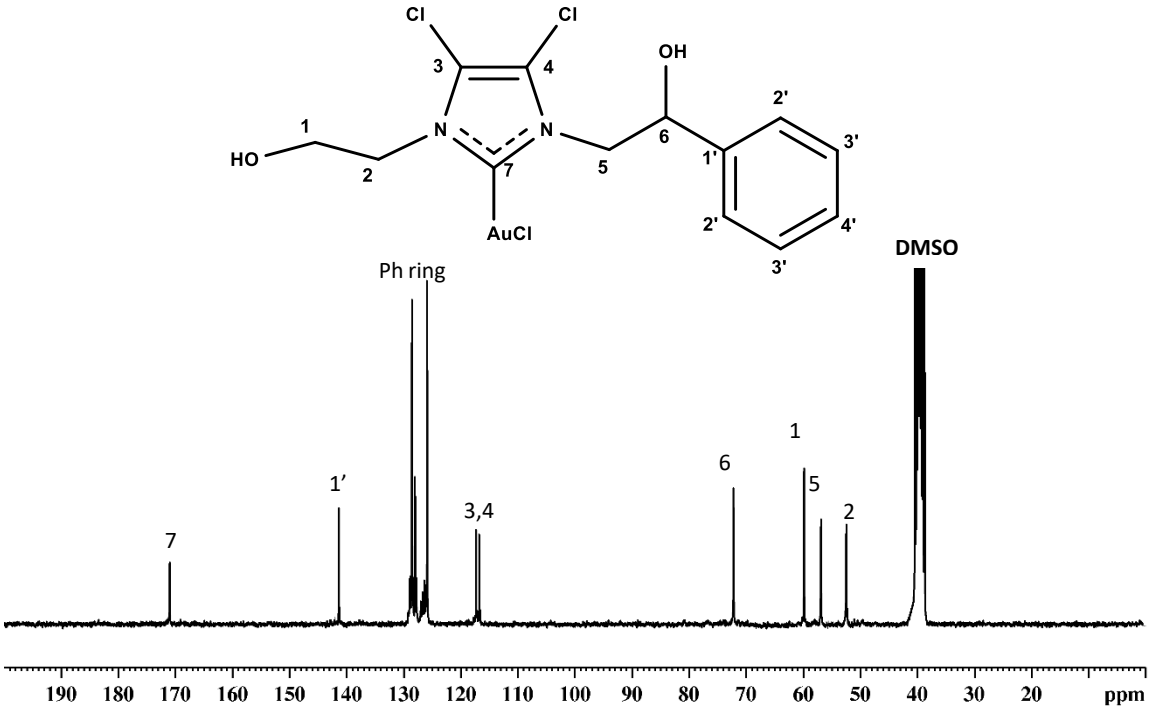

^{13}C-NMR (100 MHz, DMSO-d$_6$): δ 170.9$_0$ (N***C***N), 141.3$_5$ (*ipso* carbon of ***Ph ring***), 128.4$_1$, 127.9$_2$, 125.0$_8$ (aromatic carbon, ***Ph ring***), 117.2$_0$, 116.7$_4$ (*backbone carbons*), 72.1$_4$ (***C***HOH), 59.8$_9$ (***C***H$_2$OH), 56.8$_9$ (N***C***H$_2$CHOH), 52.3$_7$ (N***C***H$_2$CH$_2$OH).

ESI-MS (CH$_3$CN m/z): 707.99716 Da attributable to [C$_{26}$H$_{32}$AgN$_4$O$_4$]$^+$

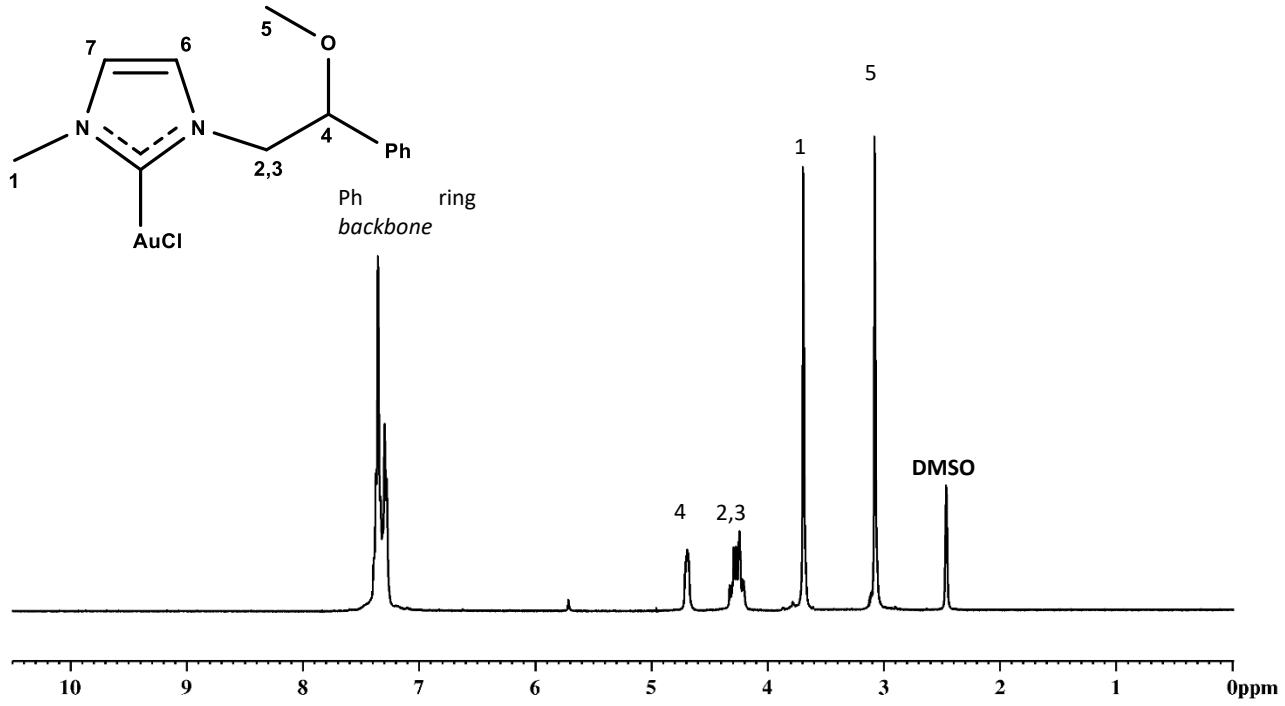

^{1}H NMR (400MHz, DMSO-d$_6$): δ 7.3$_5$-7.2$_9$ (m, 7H, ***Ph ring, backbone***), 4.6$_9$(m, 1H, OC***H***), 4.3$_2$-4.2$_6$(m, 2H, NC***H***$_2$), 3.7$_0$(s,3H, NC***H***$_3$), 3.0$_7$(s,3H, OC***H***$_3$).

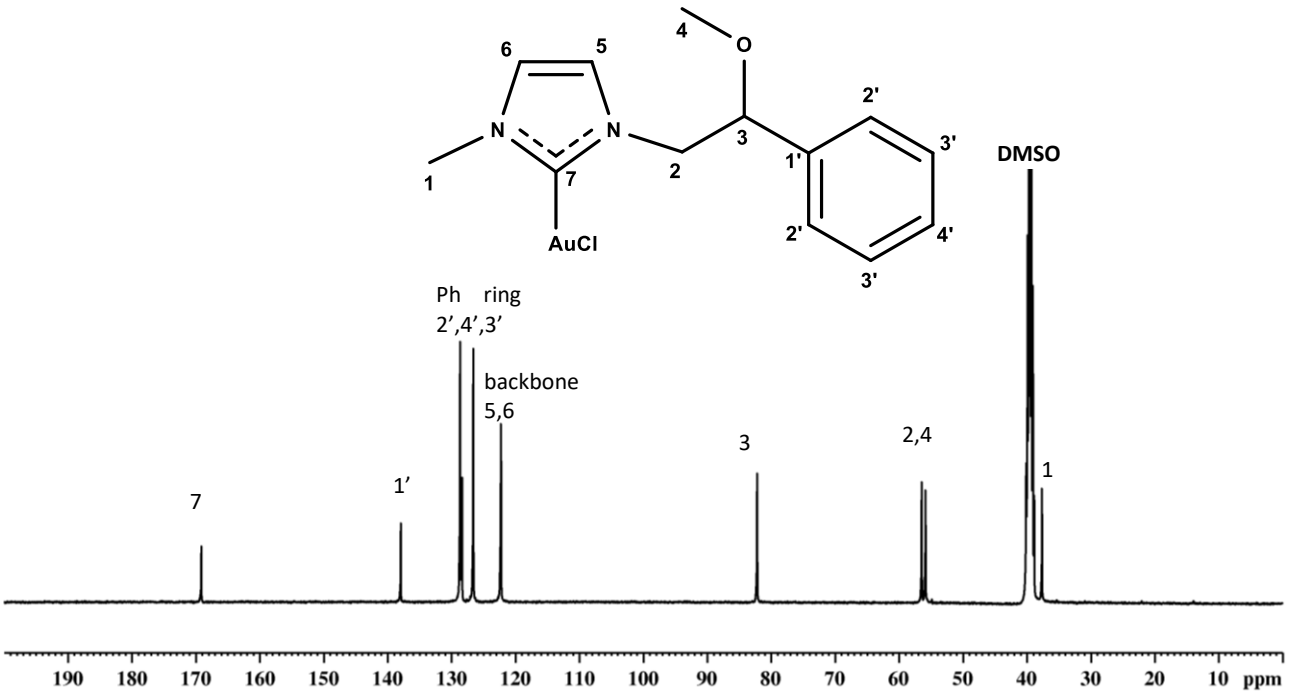

^{13}C-NMR (100 MHz, DMSO-d$_6$): δ 169.1$_0$ (N***C***N), 137.9$_1$ (*ipso* carbon of ***Ph ring***), 128.6$_1$, 128.3$_2$, 126.6$_8$ (aromatic carbon, ***Ph ring***), 122.3$_0$, 122.2$_5$ (*backbone carbons*), 82.2$_4$ (***C***HO), 56.5$_9$ (N***C***H$_2$), 55.8$_7$ (O***C***H$_3$), 37.6$_6$(N***C***H$_3$).

MALDI-ToF (m/z): 629.2267 Da attributable to [C$_{26}$H$_{32}$AgN$_4$O$_2$]$^+$

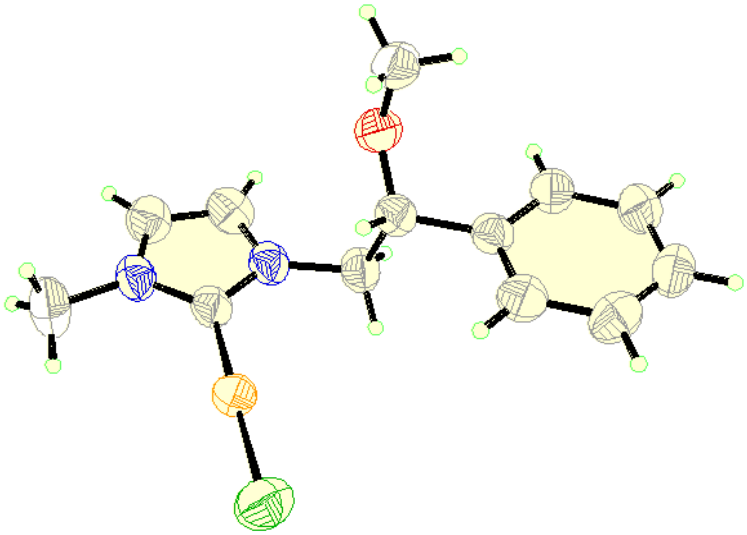

Figure 53 ORTEP of the complex AuL7

The molecular structure of complex **AuL7** has been determined by Prof. Alessandra Crispini of the University of Calabria. The X-ray analysis of the complex AuL7 (**Figure 53**) has revealed a neutral mono carbene structure. The C $_{carbene}$-Au-Cl bond is approximately linear, with an angle of 177.38(9)°. The length of the bonds C$_{carbene}$Au and Au-Cl are respectively 1.937(3) Å and 2.294(1) Å; these lengths are comparable with other known Au-NHC complexes[142–144]. The lowest distance among Au-Au atoms is found to be 5.84 Å, in 3D packaging (**Figure 54**). Thus, it was not observed any aurophlic interactions. The methylene group, of each molecule, interacts with the chlorine atom[145]. The length and the angle of this bond are respectively 2.947 Å and 155.3°. Every single ring interacts with the methyl group and with another benzene ring through CH-π interaction.

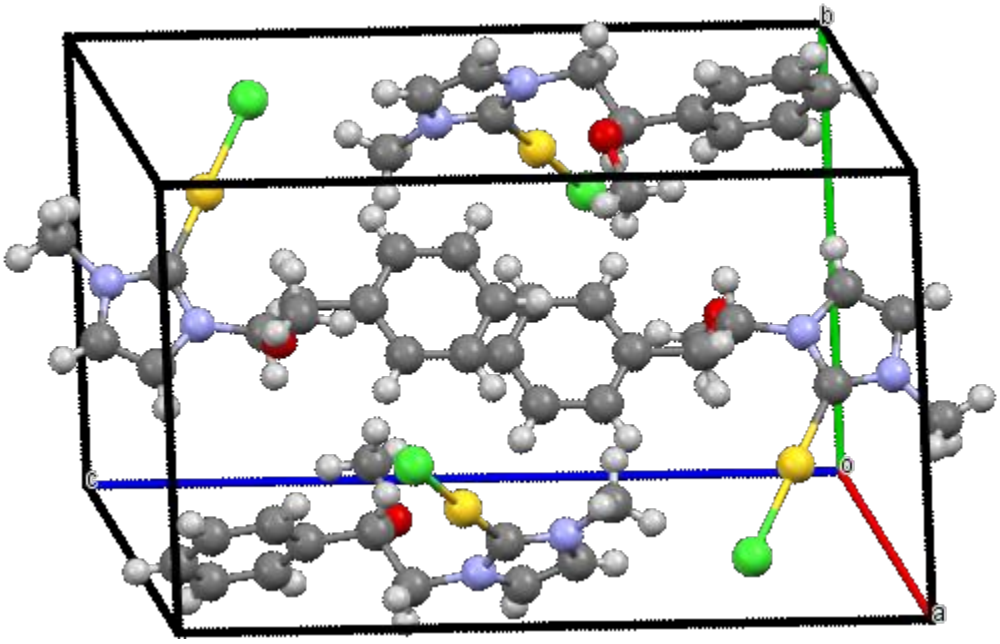

Figure 54 Crystal packing of complex AuL7. Showing the intermolecular interactions

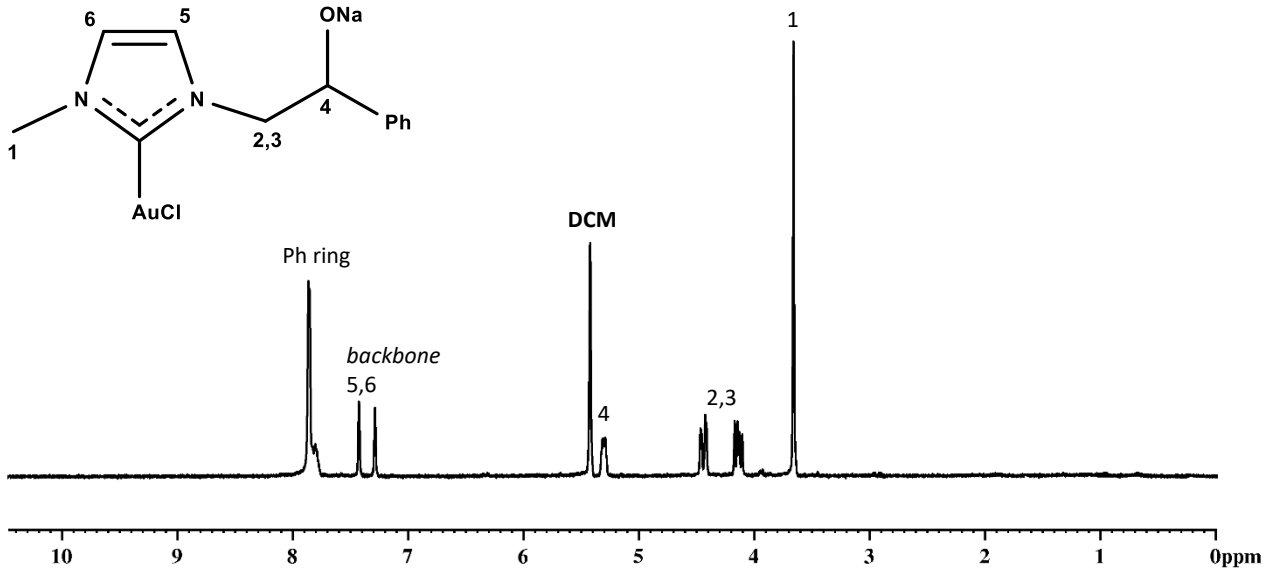

^{1}H NMR (400MHz, CD_2Cl_2-d_2): δ 7.3$_6$-7.3$_3$ (m, 5H, ***Ph ring***), 6.8$_9$-6.7$_9$ (s, 2H, ***backbone***), 5.1$_3$(t, 1H, $^{-}$OC***H***), 4.4$_0$-4.3$_0$(m, 2H, NC***H***$_2$), 3.8$_6$(s,3H, NC***H***$_3$).

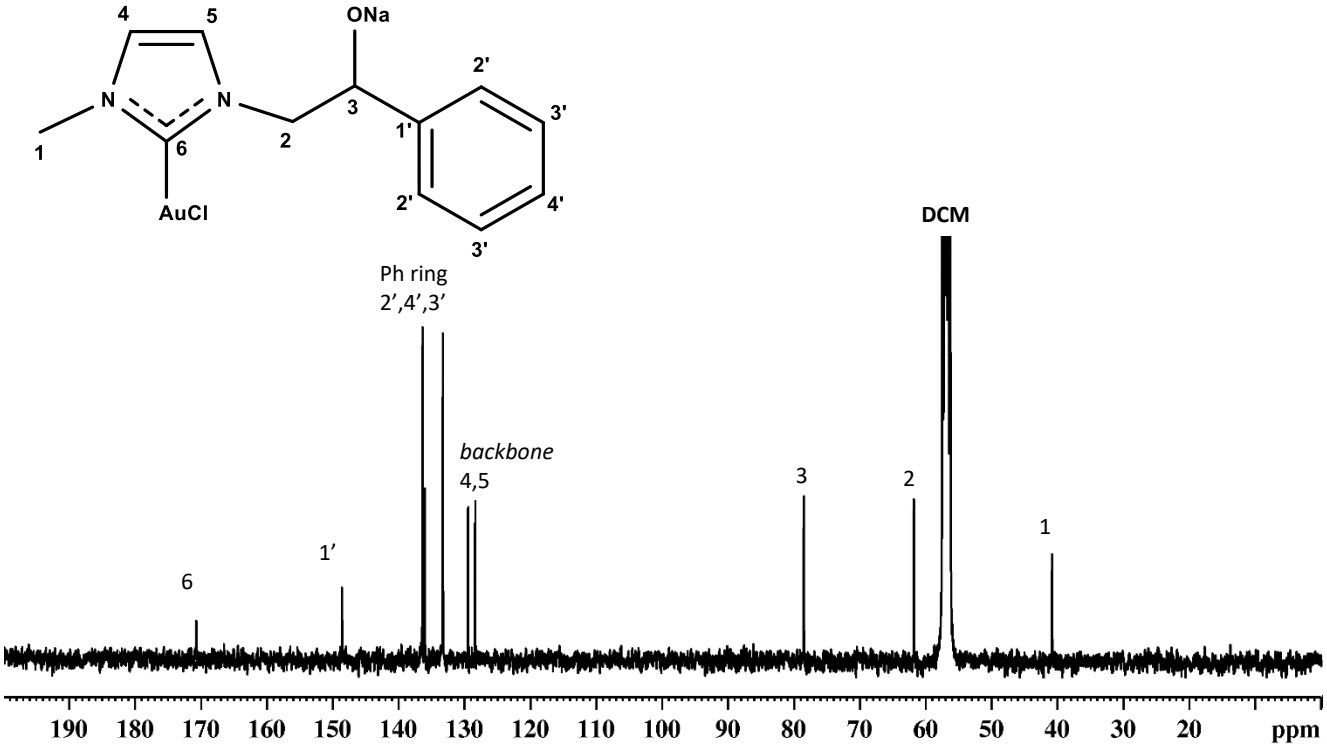

^{13}C-NMR (100 MHz, CD_2Cl_2-d_2): δ 171.9$_0$ (N***C***N), 141.8$_1$ (*ipso* carbon of ***Ph ring***), 129.5$_1$, 129.3$_2$, 129.1$_8$ (aromatic carbon, ***Ph ring***), 122.9$_0$, 121.8$_5$ (*backbone carbons*), 74.5$_3$ (***C***HO^{-}), 58.7$_9$ (N***C***H$_2$), 38.8$_6$(N***C***H$_3$).

ESI-MS (CH_2Cl_2, m/z): 612.3657 Da attributable to $[C_{22}H_{18}AuN_4O_2Na_2]^+$

The complete characterization of complexes **AuL8**, **AuL9**, **AuL10** is reported in literature by us[128,129].

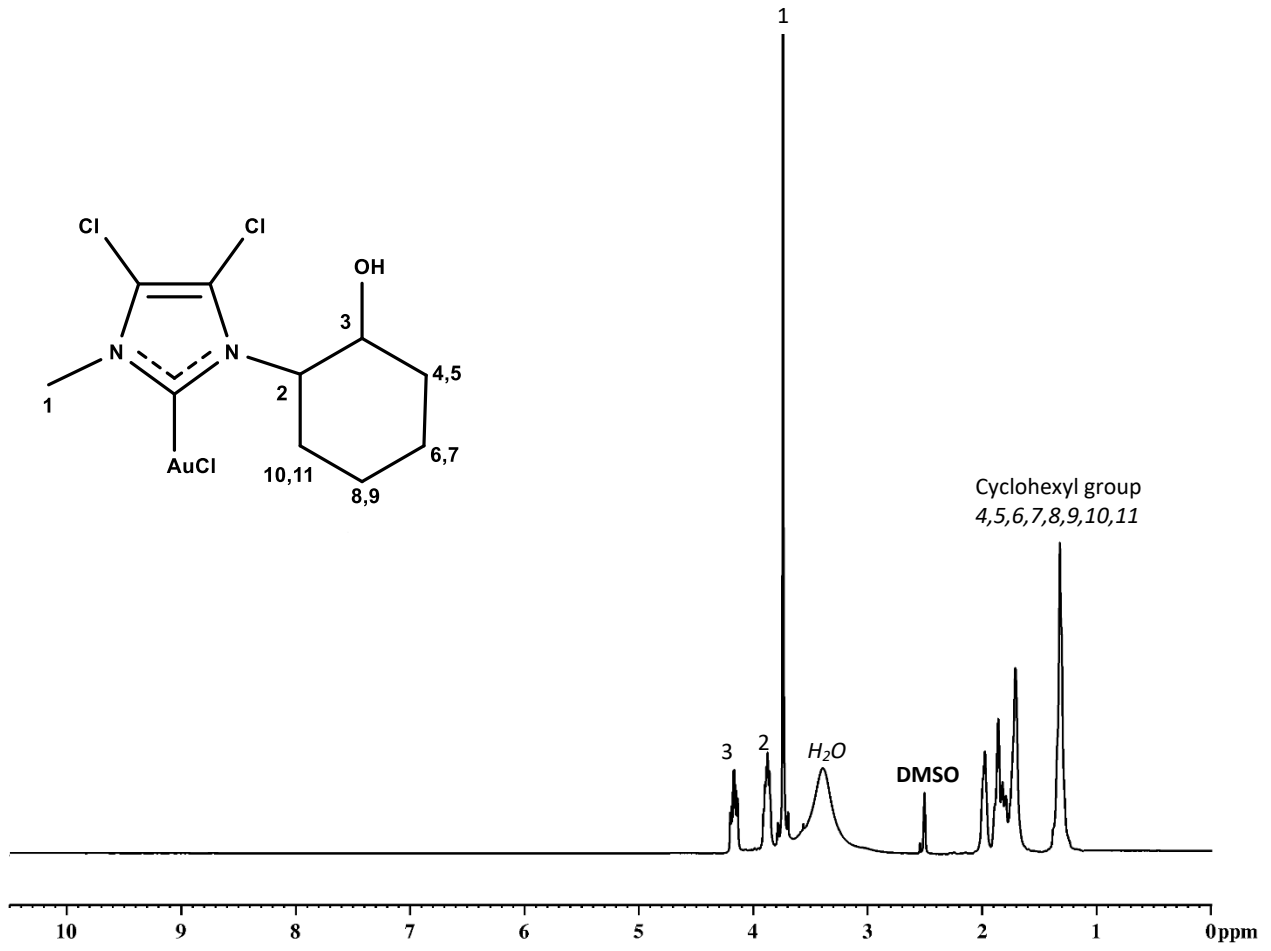

^{1}H-NMR (400MHz, DMSO-d_6): δ 4.1$_7$-4.1$_2$(m, 1H, HOC***H***), 3.8$_9$-3.8$_6$(s,1H, NC***H***), 3.7$_3$ (s, 3H, NC***H***$_3$), 1.9$_7$-1.2$_9$ (***Cyclohexyl*** group).

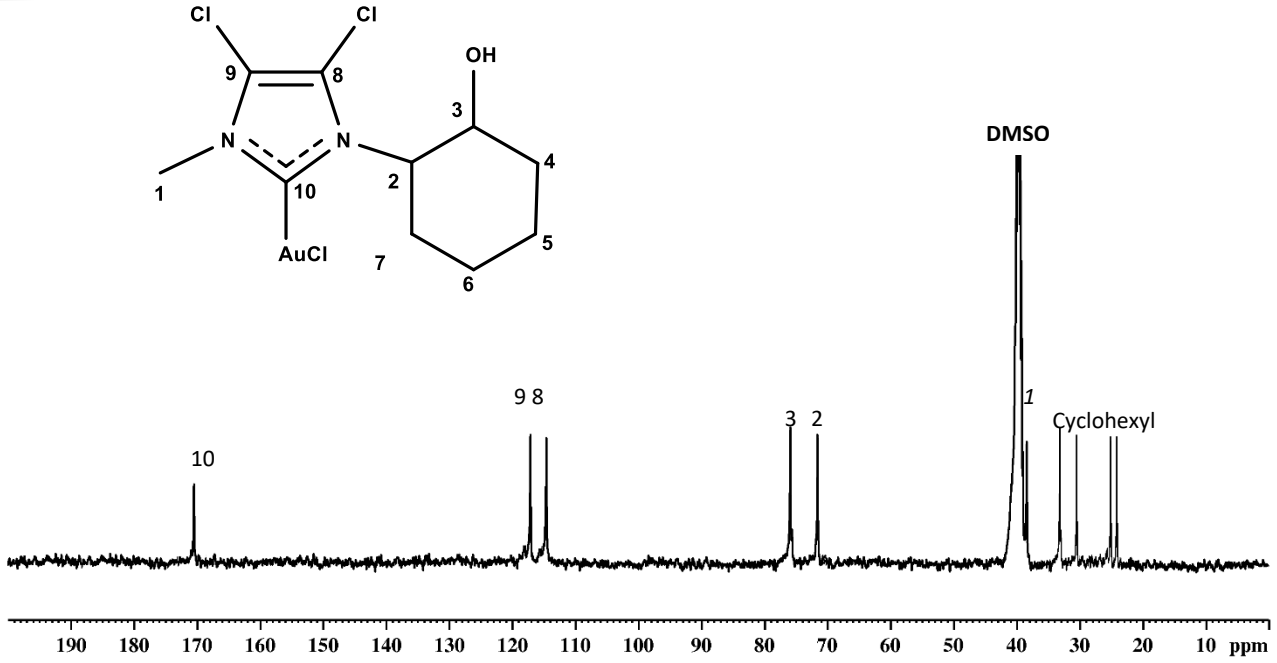

^{13}C-NMR (100 MHz, DMSO-d$_6$): δ 171.2$_0$ (N***C***N), 119.6$_5$, 117.2$_5$ (*backbone carbons*), 77.1$_3$ (***C***HOH), 71.3$_9$ (N***C***H), 39.1$_6$(N***C***H$_3$), 35.0$_1$-23.9$_3$ (***Cyclohexyl carbons***).

ESI-MS (CH$_2$Cl$_2$, m/z): 693.06319 Da attributable to [C$_{20}$H$_{28}$AuCl$_4$N$_4$O$_2$]$^+$

2.4.2 Characterization of caffeine-based gold NHC complexes AuL12-AuL13-AuL14

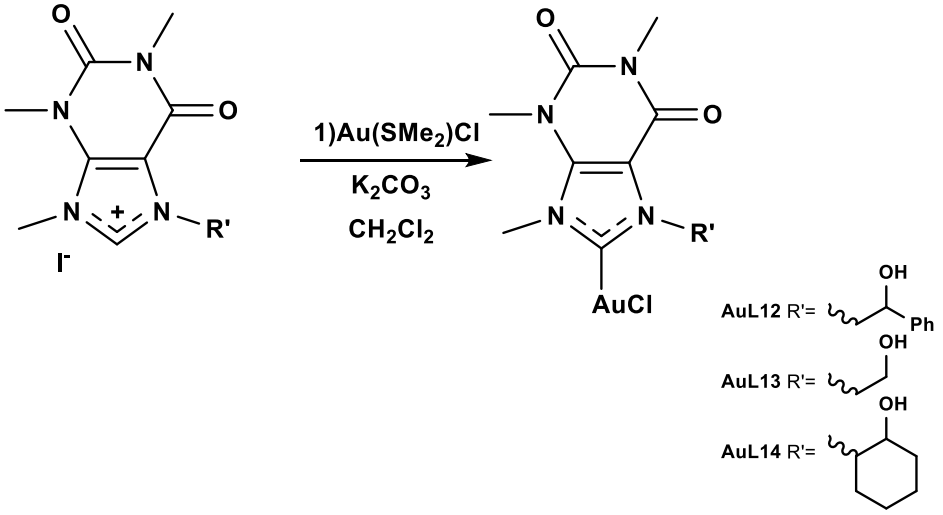

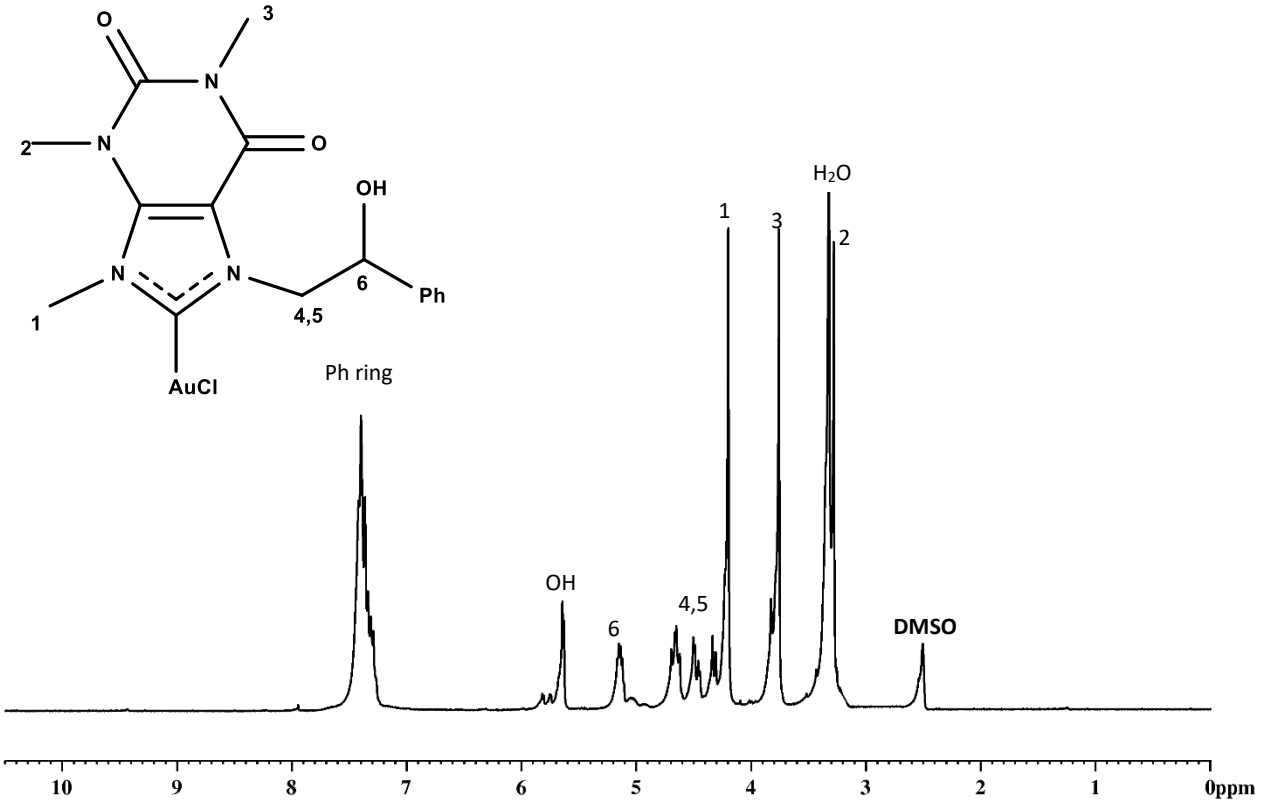

^{1}H-NMR (400 MHz DMSO-d_6): δ 7.4$_1$-7.2$_9$ (m,5H, ***Ph-group***), 5.6$_2$ (s,1H, O***H***), 5.1$_6$ - 5.1$_0$(m,1H, C***H***OH), 4.6$_0$-4.3$_2$ (m,2H, NC***H***$_2$), 4.1$_9$ (s,3H, NC***H***$_3$ imidazolium ring), 3.7$_5$ (s,3H, NC***H***$_3$), 3.2$_7$ (s,3H, NC***H***$_3$)

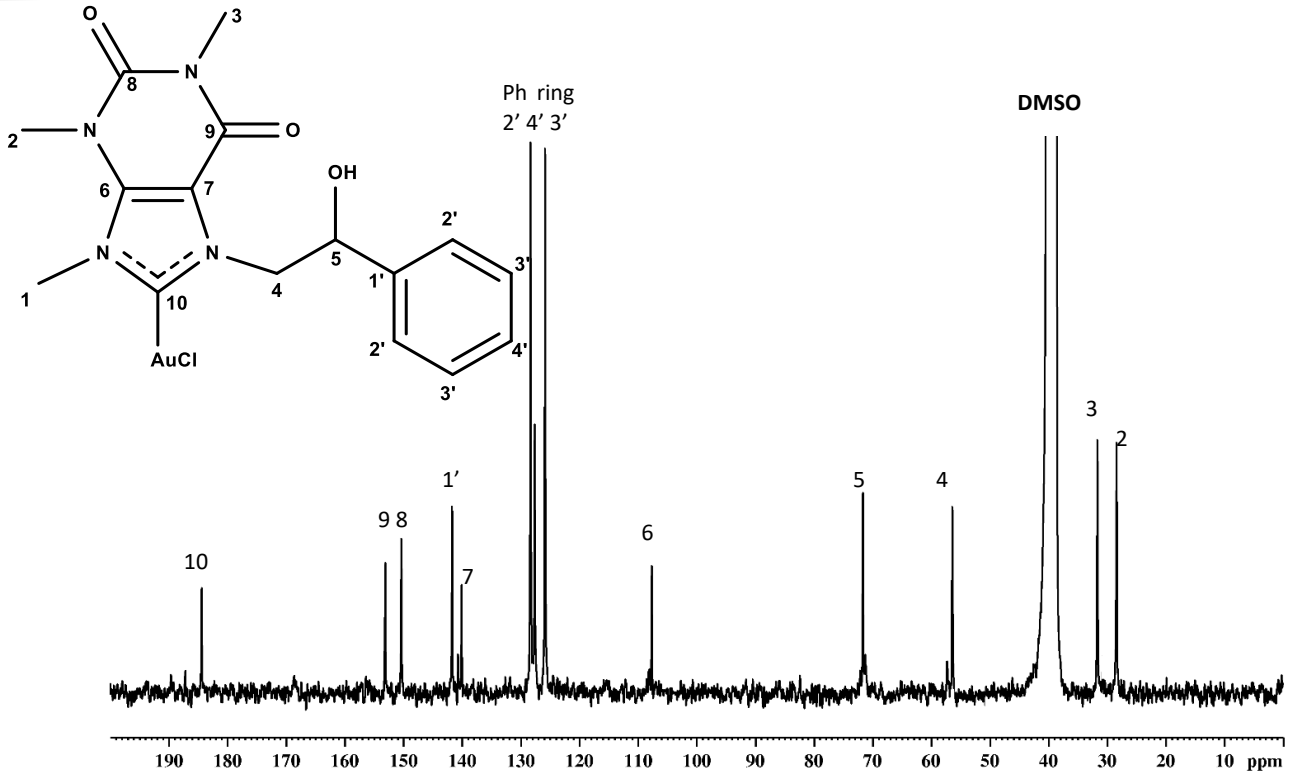

^{13}C-NMR (400MHz DMSO-d_6): δ 184.0$_0$(N***C***N), 153.5$_3$-150.4$_9$ (***C***=O *purine ring*), 141.7$_5$(*ipso aromatic carbon*, **Ph-ring**), 139.8$_3$(*backbone carbon*, ***C***=C), 128.3$_6$, 127.6$_1$, 125.8$_7$(*aromatic carbons*, **Ph ring**), 107.6$_2$ (*backbone carbon*, C=***C***), 71.6$_0$ (***C***HOH), 56.3$_5$(N***C***H$_2$), 31.6$_8$, 28.3$_6$ (N***C***H$_3$ purine ring)

ESI-Ms (CH_2Cl_2 m/z): 681.32325 Da attributable to $[C_{22}H_{22}LiAuN_8O_5]^+$

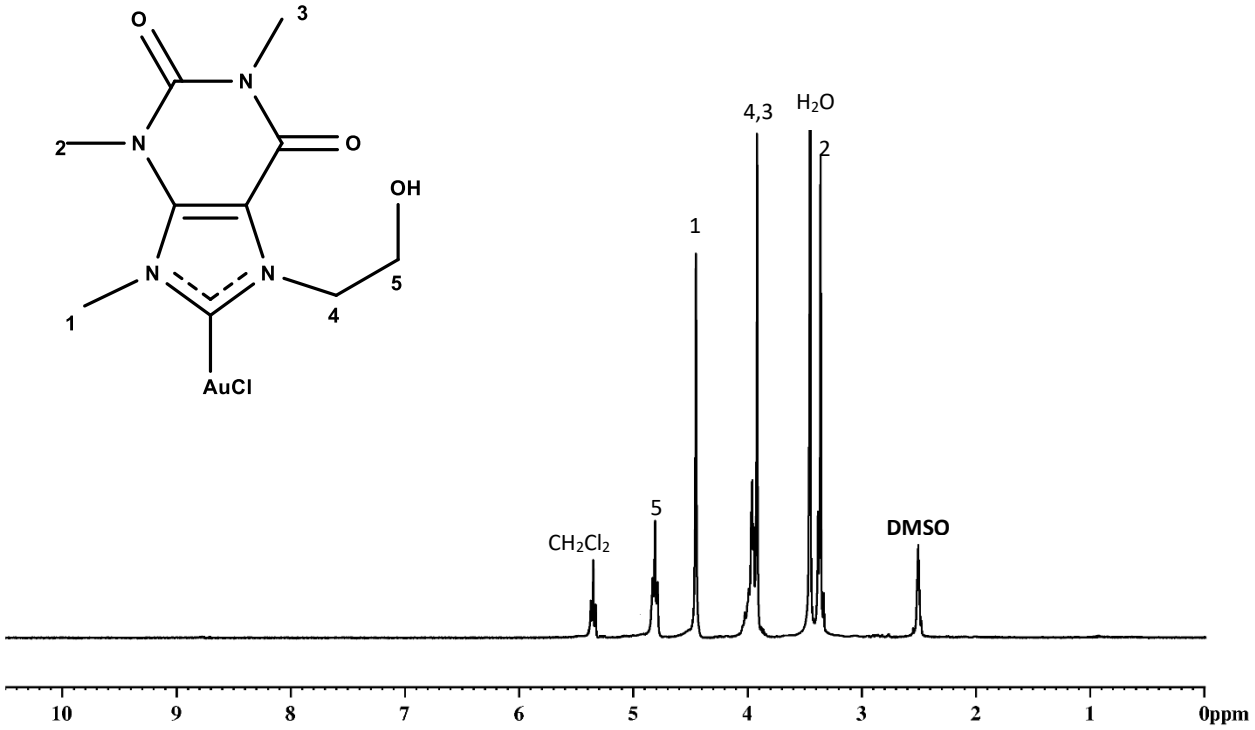

^{1}H-NMR (400 MHz DMSO-d_6): δ 4.8$_3$-4.7$_6$ (m,2H, C***H***$_2$OH), 4.4$_9$ (s,3H, NC***H***$_3$ imidazolium ring), 3.8$_6$-3.7$_3$ (b,5H, NC***H***$_2$, NC***H***$_3$), 3.2$_1$ (s,3H, NC***H***$_3$),

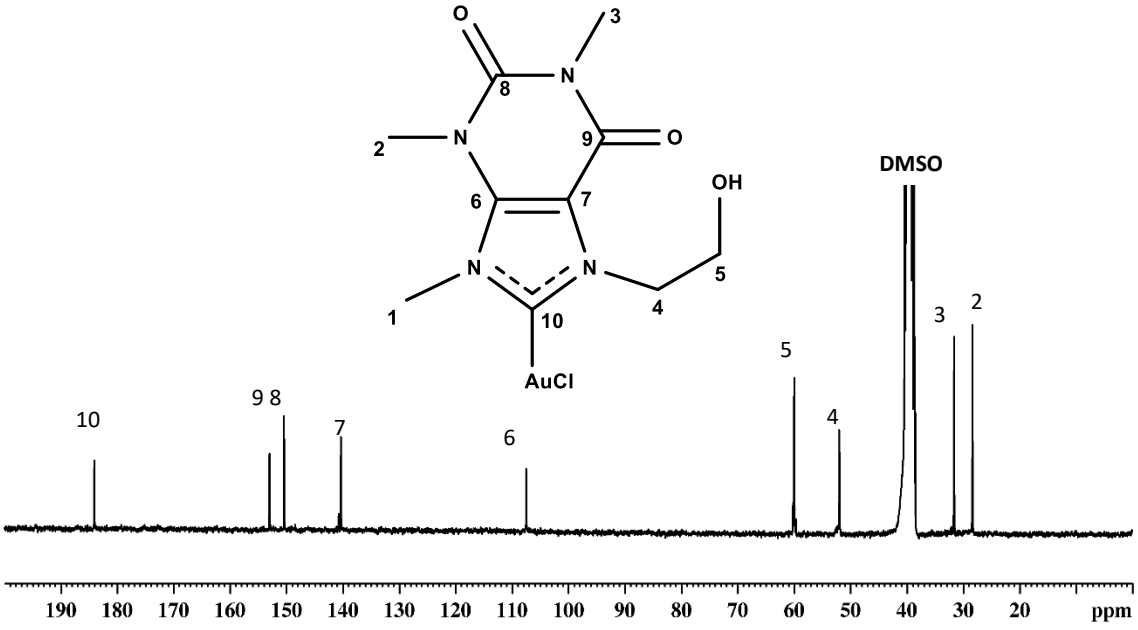

^{13}C-NMR (400MHz DMSO): 184.6$_8$(N***C***N),153.4$_3$-150.3$_2$(***C***=O *purine ring*), 139.7$_2$ (*backbone carbon* ***C***=C), 107.2$_3$(*backbone carbon*, C=***C***) 60.2$_2$ (***C***H$_2$OH), 52.9$_9$(N***C***H$_2$), 31.5$_1$ 28.2$_4$(N***C***H$_3$ imidazolium *ring*), 31.4$_0$, 28.4$_9$ (N***C***H$_3$ *purine ring*)

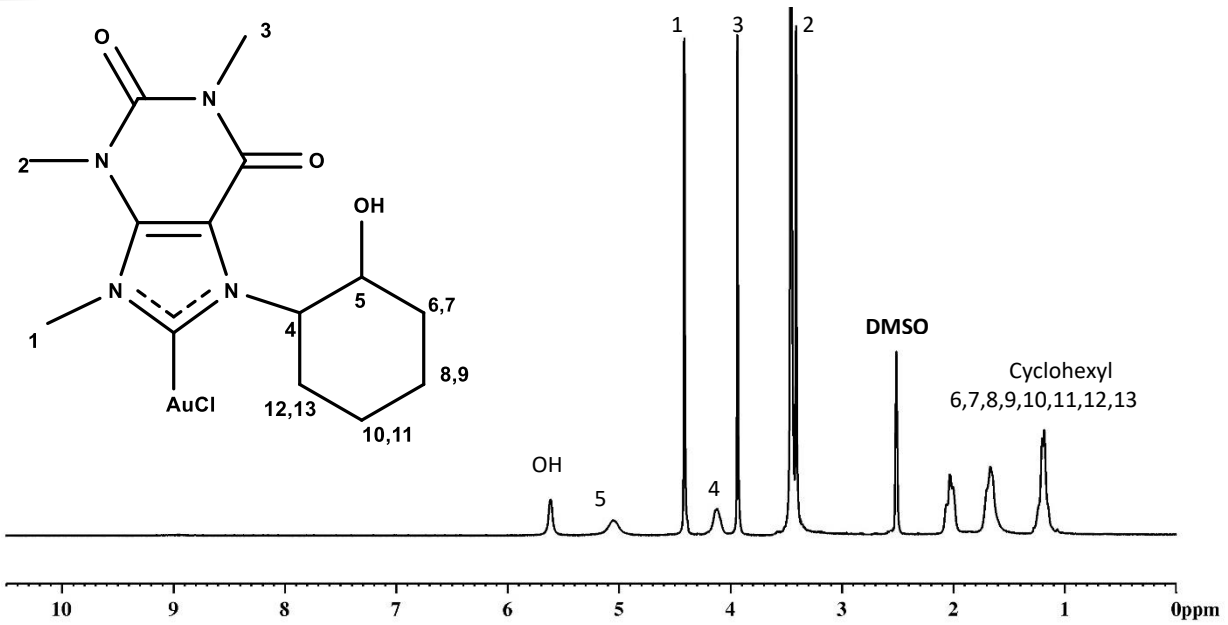

^{1}H-NMR (400 MHz DMSO-d_6): δ 5.5$_6$ (s,1H, O***H***), 5.1$_7$ (b,1H, C***H***OH), 4.2$_6$ (s,3H, NC***H***$_3$ imidazolium ring), 4.0$_8$ (b, 1H, NC***H***), 3.8$_6$(s,3H, N***C*H**$_3$), 3.2$_5$ (s,3H, NC***H***$_3$), 2.2$_0$-1.7$_5$(m, 11H, O=CC***H***$_3$, ***Cyclohexyl***)

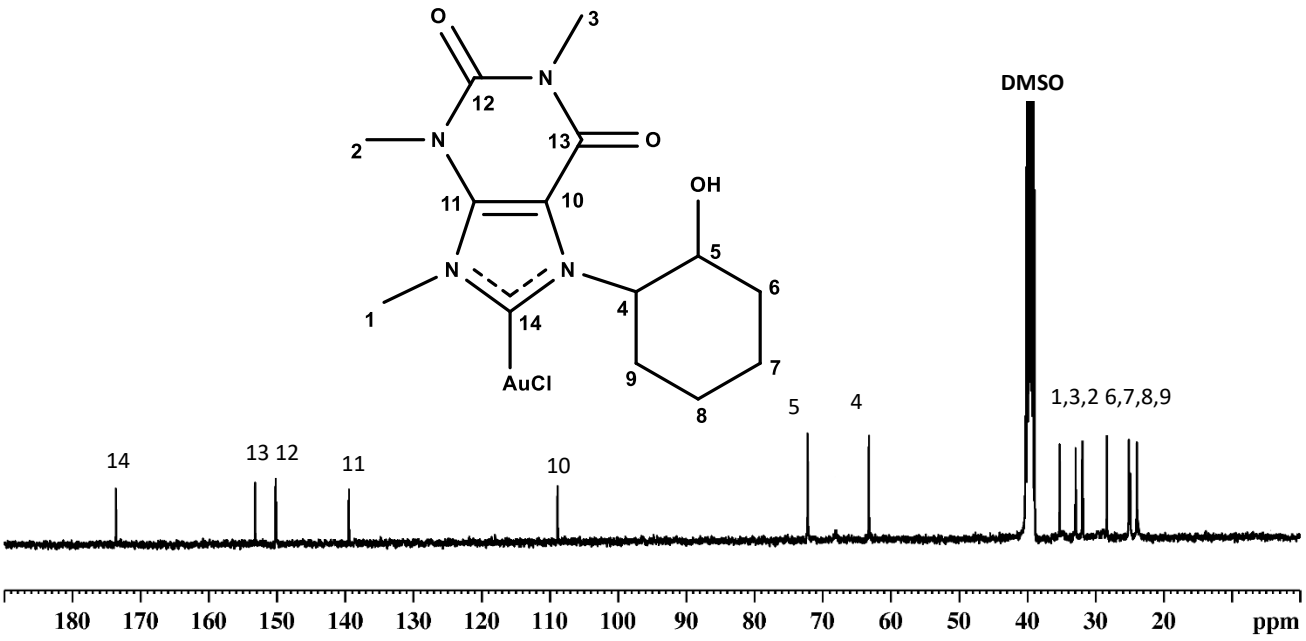

^{13}C-NMR (100 MHz, DMSO-d_6): δ 175.6$_5$(N***C***N), 153.3$_3$-149.2$_2$(***C***=O *purine ring*) 139.6$_7$ (*backbone carbon* ***C***=C),108.7$_7$ (*backbone carbon* C=***C***),72.3$_3$(O***C***H), 62.9$_0$(N***C***H), 36.8$_0$(N***C***H$_3$), 33.4$_0$, 28.4$_9$ (N***C***H$_3$ *purine ring*) 34.0$_2$-23.5$_5$(***Cyclohexyl group***) 22.8$_2$(O=C***C***H$_3$)

2.5 A³coupling reaction catalysed by Ag and Au(I) *N*-heterocyclic carbene complexes

2.5.1 Synthesis of propargylamine through A³-coupling reaction

One of the trendiest topics in contemporary chemistry is the development of more efficient and sustainable synthetic strategies for the production of fine chemicals and pharmaceuticals, and their possible application/scale up in chemical industries. [146–150]. In this regard, multicomponent reactions (MCRs) are a useful tool for the synthesis of more complex molecules, with the adoption of cleaner methodologies, and for these reasons have received much attention, in the last few years. MCR is defined as any process that involves more than two reactants, added simultaneously in the same reactor, to lead to a final product, which contains almost all the atoms of the starting compounds[151,152]. The principal advantages of MCRs are the intrinsic sustainability of the process, the simplicity of the operations, avoiding any purification step of intermediates, and high conversions. Their importance is substantiated by the large number of publications reported in the literature [153,154] and above all, by the expansion of chemical libraries of bioactive molecules, provided by the extensive application of MCRs to the total synthesis [155–157]. During the last decades, a multicomponent reaction that has gained a lot of attention is the A³coupling reaction.

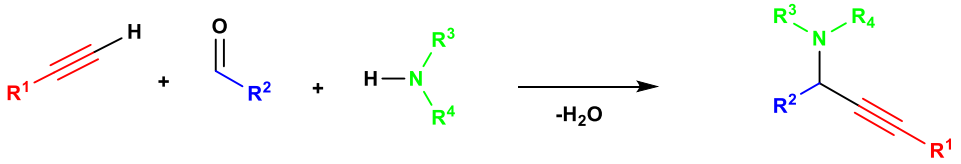

Figure 55 General scheme of the A³ coupling reaction

A³coupling reaction is a transformation among aldehyde, amine, and terminal alkyne, catalyzed by transition metal salts/complex, to lead propargylamines and water as a by-product. The study on this type of reaction has been started at the end of the XX century by Dax [157] and Rivero[159]. They have, separately, reported the synthesis of the propargylamines, using an aldehyde, an amine, and a terminal alkyne using a carbophilic transition metal salt (CuCl) in Solid Phase Organic Synthesis (SPOS), and they have demonstrated the enormous potential, of A³-coupling reaction, to produce different propargylamines.

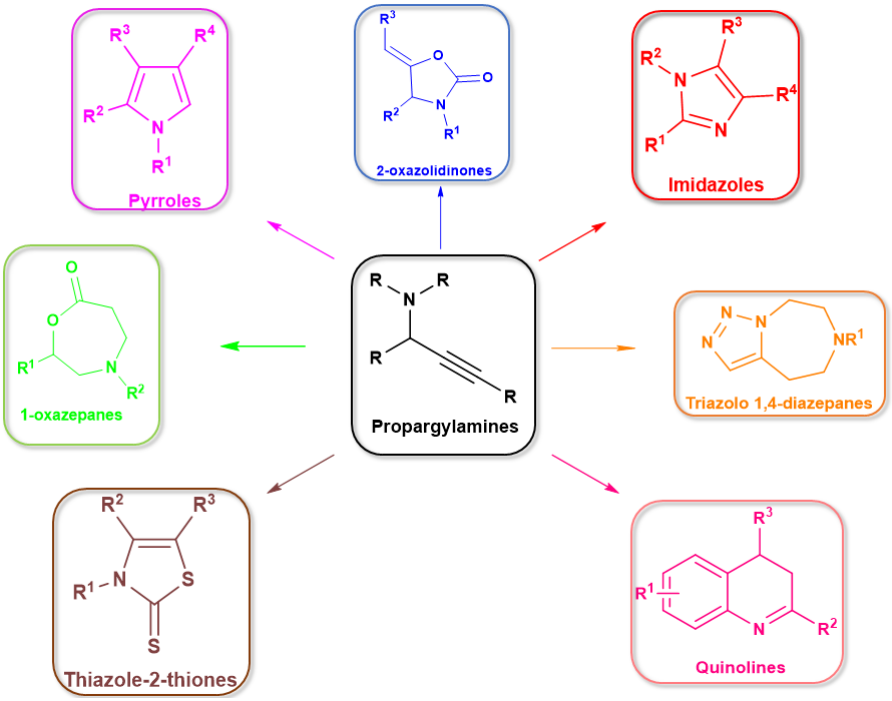

Figure 56 Example of molecules synthesized by propargylamines

Propargylamine is a crucial and versatile class of organic scaffolds, used as intermediates for the formation of heterocyclic compounds (pyrroles, pyrrolidine, imidazoles, oxazolidines, thiazoles, quinolines, *etc.)*, nitrogen-containing bioactive molecules and pharmaceuticals. Pargyline (*N*-methyl-*N*-propargylbenzylamine) [160], selegiline ((2R)-*N*-methyl-1-phenyl-*N*-propynylpropanamine)[161], and rasagiline(N-methyl-1-(R)-aminoindan) [162] are propargylamine derivatives, used for the treatment of early phases of neurodegenerative disease, such as Parkinson[163] and Alzheimer [164].

In particular, the efficacy of propargylic compounds in the treatment of neurodegenerative diseases is attributable to their irreversible and selective inhibitor action against MAO-B (monoamine oxidase). MAO-B is a mitochondrial enzyme FAD-dependent that catalyzes, together with MAO-A, the deamination oxidative of various amines (2-phenylethylamine, benzylamine, dopamine, tyramine, *etc.)*[165]. Furthermore, pargyline is described as a chemotherapeutic action, due to its inhibition action versus cancer cell lines [166], while, for rasagiline, it was observed as an antiapoptotic activity, through the reduction of oxidative stress, and a neurorestorative action[167].

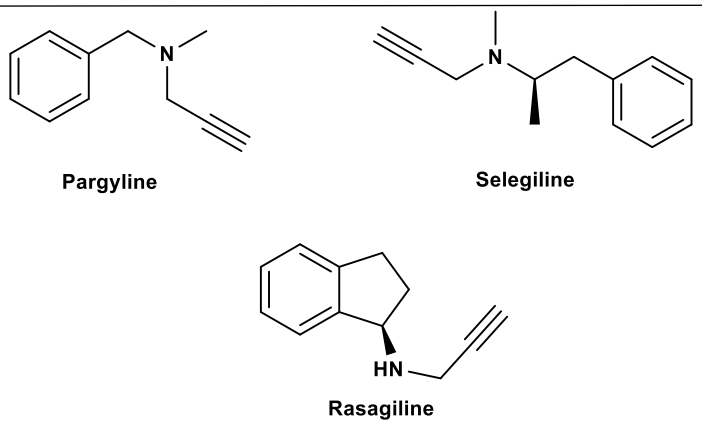

Figure 57 Structure of MAO-B inhibitors: pargyline, selegiline, rasagiline

The versatility of the propargylamines is due to their unique molecular structure; in fact, they are provided by an amine moiety in β position to triple carbon-carbon bond. The amine group can act as nucleophilic in different reactions, while the alkyne moiety can react both as electrophilic and as nucleophilic[168]. For this fundamental reactivity, propargylamines can be used as substrates in different chemical transformations.

Before the development of the A^3coupling reaction, racemic propargylamines were synthesized by direct alkylation of imines and their derivatives, through lithium and Grignard acetylides. However, these methodologies require harsh and controlled reaction conditions (anhydrous solvent, very low temperature) and they produce a stoichiometric quantity of waste (inorganic salts). Since the publication of the twelve principles of green chemistry and the growing interest in environmental issues, the scientific community is aimed to develop new synthetic strategies that are simpler and less dangerous and does not produce waste [150]. In this scenario, transition metal-catalyzed A^3-coupling reaction is a green alternative synthetic strategy for the production of propargylamines[169–172]. Recently, *N*-heterocyclic carbene complexes of silver and gold (I) have gained exponential interest due to their activity in A^3-coupling reactions[80–82,120,121,173].

2.5.2 Catalytic Performance of Ag and Au NHC complexes

Because of the good results reported in the literature by silver and gold NHC complexes in A^3coupling reaction, we have tested the catalytic behavior of synthesized silver and gold complexes shown in **Figures 44-45**. Their catalytic behavior was evaluated using three different aldehydes (p-formaldehyde, cyclohexanecarboxaldehyde, and benzaldehyde) with piperidine, as secondary amine, and phenylacetylene, as terminal alkyne, in neat conditions or water at 80°C, using the same reaction condition adopted in literature[174]. All the yields of the runs were detected through ^{1}H-NMR spectroscopy, using the internal standard method (2-bromesitylene was selected as the internal standard), by the comparison of the area of aromatic protons of 2-bromesitylene, δ=6.8$_9$ $CDCl_3$, with the signal attributable to proton(s) in α position to amine moiety, of the produced propargylamine. **Figure 58** shows the general scheme of the A^3-coupling reaction.

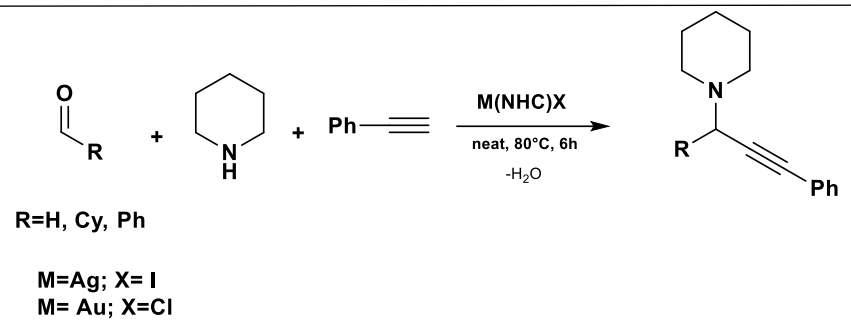

Figure 58 General A³ coupling reaction with three different aldehydes

The obtained results are cataloged by the *N*-heterocyclic carbene ligand bonded to the metal center. We initially tested the catalytic activity of silver and gold complexes derived from imidazole (L1), 4,5-dichloro imidazole (L2), 4,5-diphenyl imidazole (L3), and benzimidazole (L4).

Table 7 Obtained result with the AgL1-4, AuL1-4 [a]

Run	Catalyst	Aldehyde	Yield [b] (%)
1	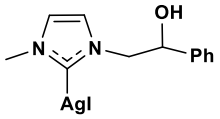 **AgL1**	p-formaldehyde	13
2		cyclohexanecarboxaldehyde	99
3		benzaldehyde	13
4	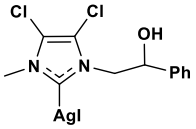 **AgL2**	p-formaldehyde	94
5		cyclohexanecarboxaldehyde	99
6		benzaldehyde	38
7	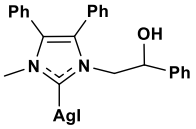 **AgL3**	p-formaldehyde	15
8		cyclohexanecarboxaldehyde	20
9		benzaldehyde	5
10	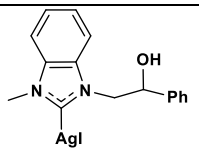 **AgL4**	p-formaldehyde	10
11		cyclohexanecarboxaldehyde	78
12		benzaldehyde	4
13	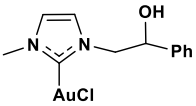 **AuL1**	p-formaldehyde	99
14		cyclohexanecarboxaldehyde	99
15		benzaldehyde	83
16	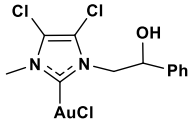 **AuL2**	p-formaldehyde	99
17		cyclohexanecarboxaldehyde	96
18		benzaldehyde	86
19	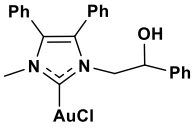 **AuL3**	p-formaldehyde	62
20		cyclohexanecarboxaldehyde	84
21		benzaldehyde	46
22	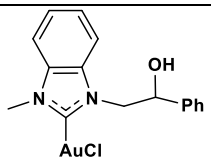 **AuL4**	p-formaldehyde	99
23		cyclohexanecarboxaldehyde	90
24		benzaldehyde	28

[a] Reaction conditions: aldehyde (1.0 mmol), piperidine (1.2 mmol) phenylacetylene (1.5mmol), AuNHC (3%mol) 80°C, 6h. nitrogen atmosphere. [b] Yields were average of two runs and determined by ^{1}H-NMR analysis through internal standard.

As shown in **Table 7**, all the complexes were able to catalyze the condensation among aldehyde, amine, and terminal alkyne, in the adopted reaction conditions. By the comparison of runs 1-12 with 13-24, it is possible to assert that the catalytic activity is dependent on the metal and as well as by the substituents on NHC's backbone: silver

complexes were less reactive than gold analogs, and the best catalytic activities have been observed with the complexes bearing two chlorine atoms on the backbone of imidazole rings. The lower reactivity of silver complexes is probably attributable to the major lability of the Ag-NHC bond than gold analogs. whereas the better catalytic activity of **AgL2** and **AuL2** is attributed to a more positive charge on the metal center, due to the presence of electron-withdrawing substituents on the backbone.

In **Table 8** are reported the Mulliken charges and BDE (bond dissociation energy), for complexes **AgL1**, **AgL2**, **AuL1,** and **AuL2,** calculated by Prof. Chiara Costabile, of the University of Salerno. [130]. By the analysis of the results reported in **Table 8**, the complexes **AgL2** and **AuL2** have shown a major positive charge (Mulliken charge) and lower bond-dissociation energy than **AgL1** and **AuL2**. That is an indication of a weaker bond between the metal center and the NHC ligand. Also, a greater BDE in presence of halogen suggests a less σ donation of the NHC ligand to the metal. Based on these results, the higher catalytic activity of **AgL1** and **AuL2** might be assigned to a more electrophilic behavior of the metal center, which could consent to easy coordination of the alkyne.

Table 8 Mulliken charge on the metal and bond-dissociation energies (BDE) of NHC and halogen for AgL1, AgL2, AuL1, and AuL2. Values were obtained with DFT calculations using the PBE0/6-311 G(d,p) basis set[130].

Complex	Mulliken charge	BDE (NHC)[a]	BDE (halogen)
AgL1	+0.151	55.2	116.0
AgL2	+0.158	51.3	119.8
AuL1	+0.279	82.4	142.0
AuL2	+0.314	78.1	146.2

[a] BDE= Bond-dissociation energy referred to the metal-NHC bond

For all complexes, benzaldehyde was found to be less reactive than the other used aldehyde, whereas **AgL2**, **AuL1**, **AuL2**, and **AuL4** have shown to be able to convert completely p-formaldehyde and cyclohexanecarboxyaldehyde. By the analysis of the yields, the best catalytic activity is due to the gold complex bearing the two chlorine atoms on the backbone of the NHC ligand.

Afterward, we tested the silver and gold complexes, derived from imidazole and 4,5-dichloroimidazole with an additional hydroxyl function on the nitrogen atom, (**AgL5, AgL6**, **AuL5,** and **AuL6**). The catalytic activities are reported in **Table 9**[136].

Table 9 Obtained results with the AgL5-6, AuL5-6 [a]

Run	Catalyst	Aldehyde	Yield [b] (%)
25	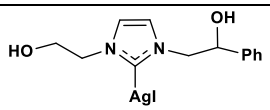	p-formaldehyde	25
26		cyclohexanecarboxaldehyde	47
27	**AgL5**	benzaldehyde	23
28	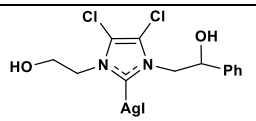	p-formaldehyde	65
29		cyclohexanecarboxaldehyde	52
30	**AgL6**	benzaldehyde	36
31	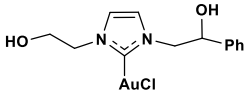	p-formaldehyde	86
32		cyclohexanecarboxaldehyde	65
33	**AuL5**	benzaldehyde	60
34	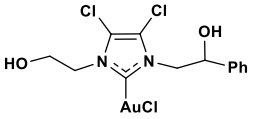	p-formaldehyde	99
35		cyclohexanecarboxaldehyde	99
36	**AuL6**	benzaldehyde	60

[a] Reaction conditions: aldehyde (1.0 mmol), piperidine (1.2 mmol) phenylacetylene (1.5mmol), AuNHC (3%mol) 80°C, 6h. nitrogen atmosphere. [b] Yields were average of two runs and determined by ^{1}H-NMR analysis through internal standard.

As is illustrated in **Table 9**, we have conducted the catalytic test with the same aldehydes, used in the first preliminary work, to compare the activities of the complexes. As seen before for compounds **Ag/Au L1-4**, all complexes were able to catalyze the A^3-coupling reactions in the same reaction conditions. According to the results listed in **Table 9**, it is possible to descript the following trend **AuL6>AuL5>AgL6>AgL5**, where the gold complexes were more active than the silver ones. **AuL6** was able to convert completely p-formaldehyde and cyclohexylcarboxyaldehyde. Whereas **AuL4** has shown a better catalytic behavior in comparison to **AuL6**, with benzaldehyde (**Run 15, Table 7 vs Run 36, Table 9**). The lower reactivity might be attributed to the presence of an additional hydroxyl functionality, that could coordinate with the metal center, giving it electronic density, and making it less electrophilic and, consequently, less reactive. On the other hand, the presence of a hydroxyl group also on the second nitrogen atom could make the complexes more soluble in green solvents, such as water, ethylene carbonate, *etc*., and therefore more interesting in sustainable chemistry.

Furthermore, it was investigated the catalytic behavior of silver complexes, **AgL7-AgL7'** and the corresponding gold analogs **AuL7- AuL7'**, in the A^{3}coupling reaction. These complexes are characterized by the substitution of the hydroxyl group of the complexes **AgL1-AuL1**, with methoxyl (**AgL7-AuL7**) or sodium alcoholate group (**AgL7'-AuL7'**), with the aim of enhancing the solubility in the reagents, when the reactions are carried out in neat conditions[132].

Table 10 Obtained results with methoxyl and sodium alcoholate substituted NHC silver and gold complexes

Run	Catalyst	Aldehyde	Yield [b] (%)
37	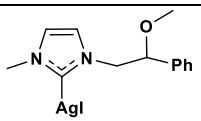 **AgL7**	p-formaldehyde	29
38		cyclohexanecarboxaldehyde	43
39		benzaldehyde	11
40	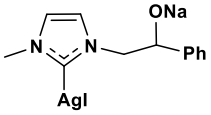 **AgL7'**	p-formaldehyde	20
41		cyclohexanecarboxaldehyde	40
42		benzaldehyde	10
43	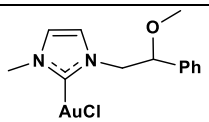 **AuL7**	p-formaldehyde	88
44		cyclohexanecarboxaldehyde	76
45		benzaldehyde	43
46	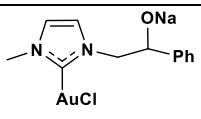 **AuL7'**	p-formaldehyde	90
47		cyclohexanecarboxaldehyde	60
48		benzaldehyde	47

[a] Reaction conditions: aldehyde (1.0 mmol), piperidine (1.2 mmol) phenylacetylene (1.5mmol), AuNHC (3%mol) 80°C, 6h. nitrogen atmosphere. [b] Yields were average of two runs and determined by ^{1}H-NMR analysis through internal standard.

According to the results listed in **Table 10**, the complexes bearing N-methyl-N'-(2-methoxy-2-phenyl) ethyl-2-ylidene-imidazole (**L7**) are generally more active than the sodium alcoholate substituted NHC complexes. The catalytic behavior of **AuL7** and **AuL7'** was compared to **AuL1** and **AuL2**, using water as a solvent.

Table 11 The catalytic activities in the A3 coupling reaction catalyzed by AuL1, AuL2, AuL7, and AuL7', using water as solvent

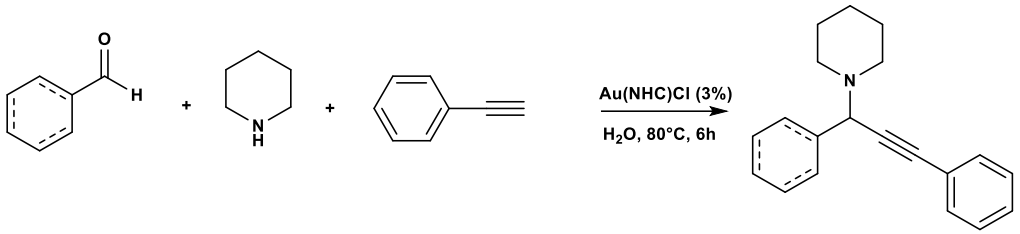

Run	Catalyst	Aldehyde	Yield [b] (%)
49	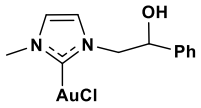 **AuL1**	cyclohexanecarboxaldehyde	66
50		benzaldehyde	19
51	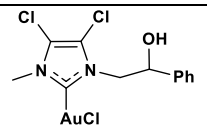 **AuL2**	cyclohexanecarboxaldehyde	70
52		benzaldehyde	25
53	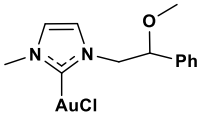 **AuL7**	cyclohexanecarboxaldehyde	37
54		benzaldehyde	11
55	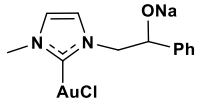 **AuL7'**	cyclohexanecarboxaldehyde	43
56		benzaldehyde	20

[a] Reaction conditions: aldehyde (1.0 mmol), piperidine (1.2 mmol) phenylacetylene (1.5mmol), AuNHC (3%mol) 80°C, 6h, water (3.0mL). nitrogen atmosphere. [b] Yields were average of two runs and determined by ^{1}H-NMR analysis through internal standard

In reaction carried out in water, **AuL2** was the most active catalyst, while **AuL7** showed the lowest conversions, due to its less solubility in reaction media. The comparison of catalytic behavior of gold complexes **AuL1** and **AuL7'**, which are different for N-substituents, revealed that **AuL1** is more active than other gold complexes. To try to understand the reasons for differences in catalysis, DFT (density functional theory) at the PBE0/6-311 G(d,p) level was executed on **AuL1** and **AuL7'**, calculated by Prof. Chiara Costabile of the University of Salerno. The reaction was modeled in line with the accepted mechanism [79] reported in **Scheme 1**, using acetylene as an alkyne, for computational simplicity. In such mechanism, the alkyne coordinates to the metal center through π-bond and, it is deprotonated to form the nucleophilic metal acetylide compound. In **Figure 58**, are illustrated the minimum energy of intermediates. The free energy coordination of the benzaldehyde to the metal center was -18.0 kcal/mol for AuL1 and -24.0 kcal/mol for AuL7'. The major stability of the neutral metal-alkyne specie could be rationalized by the observation of **Figure 59**. In **AuL1**, the alkyne is orthogonally oriented to NHC plane, the carbene metal bond is about 2.2 Å, and the alkyne angle bond (HCC). In neutral metal

alkyne specie, the olefin is on the same plane of AuNHC. Furthermore, the intermediate has a longer $C_{carbene}$-Au bond and the angle bond HCC_{alkyne} bent at 151°. The longer distance among the NHC-M and the shorter distance between carbon atoms in alkyne moieties could be attributable to a stronger electron donation from olefin to the metal center, in a square planar intermediate.

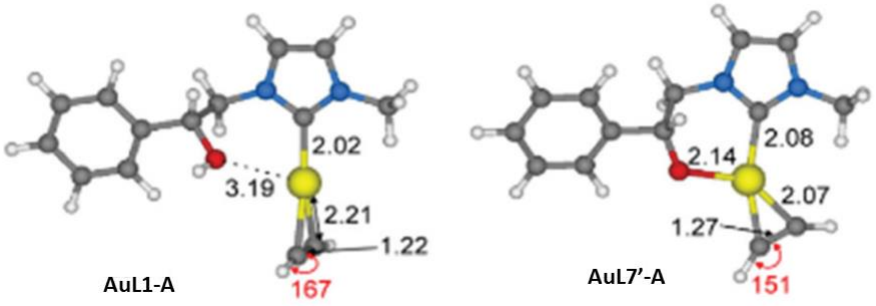

Figure 59 Minimum energy intermediates AuL1-A and AuL7'-A. The distances are expressed in Å. Reproduced from Ref.[132] with permission from the Royal Society of Chemistry.

The coordination of the alkyne to the metal center is followed by its deprotonation, with the secondary amine (piperidine). We have investigated the deprotonation step for both complexes. In **Figures 60-61** are represented the energy of intermediates and the geometry involved for the complexes AuL1 e AuL7'. As shown in **Figure 60**, the amine deprotonates the alkyne from the opposite site to the hydroxyl group (AuL1-B) for steric reasons, to lead to the corresponding metal acetylide compound (AuL1-C). The energy barrier for this step is very low (ΔG=2.5 kcal/mol).

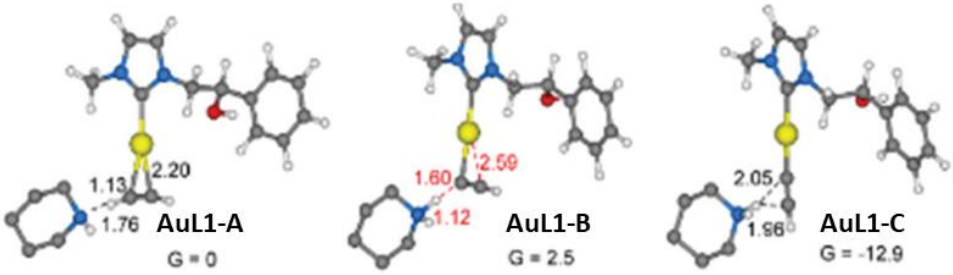

Figure 60 Energies and geometries involved in the reaction of deprotonation of acetylene. The energies calculated are reported in kcal/mol. Reproduced from Ref.[132] with permission from the Royal Society of Chemistry.

Due to the chelating alkoxy group, the deprotonation of the alkyne involves a different pathway. The base deprotonates acetylene involving a six-member cycle (AuL7'-BC$^{\neq}$), with a double hydrogen transfer: the amine provides the proton to the alkoxy group, while the alkyne gives the proton to the amine. The energy calculated is slightly higher than that observed in the deprotonation of the complex AuL1 (ΔG=2.8 kcal/mol). The deprotonation leads to the formation of the same group present on catalyst AuL1 (AuL7'-C) but in a more basic reaction environment. Thus, we have the nucleophilic attack on imine by phenylacetilide, rather than iminium ion. The greater catalytic activity for the complex AuL1

might be associated with the second part of the catalytic cycle, where the acidity is necessary to consent to the carrying-out of the reaction.

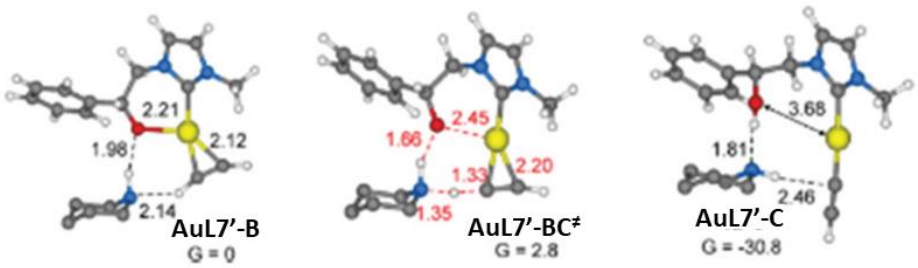

Figure 61 Energies and geometries of intermediates and transition state involved in the deprotonation in the presence of AuL7'. Free energies are reported in kcal/mol. Reproduced from Ref.[132] with permission from the Royal Society of Chemistry.

The xanthine-based *N*-heterocyclic carbene complexes have been largely studied as antibacterial [53] and antitumoral compounds [92,93]. These complexes have shown an interesting biological activity due to their solubility in aqueous media. In this regard, caffeine-based NHC ligands and their relative complexes have been applied for catalytic purposes [137], for the design of homogeneous and heterogeneous catalysts, and used in aqueous solutions. [174–176]. Based on this interesting research field, we have preliminarily tested the catalytic behavior of caffeine-based NHC silver and gold complexes in A^3-coupling reaction in neat conditions, and the results are listed in **Table 12**.

Table 12 Results obtained with NHC-caffeine based silver and gold complexes

Run	Catalyst	Aldehyde	Yield [b] (%)
57	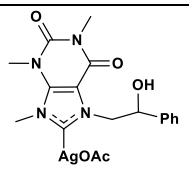	p-formaldehyde	95
58		cyclohexanecarboxaldehyde	60
59		benzaldehyde	15
	AgL12		
60	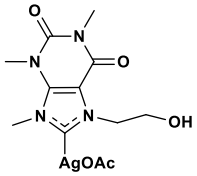	p-formaldehyde	95
61		cyclohexanecarboxaldehyde	50
62		benzaldehyde	15
	AgL13		
63	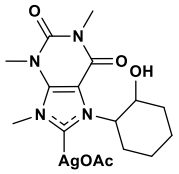	p-formaldehyde	77
64		cyclohexanecarboxaldehyde	53
65		benzaldehyde	20
	AgL14		
67	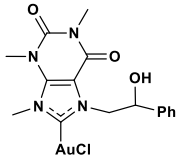	p-formaldehyde	95
68		cyclohexanecarboxaldehyde	76
69		benzaldehyde	44
	AuL12		
70	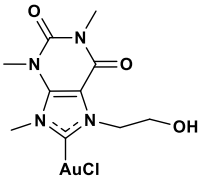	p-formaldehyde	95
71		cyclohexanecarboxaldehyde	76
72		benzaldehyde	44
	AuL13		
73	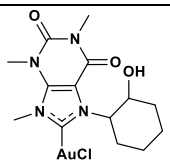	p-formaldehyde	99
74		cyclohexanecarboxaldehyde	68
75		benzaldehyde	47
	AuL14		

[a] Reaction conditions: aldehyde (1.0 mmol), piperidine (1.2 mmol) phenylacetylene (1.5mmol), AuNHC (3%mol) 80°C, 6h. nitrogen atmosphere. [b] Yields were average of two runs and determined by ^{1}H-NMR analysis through internal standard.

All the caffeine NHC complexes have catalyzed the condensation reaction among the aldehyde, amine, and alkyne. The analysis of the obtained yields shows that the silver caffeine-based complexes have catalyzed the A^3-coupling reaction as well as other complexes previously seen. The silver complexes have completely converted p-formaldehyde in the resulting propargylamine, with the only exception of **AgL14** (**Run 63, Table 12**). As already seen before, gold complexes have shown a better catalytic activity than silver analogs. In particular, the gold caffeine-based complexes were less reactive towards cyclohexylacarboxyaldehyde than benzimidazole based gold complex, **AuL4**, (See

runs 68, 71, 74 of Table 11 vs **Run 23 of table7**), but they have surprisingly shown a better activity toward benzaldehyde (**Runs 69, 72, 75 of Table 12** vs **Run 24 of Table 12**).

2.5.3 Kinetic studies on A³coupling reaction catalyzed by AuL2 and its halo and (pseudo)halo-derivates

By the analysis of the evaluated yields in the A³ coupling reaction, gold complex **AuL2** showed the best catalytic performance in the A³ coupling reaction, in fact it has completely converted p-formaldehyde and cyclohexylcarboxyaldehyde, in six hours (see **Runs 16**, **17** of **Table 7**) in the corresponding propargylamines, and have shown the higher activity in the same reaction using benzaldehyde (Yield 86%) [130]. The catalytic activity was attributed to its higher electrophilicity (see **Table 8**), due to the presence of two chlorine atoms on the NHC backbone, which reduce the electronic density of the metal center.

A logical consequent investigation was the analysis of the counterion effect in this type of reaction. In this regard, we have synthesized, characterized, and tested the halo and pseudo (halo) analogs of **AuL2**, in the A³ coupling reaction of benzaldehyde with piperidine and phenylacetylene in neat conditions at 80°C for six hours. As seen above, the yields of propargylamine were monitored by ¹H-NMR using 2-bromesitilene as an internal standard. The complexes tested are illustrated in **Figure 62**.

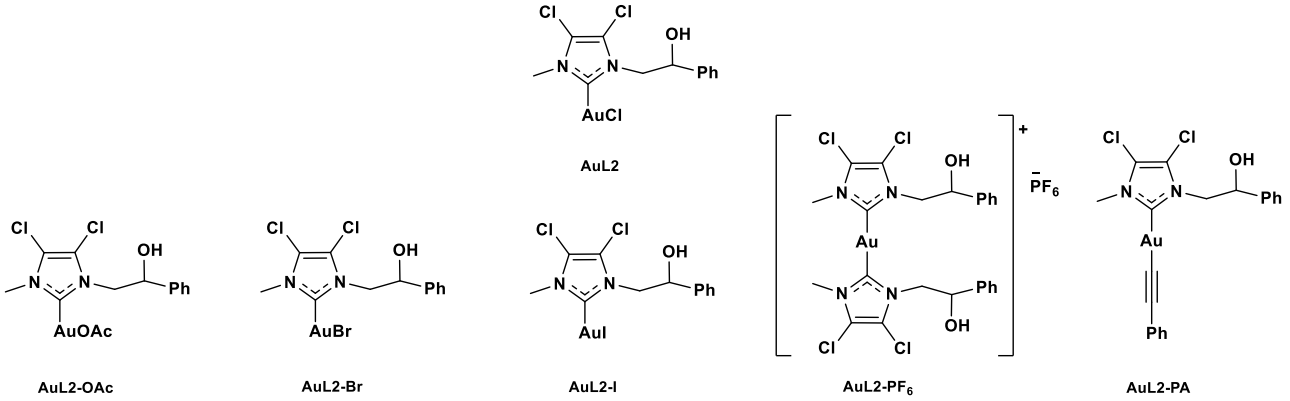

Figure 62 Halo and pseudo halo derivates of AuL2

2.5.3.1 Synthesis and characterization of halo and pseudo halo analogues of AuL2

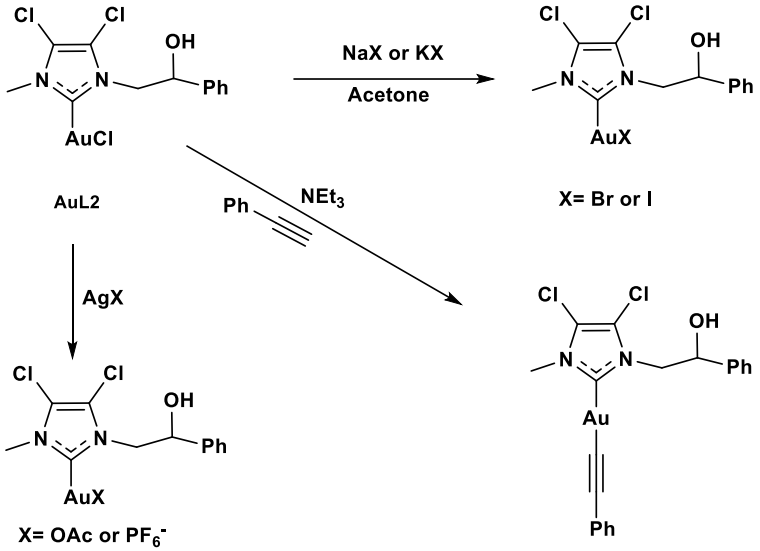

Figure 63 Synthetic routes for the synthesis of AuL2 derivates

The synthetic routes are summarized in **Figure 63**, following the published literature procedures[178–180]. Bromo and iodo derivates were synthesized by the reaction of the gold complex with an excess of sodium or potassium halogenide salt, in acetone. Acetate and hexafluorophosphate gold complexes were produced using the corresponding silver salts. The halide abstraction using silver salts with non-coordinating anions is an efficient methodology to generate electrophilic gold species. The main limitation is the difficult isolation of these complexes due to their facile decomposition to colloidal gold (0) [179]. To prevent the decomposition, the reaction with silver hexafluorophosphate has been conducted in acetonitrile. Echavarren and Nolan have reported the synthesis of gold complexes bearing phosphine and N-heterocyclic carbene ligand with non-coordinating anions demonstrating the importance of the coordination of solvent molecules in the stabilization of these complexes[179,181].

The alkynyl gold complex was synthesized following the literature procedure [180], slightly modified by us, by reaction of **AuL2** with an excess of NEt_3 and phenylacetylene. We synthesized the alkynyl functionalized compound to study the effect in the A^3coupling reaction, starting from the acetylide derivative.

The ^1H and ^{13}C NMR spectra of all complexes were recorded. The ^1H-NMR spectra of the complexes have not shown any signal of decomposition, and the pattern remained the same. Only acetate gold NHC complex shows other signals: a singlet signal at 1.83 ppm attributable to the methyl group of acetate anion in the ^1H NMR spectrum, and two signals in the ^{13}C-NMR spectrum attributable to the carbonyl and methyl group at 174.85 and 23.87 ppm, respectively. Moreover, the carbene carbon shifts from 170.69 to 163.69 ppm. The ^{13}C-NMR spectra of other halo and pseudo halo gold complexes have presented a significant downfield shift of the signal attributable to carbenic carbon (**Table 13**). Backer attributed the

increase of ^{13}C chemical shift of the carbene carbon, in Au(NHC)X complexes, to the increase of the σ-donor ability of the counter-ion [178].

Table 13 Chemical Shift of carbenic carbon of gold NHC complexes

δ_C (DMSO)	
X	**Au-*C***
OAc	163.69
Cl	170.69
Br	173.89
I	182.92
PF_6	183.82
Ph-C≡C	186.95

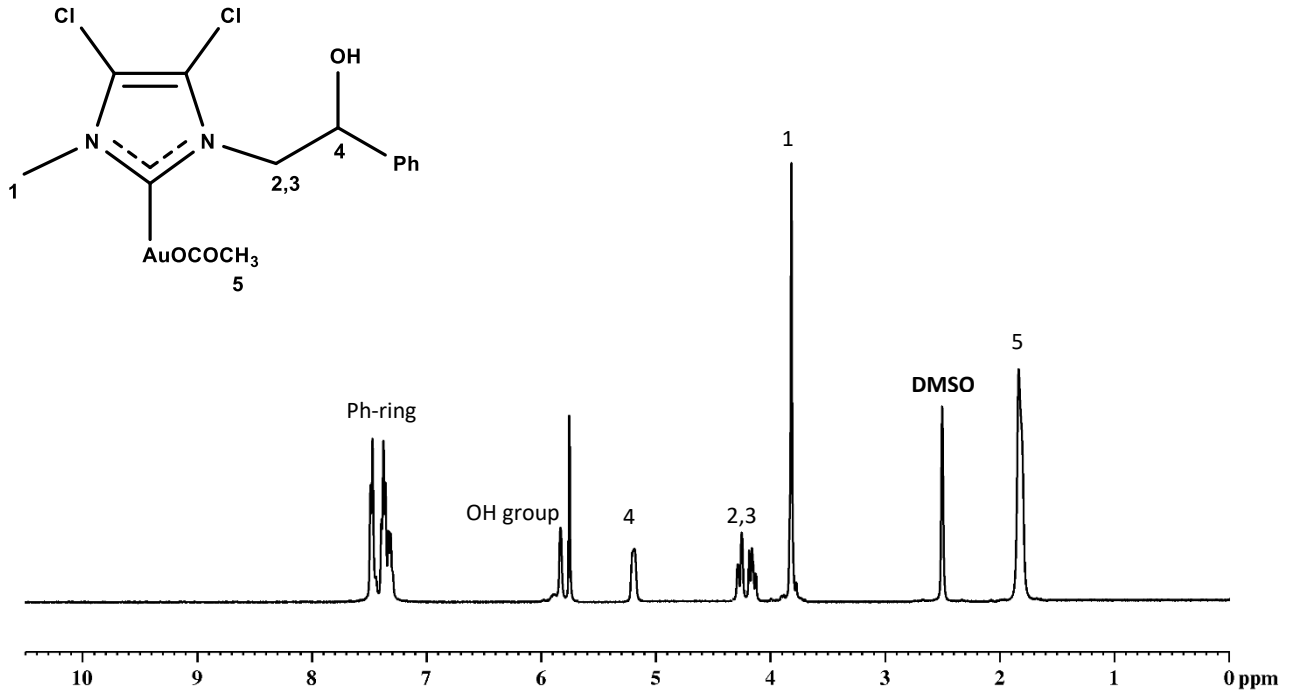

^{1}H-NMR (400MHz, DMSO-d_6): δ 7.48-7.31 (m, 5H, ***Ph ring***) 5.83(m, 1H, ***OH group***); 5.2 (m, 1H, OC***H***) 4.20-4.12(m, 2H, NC$\boldsymbol{H_2}$); 3.81(s,3H, NC$\boldsymbol{H_3}$)1.83 (s. 3H, COC$\boldsymbol{H_3}$).

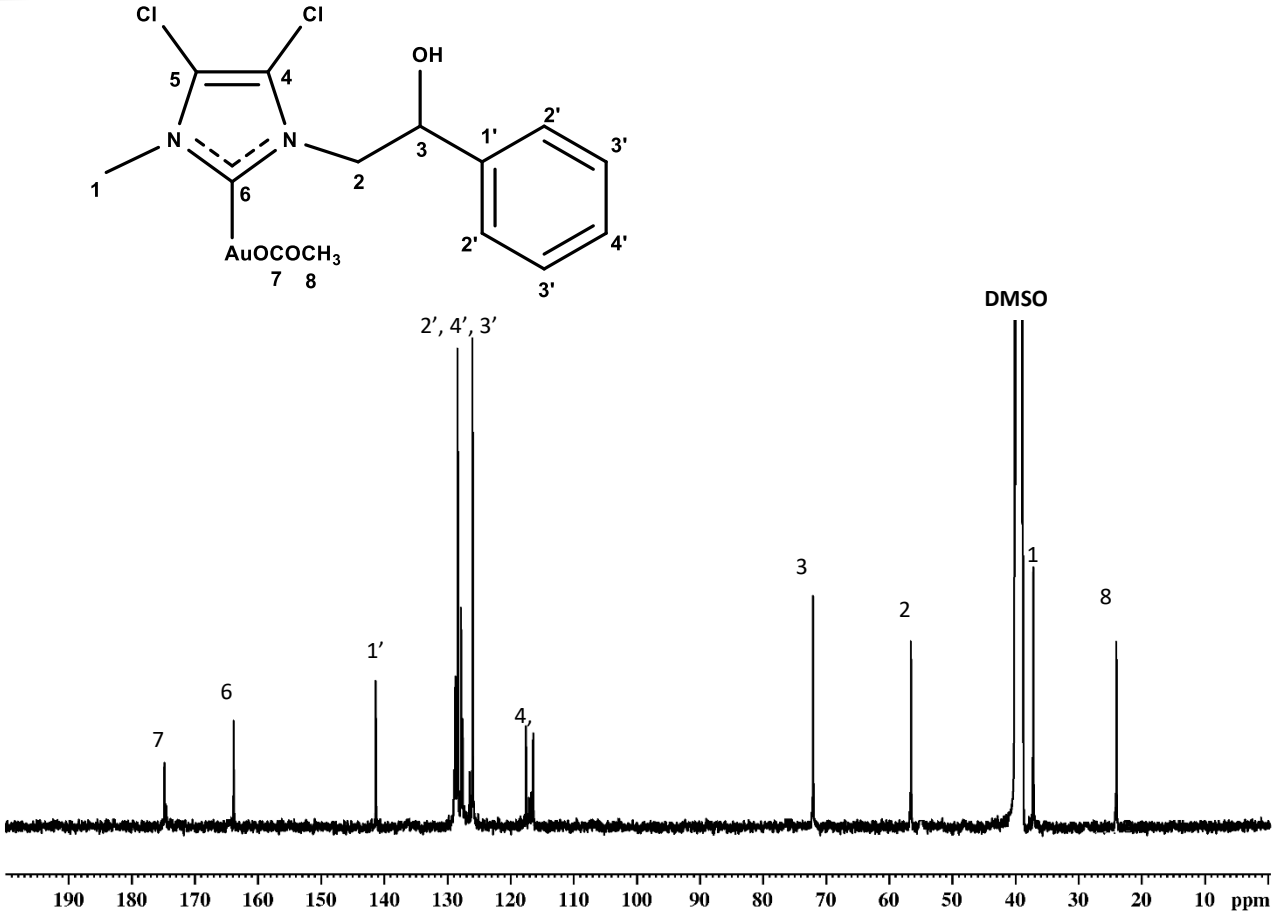

^{13}C-NMR (100 MHz, DMSO-d_6): δ 174.8$_5$ (O***C***OCH$_3$) 163.9$_6$ (N***C***N) 141.4$_4$ (*ipso aromatic carbon*, **Ph-ring**), 128.3$_5$-125.9$_8$ (*aromatic carbons*, **Ph rings**) 117.5$_9$-116.5$_6$ (*backbone carbons*, N***C***=***C***N), 72.2$_6$(O***C***H), 56.5$_1$(N***C***H$_2$), 37.6$_7$(N***C***H$_3$), 23.8$_7$ (OCO***C***H$_3$)

MALDI-ToF (m/z): 739.07459 Da attributable to a structure a bis-carbene structure $[C_{24}H_{24}AuCl_4N_4O_2]^+$

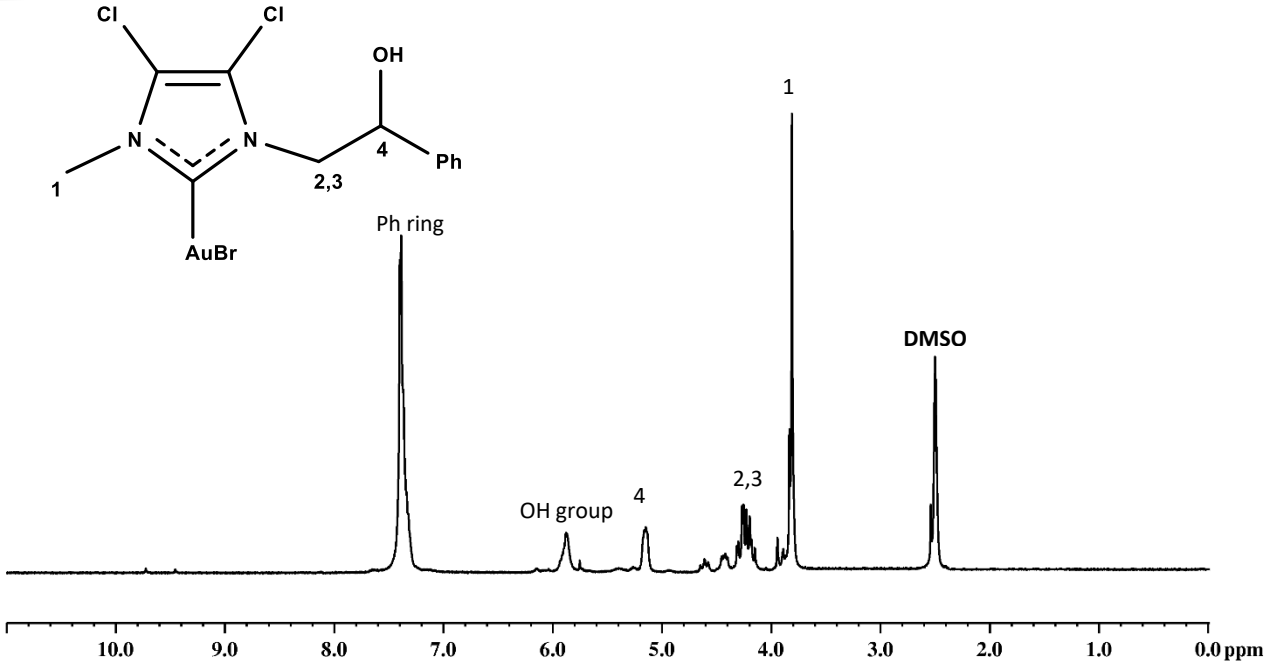

^{1}H-NMR (400MHz, DMSO-d_6): δ 7.4$_0$-7.3$_6$ (m, 5H, ***Ph ring***) 5.8$_7$(m, 1H, ***OH group***); 5.1$_4$ (m, 1H, OC***H***) 4.2$_6$-4.1$_9$(m, 2H, NC***H***$_2$); 3.8$_1$(s,3H, NC***H***$_3$)

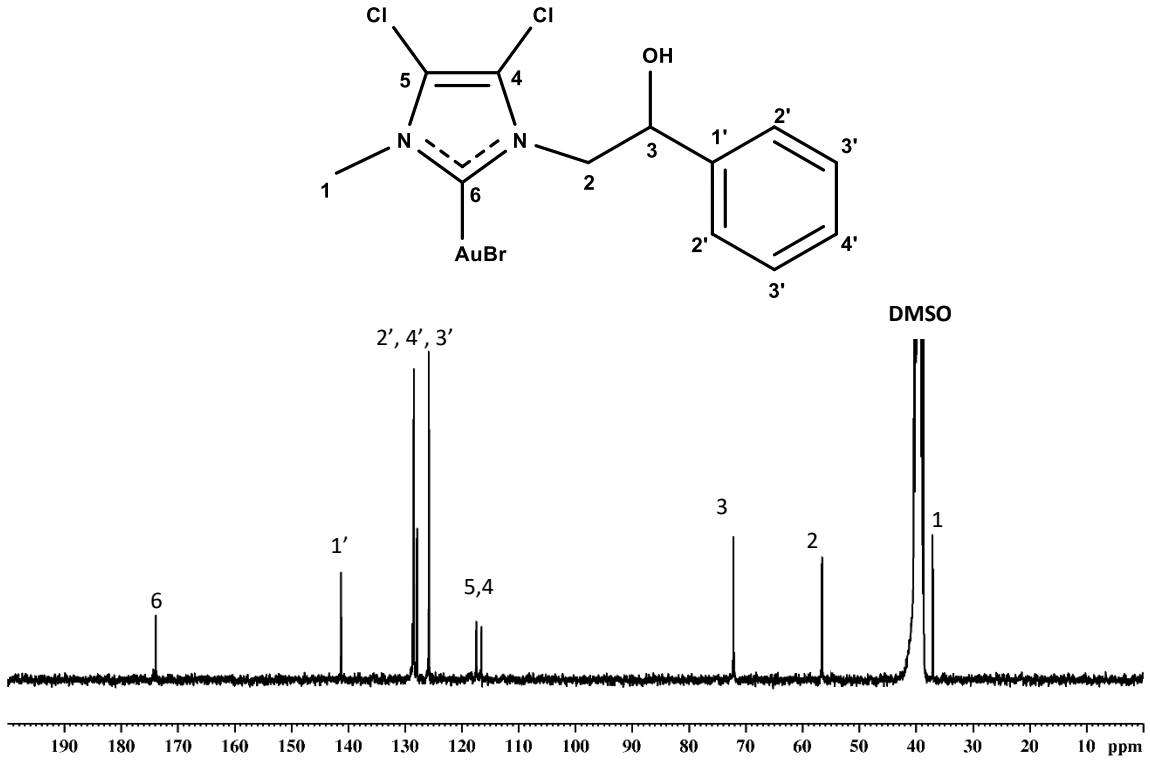

^{13}C-NMR (100 MHz, DMSO-d_6): δ 173.8$_9$ (N***C***N) 141.2$_4$ (*ipso aromatic carbon*, **Ph-ring**), 128.4$_3$-125.7$_8$ (*aromatic carbons*, **Ph rings**) 117.4$_2$-116.5$_4$ (*backbone carbons*, N***C***=***C***N), 72.1$_4$(O***C***H), 56.5$_6$(N***C***H$_2$), 37.0$_4$(N***C***H$_3$)

MALDI-ToF (m/z): 739.03526 Da attributable to a structure a bis-carbene structure $[C_{24}H_{24}AuCl_4N_4O_2]^+$

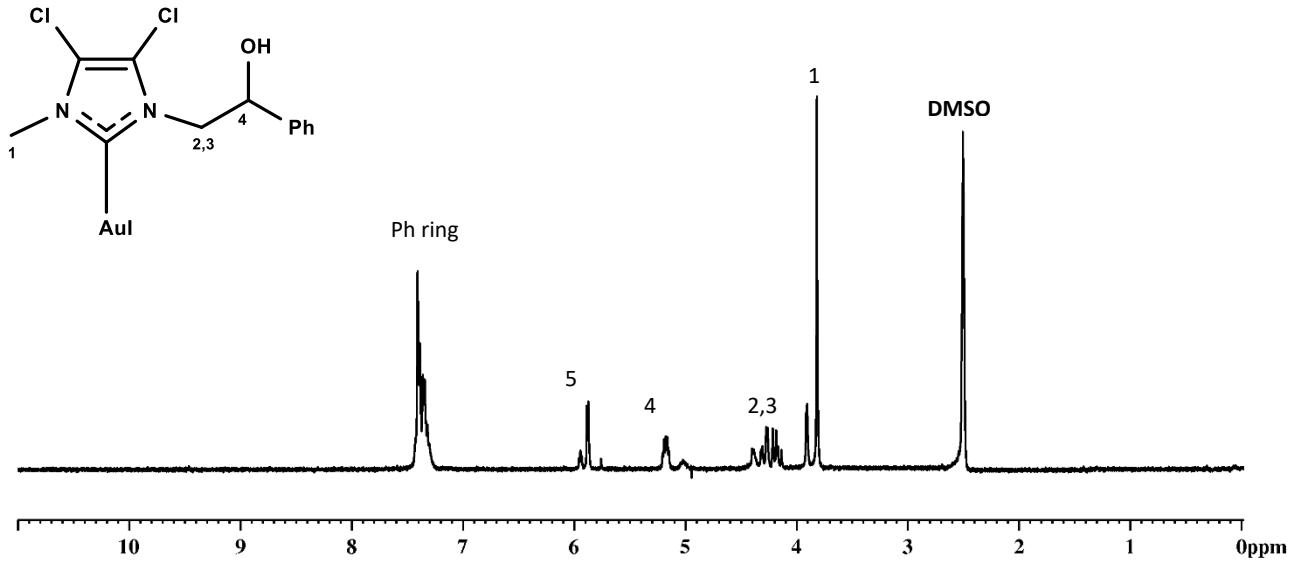

^{1}H-NMR (400MHz, DMSO-d_6): δ 7.40-7.34 (m, 5H, ***Ph ring***) 5.95 -5.75(m, 1H, ***OH group***); 5.18 - 5.17 (m, 1H, OC***H***) 4.39-4.05(m, 2H, NC$\boldsymbol{H_2}$); 3.91-3.81(s,3H, NC$\boldsymbol{H_3}$)

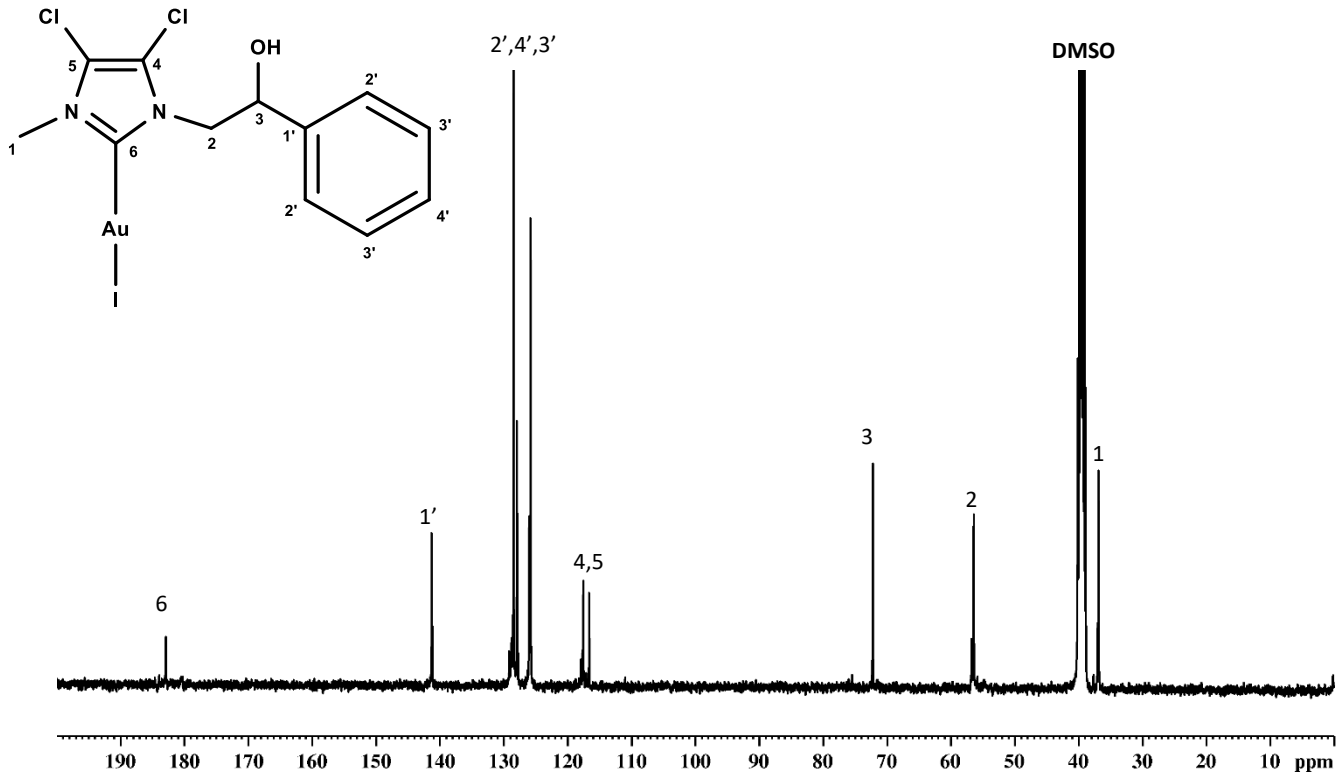

^{13}C-NMR (100 MHz, DMSO-d_6): δ 182.92 (N***C***N) 141.28 *(ipso aromatic carbon*, **Ph-ring**), 128.47-125.78 (*aromatic carbons*, **Ph rings**) 117.54-116.62 (*backbone carbons*, N***C*=*C***N), 72.22(O***C***H), 56.41(N***C***H$_2$), 36.84(N***C***H$_3$)

MALDI-ToF (m/z): 739.06311 Da attributable to a bis-carbene structure $[C_{24}H_{24}AuCl_4N_4O_2]^+$

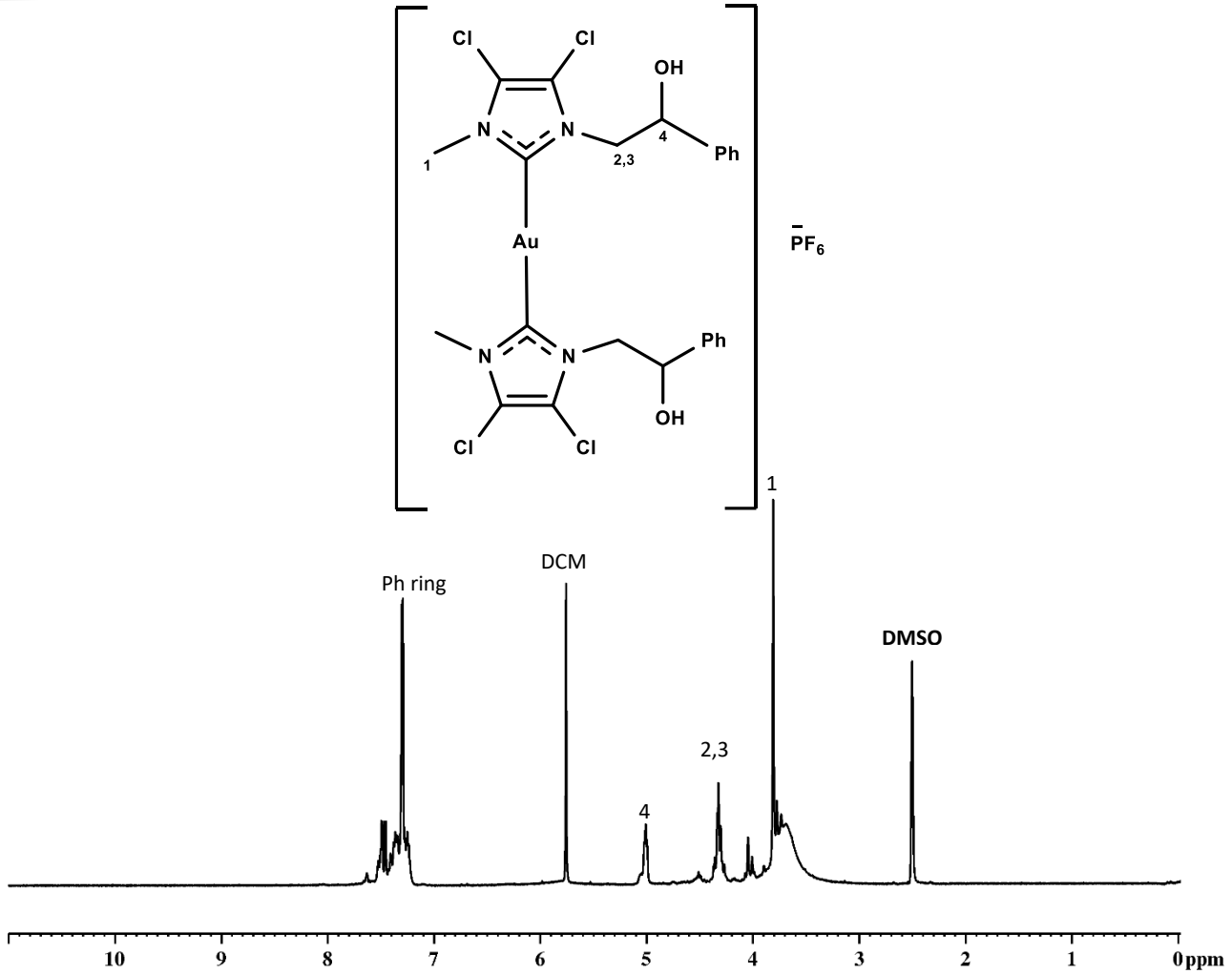

^{1}H-NMR (400MHz, DMSO-d_6): δ 7.4$_0$-7.2$_9$ (m, 5H, ***Ph ring***) 4.9$_9$ (m, 1H, OC***H***) 4.3$_3$-4.3$_0$(m, 2H, NC***H***$_2$); 3.80(s,3H, NC***H***$_3$)

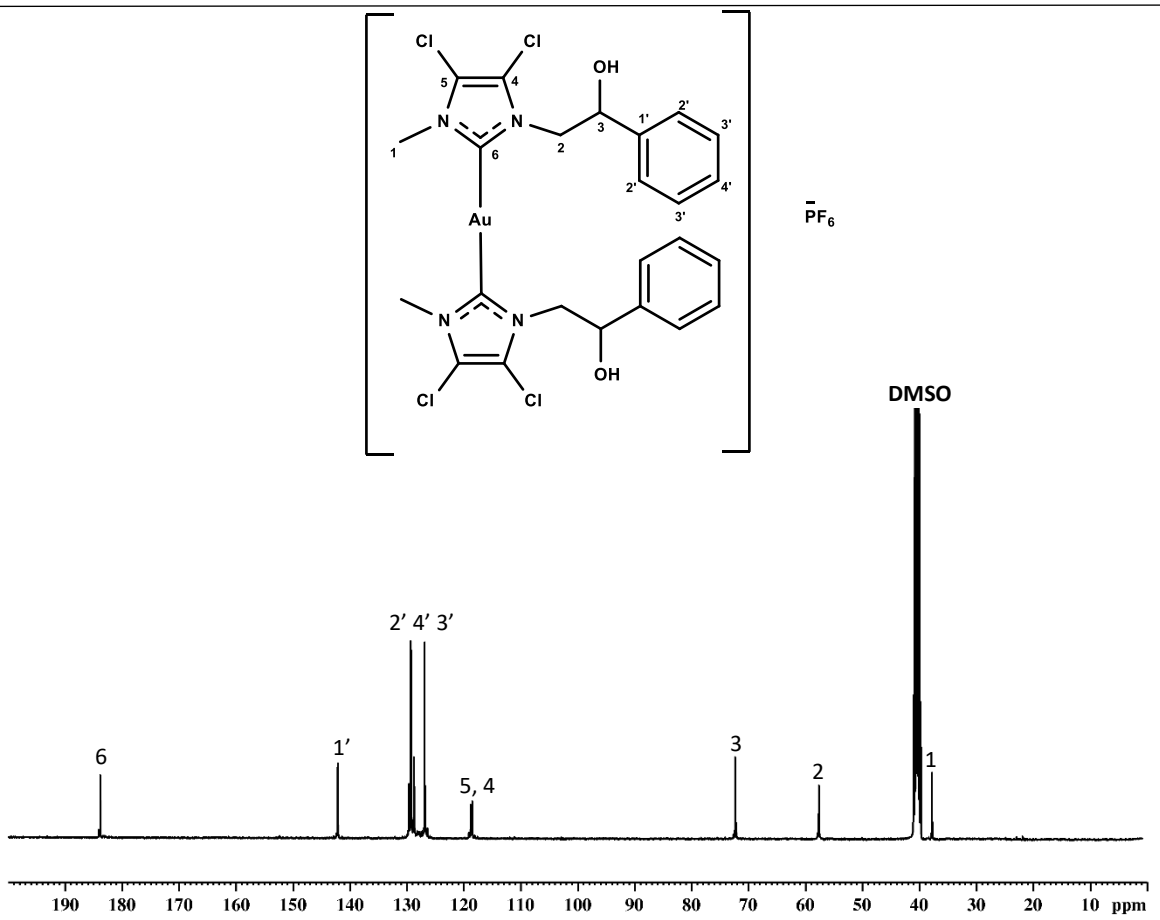

^{13}C-NMR (100 MHz, DMSO-d_6): δ 183.8$_2$ (N***C***N) 142.1$_4$ (*ipso aromatic carbon*, **Ph-ring**), 129.2$_9$-126.8$_8$ (*aromatic carbons*, **Ph rings**) 118.7$_8$-118.5$_1$ (*backbone carbons* N***C*=*C***N), 72.3$_3$(O***C***H), 57.6$_3$(N***C***H$_2$), 37.8$_0$(N***C***H$_3$)

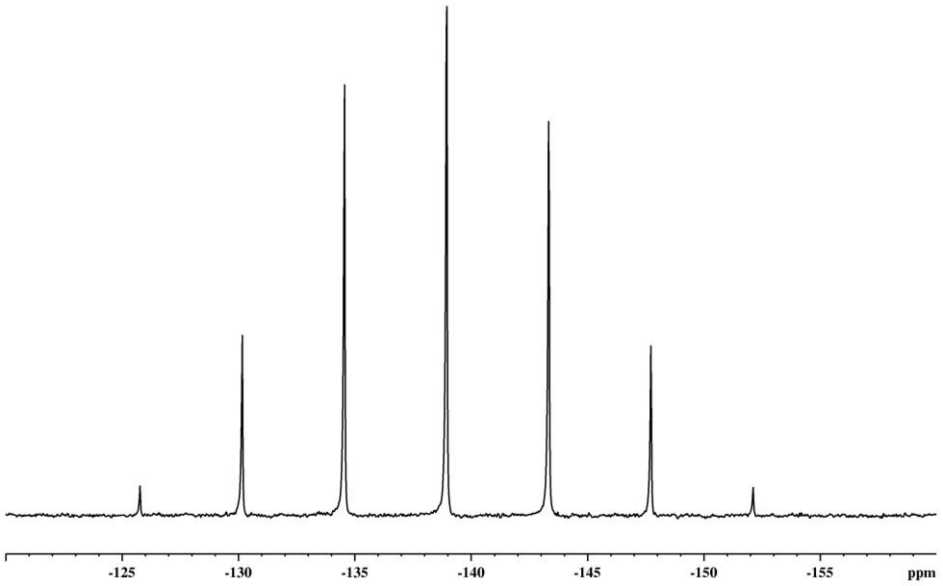

^{31}P-NMR (162.60 MHz; DMSO-d_6): δ 193.9$_3$ (septuplet)

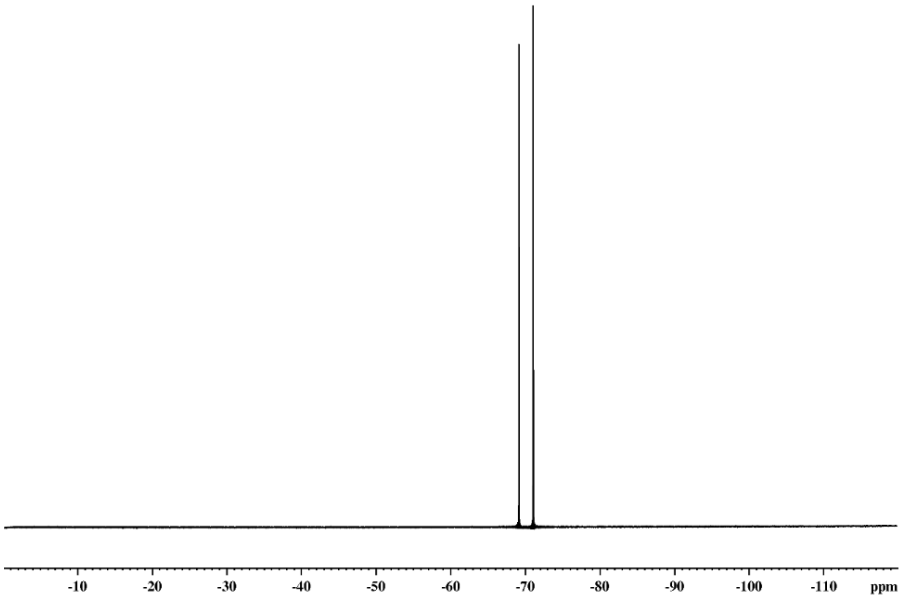

^{19}F-NMR (377.35 MHz, DMSO-d_6): δ 70.10 (duplet)

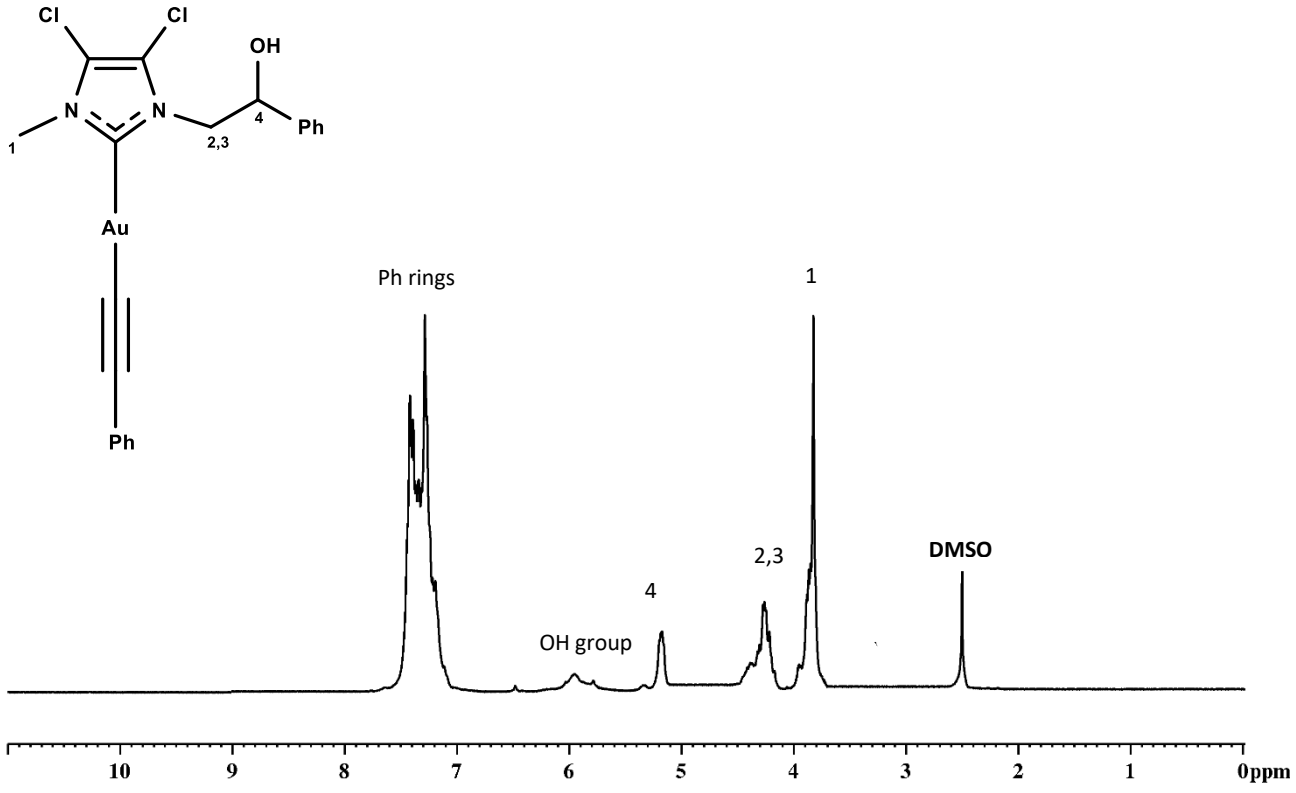

^{1}H-NMR (400MHz, DMSO-d_6): δ 7.42-7.27 (m, 10H, ***Ph rings***) 5.9$_7$(m, 1H, ***OH group***); 5.1$_7$ (m, 1H, OC***H***) 4.2$_7$-4.2$_6$(m, 2H, NC***H***$_2$); 3.8$_2$(s,3H, NC***H***$_3$)

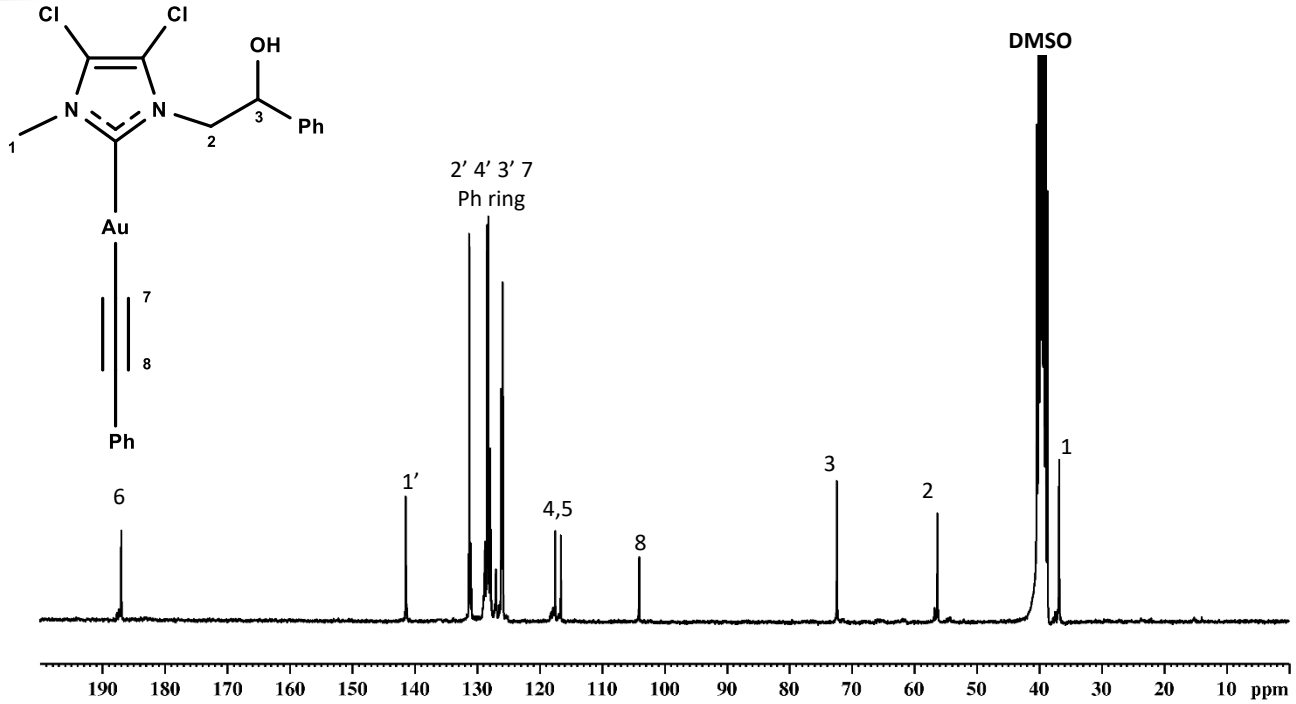

^{13}C-NMR (100 MHz, DMSO): 186.9$_5$ (N***C***N) 141.3$_9$ (*ipso aromatic carbon*, **Ph-ring**), 131.2$_4$-125.8$_5$ (*aromatic carbons*, **Ph rings,** Au***C***≡C-Ph) 117.4$_7$-116.5$_6$ (*backbone carbons* N***C***=***C***N,), 104.0$_3$ (AuC≡***C***-Ph) 72.3$_6$(O***C***H), 56.2$_7$(N***C***H$_2$), 36.7$_8$(N***C***H$_3$).

The kinetic results in A^3-coupling reaction, catalyzed by halo and pseudo halo analogs of AuL2 are shown in **Table 14** and displayed in **Figure 64**

Table 14 Monitoring of A^3-coupling reaction of benzaldehyde catalyzed by AuL2X complex

Tempo(h)	Yield (%)					
	(NHC)Au-Cl	(NHC)Au-Br	(NHC)Au-I	(NHC)Au-OAc	[Au(NHC)$_2$]$^+$PF$_6^-$	(NHC)AuCCPh
0	0	0	0	0	0	0
0.16	0	0	0	0	0	0
0.33	0	0	0	0	0	0
0.5	0	0	0	0	0	0
0.66	7	6	0	6	0	0
0.83	13	11	4	11	0	0
1.00	18	16	9	17	0	0
2.00	36	30	18	36	0	0
3.00	58	37	27	48	0	13
4.00	72	42	36	59	0	20
5.00	77	45	40	61	0	24
6.00	84	53	45	64	9	31
24.0	99	71	60	70	46	67

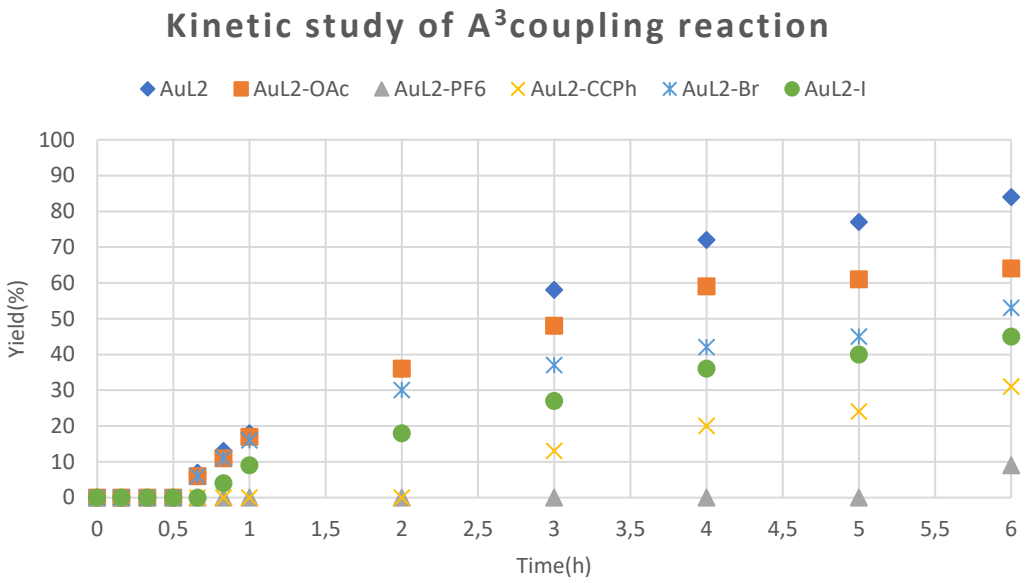

Figure 64 Plot of yields versus time for the first 6 hours of the reaction with benzaldehyde

The catalytic activity of the complexes was strictly influenced by the nature of the counter-ion, in the order, Cl > Br ≈ OAc > I > C≡CPh > PF_6, according to the literature [81]. Considering halide gold complexes, the lowering of catalytic activity, descending along with the group, is due to the decreasing of the Lewis acidity of the metal center, as was observed by Backer and coworkers in their spectroscopic studies[178]. While, the worst catalytic activity was displayed by the hexafluorophosphate gold complex, and it was attributed to the exclusive presence of bis carbenic metallic species[$(NHC)_2Au]PF_6$.

2.5.4 Conclusion

Silver and gold NHC complexes have attracted scientific attention due to their ability to catalyze various interesting reactions, such as A^3-coupling reaction. To explore the potentialities of these compounds, we have tested silver and gold complexes, bearing L1-L14 ligands, in A^3-coupling reaction with three different aldehydes (p-formaldehyde, cyclohexanal, and benzaldehyde) with piperidine and phenylacetylene, in neat conditions at 80°C. All complexes were able to catalyze the reaction, while the best catalytic activity was achieved by **AuL2**. The higher catalytic activity is attributed to the presence of the chlorine atoms on the backbone, which makes the metal center more electrophilic and more prone to coordinate the alkyne.

Then, to deepen the studies on A^3 coupling reaction, we have synthesized, characterized, and tested the activity of halo and pseudo halide analogs with the highest catalytic activity (**AuL2**). The chloride anion was substituted by bromide, iodide, acetate, phenylacetilide, and hexafluorophosphate, with opportune silver or alkali salts.

By the analysis of the yields, the activity of the complex was closely influenced by the nature of the anion, in fact chloride gold NHC complex (**AuL2**) has displayed the greatest activity in the condensation of benzaldehyde with piperidine and phenylacetylene.

2.6 Hydroamination of alkynes catalyzed by Au(I) *N*-heterocyclic carbene complexes

2.6.1. Hydroamination reaction

The compounds containing C-N bonds are significant and commercially important starting materials for the synthesis of value-added products such as polymers, solvents, biologically active molecules, and pharmaceuticals[182–185]. Thus, the hydroamination reaction, due to its high efficiency and sustainability, is one of the most useful synthetic strategies to obtain these compounds. It consists of the addition of amine moiety to C-C multiple bonds (alkenes and alkynes) providing a 100% of atom economy. Due to their lower electron density, the addition of amines to alkenes is more difficult than that to alkynes[186,187]. Another important factor in this reaction is the regiochemistry of the product. The anti-Markovinikov addition of amines to the olefin is listed as one of the ''Ten Challenges for Catalysis''[186].

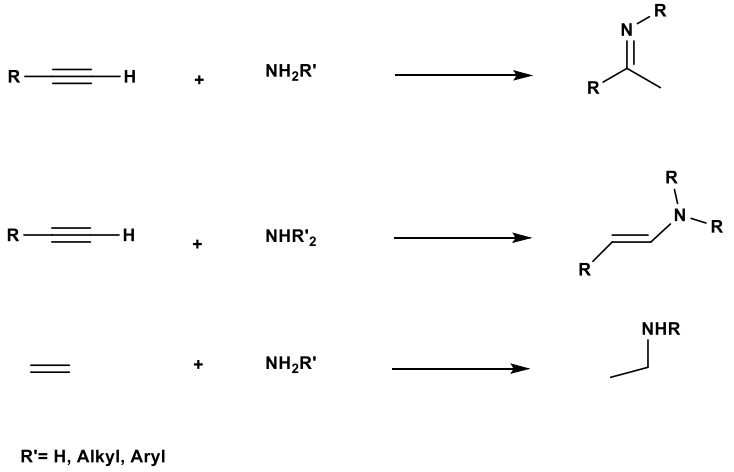

Figure 65 General Scheme of hydroamination reaction

Despite the reaction is thermodynamically achievable, it is necessary to overcome a high activation barrier owing to the repulsion between the electron density of amine and the π-system of electrophile. This high activation barrier can be reduced by using the metal catalysis pathway by the coordination of the alkene/alkyne or amine to the metal center and subsequently protonolysis, giving the desired product. Hydroamination reaction is catalyzed by different kinds of main groups and transition metals. The catalytic hydroamination is strictly related to the choice of the metal catalyst. Early transition metals, alkali, earth alkali metals, and lanthanides have shown a good activity[188–192] following an amine activation pathway[193,194]. The main limitation of these catalytic systems is the air and moisture instability due to their oxophilicity. Instead, late transition metals are less oxophilic and more tolerant to air and moisture and have shown good activity in catalytic hydroamination [118,195–199]. For these catalysts, an alkyne coordination pathway is hypothesized[200]. In this regard, gold has emerged as a catalyst in the hydroamination reaction; in particular, Au-NHC complexes, activated by halide scavenger as a silver salt,

have attracted the attention for their application in this catalytic transformation [118,199,201].

2.6.2 Aim of the project

Based on the interesting results obtained by our gold complexes in the A^3-coupling reaction, we have extended the studies on their performance in hydroamination reactions. We have tested the gold complexes **AuL1**, **AuL2**, **AuL3**, **AuL4**, **AuL5**, **AuL6**, **AuL10**, and **AuL11** (Figure 45, Chapter 2) in the hydroamination reaction, using as halide scavenger silver hexafluoro antimoniate ($AgSbF_6$), because it has shown the best performance in the screening test of the cocatalyst[118,202] (see **Table 15**).

In the first instance, we tested all the complexes in the addition of aniline to phenylacetylene, in acetonitrile (CH_3CN), following the literature procedure [117,202], at 90°C for sixteen hours.

Subsequently, it was performed a screening of the reaction in diverse solvents such as 1,4-dioxane, dimethyl sulfoxide (DMSO), ethylene carbonate, toluene, and tetrachloroethane (see **Table 16**).

Finally, it was tested the catalytic activity of the best performer gold complex (**AuL2**) in the addition of different arylamine to phenylacetylene and internal alkynes (diphenylacetylene) (see **Table 17).**

2.6.3 Screening of the Gold (I) complexes as Catalyst in the Hydroamination of Phenylacetylene with Aniline

The gold complexes **AuL1**, **AuL2**, **AuL3**, **AuL4**, **AuL5**, **AuL6**, **AuL10**, **AuL11** were tested in the hydroamination reaction of phenylacetylene with aniline, in acetonitrile at 90°C, using 1%mol of gold precatalyst and the 2% mol of the halide-scavenger silver salt, to lead the corresponding ketoimine. In **Table 7** are reported the activities of these gold NHC complexes. The yields were determined by ^{1}H-NMR spectroscopy, using the internal standard method (dibromomethane, CH_2Br_2), with the integration of the singlet signal of the standard, at 4.9$_3$ ppm, with the signal of the methyl group of ketoimine at 2.2$_4$ ppm. By the analysis of the NMR spectra, it was observed the singlet signal attributable to the acetophenone (2.6$_0$ ppm). The formation of the ketone is ascribed to the capacity of gold NHC complexes to catalyze the addition of the water of alkynes [109–111] and/or by the hydrolysis of the imine, given by the hygroscopicity of the silver cocatalyst salt.

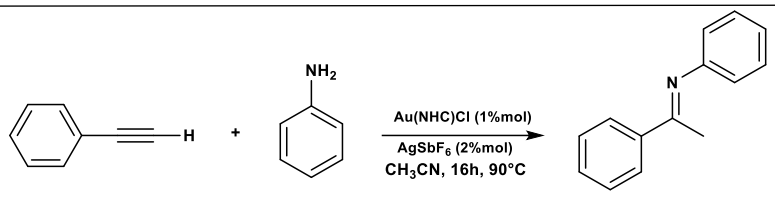

Figure 66 Hydroamination of phenylacetylene catalyzed by Au(I) NHC complexes

Table 15 Catalytic activity of Au-NHC complexes in hydroamination reaction

Run[a]	Catalyst	Yield [b] (%)
1	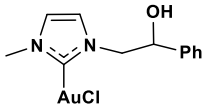 **AuL1**	55%
2	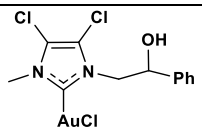 **AuL2**	70%
3	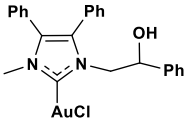 **AuL3**	53%
4	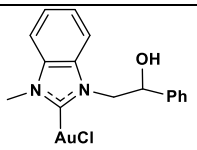 **AuL4**	35%
5	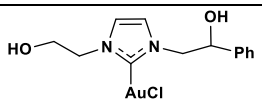 **AuL5**	34%
6	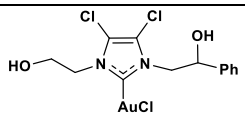 **AuL6**	55%
7	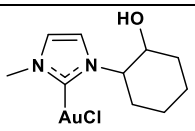 **AuL10**	30%
8	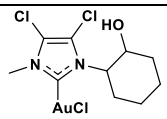 **AuL11**	60%
9	**$Au(SMe_2)Cl$**	10%
10	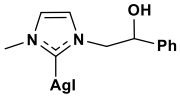 **AgL1**	10%
11	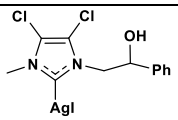 **AgL2**	15%

[a] Reaction conditions: aniline (1.0 mmol), phenylacetylene (1.5mmol), AuNHC (1%mol), $AgSbF_6$ (2%mol), 90°C, 16h. CH_3CN (1mL), nitrogen atmosphere. [b] Yields were average of two runs and determined by ^{1}H-NMR analysis through internal standard.

As shown in **Table 15**, all tested complexes were able to catalyze the hydroamination reaction of phenylacetylene. The gold complexes were more active than the silver analogs (**Run 1,2 vs 10,11**). This observation underlines the role of gold in this type of reaction. Another interesting observation was the important different catalytic activity of gold NHC complexes, in comparison with the gold precursor [**Au(SMe$_2$)Cl**]. This suggests the importance of the NHC ligand in the stabilization of the cationic gold catalyst. Gold complexes with chlorine atoms on the backbone of the ligand (**AuL2**, **AuL6**, **AuL11**) were more active than other gold complexes. This better catalytic activity is imputable to a major positive charge on the metal center, as seen in A^3 coupling reactions, in fact the presence of the chlorine atoms makes more electrophilic the metal center, thus more prone to receive the π-electron density of the alkyne.

2.6.4 Screening of the Solvent for the Hydroamination of Phenylacetylene with Aniline, promoted by AuL2.

After the preliminary studies that allowed the choice of the catalyst, we have used various solvents to optimize the reaction conditions. It was screened the hydroamination reaction of phenylacetylene with aniline, in 1,4-dioxane, dimethyl sulfoxide (DMSO), ethylene carbonate, toluene, and tetrachloroethane. In **Table 16**, are reported the yield of the hydroamination reaction with tested solvent, catalyzed by **AuL2**. As seen in the previous section, the yields of the reaction are calculated by the ^{1}H-NMR, using the internal standard method.

Table 16 Screening of the solvent in the reaction of hydroamination

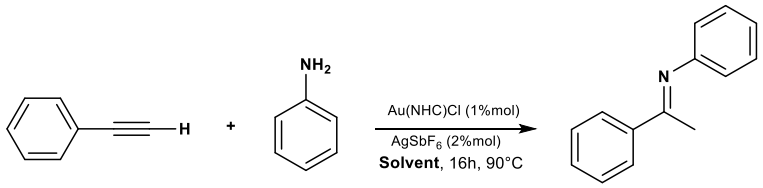

Run[a]	Solvent	Yield [b] (%)
1	**CH_3CN**	70%
2	**1,4-Dioxane**	20%
3	**DMSO**	13%
4	**TCDE**	45%
5	**toluene**	50%
6	**Ethylene Carbonate**	35%

[a] Reaction conditions: aniline (1.0 mmol), phenylacetylene (1.5mmol), AuL2 (1%mol), $AgSbF_6$ (2%mol), 90°C, 16h. Solvent (1mL), nitrogen atmosphere. [b] Yields were average of two runs and determined by ^{1}H-NMR analysis through internal standard.

As shown in **Table 16**, CH_3CN has provided the highest yield in the adopted reaction conditions, in accordance with the data present in the literature [117,199,202,203]. A plausible explanation of the best performance in acetonitrile is given by the possibility of

the solvent coordinating and stabilizing the cationic metal center, after the precipitation of chloride by silver salt (see **Scheme 3**)[116].

2.6.5 Hydroamination of alkyne with different arylamine.

Once the reaction conditions were optimized, **AuL2** was tested in the hydroamination reaction of phenylacetylene and another internal alkyne with different arylamines. All the results are reported in **Table 17**.

Table 17 Hydroamination test with different aryl substrate

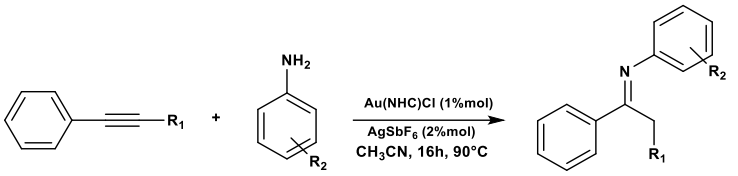

Entry	R_1	Amine	Product	Yield (%)
1	H	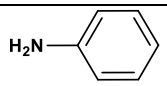	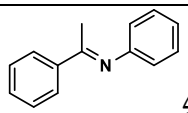 **4a**	70
2	H	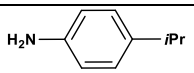	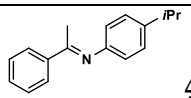 **4b**	71
3	H	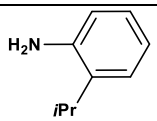	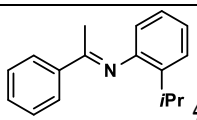 **4c**	73
4	H	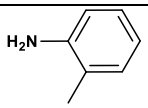	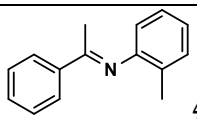 **4d**	62
5	H	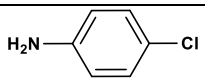	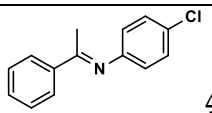 **4e**	33
6	H	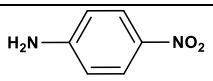	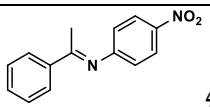 **4f**	10
7	H	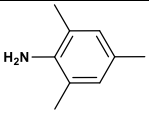	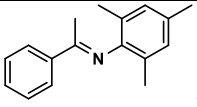 **4g**	57
8	H	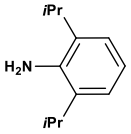	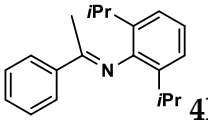 **4h**	55
9	H	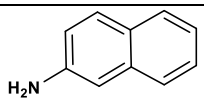	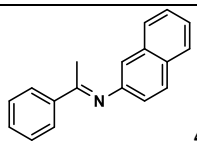 **4i**	47

10	H	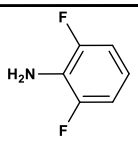	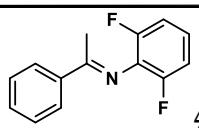 **4j**	38
11	H	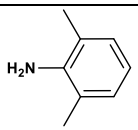	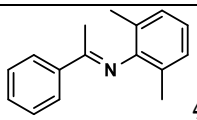 **4k**	55
12	H	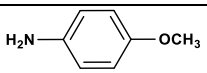	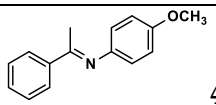 **4l**	72
13	Ph	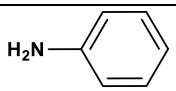	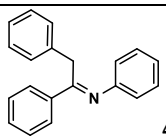 **4m**	20 60[c]

[a] Reaction conditions: arylamine (1.0 mmol), alkyne (1.5mmol), AuL2 (1%mol), $AgSbF_6$ (2%mol), 90°C, 16h. Solvent (1mL), nitrogen atmosphere. [b] Yields were average of two runs and determined by ^{1}H-NMR analysis through internal standard, [c] AuL2Cl (3%mol), $AgSbF_6$ (6%mol).

Several arylamines were found to react with an alkyne, giving the desired ketoimine. Electron-rich arylamines (o-isopropyl aniline, p-isopropyl aniline, anisole) have shown good reactivity (**entries 2,3,12**). Naphthylamine and more steric hindered arylamines (mesitylamine, 2,6-diisopropyl aniline, 2,6-methyl aniline) have reacted well with phenylacetylene (**entries 7,8,11**). Instead, electron-poor arylamines (p-chloroaniline, p-nitroaniline and 2,6-difluoroaniline) did not show a good reactivity in the intermolecular hydroamination reaction of phenylacetylene (**entries 5,6,10**). Probably, the presence of an electron-withdrawing group makes the arylamine less reactive toward the nucleophilic attack of the alkyne. Finally, the hydroamination reaction diphenylacetylene with aniline was performed (entry 13). For the reaction, the use of 3% mol of catalyst to active the alkyne in the nucleophilic addition of aniline was necessary to obtain a good yield of the ketomine (60%).

2.6.7 Conclusions

In summary, the gold NHC complexes, synthesized and characterized by us, were tested in the intermolecular hydroamination. All the complexes were active toward the hydroamination reaction of phenylacetylene with aniline. By the analysis of the yields (**Table 15**), the gold complexes bearing two chlorine atoms on their backbone have shown the best catalytic activity. In the same manner, as the A^3-coupling reaction, a possible reason for this behavior is the higher electrophilicity of the gold complex, which allows for stronger coordination of the olefin and a consequent nucleophilic attack by the arylamine.

To optimize the reaction conditions, a series of solvents were screened using the best performer gold precatalyst (**AuL2**). Best catalytic performance was recorded in CH_3CN, which gives a superior catalytic activity of the precatalyst than the other used solvent (DMSO, 1,4-dioxane, toluene, ethylene carbonate, tetrachloroethane).

Finally, in the optimized reaction conditions, **AuL2** was tested in the hydroamination reaction with different arylamines. The activity of the complex is influenced by electron and steric factors, in fact, by the analysis of the yields, the electron-rich aryl amines give interesting yields in the addition to alkyne moiety, whereas the electron-poor arylamine has not shown the same behavior in the reaction. Moreover, increasing the steric hindrance, it was observed a slight worsening of the catalytic activity. Thus, for the reaction of the diphenylacetylene was necessary the 3%mol of the precatalyst to obtain a good yield (60%).

2.7 Biological activity

Considering the interesting results shown by silver and gold complexes in bioinorganic chemistry [204], the antibacterial and antitumoral activities of these complexes have been preliminarily evaluated.

Since the widespread use of silver salts as antibacterial compounds and considering the efficacy of silver *N*-heterocyclic carbene complexes in this regard, has been preliminary tested the antimicrobial activity of AgNHC complexes [126].

Table 18 Preliminary test of silver N-heterocyclic carbene complexes as antimicrobial

Compound	MIC (Minimal inhibitory Concentration µg/mL [a]	
	E. Coli (Gram Negative)	*B.subtilis (Gram Positive)*
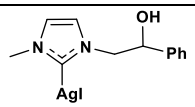 **AgL1**	5	5
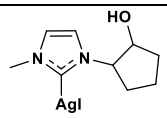 **AgL8**	5	50
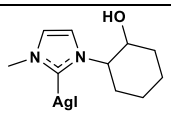 **AgL10**	5	50

The analysis of the results suggests that silver complexes have good antimicrobial activity. They inhibited the growth of *E. coli* at a concentration of 5µg/mL. Furthermore, AgL1 has exhibited the same inhibition concentration against *B.subtillis*. **AgL8** and **AgL9** inhibited the growth of *B. subtillis* at higher concentrations. The antitumoral activity of silver and gold (I) NHC complexes were evaluated for the first time by some of us in 2016 [128]. Silver compound (**AgL1**, **AgL8**, **AgL10**), and gold analogs (AuL1, AuL8, AuL10) were tested toward tumorigenic cell lines (MCF-7), and the cytotoxic activity was evaluated by the calculation of IC_{50}. **AgL1** and **AuL1** have exhibited an interesting biological activity, in fact the IC_{50} were respectively 4.0±0.2 µM and 1.0±0.2 µM. Whereas, other complexes did not reveal any activity.

Based on these preliminary results, Iacopetta and coworkers synthesized two new silver and gold complexes, starting by 4,5-dichloro imidazole (**AgL9**, **AuL9**), and studied their antiproliferative activity against two tumoral breast cell lines (MCF-7 and MDA-MB 231) and two tumorigenic uterine cell lines (ISHIKAWA, HeLa)[129]. The results are reported in **Table 19**. **AuL9** resulted more active than the silver analogs, inducing the reduction of cell growth. Furthermore, the complexes were inactive toward non-tumorigenic cell lines (MCF-10A and HEK-293).

Table 19 IC50 of Ag and Au NHC complexes expressed in micromolar μM[129]

	IC_{50} μM					
compound	**MCF-7**	**MDA-MB231**	**HeLa**	**ISHIKAWA**	**MCF-10A**	**HEK-293**
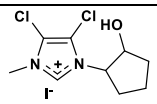 **P-L9**	>200	>200	>200	>200	>200	>200
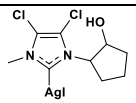 **AgL9**	16.5±0.8	20.8±1.2	15.6±0.6	15.0±0.9	>200	>200
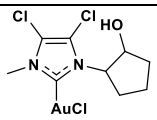 **AuL9**	3.98±0.4	6.02±0.7	1.63±0.5	4.81±0.9	>200	>200

The activity of complex **AuL9** was attributed to its ability to induce mitochondrial apoptotic pathway, increasing ROS (reactive oxygen species) production.

Starting from these preliminary results, we have evaluated the biological activity of newly synthesized silver and gold complexes.

2.7.1 Antimicrobial activity of silver and gold N-heterocyclic carbene complexes

Based on the interesting preliminary obtained results, we have tested the antibacterial activity of other silver and gold NHC complexes. The antibacterial activity of silver and gold complexes was evaluated with the determination of the MIC, following Clinical and Laboratory Standards Institute (CLSI) guidelines [205], by the research group of Prof. Giovanni Vigliotta of the University of Salerno. Silver and gold complexes were tested against *Staphylococcus aureus* (Gram-positive) and *Escherichia coli* (Gram-negative) bacterial strains. The results are reported in **Table 20**[136].

Table 20 Antibacterial activity of silver and gold (I) N-heterocyclic carbene complexes towards Gram – and Gram + bacteria

Compound	MIC (Minimal inhibitory Concentration μg/mL [a]	
	E. Coli (Gram Negative)	*S. Aureus (Gram Positive)*
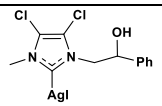 **AgL2**	10	>150
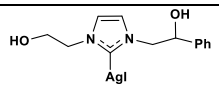 **AgL5**	15	50
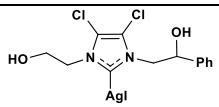 **AgL6**	15	>150
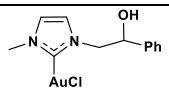 **AuL1**	>150	40
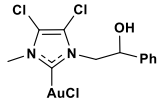 **AuL2**	75	0.5
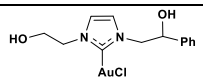 **AuL5**	100	25
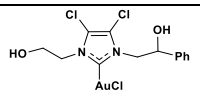 **AuL6**	75	2.5

The results were determined by three independent assays, each in triplicate. [a]150 μg/mL is the highest concentration tested for each compound.

By the analysis of the results, AgNHC complexes have shown an antibacterial selectivity toward Gram – bacteria strain, showing MIC values between 10 and 15 μg/mL. Instead, they have not shown efficacy against tested Gram + strain (*S. Aureus)*, with the exclusion of **AgL5**, that have shown a modest activity (MIC 50 μg/mL). **AgL1** have exhibit the best antibacterial activity against *E. coli* (6.5 μg/mL). Unlike silver complexes, gold compounds have shown a better antibacterial activity toward Gram + strain, in accordance with the literature[90]. Gold complexes have exhibited an interesting antibacterial activity toward *S. Aureus,* showing low values of MIC, **AuL2** revealed a minimum inhibition concentration of 0.5 μg/mL. Furthermore, AuNHC complexes have revealed an activity toward *E. coli*, with MIC values among 75-150 μg/mL, suggesting a wider range of antibacterial activity than silver analogs. Finally, the corresponding imidazolium pro-ligands were tested, and they have not shown any growth inhibition up to the concentration of 200 μg/mL. The promising activity of N-heterocyclic carbene silver halide complexes (**AgL1**, **AgL2**) as antibacterial compounds, led us to evaluate the antimicrobial activity of their acetate analog, shown in **Figure 67**.

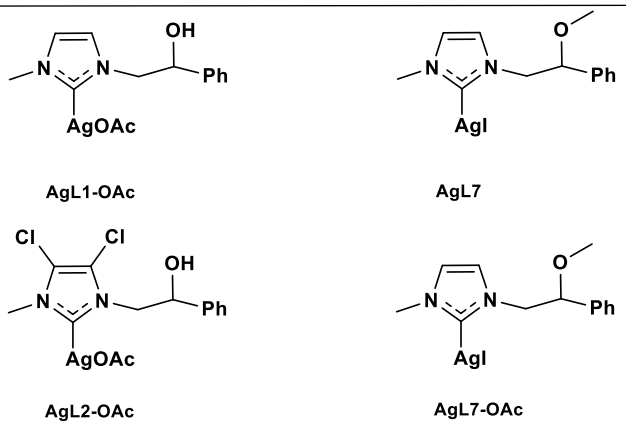

Figure 67 Structure of AgNHC complexes tested as antimicrobial

These complexes were synthesized by metathesis reaction of the counterion, using silver NHC complexes with silver acetate in a mixture of methanol and dichloromethane, at room temperature.

The complexes have shown a low value of MIC against *E. coli*, *S. Aureus,* and *E. faecalis*. All the MIC values are listed in **Table 21**. The **AgL1-OAc** and **AgL2-OAc** have inhibited the growth of E. coli at 10μg/mL, while other complexes have revealed lower inhibition concentrations (5 μg/mL). By the analysis of the results against Gram+ bacterial strains (*S. Aureus E. faecalis)*, higher concentrations of silver NHC compounds were required to inhibit their growth (MIC from 5μg/mL to 10μg/mL for *S. Aureus*, and 10 μg/mL to 20 μg/mL for *E. faecalis*). For these complexes was evaluated the minimal bactericidal concentration (MBC), the lowest concentration able to kill bacteria. All the complexes have exhibited an MBC equal to or greater than 100 μg/mL.

Table 21 MIC values of silver NHC complexes

compound	MIC (Minimal inhibitory Concentration μg/mL		
	E. coli	*S. Aureus*	*E. faecalis*
AgL1-OAc	10	5	20
AgL2-OAc	10	5	10
AgL7	5	5	10
AgL7-OAc	5	5	20

2.7.1 Antitumoral activity of silver and gold N-heterocyclic carbene complexes

With the purpose to deepen the obtained results on cytotoxic silver and gold NHC complexes, we have adopted structural modifications to enhance the antitumoral activity. In this regard, we have evaluated the antitumoral activity of two silver and gold complexes, derived from 4,5-dichloro imidazole (**AgL2**, **AuL2**) [206]. The complexes were evaluated on MCF-7, MDA-MB-231, HeLa, and ISHIKAWA, by the research group of Prof. Maria Stefania Sinicropi of the University of Calabria. The gold complex has shown an intriguing activity

on all tumorigenic cell lines, particularly against MDA-MB-231 cell lines (IC_{50}=2.10±0.7μM). The silver analog has also exhibited an interesting cytotoxic activity against uterine carcinoma cell lines (IC_{50}=9.76±0.6μM on HeLa and 6.55±0.7μM on ISHIKAWA). Also, these complexes, as seen above for **AgL9** and **AuL9**, did not interfere with healthy cell lines. The imidazolium pro-ligand was not effective against all cell lines.

Table 22 IC_{50} of Ag and Au complexes derived by 4,5-dichloro imidazole expressed in micromolar

	IC_{50} μM				
compound	**MCF-7**	**MDA-MB231**	**HeLa**	**ISHIKAWA**	**MCF-10A**
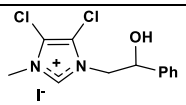 **P-L2**	>200	>200	>200	>200	>200
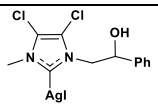 **AgL2**	10.5±0.8	3.2±1.2	9.8±0.6	6.6±0.9	>200
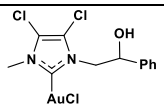 **AuL2**	5.2±0.4	2.1±0.7	31.9±0.5	29.9±0.9	>200

By the analysis of *in vitro* and *in silico* studies, it was demonstrated that AuL2 can inhibit human Topoisomerase I and II and it interferes with the tubulin polymerization. In this regard, this ability can make **AuL2** a promising compound for the development of a multi-target agent in the treatment of tumors.

Further studies have been conducted on cationic silver and gold NHC complexes stabilized by acetate counterion. Silver and gold NHC complexes have been synthesized following the procedure reported in sections 2.3.5 and 2.5.3.1, by the reaction of the halo NHC complex with silver acetate[178]. Below, are reported the NMR characterization of **AuL1-OAc** and **AuL7-OAc**. The formation of acetate gold NHC complexes has been confirmed by the appearance of the methyl group in the ^{1}H-NMR spectrum, and by the ''shifting'', at high-field, of the signal attributable to the carbene carbon atom, in ^{13}C-NMR, as seen above for the complex **AuL2-OAc** in section 2.5.3.1.

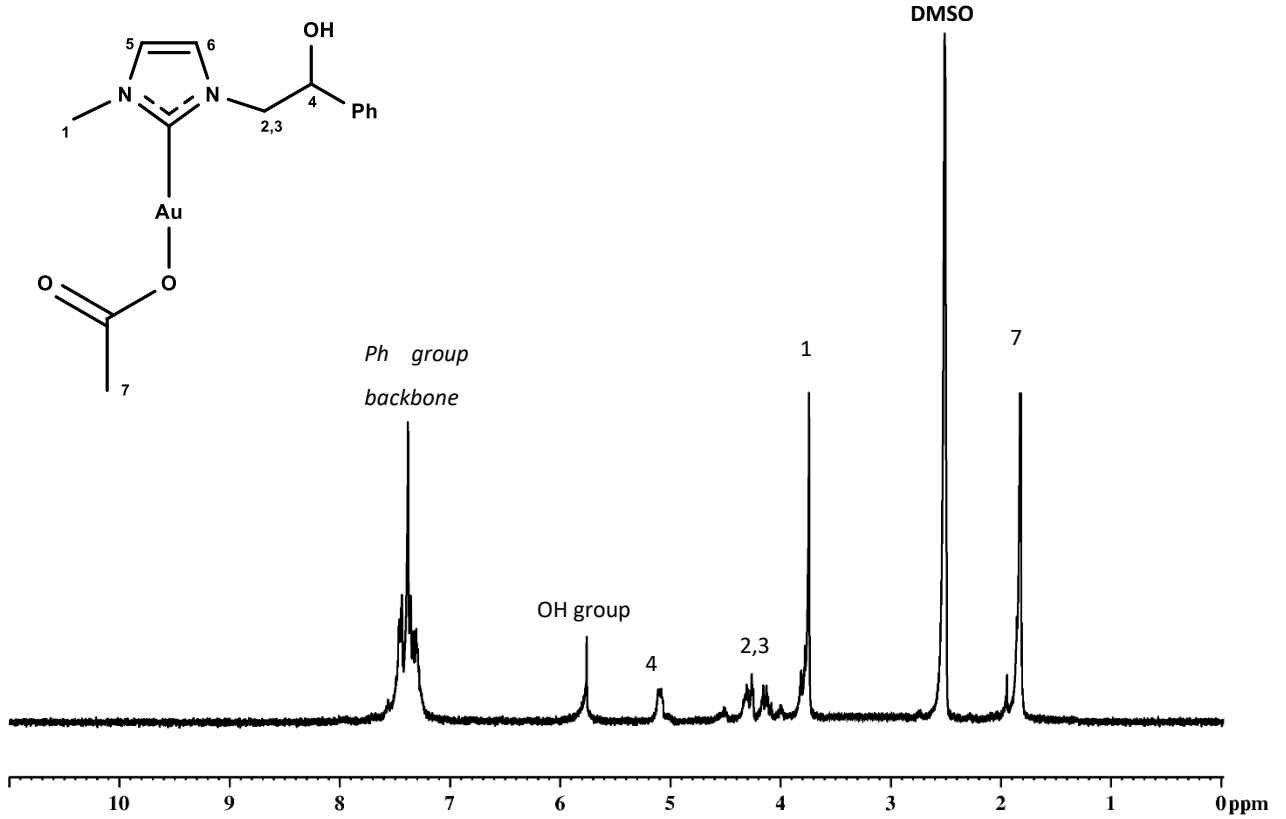

^{1}H-NMR (400MHz, DMSO-d_6): δ 7.4$_5$-7.3$_0$ (m, 7H, ***Ph ring, backbone***) 5.8$_5$ (s, 1H, ***OH group***); 5.1$_0$-5.0$_7$(m, 1H, OC***H***) 4.3$_0$-4.1$_0$(m, 2H, NC***H***$_2$); 3.7$_3$(s,3H, NC***H***$_3$)1.8$_1$(s. 3H, COC***H***$_3$).

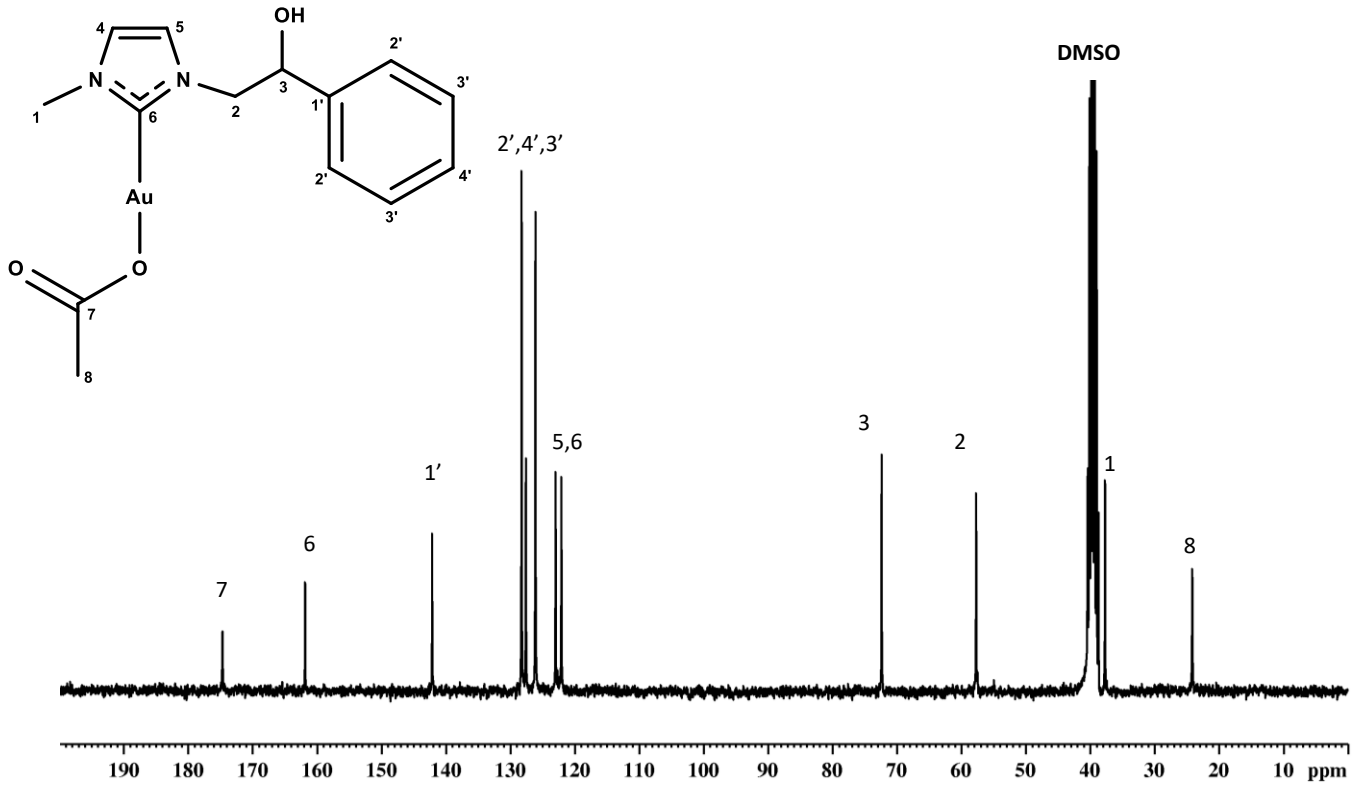

^{13}C-NMR (100 MHz, DMSO-d$_6$): δ 174.6$_5$ (O***C***OCH$_3$) 161.8$_5$ (N***C***N) 142.1$_4$ *(ipso aromatic carbon*, **Ph-ring**), 128.2$_2$-126.0$_8$ (*aromatic carbons*, **Ph rings**) 122.9$_4$-122.0$_6$ (*backbone carbons*, N***C*=*C***N), 72.3$_0$(O***C***H), 57.6$_7$(N***C***H$_2$), 37.6$_6$(N***C***H$_3$), 24.1$_2$ (OCO***C***H$_3$)

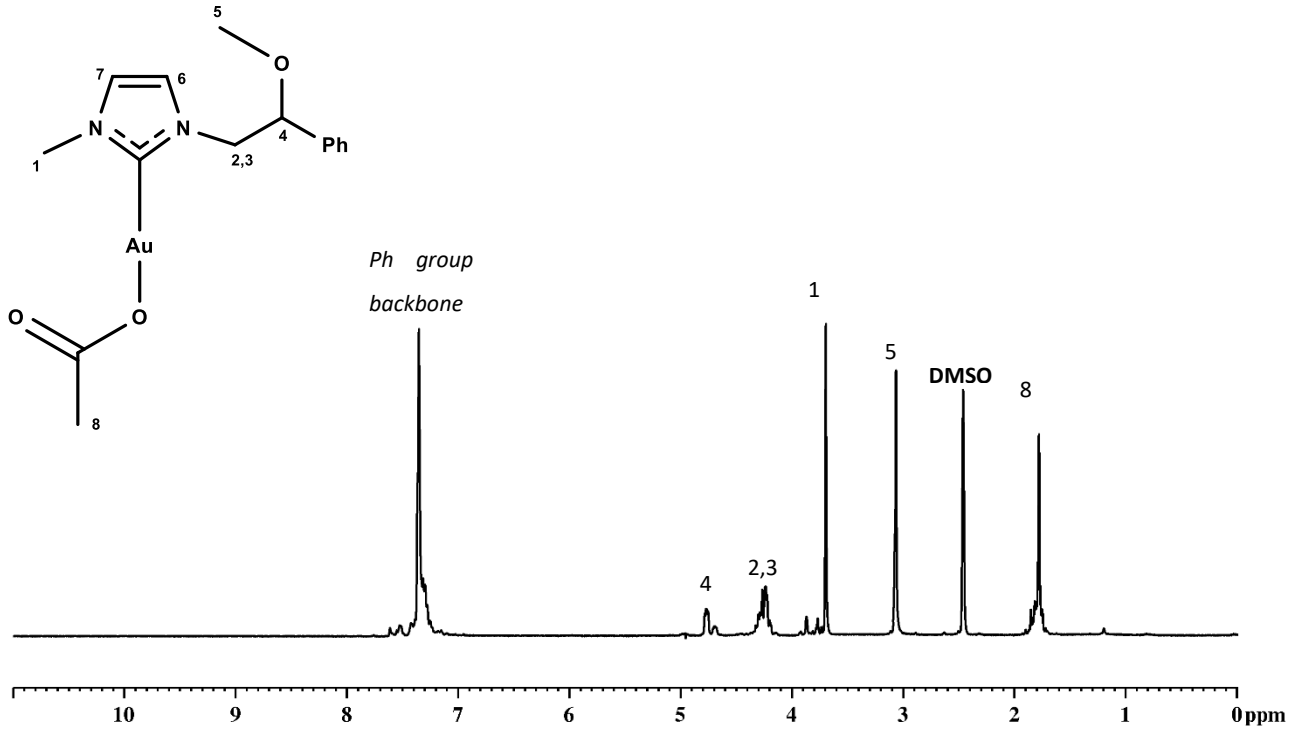

^{1}H-NMR (400MHz, DMSO-d$_6$): δ 7.3$_5$-7.2$_9$ (m, 7H, ***Ph ring, backbone***); 4.7$_8$-4.7$_4$ (m, 1H, OC***H***) 4.3$_0$-4.1$_9$(m, 2H, NC***H*$_2$**); 3.6$_9$(s,3H, NC***H*$_3$**); 3.0$_6$ (s,3H, NC***H*$_3$**);1.8$_1$(s. 3H, COC***H*$_3$**).

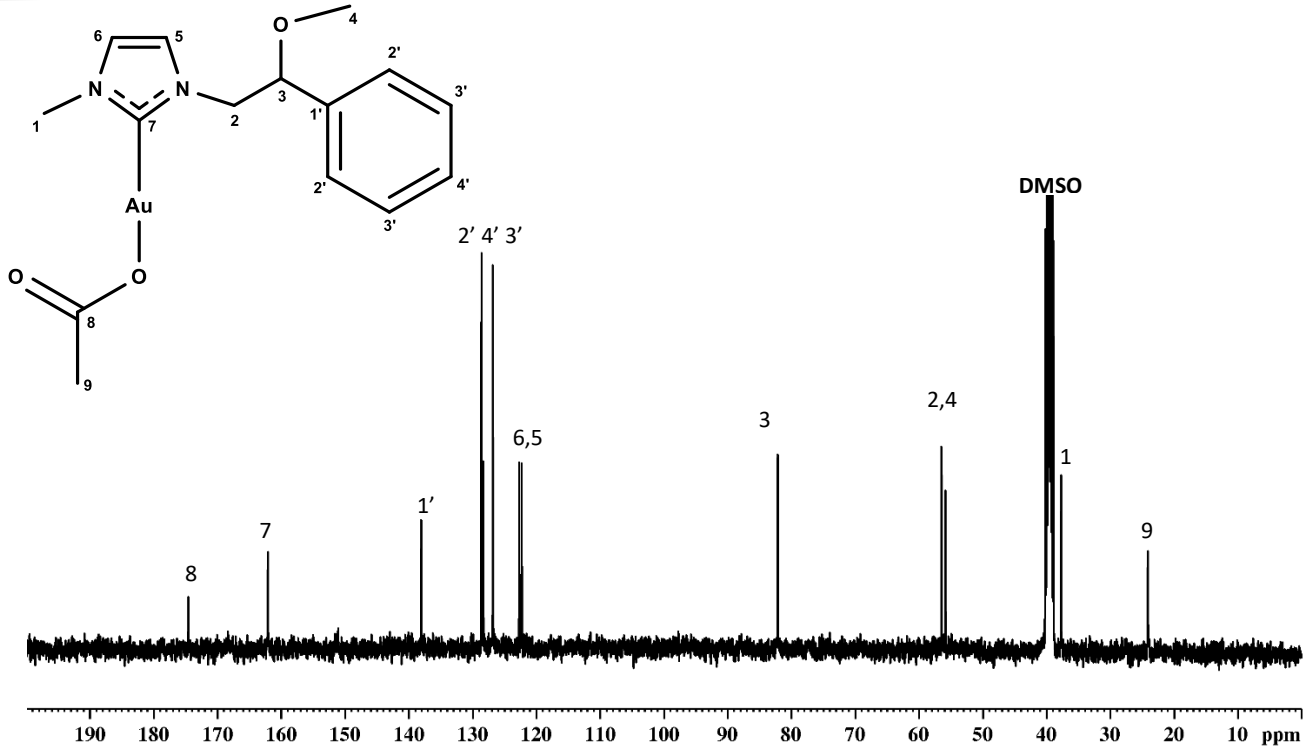

^{13}C-NMR (100 MHz, DMSO-d_6): δ 174.5$_5$ (O***C***OCH$_3$) 162.0$_8$ (N***C***N) 138.0$_4$ (*ipso aromatic carbon*, **Ph-ring**), 128.5$_8$-126.8$_0$ (*aromatic carbons*, **Ph rings**) 122.6$_6$-122.2$_7$ (*backbone carbons*, N***C***=***C***N), 82.1$_4$ (O***C***H), 56.4$_3$(N***C***H$_2$), 55.8$_1$(O***C***H$_3$) 37.6$_7$(N***C***H$_3$), 24.0$_7$ (OCO***C***H$_3$)

Acetate silver and gold NHC complexes were tested against breast cancer cell lines (MCF-7 and MDA-MB 231), and the IC_{50}, examined by MTT-assay, are reported in **Table 23**.

Table 23 Cytotoxic activity of silver acetate and halogen complexes

Compound	IC_{50}(μM)		
	MCF-7	MDA-MB231	MCF-10A
AgL1-OAc	18.4±0.6	>100	>200
AuL1-OAc	21.9±0.5	58.5±1.2	27.8±0.7
AgL2-OAc	38.1±0.8	13.2±0.3	>200
AuL2-OAc	1.2±0.3	16.8±1.2	24.4±0.9
AgL7	52.6±0.3	31.8±0.8	>200
AgL7-OAc	20.9±1.1	30.7±0.7	>200
AuL7	3.3±1.4	2.2±1.1	13.3±1.0
AuL7-OAc	9.4±0.6	3.0±0.7	5.2±0.9

By the analysis of the outcome, silver acetate NHC complexes have not shown any cytotoxicity against healthy cell lines (MCF-10A), instead, gold analogs showed modest values of IC_{50}.

AuL2-OAc has shown the highest activity against the MCF-7 cell line, in fact it reduced the cellular growth with a concentration of 1.2±0.3 μM, while a lower activity was recorded against highly aggressive and metastatic cells, MDA-MB 231 (16.8±1.2 μM). Furthermore,

AuL2-OAc has presented slight toxicity against non-tumoral cell lines (IC_{50} 24.4±0.9 μM), nevertheless nearly 20-fold less active against MCF-7. Surprisingly, **AgL2-OAc** has not demonstrated any cytotoxicity against MCF-10A cells, but otherwise, it exhibited a lesser activity against tumoral cells (IC_{50}. 13.2±0.3μM for MDA-MB 231 and 38.1±0.8 μM for MCF-7). **AuL7** and **AuL7-OAc** were active on both tumorigenic cell lines, but were very toxic against healthy cell lines, while silver analogs (**AgL7** and **AgL7-OAc**) were less active. As seen above, the activity of gold complexes was attributed to their ability to inhibit the human Topoisomerases I and II.

Recently we have investigated the anticancer activity, against the same cell lines seen so far, of the new four silver and gold complexes, derived by imidazole (**AgL5 AuL5**) and 4,5-dichloroimidazole (**AgL6**, **AuL6**)[136]. To improve the biological activity, we have substituted the methyl group, with the 2-hydroxyethyl group on the nitrogen atom, whereas the second nitrogen atom is functionalized with the 2-hydroxyethyl-phenyl group, due to its importance in the biological activity of the corresponding silver and gold complexes[128,206]. We have carried out this type of modification on the molecular structure of complexes, to increase their solubility in the biological environment, with the introduction of another hydroxyl group.

From the analysis of the results, listed in **Table 24**, **AgL5** and **AgL6** showed similar activities and were particularly effective against HeLa cells (12.2±1.0 μM for **AgL5** and 11.9±0.4 μM for **AgL6**) Furthermore, they have displayed a modest activity toward MCF-7 cell line with values 20.3±1.1 μM and 19.5±0.9 μM respectively. Unexpectedly, gold complexes have not shown biological activity, with the only exception of **AuL6**, that have exhibited an interesting activity in breast cell line (MCF-7 IC_{50} 12.2 ±1.2 μM), and a greater inhibition value against MDA-MB 231 cell line (49.5±0.7 μM). Both gold complexes were not active toward HeLa. As seen before, pro-ligands (**P-L5**, **P-L6**) have not efficacy against all the tested cell lines.

Table 24 Antitumoral activity of silver and gold (I) complexes (AgL5, L6 and AuL5, L6) and the imidazolium pro-ligands (P-L5, P-L6) expressed in μM

	IC_{50} μM				
compound	**MCF-7**	**MDA-MB231**	**HeLa**	**HEK-293**	**MCF-10A**
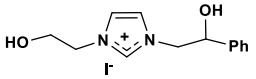 **P-L5**	>200	>200	>200	>200	>200
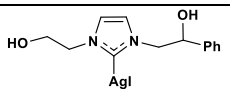 **AgL5**	20.3±1.1μM	>200	12.2±1.0μM	>200	>200
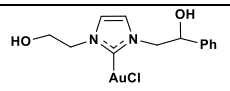 **AuL5**	>200	>200	>200	>200	>200

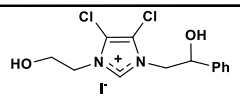 **P-L6**	>200	>200	>200	>200	>200
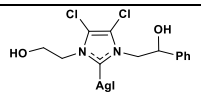 **AgL6**	>200	19.5±0.9μM	11.9±0.4μM	>200	>200
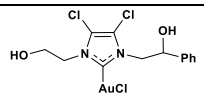 **AuL6**	49.5±0.7μM	12.2±1.2μM	>200	>200	>200

2.7.3 Conclusion

In summary, we have evaluated the biological activity of silver, gold(I) NHC complexes either as antibacterial and anticancer.

The antibacterial activity of the complexes was evaluated against *E. coli* (Gram -) and *S. aureus* (Gram +). They were more active toward *E. coli* cells, showing MIC values in the range from 10 to 15 μg/mL, while gold analogs have shown a better activity against Gram + cell (MIC from 0.5 to 40 μg/mL). While, gold complexes bearing chlorine atoms on their substituents, **AuL2** and **AuL6**, have exhibited a modest activity against *E. coli* cells (MIC 75 μg/mL).

Cytotoxic studies demonstrated that gold and silver complexes are very promising candidates for the development of new metal-based pharmaceutics for the treatment of tumors. In this regard, **AuL2** has exhibited the lowest inhibitory concentration against very aggressive breast cancer cells (MDA-MB231 IC_{50}=2.1±0.7 μM). Furthermore, **AuL2** has demonstrated good activity against the MCF-7 cell line (IC50=5.2±0.4μM), in line with the gold NHC complex with hydrogen atoms on the backbone (**AuL1**). The acetate gold complex (**AuL2-OAc**) has exhibited an interesting activity against MCF-7 cell lines. The silver analog (**AgL2**) has also shown an interesting cytotoxic activity against the same cancer cell lines (MDA-MB231 IC_{50}=3.2±1.2 μM, MCF-7 IC_{50}=10.5±0.8 μM). Silver and gold complexes bearing another hydroxyl group have not shown an interesting biological activity, with the exclusion of AuL6, that demonstrated a modest activity against breast cell lines (MCF-7 IC_{50}=12.2±1.2 μM MDA-MB231 IC_{50}=49.5±0.7 μM). The antitumor activity of **AuL2** has been attributed to the ability of these complexes to inhibit the human Topoisomerase I and II. Another interesting characteristic of these complexes is the selectivity toward tumorigenic cells, in fact all the tested complexes have not shown any activity against healthy cells. While *N*-heterocyclic pro-ligands have not exhibited any biological activity, in both fields.

Chapter 3: Conclusion and Perspective

In this doctoral thesis, novel *N*-heterocyclic carbene pro-ligands and relative silver and gold(I) complexes were synthesized and characterized.

For these complexes has been evaluated the catalytic activity in the coupling among aldehyde, amine, and terminal alkyne (named A^3-coupling reaction), using p-formaldehyde, cyclohexanal and benzaldehyde as aldehyde, piperidine as amine, and phenylacetylene as an alkyne, we obtained the corresponding propargylamine. All silver and gold complexes were able to catalyze this reaction, in neat conditions at 80°C for six hours. The higher yields were achieved using gold complexes. The best performance was achieved with **AuL2**, due to the presence of the chlorine atoms on the backbone, which makes the metal center more electrophilic and more predisposed to the coordination of the alkyne, by π interaction.

Gold(I) complexes were tested in the hydroamination of phenylacetylene with anilines in acetonitrile, to lead aryl-imines. As for the A^3coupling reaction, **AuL2** has shown the best activity, and it was tested with different electron-rich and electron-poor arylamines.

Finally, silver and gold complexes were tested as antibacterial and antitumoral compounds. By the analysis of the antimicrobial test, AgNHC complexes have exhibited lower inhibition concentrations against *E. coli* (Gram-), while gold analogs were more active toward *B. subtilis* (Gram+) bacterial strain. Furthermore, these complexes have exhibited an interesting antitumoral activity against breast cancer cell lines.

Chapter 4: Experimental part

4.1 General Procedure

All the manipulation, synthesis, and characterization of the NHC-ligands and their relative silver and gold complexes were carried out under an inert atmosphere using Schlenk and glovebox techniques. All chemical reagents were bought from TCI Chemicals and Merck-Life Science and used without further manipulation or purification. CH_2Cl_2 (dichloromethane) and Et_2O (diethyl ether) were dried on CaH_2 and distilled before the use. All deuterated solvents were degassed under N_2 flow and stored with the exclusion of the light, over activated molecular sieve (4Å) in glovebox. NMR spectra were recorded on Bruker AM 300 spectrometers (300 MHz for ^1H; 75 MHz for ^{13}C) and Bruker AVANCE 400 spectrometer (400 MHz for ^1H; 100 MHz for ^{13}C). The samples were prepared by dissolving 20 mg of compounds in 0.5 mL of deuterated solvent. The ^1H and ^{13}C NMR chemical shifts are referenced to $SiMe_4$ ($\delta = 0$ ppm) using the residual proton impurities of the deuterated solvents as the internal standard. The spectrum multiplicities are abbreviated in this manner: singlet (s), doublet (d), triplet (t), multiplet (m), and broad (br).

ESI-MS measurements of the complexes and NHC pro-ligands were carried out using a Brucker Solaris XR instrument. MALDI-MS were obtained using a Brucker SolariX XR Fourier transform ion cyclotron resonance mass spectrometer (Brucker Daltonik GmbH, Bremen, Germany) equipped with a 7T refrigerated actively shielded superconducting magnet (Brucker Biospin, Wissembourg, France). The laser power was 28%, and 22 laser shots were used for each scan. The mass range was set to m/z 200–3000. To improve the accuracy of the measurement, the spectra of the samples were recalibrated internally by matrix ionization (2,5-dihydroxybenzoic acid).

DFT and computational studies were performed by Prof. Chiara Costabile of the University of Salerno. The antibacterial activity of compounds was evaluated by research groups of Prof. Giovanni Vigliotta of the University of Salerno. The antitumoral activity of complexes was evaluated by the research group of Prof. Maria Stefania Sinicropi of the University of Calabria.

The X-ray analyses were conducted by Prof. Alessandra Crispini of the University of Calabria.

4.2 Synthesis of imidazolium salts

4.2.1 General procedure for Synthesis of N-Heterocyclic carbene Proligands P-L1-6, P-L8-11

NHC-proligands P-L1-6 and P-L8-11 were obtained following the synthetic strategies published in the literature [122–124] and applying the procedure reported by us [126–130,136]. Imidazole (1.0 eq) was reacted with epoxy alkylating reactant (styrene oxide, cyclopentene oxide, cyclohexene oxide) for 12 h by heating it at reflux, and subsequently,

iodomethane (5.0 eq) or 2-iodoethanol (2.0 eq) was added. The imidazolium salts were obtained by precipitation and washed with hexane (3x20 mL) and diethyl ether (3x30 mL).

4.2.2 Synthesis of *N*-methyl, *N'*-(2-Hydroxy-2-phenyl ethyl) imidazolium iodide (P-L1)

The synthesis and characterization of P-L1 are reported in our published paper [126].

4.2.3 Synthesis of 4,5-dichloro-*N*-methyl, N'-(2-Hydroxy-2-phenyl ethyl) imidazolium iodide (P-L2)

The synthesis and characterization of P-L1 are reported in our published paper[130].

4.2.4 Synthesis of 4,5-diphenyl-*N*-methyl, N'-(2-Hydroxy-2-phenyl ethyl) imidazolium iodide (P-L3)

4,5-diphenyl imidazole (1.00 g, 4.53 mmol) and K_2CO_3 (1.25g, 9.06 mmol) were suspended in CH_3CN (25 mL) and stirred at refluxing temperature for two hours under nitrogen atmosphere. After it was added styrene oxide (0.65 g, 5.43 mmol, 1.2 eq), the mixture was stirred for another 12 h. Subsequently, the reaction mixture was cooled to consent to the addition of iodomethane (3.21g, 22.65 mmol, 5.0 eq). The resulting mixture was warmed up to refluxing temperature and stirred for other eight hours. The product was recovered by removing the solvent, and precipitation in cold acetone. The imidazolium salt (1.92 g, 4.00 mmol,) was washed with hexane (3x20 mL) and diethyl ether (2x20 mL).

Yield: 88%

^{1}H NMR (400 MHz, DMSO-d_6): δ 9.5$_0$ (s, 1H, NC***H***N); 7.4$_6$-7.1$_1$ (m, 15H, ***Ph rings***); 6.1$_2$ (s, 1H, O***H***); 4.7$_2$ (m, 1H, OC***H***); 4.2$_6$-4.1$_1$ (m, 2H, NC***H***$_2$); 3.8$_4$ (s, 3H, NC***H***$_3$).

^{13}C-NMR (100 MHz, DMSO-d_6): δ 140.7$_7$ *(ipso aromatic carbon* (1'), **Ph-ring**), 136.8$_8$ (N***C***N), 131.3$_7$-125.5$_9$, (*aromatic carbons*, **Ph rings**), 125.5$_9$-125.0$_3$ (*backbone carbons*, N***C***Ph=***C***PhN), 70.0$_6$ (O***C***H), 54.0$_2$ (N***C***H$_2$), 34.4$_7$ (N***C***H$_3$).

MALDI-ToF (m/z): 355.18080 attributable to the cationic portion of the imidazolium salt $[C_{24}H_{23}N_2O]^+$

4.2.5 Synthesis of *N*-methyl, *N'*-(2-Hydroxy-2-phenyl ethyl) benzimidazolium iodide (P-L4)

Benzimidazole (1.00 g, 8.46 mmol) was stirred with K_2CO_3 (2.33 g, 16.92 mmol) in CH_3CN (45 mL) at refluxing temperature for two hours, under nitrogen atmosphere. In second time, it was added styrene oxide (1.22 g, 10.15 mmol, 1.2 eq) and the mixture was stirred for twelve hours. After this time, it was added the second alkylating agent, iodomethane (6.00 g, 42.3 mmol, 5.0 eq), and the mixture was stirred for eight hours at refluxing temperature. The solvent was removed *in vacuo*. The desired product was obtained by filtration after precipitation in cold acetone. Benzimidazolium salt (2.85 g,7.50 mmol) was washed with hexane (3x30 mL) and diethyl ether (2x20 mL).

Yield: 88%

^{1}H NMR (400 MHz, DMSO-d_6): δ 9.7$_7$ (s, 1H, NC***H***N); 8.0$_6$-7.3$_1$ (m, 9H, ***Ph rings***); 5.9$_9$ (d, 1H, O***H***); 5.1$_0$-5.0$_7$ (dd, 1H, OC***H***); 4.6$_1$-4.5$_2$ (m, 2H, NC***H***$_2$); 4.1$_4$ (s, 3H, NC***H***$_3$).

^{13}C-NMR (100 MHz, DMSO-d_6): δ 144.0$_6$ (N***C***N) 141.9$_0$ *(ipso aromatic carbon* (1'), **Ph-ring**), 131.6$_0$-131.3$_6$ (*backbone carbons*, N***C*=*C***N), 128.3$_7$-113.1$_1$ (*aromatic carbons*, **Ph rings**), 70.0$_6$ (O***C***H), 54.0$_2$ (N***C***H$_2$), 34.4$_7$ (N***C***H$_3$).

MALDI-ToF (m/z): 253.13474 Da attributable to the cationic portion of the imidazolium salt $[C_{16}H_{17}N_2O]^+$

4.2.6 Synthesis of *N*-[2-Hydroxyethyl], *N'*-(2-Hydroxy-2-phenyl ethyl) imidazolium iodide (P-L5)

Imidazole (1.00 g, 15.4 mmol,) and styrene oxide (2.40 g, 18.5 mmol) were dissolved in 25 mL of CH_3CN and stirred at refluxing temperature under nitrogen atmosphere for twelve hours. Later, was added 2-iodoethanol (5.29 g, 30.8 mmol). The reaction mixture was stirred for 8 hours. The product was obtained after removing the solvent, and by the precipitation in cold acetone. The salt was washed with hexane (3x20 mL) and diethyl ether (2x20 mL). The imidazolium iodide salt (5.40 g, 15.0 mmol) was obtained as a white powder.

Yield: 97%

^{1}H NMR (400 MHz, DMSO-d_6): δ 9.1$_2$ (s, 1H, NC***H***N); 7.7$_5$-7.3$_5$ (m, 7H, ***Ph rings***); 5.9$_9$ (s, 1H, O***H***); 5.1$_7$ (s, 1H, O***H***); 4.9$_7$ (m, 1H, OC***H***); 4.4$_6$-4.2$_5$ (m, 4H, NC***H***$_2$CH$_2$OH, NC***H***$_2$CHOH); 3.7$_5$ (s,2H, NCH$_2$C***H***$_2$OH).

^{13}C-NMR (100 MHz, DMSO-d_6): δ 144.0$_6$ (N***C***N) 141.9$_0$ *(ipso aromatic carbon* (1'), **Ph-ring**), 131.6$_0$-131.3$_6$ (*backbone carbons*, N***C*=*C***N), 128.3$_7$-113.1$_1$ (*aromatic carbons*, **Ph rings**), 70.0$_6$ (O***C***H), 54.0$_2$ (N***C***H$_2$), 34.4$_7$ (N***C***H$_3$).

MALDI-ToF (m/z): 253.13474 Da attributable to the cationic portion of the imidazolium salt $[C_{16}H_{17}N_2O]^+$

4.2.7 Synthesis of 4,5-dichloro *N*-[2-Hydroxyethyl], *N'*-(2-Hydroxy-2-phenyl ethyl) imidazolium iodide (P-L6)

In a round bottom flask, under nitrogen flow, 4,5-dichloroimidazole (1.00 g, 7.33 mmol) and styrene oxide (1.32 g, 11.0 mmol) were dissolved in CH_3CN (18 mL) and stirred at refluxing temperature for twelve hours. After cooling the mixture, it was added 2-iodoethanol (2.52 g, 14.6 mmol). The reaction mixture was heated to refluxing temperature and stirred for other eight hours. The solvent was removed *in vacuo* and the salt (1.88 g, 4.39 mmol) was obtained by filtration after the precipitation with cold acetone.

Yield:60%

^{1}H NMR (400 MHz, DMSO-d_6): δ 9.5$_1$ (s, 1H, NC***H***N);7.4$_0$-7.3$_3$ (m, 5H, ***Ph rings***); 6.0$_5$ (s, 1H, O***H***); 5.1$_8$ (s, 1H, O***H***); 4.9$_9$ (m, 1H, OC***H***); 4.4$_9$-4.3$_4$ (m, 4H, NC***H***$_2$CH$_2$OH, NC***H***$_2$CHOH); 3.7$_7$ (s, 2H, NCH$_2$C***H***$_2$OH).

^{13}C-NMR (100 MHz, DMSO-d_6)**:** δ 140.44 (*ipso* carbon of ***Ph ring***), 137.39 (N***C***HN), 128.44, 128.10, 125.96 (aromatic carbon, ***Ph ring***), 118.91, 118.47 (backbone carbons), 69.80 (***C***HOH), 58.18 (***C***H_2OH), 54.85 (N***C***H_2CHOH), 51.06 (N***C***H_2CH_2OH).

MALDI-ToF (m/z): 301.05142 Da attributable to the cationic portion of the imidazolium salt $[C_{13}H_{15}Cl_2N_2O_2]^+$

4.2.8 Synthesis of *N*-methyl, *N*′-(2-methoxy-2-phenyl) ethyl) imidazolium iodide (P-L7)

The imidazolium salt was obtained following the synthetic strategy published in the literature [131] and slightly modified by us. To a solution of *N*-(2-hydroxy phenyl) ethyl imidazole (1.00 g, 5.31 mmol) in CH_3CN was added NaH (0.25 g, 10.6 mmol) at 4 °C. The reaction mixture was stirred for 2 h before the addition of CH_3I (5.27 g, 37.1 mmol), and it was stirred for twenty hours. The product was obtained by filtration as an off-white solid (1.26 g, 3.66 mmol).

Yield: 69%

^{1}H NMR (400 MHz, DMSO-d_6): δ 7.34-7.26 (m, 7H, ***Ph ring, backbone***), 4.60(m, 1H, OC***H***), 4.30-4.27(m, 2H, NC***H***$_2$), 3.74(s,3H, NC***H***$_3$), 3.07(s,3H, OC***H***$_3$).

^{13}C-NMR (100 MHz, DMSO-d_6): δ137.32 (*ipso aromatic carbon*, **Ph-ring**), 136.94 (N***C***N), 128.72, 128.64, 126.81 (*aromatic carbons*, **Ph ring**), 123.33 (*backbone carbons*, N***C***H=***C***HN), 80.46 (O***C***H), 56.46 (N***C***H_2), 54.06 (N***C***H_3), 35.97 (N***C***H_3).

MALDI-ToF (m/z): 217.1342 Da attributable to the cationic portion of the imidazolium salt $[C_{13}H_{17}N_2O]^+$

4.2.9 Synthesis of *N*-methyl, *N*′-(cyclopentane-2-ol) imidazolium iodide (P-L8)

The synthesis and characterization of P-L8 are reported in our published paper [126].

4.2.10 Synthesis of 4,5-dichloro *N*-methyl, *N*′-(cyclopentane-2-ol) imidazolium iodide (P-L9)

The synthesis and characterization of P-L9 are reported in our published paper [129].

4.2.11 Synthesis of *N*-methyl, *N*′-(cyclohexane-2-ol) imidazolium iodide (P-L10)

The synthesis and characterization of P-L10 are reported in our published paper [126].

4.2.12 Synthesis of 4,5-dichloro-*N*-methyl, *N*′-(cyclohexane-2-ol) imidazolium iodide (P-L10)

In a round bottom flask, 4,5-dichloroimidazole (1.00 g, 7.33 mmol) and cyclohexene oxide (0.863 g, 8.8 mmol) were dissolved in CH_3CN (25 mL), and the mixture was stirred for twelve hours, under nitrogen atmosphere. Then, the solution was cooled to room temperature, it was added iodomethane (5.16 g, 36.6 mmol) and the solution was warmed to refluxing temperature and stirred for another six hours. After this time, the solvent was

removed at reduced pressure, and the product was precipitated as a white powder (1.93 g, 5.13 mmol) with the addition of cold acetone.

Yield: 70%

^{1}H NMR (400 MHz, DMSO-d_6): δ 9.7$_2$ (s, 1H, NC***H***N); 5.2$_5$ (m, 1H, O***H***); 4.1$_2$-4.0$_7$ (m, 1H, OC***H***); 3.8$_4$ (s, 3H, NC***H***$_3$) 3.7$_4$-3.7$_0$ (m, 1H, NC***H***); 2.0$_8$ 1.3$_6$ (s, 8H, Cyclohexyl).

^{13}C-NMR (100 MHz, DMSO-d_6): δ135.6$_7$ (N***C***N), 118.8$_6$ (*backbone carbons*, N***C***Cl=***C***ClN), 71.5$_3$ (O***C***H), 65.2$_0$ (N***C***H), 35.2$_0$ (N***C***H$_3$), 34.0$_2$-23.5$_5$ (Cyclohexyl group).

MALDI-ToF (m/z): 249.05614 Da attributable to the cationic portion of the imidazolium salt $[C_{10}H_{15}Cl_2N_2O]^+$

4.2.13 General procedure for the synthesis of xanthinium *N*-Heterocyclic carbene Proligands P-L12-14

Caffeine-based NHC proligands were obtained following the procedure published in the literature [54,102,125,137] and slightly modified by us. Theophylline (1.0 eq) was dissolved in dimethylformamide (DMF) and has been reacted with K_2CO_3 (2.0 eq), at refluxing temperature. Subsequently, it was added the first alkylating agent (styrene oxide, 2-iodoethanol, or cyclohexene oxide) and the reaction mixture was stirred for twelve hours. After, it was added the second alkylating agent (iodomethane), and the mixture was stirred for another six hours, at refluxing temperature. The caffeine-based salt was recovered after removing the solvent, and precipitation with the addition of cold acetone.

4.2.14 Synthesis of *N'*-[2-(hydroxy-phenyl) ethyl] trimethyl xanthinium iodide (P-L12)

In a round bottom flask, under a nitrogen atmosphere, it was dissolved theophylline (2.00 g, 11.0 mmol) in DMF (40 mL). After, the solubilization of the xanthine, it was added K_2CO_3 (1.52 g, 11.0 mmol), and stirred for two hours at refluxing temperature. Then, the mixture was cooled at room temperature and was added styrene oxide (1.32 g, 13.2 mmol). The resulting mixture was stirred and refluxed for twelve hours. After this time, was added iodomethane (7.75 g, 55.0 mmol) and stirred for another six hours. Afterward, the solvent was removed under reduced pressure, and the xanthium salt (3.53 g, 8.00 mmol) was obtained by precipitation in cold acetone and washed with hexane (5x50 mL).

Yield: 72%

^{1}H NMR (400 MHz DMSO-d_6)**:** δ9.3$_9$ (s, 1H, NC***H***N), 7.4$_4$-7.3$_0$ (m, 5H, ***Ph-group***), 5.9$_6$ (s, 1H, O***H***), 4.7 $_3$(s,1H, C***H***OH), 4.6$_9$-4.4$_0$ (m, 2H, NC***H***$_2$), 4.3$_5$ (s, 3H, NC***H***$_3$ imidazolium ring), 3.7$_4$ (s, 3H, NC***H***$_3$), 3.2$_7$ (s, 3H, NC***H***$_3$).

^{13}C-NMR (100 MHz DMSO-d_6)**:** δ 186.3$_6$ (N***C***N), 174.5$_1$ (CH$_3$***C***=O), 153.3$_3$-150.3$_9$ (***C***=O *purine ring*), 142.4$_5$ (*ipso aromatic carbon*, **Ph-ring**), 140.6$_3$ (*backbone carbon*, ***C***=C), 128.2$_6$, 128.1$_1$, 125.7$_7$ (*aromatic carbons*, **Ph ring**), 108.8$_2$ (*backbone carbon*, C=***C***), 72.1$_0$ (***C***HOH), 57.1$_5$ (N***C***H$_2$), 31.4$_8$, 28.3$_6$ (N***C***H$_3$ purine ring), 22.9$_6$ (O=C***C***H$_3$).

ESI-MS (CH_2Cl_2 m/z): 705.44325 Da attributable to $[C_{30}H_{30}AgN_8O_6]^+$

4.2.15 Synthesis of *N'*-[2-(hydroxy) ethyl] trimethyl xanthinium iodide (P-L13)

Under an inert atmosphere, in a round bottom flask, was dissolved theophylline (2.00 g, 11.0 mmol) in DMF (40 mL). In the solution was added K_2CO_3 (1.52 g, 11.0 mmol), and stirred for two hours at refluxing temperature. After that, at reaction mixture was added 2-iodoethanol (2.83 g, 17.0 mmol), and stirred for another ten hours. Later, it was added iodomethane (7.75 g, 55.0 mmol) and stirred for another six hours. The caffeine-based salt (3.13 g, 8.50 mmol) was obtained after removing the solvent and washing the light-yellow powder with hexane (5x50 mL).

Yield: 77%

^{1}H NMR (400 MHz DMSO-d_6)**:** δ 9.37 (s, 1H, NC***H***N), 5.16 (s, 1H, O***H***), 4.52-4.50 (m, 2H, C***H***$_2$OH), 4.19 (s, 3H, NC***H***$_3$ imidazolium ring), 3.75 (b, 5H, NC***H***$_2$, N***C*****H**$_3$), 3.27 (s,3H, NC***H***$_3$).

^{13}C-NMR (175 MHz DMSO-d_6)**:** δ 153.23-150.12 (***C***=O), 139.63 (N***C***HN), 107.03 (*backbone carbons*, ***C***=***C***), 58.35 (***C***H$_2$OH), 51.39 (N***C***H$_2$), 36.91 (N***C***H$_3$ imidazolium *ring*), 31.40 (N***C***H$_3$ purine ring), 28.49 (N***C***H$_3$ purine ring)

MALDI-ToF (m/z): 239.11513 Da attributable to cationic part of imidazolium pro-ligand $[C_{10}H_{15}N_4O_3]^+$

4.2.16 Synthesis of *N'*-[cyclohexan-2-ol] trimethyl xanthinium iodide (P-L14)

Both, theophylline (2.00 g, 11.0mmol) and K_2CO_3 (1.52 g, 11.0 mmol) were suspended in DMF (40 mL) under nitrogen atmosphere and stirred for two hours. Later, at reaction mixture was added cyclohexene oxide (1.30 g,13.2 mmol), and stirred for ten hours at refluxing temperature, before adding iodomethane (7.75 g, 55.0 mmol). The desired product (2.52 g, 6.0 mmol) was obtained by filtration in cold acetone, after removing the solvent *in vacuo*, and washed with hexane (5x50 mL).

Yield: 54%

^{1}H-NMR (400 MHz DMSO-d_6)**:** 9.54 (s, 1H, NC***H***N), 5.26 (s,1H, O***H***), 4.78-4.70 (m,1H, C***H***OH), 4.16 (s, 3H, NC***H***$_3$ imidazolium ring), 3.91-3.90 (b,1H, NC***H***), 3.75 (s, 3H, N***C*****H**$_3$), 3.28 (s, 3H, NC***H***$_3$), 2.10-175 (m, 8H, *Cyclohexyl*).

^{13}C-NMR (100 MHz DMSO)**:** δ 153.20-150.12 (***C***=O), 139.69 (*backbone carbons*, ***C***=C) 138.55 (N***C***HN), 107.70 (*backbone carbons*, C=***C***), 70.16 (***C***HOH), 65.47 (N***C***H), 37.24 (N***C***H$_3$ imidazolium *ring*), 34.41-28.72, (*cyclohexyl carbons*), 24.44 (N***C***H$_3$ purine ring)-23.67 (N***C***H$_3$ purin ring).

MALDI-ToF(m/z):293.16137 Da attributable to the cationic part of imidazolium pro-ligand$[C_{14}H_{21}N_4O_3]^+$

4.3 Synthesis of *N*-heterocyclic carbene silver complexes

4.3.1 General procedure for the synthesis of *N*-Heterocyclic silver carbene complexes AgL1-L6, AgL8-L11

Under nitrogen atmosphere, imidazolium pro-ligand (1.0 eq) was suspended in dry dichloromethane (25 mL). After, active molecular sieves (4Å) and silver oxide (Ag_2O, 0.7 eq) were added to the mixture and stirred for four hours, at room temperature, with the exclusion of light. The silver complex was obtained after filtration on a pad of Celite, to eliminate silver iodide by-product, and the molecular sieves and the volatiles were removed under reduced pressure to afford the silver complex as a white solid.

4.3.2 Synthesis of Iodo [*N*-(methyl)-*N'*(2-hydroxy phenyl)ethyl-imidazolyden]silver(I) (AgL1)

The synthesis and characterization of AgL1 are reported in our published paper by us[126].

4.3.3 Synthesis of Iodo 4,5-dichloro-[*N*-(methyl)-*N'*(2-hydroxy phenyl)ethyl-imidazolyden]silver(I) (AgL2)

The synthesis and characterization of AgL2 are reported in our published paper by us [130].

4.3.4 Synthesis of Iodo 4,5-diphenyl-[*N*-(methyl)-*N'*(2-hydroxy phenyl)ethyl-imidazolyden]silver(I) (AgL3)

The silver complex AgL3 was obtained by the reaction of imidazolium salt P-L3 (0.48 g, 1.0 mmol) and Ag_2O (0.16 g, 0.7 mmol) in dry DCM (25 mL) with molecular sieves (4Å). The reaction mixture was stirred for four hours at room temperature with the exclusion of light. The mixture reaction was filtered through a pad of Celite to remove the molecular sieves and the silver iodide byproduct. The solvent was removed *in vacuo,* and the silver complex was obtained as a light grey powder (0.41 g, 0.7 mmol).

Yield: 70%

^{1}H NMR (400 MHz, DMSO-d_6): δ 7.46-7.04 (m, 15H, ***Ph rings***); 4.76 (m, 1H, OC***H***); 4.24-4.14 (m, 2H, NC$\boldsymbol{H_2}$); 3.82 (s, 3H, NC$\boldsymbol{H_3}$).

^{13}C-NMR (100 MHz, DMSO-d_6): δ 181.38 (N***C***N), 142.17 *(ipso aromatic carbon* (1'), **Ph-ring**), 131.97-125.59, (*aromatic carbons*, **Ph ring**), 72.16(O***C***H), 56.02(N***C***H_2), 37.37(N***C***H_3)

MALDI-ToF (m/z): 817.26229 Da attributable to a structure a bis-carbene structure $[C_{48}H_{44}AgN_4O_2]^+$

4.3.5 Synthesis of Iodo-[*N*-(methyl)-*N'*(2-hydroxy phenyl)ethyl-benzimidazolyden]silver(I) (AgL4)

AgL4 was synthesized by the reaction of *N*-(methyl)-*N'*(2-hydroxy phenyl)ethyl-benzimidazolium iodide (P-L4, 0.38 g, 1.0 mmol) with silver oxide(0.16 g, 0.7 mmol) in 25 mL of dry CH_2Cl_2, under nitrogen atmosphere. The silver NHC complex (0.27 g, 0.55 mmol) was recovered by the filtration on a pad of Celite, and by the removal of the solvent *in vacuo*.

Yield: 55%

^{1}H NMR (400MHz, DMSO-d_6): δ 7.8$_2$-7.2$_4$ (m, 9H, ***Ph ring***); 5.8$_6$ (s, 1H, O***H***); 5.0$_9$-5.0$_7$ (dd, 1H, OC***H***); 4.6$_9$-4.6$_2$(m, 2H, NC***H***$_2$); 4.0$_4$ (s, 3H, NC***H***$_3$).

^{13}C-NMR (100 MHz, DMSO-d_6): δ 190.9$_1$ (N***C***N), 142.2$_7$ *(ipso aromatic carbon* (1'), **Ph-ring**), 134.4$_0$-133.8$_2$ (*backbone carbons*, N***C*=*C***N), 128.2$_1$-111.7$_0$, (*aromatic carbons*, **Ph rings**), 72.0$_6$ (O***C***H), 55.8$_2$ (N***C***H$_2$), 3 5.5$_0$(N***C***H$_3$).

MALDI-ToF (m/z): 517.26179 Da attributable to structure bis-carbenic $[C_{26}H_{25}AgN_4O]^+$

4.3.6 Synthesis of Iodo-[*N*-(2-hydroxyethyl)-*N'*(2-hydroxy phenyl)ethyl-imidazolyden]silver(I) (AgL5)

P-L5 (0.36 g, 1.00 mmol), Ag_2O (0.16 g, 0.7 mmol), and molecular sieves (4Å) were suspended and stirred in dry DCM (25 mL) for four hours with the exclusion of the light, under inert atmosphere. The solvent was removed at reduced pressure and the complex was recovered as a light-grey powder (0.330 g, 0.7mmol).

Yield: 70%

^{1}H NMR (400 MHz, DMSO-d_6): δ7.3$_8$-7.3$_1$ (m, 7H, ***Ph rings***); 5.8$_8$ (s, 1H, O***H***); 5.0$_7$ (s, 1H, O***H***); 4.9$_9$ (m, 1H, OC***H***); 4.3$_6$-4.2$_7$ (m, 4H, NC***H***$_2$CH$_2$OH, NC***H***$_2$CHOH); 3.7$_3$(s,2H, NCH$_2$C***H***$_2$OH).

^{13}C-NMR (100 MHz, DMSO)**:** 181.2$_8$ 179.2$_8$ (N***C***N), 142.5$_3$ (*ipso* carbon of ***Ph ring***), 128.1$_0$, 127.1$_0$, 126.0$_6$ (aromatic carbon, ***Ph ring***), 122.4$_0$, 121.8$_5$ (*backbone carbons*), 72.4$_6$ (***C***HOH), 61.1$_9$ (***C***H$_2$OH), 58.4$_0$ (N***C***H$_2$CHOH), 53.6$_2$ (N***C***H$_2$CH$_2$OH).

ESI-MS (CH$_3$CN m/z): 573.14690 Da attributable to $[C_{26}H_{32}AgN_4O_4]^+$

4.3.7 Synthesis of Iodo-4,5-dichloro-[*N*-(2-hydroxyethyl)-*N'*(2-hydroxy phenyl)ethyl-imidazolyden]silver(I) (AgL6)

The imidazolium pro-ligand P-L6 (0.43 g, 1.0 mmol), silver oxide (0.16 g, 0.7 mmol), and molecular sieves 4Å were stirred for four hours in the dark, under a nitrogen atmosphere. The reaction mixture was filtered on a pad of Celite, the solvent was **removed under reduced pressure**, and the residual product was recovered as a light grey powder (0.36 g, 0.67 mmol).

Yield: 67%

^{1}H NMR (400 MHz, DMSO-d_6): δ 7.3$_8$-7.2$_7$ (m, 5H, ***Ph ring***); 5.8$_9$ (s, 1H, O***H***); 5.0$_7$ (s, 1H, O***H***); 4.9$_9$ (m, 1H, OC***H***); 4.3$_3$-4.2$_7$ (m, 4H, NCH$_2$C***H***$_2$OH, NC***H***$_2$CHOH); 3.7$_4$ (s,2H, NC***H***$_2$CH$_2$OH).

^{13}C-NMR (100 MHz, DMSO-d_6)**:** δ 181.3$_0$ (N***C***N), 141.5$_1$ (*ipso* carbon of ***Ph ring***), 128.3$_1$, 127.7$_2$, 126.0$_8$ (aromatic carbon, ***Ph ring***), 117.1$_0$, 116.7$_5$ (*backbone carbons*), 71.6$_3$ (***C***HOH), 60.2$_9$ (***C***H$_2$OH), 56.9$_9$ (N***C***H$_2$CHOH), 52.5$_7$ (N***C***H$_2$CH$_2$OH).

ESI-MS (CH$_3$CN m/z): 707.99716 Da attributable to $[C_{26}H_{28}Cl_4AgN_4O_4]^+$

4.3.8 Synthesis of Iodo [*N*-(methyl)-*N'*(2-methoxy phenyl)ethyl-imidazolyden]silver(I) (AgL7)

The reaction among P-L7 proligand (0.34 g, 1.0 mmol) and silver oxide (0.17 g, 0.7 mmol), in an inert atmosphere with molecular sieves 4Å, has led to silver complex (0.32 g, 0.7 mmol). The complex was obtained after filtration and the removal of the solvent *in vacuo*.

^{1}H NMR (400 MHz, DMSO-d_6): δ 7.34-7.26 (m, 7H, ***Ph ring, backbone***), 4.60 (m, 1H, OC***H***), 4.30-4.27 (m, 2H, NC***H***$_2$), 3.74 (s, 3H, NC***H***$_3$), 3.07 (s, 3H, OC***H***$_3$).

^{13}C-NMR (100 MHz, DMSO-d_6)**:** δ 181.60 (N***C***N), 138.21 (*ipso* carbon of ***Ph ring***), 128.51, 128.22, 126.88 (aromatic carbon, ***Ph ring***), 122.60, 122.35 (*backbone carbons*), 82.23 (***C***HO), 56.49 (N***C***H$_2$), 52.27 (O***C***H$_3$), 38.16 (N***C***H$_3$).

MALDI-ToF (m/z): 539.1567 Da attributable to $[C_{26}H_{32}AgN_4O_2]^+$

4.3.9 Synthesis of Iodo [*N*-(methyl)-*N'*(sodium alcholate-2-phenyll)ethyl-imidazolyden]silver(I) (AgL7')

The complex AgL7' was synthesized by the reaction among AgL1 (0.25 g, 0.57 mmol) and sodium hydride (NaH, 18.5 mg, 0.77 mmol) in dry DCM (30 mL). The reaction mixture was stirred for twenty hours with the exclusion of light. The solution was filtered through a pad of Celite. The residual solution was dried under reduced pressure, and the crude product was washed with dry Et_2O (3x10 mL). The complex was recovered as a yellow powder (0.24 g, 0.51 mmol)

Yield: 90%

^{1}H NMR (400 MHz, CD_2Cl_2): δ 7.36-7.33 (m, 5H, ***Ph ring***), 6.89-6.79 (s, 2H, ***backbone***), 5.13 (t, 1H, $^{-}$OC***H***), 4.40-4.30 (m, 2H, NC***H***$_2$), 3.86 (s, 3H, NC***H***$_3$).

^{13}C-NMR (100 MHz, CD_2Cl_2)**:** δ 184.60 (N***C***N), 141.81 (*ipso* carbon of ***Ph ring***), 129.11, 128.42, 126.78 (aromatic carbon, ***Ph ring***), 123.40, 122.85 (*backbone carbons*), 78.13 (***C***HO^{-}), 59.49 (N***C***H$_2$), 39.26 (N***C***H$_3$).

ESI-MS (CH_2Cl_2, m/z): 528.0035 Da attributable to $[C_{22}H_{22}AgN_4O_2Na_2]^+$

4.3.10 Synthesis of Iodo [*N*-(methyl)-*N'*(cyclopent-2-ol)-imidazolyden] silver(I) (AgL8)

The synthesis and characterization of AgL8 are reported in our published paper by us[126].

4.3.11 Synthesis of Iodo 4,5-dichloro-[*N*-(methyl)-*N'*(cyclopent-2-ol)-imidazolyden] silver(I) (AgL9)

The synthesis and characterization of AgL9 are reported in our published paper by us[129].

4.3.12 Synthesis of Iodo [*N*-(methyl)-*N'*(cyclopent-2-ol)-imidazolyden] silver(I) (AgL10)

The synthesis and characterization of AgL10 are reported in our published paper by us[126].

4.3.13 Synthesis of Iodo 4,5-dichloro-[*N*-(methyl)-*N'*(cyclopent-2-ol)-imidazolyden] silver(I) (AgL11)

In a Schlenk tube, under a nitrogen atmosphere P-L11 (0.38 g, 1.00 mmol), silver oxide (0.17 g, 0.7 mmol), and molecular sieves were stirred for 4 hours, without the light.

After completion of the reaction, the mixture was filtered on a pad of Celite, and the solvent was removed under vacuum to lead the silver complex (0.31 g, 0.64 mmol).
Yield: 64%
^{1}H NMR (400 MHz, DMSO-d_6): δ 4.9$_3$ (b, 1H, O***H***), 4.0$_7$-3.9$_2$ (m, 1H, HOC***H***), 3.8$_6$ (s,4H, NC***H***, NC***H***$_3$), 1.9$_6$-1.3$_1$ (*Cyclohexyl* group).
^{13}C-NMR (100 MHz, CD_2Cl_2)**:** δ 182.9$_0$ (N***C***N), 118.6$_5$, 117.2$_5$ (*backbone carbons*), 76.1$_3$ (***C***HOH), 70.3$_9$ (N***C***H), 38.7$_6$ (N***C***H$_3$), 35.0$_1$-23.9$_3$ (*Cyclohexyl carbons*).
ESI-MS (CH_2Cl_2, m/z): 603.0017 Da attributable to $[C_{20}H_{28}AgCl_4N_4O_2]^+$

4.3.14 General procedure for the synthesis of caffeine-based *N*-Heterocyclic carbene silver complexes AgL12-L14

Caffeine-based silver complexes were synthesized following the protocols published in the literature [53,55,125,139]. Xanthinum salt (1.0 eq), and silver acetate (2.0 eq) were dissolved and stirred in acetonitrile for eight hours, with the exclusion of the light under a nitrogen atmosphere. The complex was obtained after the removal of the solvent *in vacuo*.

4.3.15 Synthesis of acetate-[*N'*(2-hydroxy phenyl)ethyl-trimethylxanthium] silver(I) (AgL12)

In a round bottom flask, under a nitrogen atmosphere, imidazolium salt P-L12 (0.44 g,1.0 mmol) and silver acetate (0.33 g, 2.0 mmol) were dissolved in dry-acetonitrile (30 mL). The reaction mixture was stirred for eight hours, with the exclusion of light. After this time, the mixture was filtered, and the solvent was removed in a vacuum. The silver complex (0.20 g,0.4 mmol) was obtained as a white powder.
Yield: 40%
^{1}H-NMR (400 MHz DMSO-d_6)**:** δ 7.4$_1$-7.2$_9$ (m, 5H, ***Ph-group***), 5.6$_2$ (s,1H, O***H***), 5.1$_6$ - 5.1$_0$ (m, 1H, C***H***OH), 4.6$_0$-4.3$_2$ (m, 2H, NC***H***$_2$), 4.1$_9$ (s, 3H, NC***H***$_3$ imidazolium ring), 3.7$_5$ (s,3H, NC***H***$_3$), 3.2$_7$ (s, 3H, NC***H***$_3$).
^{13}C-NMR (100 MHz, DMSO-d_6): δ 181.3$_8$ (N***C***N), 142.1$_7$ *(ipso aromatic carbon* (1'), **Ph-ring**), 131.9$_7$-125.5$_9$, (*aromatic carbons*, **Ph ring**), 72.1$_6$ (O***C***H), 56.0$_2$ (N***C***H$_2$), 37.3$_7$ (N***C***H$_3$).
MALDI-ToF (m/z): 817.26229 Da attributable to bis-carbenic structure $[C_{48}H_{44}AgN_4O_2]^+$

4.3.16 Synthesis of acetate-[*N'*(2-hydroxy ethyl)-trimethylxanthium] silver(I) (AgL13)

P-L13 (0.37 g,1.00 mmol) and silver acetate (0.33 g, 2.0 mmol) were dissolved in dry CH_3CN (30 mL) under nitrogen atmosphere. The reaction mixture was stirred for eight hours without the light. After that, the mixture was filtered on a pad of Celite to remove the silver iodide byproduct. The complex (0.22 g, 0.55 mmol) was obtained after the removal of the solvent.
Yield: 55%
^{1}H-NMR (400 MHz DMSO-d_6)**:** δ 4.5$_3$-4.5$_0$ (m, 2H, C***H***$_2$OH), 4.1$_9$ (s, 3H, NC***H***$_3$ imidazolium ring), 3.7$_6$-3.7$_3$ (b, 5H, NC***H***$_2$, NC***H***$_3$), 3.2$_1$ (s,3H, NC***H***$_3$), 1.77 (s, 3H, O=CC***H***$_3$).

^{13}C-NMR (400MHz DMSO-d_6)**:** δ 186.5$_8$ (N***C***N); 173.9$_0$ (O=***C***CH3); 153.0$_3$-150.4$_2$ (***C***=O *purine ring*); 140.7$_2$ (*backbone carbon* ***C***=C); 108.2$_3$ (*backbone carbon*, C=***C***) 60.1$_2$ (***C***H$_2$OH), 52.9$_9$ (N***C***H$_2$), 31.5$_1$, 28.2$_4$ (N***C***H$_3$ imidazolium *ring*), 31.4$_0$, 28.4$_9$ (N***C***H$_3$ *purine ring*), 22.8$_2$(O=C***C***H$_3$)

4.3.17 Synthesis of acetate-[*N'*(cyclohexan-2-ol)-trimethylxanthium] silver(I) (AgL14)

Under an inert atmosphere, in a Schlenk round flask was dissolved the caffeine-based salt (0.42 g, 1.00 mmol) and AgOAc (0.33 g, 2.0 mmol) in dry CH_3CN (25 mL). The mixture was stirred in dark conditions for eight hours. Subsequently, the mixture was filtered, and the solvent was reduced *in vacuo*. The complex was recovered as an off-white powder (0.19 g, 0.4 mmol)

Yield: 40%.

^{1}H-NMR (400 MHz DMSO-d_6)**:** δ 5.1$_6$ (s, 1H, O***H***), 4.4$_3$-4.3$_5$ (m, 1H, C***H***OH), 4.2$_6$ (s,3H, NC***H***$_3$ imidazolium ring), 3.7$_6$(s,4H, NC***H***, N***CH***$_3$), 3.2$_5$ (s,3H, NC***H***$_3$), 2.1$_0$-17$_5$ (m, 11H, O=CC***H***$_3$, *Cyclohexyl*).

^{13}C-NMR (100 MHz, DMSO-d_6): δ 183.8$_5$ (N***C***N), 170.4$_0$ (CH$_3$***C***=O), 153.2$_3$-150.2$_2$ (***C***=O *purine ring*), 139.67 (*backbone carbon* ***C***=C), 109.5$_7$ (*backbone carbon* C=***C***), 72.3$_3$ (O***C***H), 62.9$_0$ (N***C***H), 37.8$_0$ (N***C***H$_3$), 33.4$_0$, 28.4$_9$ (N***C***H$_3$ *purine ring*) 34.0$_2$-23.5$_5$ (*Cyclohexyl group*) 22.8$_2$ (O=C***C***H$_3$).

4.3.18 General Procedure for the synthesis of NHC silver acetate complexes

NHC silver acetate complexes have been synthesized following the procedure published in the literature [140], slightly modified by us. NHC silver iodo complex (1.0 eq) and silver acetate (1.2 eq) were dissolved in mixture of methanol (15 mL) and dichloromethane (15 ml) and stirred for six hours with the exclusion of light and under a nitrogen atmosphere. Then, the reaction mixture was filtered to remove insoluble silver iodide. The acetate silver NHC complex was obtained by the remotion of solvent *in vacuo*.

4.3.19 Synthesis of acetate [*N*-(methyl)-*N'*(2-hydroxy phenyl)ethyl-imidazolyden]silver(I) (AgL1-OAc)

In a round bottom flask, under a nitrogen atmosphere, AgL1 (0.22 g, 0.5 mmol) and silver acetate (0.100 g, 0.6 mmol) in a mixture of methanol (15 mL) and dichloromethane (15 mL). The reaction mixture was stirred for six hours. The reaction mixture was filtered to remove insoluble silver iodide. The complex (0.13 g, 0.35 mmol) was obtained as an off-white powder.

Yield: 64%

^{1}H-NMR (400 MHz DMSO-d_6)**:** δ 7.4$_1$-7.2$_4$ (m, 7H, ***Ph ring***), 6.0$_5$ (b, 1H, ***OH group***), 4.9$_4$-4.9$_3$ (m, 1H, C***H***OH), 4.2$_9$ – 4.2$_1$ (m, 2H, NC***H***$_2$), 3.7$_5$ (s, 3H, N***CH***$_3$), 1.7$_0$ (s, 3H, OCOC***H***$_3$,).

^{13}C-NMR (100 MHz, DMSO-d_6): δ 179.2$_8$ (N***C***N), 175.2$_5$ (O***C***OCH$_3$), 142.4$_3$ *(ipso aromatic carbon* (1'), **Ph-ring**), 128.1$_0$-126.0$_9$, (*aromatic carbons*, **Ph ring**), 122.96-122.13 (*backbone carbon* ***C=C***), 72.4$_3$ (O***C***H), 58.2$_2$ (N***C***H$_2$), 38.0$_2$ (N***C***H$_3$), 24.11 (OCO***C***H$_3$).

4.3.20 Synthesis of acetate [4,5-dichloro-*N*-(methyl)-*N'*(2-hydroxy phenyl)ethyl-imidazolyden]silver(I) (AgL2-OAc)

Under nitrogen atmosphere, in a round bottom flask, a solution of AgL2 (0.25 g, 0.5 mmol) in methanol (15 mL) and dichloromethane (15 mL), was added silver acetate (0.10 g, 0.6 mmol). The reaction mixture was stirred for six hours at room temperature with the exclusion of light. The silver acetate complex (0.13 g,0.25 mmol) was obtained as a light-yellow powder.

Yield: 50%

^{1}H-NMR (400 MHz DMSO-d_6)**:** δ 7.40-7.28 (m, 5H, ***Ph ring***), 6.05 (b, 1H, ***OH group***) 4.96-4.93 (m, 1H, C***H***OH), 4.32 – 4.23 (m, 2H, NC***H***$_2$), 3.81 (s, 3H, N***CH***$_3$), 1.73 (s, 3H, COC***H***$_3$).

^{13}C-NMR (100 MHz, DMSO-d_6): δ 182.26 (N***C***N), 174.53 (O***C***OCH$_3$), 141.79 *(ipso aromatic carbon* (1'), **Ph-ring**), 128.20-126.03 (*aromatic carbons*, **Ph ring**), 117.15-116.67 (*backbone carbon* ***C=C***), 71.44 (O***C***H), 57.16 (N***C***H$_2$), 37.57 (N***C***H$_3$), 24.71 (OCO***C***H$_3$).

4.3.21 Synthesis of acetate [*N*-(methyl)-*N'*(2-methoxy phenyl)ethyl-imidazolyden]silver(I) (AgL7-OAc)

At solution of AgL7 (0.23 g, 0.5 mmol) in methanol (15 mL) and dichloromethane (15 mL), was added silver acetate (0.10 g, 0.6 mmol) under nitrogen atmosphere. The mixture was stirred for six hours with the exclusion of light. The product (0.12 g, 0.33 mmol) was obtained after filtration and the removal of the solvent at reduced pressure.

Yield: 66%

^{1}H NMR (400 MHz, DMSO-d_6): δ 7.34-7.26 (m, 7H, ***Ph ring, backbone***), 4.60 (m, 1H, OC***H***), 4.30-4.27 (m, 2H, NC***H***$_2$), 3.74 (s, 3H, NC***H***$_3$), 3.07 (s, 3H, OC***H***$_3$).

^{13}C-NMR (100 MHz, DMSO-d_6)**:** δ 182.75 (N***C***N), 173.43 (O***C***OCH$_3$), 137.21 (*ipso* carbon of ***Ph ring***), 128.72, -126.68 (aromatic carbon, ***Ph ring***), 122.60, 122.35 (*backbone carbons* ***C=C***), 83.32 (***C***HO), 56.79 (N***C***H$_2$), 54.27 (O***C***H$_3$), 38.26 (N***C***H$_3$), 24.11 (OCO***C***H$_3$).

4.4 Synthesis of gold(I) *N*-heterocyclic carbene complexes AuL1-L11

The gold complexes were formed by *trans*-metalation route [44], by the reaction of NHC silver complex (1.0 eq) with chloro(dimethylsulfide) gold(I)(1.0 eq) in dry-DCM.

4.4.1 Synthesis of chloro [*N*-(methyl)-*N'*(2-hydroxy phenyl)ethyl-imidazolyden]gold(I) (AuL1)

The synthesis and characterization of AuL1 were reported by the protocol published by us[128].

4.4.2 Synthesis of chloro 4,5-dichloro-[*N*-(methyl)-*N'*(2-hydroxy phenyl)ethyl-imidazolyden]gold(I) (AuL2)

The reaction for the synthesis and characterization of AuL2 were reported by us[130].

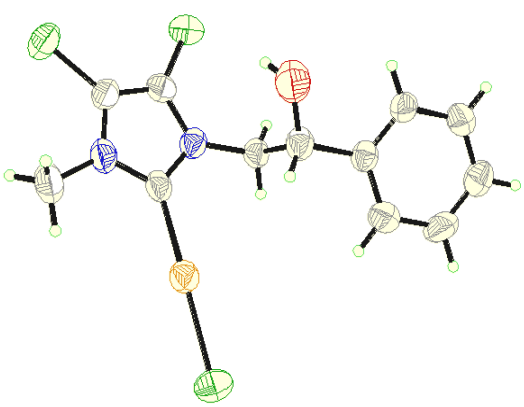

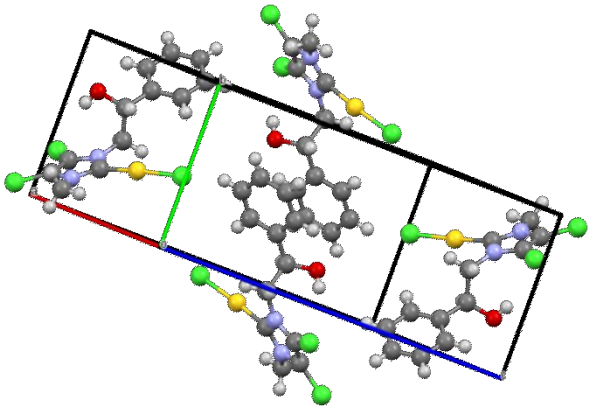

4.4.3 Synthesis of chloro 4,5-diphenyl-[*N*-(methyl)-*N'*(2-hydroxy phenyl)ethyl-imidazolyden]gold(I) (AuL3)

In a round bottom flask, under a nitrogen atmosphere, AgL3 (0.29 g,0.5 mmol) was dispersed in 25 mL of dry CH_2Cl_2. In the reaction mixture was added the chloro(dimethylsulfide) gold(I) (0.15 g, 0.5 mmol), and was stirred for three hours with the exclusion of the light. Afterward, the mixture was filtered through a pad of Celite, and the resulting solution was dried *in vacuo* to lead the gold complex (0.20 g, 0.35 mmol).

Yield: 70%

^{1}H NMR (400 MHz, DMSO-d_6): δ 7.3$_6$-7.1$_4$ (m, 15H, ***Ph rings***) 5.1$_3$ (m, 1H, OC***H***); 4.1$_7$-4.0$_6$ (m, 2H, NC***H***$_2$); 3.7$_2$ (s, 3H, NC***H***$_3$).

^{13}C-NMR (100 MHz, DMSO-d_6): δ 169.4$_6$ (N***C***N), 141.8$_4$ (*ipso aromatic carbon*, **Ph-ring**), 131.7$_0$-125.4$_9$, (*aromatic carbons*, **Ph ring**), 72.3$_0$ (O***C***H), 55.5$_7$ (N***C***H$_2$), 36.9$_1$ (N***C***H$_3$).

MALDI-ToF (m/z): 905.31858 Da attributable to bis-carbenic structure $[C_{48}H_{44}AuN_4O_2]^+$

4.4.4 Synthesis of chloro [*N*-(methyl)-*N'*(2-hydroxy phenyl)ethyl-benzimidazolyden]gold(I) (AuL4)

At a solution of AgL4 (0.24 g, 0.5 mmol) in dichloromethane (25 mL) was dissolved chloro(dimethylsulfide) gold(I) (0.15 g, 0.5 mmol) under nitrogen atmosphere. The resulting mixture was stirred for four hours with the exclusion of

light. Later, the mixture was filtered, and the resulting solution was dried to give the gold complex (0.15 g, 0.30 mmol).

^{1}H NMR (400 MHz, DMSO-d_6): δ 7.8$_0$-7.2$_8$ (m, 9H, ***Ph ring***); 5.7$_6$ (s, 1H, O***H***); 5.2$_2$-5.2$_1$ (dd, 1H, OC***H***); 4.6$_9$-4.5$_4$ - 4.5$_0$ (m, 2H, NC***H***$_2$); 4.0$_0$ (s, 3H, NC***H***$_3$).

^{13}C-NMR (100 MHz, DMSO-d_6): δ 177.4$_1$ (N***C***N), 141.9$_7$ (*ipso aromatic carbon*, **Ph-ring**), 133.5$_5$-133.1$_0$ (*backbone carbons*, N***C***=***C***N), 128.3-111.8$_2$ (*aromatic carbons*, **Ph rings**), 72.5$_6$(O***C***H), 55.4$_2$ (N***C***H$_2$), 35.0$_0$ (N***C***H$_3$).

MALDI-ToF (m/z): 701.22194 Da attributable to bis-carbenic structure $[C_{32}H_{32}AuN_4O_2]^+$

4.4.5 Synthesis of chloro [*N*-(2-hydroxy ethyl)-*N'*(2-hydroxy phenyl)ethyl-imidazolyden]gold(I) (AuL5)

AgL5 (0.233 g, 0.5 mmol) and chloro(dimethylsulfide) gold(I) (0.15 g, 0.5 mmol) were dissolved in dry DCM in a Schlenk flask, under inert atmosphere. The solution was stirred for six hours at room temperature. The AgI byproduct was filtered off through a pad of Celite, and the solution was dried *in vacuo*. The gold NHC complex was recovered as a light-yellow powder (0.148 g, 0.32 mmol).

^{1}H NMR (400 MHz, DMSO-d_6): 7.3$_8$-7.3$_1$ (m, 7H, ***Ph rings***); 5.8$_8$ (s, 1H, O***H***); 5.0$_7$ (s, 1H, O***H***) 4.9$_9$ (m, 1H, OC***H***); 4.3$_6$-4.2$_7$ (m, 4H, NCH$_2$C***H***$_2$OH, NC***H***$_2$CHOH); 3.7$_3$ (s, 2H, NC***H***$_2$CH$_2$OH).

^{13}C-NMR (100 MHz, DMSO-d_6)**:** δ 168.3$_7$(N***C***N), 142.0$_7$ (*ipso* carbon of ***Ph ring***), 128.3$_0$, 127.7$_9$, 127.6$_1$ (aromatic carbon, ***Ph ring***), 122.3$_0$, 121.5$_5$ (*backbone carbons*), 72.3$_6$ (***C***HOH), 60.4$_4$ (***C***H$_2$OH), 57.7$_9$ (N***C***H$_2$CHOH), 53.0$_0$ (N***C***H$_2$CH$_2$OH).

ESI-MS (CH$_3$CN m/z): 661.20838 Da attributable to [C$_{26}$H$_{32}$AuN$_4$O$_4$]$^+$

4.4.6 Synthesis of chloro, 4,5-dichloro-[*N*-(2-hydroxy ethyl)-*N'*(2-hydroxy phenyl)ethyl-imidazolyden]gold(I) (AuL6)

At a solution of AgL6 (0.268 g, 0.5 mmol) in dry dichloromethane (25 mL) and chloro(dimethylsulfide) gold(I) (0.15 g, 0.5 mmol), and was stirred for six hours in dark conditions. The gold complex (0.19 g, 0.35 mmol) was recovered after the filtration of the mixture and the removal of the solvent under reduced pressure.

^{1}H NMR (400 MHz, DMSO-d_6): δ 7.3$_8$-7.2$_7$ (m, 5H, ***Ph ring***); 5.8$_9$ (s, 1H, O***H***); 5.0$_7$ (s, 1H, O***H***) 4.9$_9$ (m, 1H, OC***H***); 4.3$_3$-4.2$_7$ (m, 4H, NCH$_2$C***H***$_2$OH, NC***H***$_2$CHOH); 3.7$_4$ (s, 2H, NC***H***$_2$CH$_2$OH).

^{13}C-NMR (100 MHz, DMSO-d_6)**:** δ 170.9$_0$ (N***C***N), 141.3$_5$ (*ipso* carbon of ***Ph ring***), 128.4$_1$, 127.9$_2$, 125.0$_8$ (aromatic carbon, ***Ph ring***), 117.2$_0$, 116.7$_4$ (*backbone carbons*), 72.1$_4$ (***C***HOH), 59.8$_9$ (***C***H$_2$OH), 56.8$_9$ (N***C***H$_2$CHOH), 52.3$_7$ (N***C***H$_2$CH$_2$OH).

ESI-MS (CH$_3$CN m/z): 707.99716 Da attributable to [C$_{26}$H$_{32}$AgN$_4$O$_4$]$^+$

4.4.7 Synthesis of chloro,[*N*-(methyl)-*N'*(2-methooxy phenyl)ethyl-imidazolyden]gold(I) (AuL7)

The gold complexes AuL7 was prepared by the reaction of AgL7 (0.23 g, 0.5 mmol) with chloro(dimethylsulfide) gold(I) (0.15 g, 0.5 mmol) in dry DCM (25 mL) at room temperature. The silver iodide was filtered, and the resulting solution was dried to give a yellow powder (0.20 mol,0.45 mmol).

^{1}H NMR (400 MHz, DMSO-d_6): δ 7.3$_5$-7.2$_9$ (m, 7H, ***Ph ring, backbone***), 4.6$_9$ (m, 1H, OC***H***), 4.3$_2$-4.2$_6$ (m, 2H, NC***H***$_2$), 3.7$_0$ (s, 3H, NC***H***$_3$), 3.0$_7$ (s, 3H, OC***H***$_3$).

^{13}C-NMR (100 MHz, DMSO-d_6)**:** δ 169.1$_0$ (N***C***N), 137.9$_1$ (*ipso* carbon of ***Ph ring***), 128.6$_1$, 128.3$_2$, 126.6$_8$ (aromatic carbon, ***Ph ring***), 122.3$_0$, 122.2$_5$ (*backbone carbons*), 82.2$_4$ (***C***HO), 56.5$_9$ (N***C***H$_2$), 55.8$_7$ (O***C***H$_3$), 37.6$_6$(N***C***H$_3$).

MALDI-ToF (m/z): 629.2267 Da attributable to [C$_{26}$H$_{32}$AgN$_4$O$_2$]$^+$

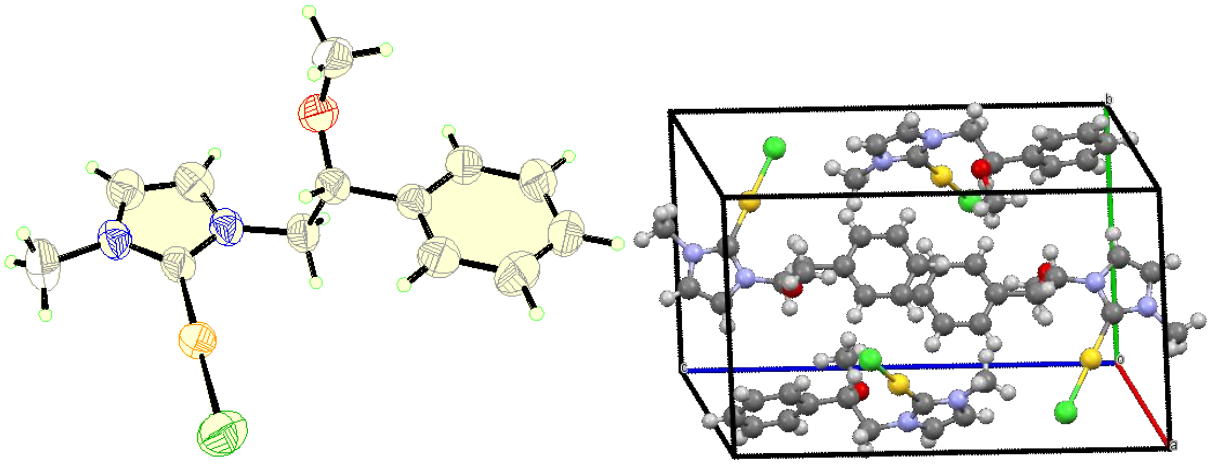

Table 1 Details of data collection and structure refinements for complex **AuL7**

Parameters	Complex **4b**
Empirical formula	$C_{13}H_{10}AuClN_2O$
Formula weight	448.7
Crystal system	Monoclinic
Space group	$P2_1/n$
T (K)	293(2)
Radiation	Mo Kα (0.7107)
a (Å)	9.012(3)
b (Å)	10.387(4)
c (Å)	16.294(5)
α (deg)	90.00
β (deg)	105.724(13)
γ (deg)	90.00
V (Å^3)	1468.2(9)
Z	4
ρ (g cm^{-1})	2.030
μ (mm^{-1})	10.192
θ range (°)	2.35–26.96
Reflections collected	23 336
Unique data	3192
Observed reflections	2858
R_1, $I > 2\sigma(I)$	0.0166
wR_2, $I > 2\sigma(I)$	0.0391
Goodness of fit, S	1.058

4.4.8 Synthesis of chloro, 4,5-[*N*-(methyl)-*N'*(2-sodium alcoholate phenyl)ethyl-imidazolyden]gold(I) (AuL7')

In a Schlenk round bottom flask, the AgL7' (0.16 g, 0.35 mmol) was suspended in dry CH_2Cl_2 (25 mL). At the suspension was added the $Au(SMe_2)Cl$ (0.11 g, 0.35 mmol), and it was stirred for four hours in the dark. The removal of the silver iodide byproduct through the filtration, and the removal of the solvent have given the gold complex (0.09 g, 0.195 mmol).

^{1}H NMR (400 MHz, CD_2Cl_2): δ 7.36-7.33 (m, 5H, ***Ph ring***), 6.89-6.79 (s, 2H, ***backbone***), 5.13 (t, 1H, $^-$OC***H***), 4.40-4.30 (m, 2H, NC***H***$_2$), 3.86 (s,3H, NC***H***$_3$).

^{13}C-NMR (100 MHz, CD_2Cl_2)**:** δ 171.90 (N***C***N), 141.81 (*ipso* carbon of ***Ph ring***), 129.51, 129.32, 129.18 (aromatic carbon, ***Ph ring***), 122.90, 121.85 (*backbone carbons*), 74.53 (***C***HO$^-$), 58.79 (N***C***H$_2$), 38.86 (N***C***H$_3$).

ESI-MS (CH_2Cl_2, m/z): 612.3657 Da attributable to $[C_{22}H_{18}AuN_4O_2Na_2]^+$

4.4.9 Synthesis of chloro [*N*-(methyl)-*N'*(cyclopentane-2-ol)-imidazolyden]gold(I) (AuL8)

The synthesis and characterization of AuL8 was reported by protocol published by us [128]

4.4.10 Synthesis of chloro4,5-dichloro[*N*-(methyl)-*N'*(cyclopentane-2-ol)-imidazolyden] gold(I) (AuL9)

The synthesis and characterization of AuL9 is reported in our published paper [129].

4.4.11 Synthesis of chloro, [*N*-(methyl)-*N'*(cyclohexane-2-ol)-imidazolyden]gold(I) (AuL10)

The synthesis and characterization of AuL10 is reported in our published paper [128].

4.4.12 Synthesis of chloro,4,5-dichloro[*N*-(methyl)-*N'*(cyclohexane-2-ol)-imidazolyden]gold(I) (AuL11)

In a round bottom flask, AgL11 (0.241 g, 0.5 mmol) was dissolved in dry-DCM (25 mL) with chloro(dimethylsulfide) gold(I) (0.15 g, 0.5 mmol). The resulting mixture was stirred for five hours. The mixture was filtered for remove the silver iodide byproduct. The gold complex was obtained as light-yellow powder (0.22 g, 0.45 mmol).

^{1}H NMR (400 MHz, DMSO-d_6): δ 4.17-4.12 (m, 1H, HOC***H***), 3.89-3.86 (s, 1H, NC***H***), 3.73 (s, 3H, NC***H***$_3$), 1.97-1.29 (*Cyclohexyl* group).

^{13}C-NMR (100 MHz, CD_2Cl_2)**:** δ 171.20 (N***C***N), 119.65, 117.25 (*backbone carbons*), 77.13 (***C***HOH), 71.39 (N***C***H), 39.16 (N***C***H$_3$), 35.01-23.93 (*Cyclohexyl carbons*).

ESI-MS (CH_2Cl_2, m/z): 693.06319 Da attributable to $[C_{20}H_{28}AuCl_4N_4O_2]^+$

4.4.13 General procedure for the synthesis of caffeine-based gold *N*-Heterocyclic carbene complexes AuL12-L14

Caffeine-based gold NHC complexes were produced following the procedure published in the literature[45,46]. Under a nitrogen atmosphere, a mixture of the imidazolium salt (1.0 eq), AuCl(SMe_2) (1.0 eq), and K_2CO_3 (10 eq), in CH_3CN (25 mL) was stirred for twenty-four hours, at room temperature.

After this time, the mixture was filtered, and the solvent was reduced to 5.0 mL. The complex was obtained by precipitation by the addition of diethyl ether (20 mL).

4.4.14 Synthesis of chloro -[*N'*(2-hydroxy phenyl)ethyl-trimethylxanthium] gold(I) (AuL12)

Imidazolium salt, P-L12 (0.22 g, 0.50 mmol) and Au(SMe_2)Cl (0.15 g, 0.5 mmol) were dissolved in dry acetonitrile (25 mL). The reaction mixture was stirred for three hours. After it was added K_2CO_3 (0.67 g, 5.0 mmol), the mixture was stirred for other twenty-four hours. After this time, the mixture was filtered, and the solvent was reduced to *ca*. 5mL. The

addition of 20 mL of diethyl ether, has caused the precipitation of the gold complex (0.16 g, 0.3mmol).

Yield: 60%

^{1}H-NMR (400 MHz DMSO-d_6)**:** δ 7.4$_1$-7.2$_9$ (m, 5H, ***Ph-group***), 5.6$_2$ (s,1H, O***H***), 5.1$_6$ - 5.1$_0$ (m, 1H, C***H***OH), 4.6$_0$-4.3$_2$ (m, 2H, NC***H***$_2$), 4.1$_9$ (s, 3H, NC***H***$_3$ imidazolium ring), 3.7$_5$ (s, 3H, NC***H***$_3$), 3.2$_7$ (s, 3H, NC***H***$_3$).

^{13}C-NMR (400 MHz DMSO-d_6)**:** δ 184.0$_0$ (N***C***N), 153.5$_3$-150.4$_9$ (***C***=O *purine ring*), 141.7$_5$ *(ipso aromatic carbon*, **Ph-ring**), 139.8$_3$ (*backbone carbon*, ***C***=C), 128.3$_6$, 127.6$_1$, 125.8$_7$ (*aromatic carbons*, **Ph ring**), 107.6$_2$ (*backbone carbon*, C=***C***), 71.6$_0$ (***C***HOH), 56.3$_5$ (N***C***H$_2$), 31.6$_8$, 28.3$_6$ (N***C***H$_3$ purine ring).

ESI-MS (CH_2Cl_2 m/z): 681.32325 Da attributable to $[C_{22}H_{22}LiAuN_8O_5]^+$

4.4.15 Synthesis of chloro -[*N'*(2-hydroxy)ethyl-trimethylxanthium] gold(I) (AuL13)

P-L13 (0.37 g, 1.00 mmol) and chloro gold(I) dimethylsulfide (0.15 g, 0.5 mmol) were dissolved in dry CH_3CN (25 mL) under nitrogen atmosphere, for three hours. In the second instance, it was added potassium carbonate (0.67 g, 5.0 mmol). The reaction mixture was stirred overnight. After that, the reaction mixture was filtered, and the solvent was reduced to ca. 5.0 mL. The gold complex (0.14 g, 0.3 mmol) was obtained by precipitation with the addition of diethyl ether (30mL).

Yield: 60%

^{1}H-NMR (400 MHz DMSO-d_6)**:** δ 4.8$_3$-4.7$_6$ (m, 2H, C***H***$_2$OH), 4.4$_9$ (s, 3H, NC***H***$_3$ imidazolium ring), 3.8$_6$-3.7$_3$ (b, 5H, NC***H***$_2$, NC***H***$_3$), 3.2$_1$ (s, 3H, NC***H***$_3$).

^{13}C-NMR (100 MHz DMSO-d_6)**:** δ 184.6$_8$ (N***C***N); 153.4$_3$-150.3$_2$ (***C***=O *purine ring*); 139.7$_2$ (*backbone carbon* ***C***=C); 107.2$_3$ (*backbone carbon*, C=***C***), 60.2$_2$ (***C***H$_2$OH), 52.9$_9$(N***C***H$_2$), 31.5$_1$, 28.2$_4$ (N***C***H$_3$ imidazolium *ring*), 31.4$_0$, 28.4$_9$ (N***C***H$_3$ *purine ring*).

4.4.16 Synthesis of chloro -[*N'*(ciclohexane-2-ol)-trimethylxanthium] gold(I) (AuL14)

Under inert atmosphere, in a round bottom flask was dissolved the caffeine-based salt (0.21 g, 0.5 mmol) and Au(SMe$_2$)Cl (0.15 g, 0.5 mmol) in dry-CH_3CN (25 mL). The resulting mixture was stirred for three hours, and subsequently, was added K_2CO_3 (0.67 g, 5.0 mmol) was stirred for other twenty-four hours. After, the mixture was filtered, and the solvent was reduced *in vacuo*. The complex was recovered as an off-white powder (0.10 g, 0.2 mmol), by precipitation with the addition of diethyl ether (25 mL).

Yield: 40%.

^{1}H-NMR (400 MHz DMSO-d_6)**:** δ 5.5$_6$ (s, 1H, O***H***), 5.1$_7$ (b, 1H, C***H***OH), 4.2$_6$ (s, 3H, NC***H***$_3$ imidazolium ring), 4.0$_8$ (b, 1H, NC***H***), 3.8$_6$ (s, 3H, N***CH***$_3$), 3.2$_5$ (s, 3H, NC***H***$_3$), 2.2$_0$-1.7$_5$ (m, 11H, O=CC***H***$_3$, *Cyclohexyl*).

^{13}C-NMR (100 MHz, DMSO-d_6): δ 175.6$_5$ (N***C***N), 153.3$_3$-149.2$_2$ (***C***=O *purine ring*), 139.6$_7$ (*backbone carbon* ***C***=C), 108.7$_7$ (*backbone carbon* C=***C***), 72.3$_3$ (O***C***H), 62.9$_0$ (N***C***H), 36.8$_0$ (N***C***H$_3$), 33.4$_0$, 28.4$_9$ (N***C***H$_3$ *purine ring*), 34.0$_2$-23.5$_5$ (*Cyclohexyl group*) 22.8$_2$ (O=C***C***H$_3$).

4.4.17 Synthesis of acetato 4,5-dichloro-[*N*-(methyl)-*N'*(2-hydroxy phenyl)ethyl-imidazolyden]gold(I) (AuL2-OAc)

A mixture of silver acetate (0.020g,0.12mmol, 1.2eq) and gold complex AuL2 (0.050g, 0.1 mmol, 1.0 eq) in dichloromethane (10mL), was stirred for 12 h at room temperature, with the exclusion of the light. The mixture was filtered, to remove AgCl by-product and the solution was dried to give the acetate gold NHC complex (0.042g, 0.08mmol) as a white powder.

Yield: 80%

^{1}H-NMR (400MHz, DMSO-d_6): δ 7.4$_8$-7.3$_1$ (m, 5H, ***Ph ring***) 5.8$_3$(m, 1H, ***OH group***); 5.2 (m, 1H, OC***H***) 4.2$_0$-4.1$_2$(m, 2H, NC***H***$_2$); 3.8$_1$(s,3H, NC***H***$_3$)1.83 (s. 3H, COC***H***$_3$).

^{13}C-NMR (100 MHz, DMSO): 174.8$_5$ (O***C***OCH$_3$) 163.9$_6$ (N***C***N) 141.4$_4$ *(ipso aromatic carbon*, **Ph-ring**), 128.3$_5$-125.9$_8$ (*aromatic carbons*, **Ph rings**) 117.5$_9$-116.5$_6$ (*backbone carbons*, N***C***=***C***N), 72.2$_6$(O***C***H), 56.5$_1$(N***C***H$_2$), 37.6$_7$(N***C***H$_3$), 23.8$_7$ (OCO***C***H$_3$)

MALDI-ToF (m/z): 739.07459 Da attributable to a structure a bis-carbene structure $[C_{24}H_{24}AuCl_4N_4O_2]^+$

4.4.18 Synthesis of bromo 4,5-dichloro-[N-(methyl)-N'(2-hydroxy phenyl)ethyl-imidazolyden]gold(I) (AuL2-Br)

At solution of gold complex AuL2 (0.050g, 0.1 mmol, 1.0 eq) in acetone (10 mL) was added LiBr (0.09g, 1mmol, 10 eq). The reaction mixture was stirred for 24 h at room temperature. Then, the solvent was removed *in vacuo*, and the was added 10 mL of dichloromethane. The mixture was filtered to remove the excess of LiBr and LiCl by-products. The Bromo NHC gold complex (0.049g, 0.09mmol) was obtained by removing the solvent *in vacuo*.

Yield: 90%

^{1}H-NMR (400MHz, DMSO-d_6): δ 7.4$_0$-7.3$_6$ (m, 5H, ***Ph ring***) 5.8$_7$(m, 1H, ***OH group***); 5.1$_4$ (m, 1H, OC***H***) 4.2$_6$-4.1$_9$(m, 2H, NC***H***$_2$); 3.8$_1$(s,3H, NC***H***$_3$).

^{13}C-NMR (100 MHz, DMSO-d_6): δ 173.8$_9$ (N***C***N) 141.2$_4$ *(ipso aromatic carbon*, **Ph-ring**), 128.4$_3$-125.7$_8$ (*aromatic carbons*, **Ph rings**) 117.4$_2$-116.5$_4$ (*backbone carbons*, N***C***=***C***N), 72.1$_4$(O***C***H), 56.5$_6$(N***C***H$_2$), 37.0$_4$(N***C***H$_3$)

MALDI-ToF (m/z): 739.03526 Da attributable to a structure a bis-carbene structure $[C_{24}H_{24}AuCl_4N_4O_2]^+$

4.4.19 Synthesis of iodo 4,5-dichloro-[N-(methyl)-N'(2-hydroxy phenyl)ethyl-imidazolyden]gold(I) (AuL2-I)

A solution of AuL2 (0.050g, 0.1 mmol, 1.0 eq) and sodium iodide (0.140g, 1.0mmol, 10 eq) in acetone (10mL) was stirred for 24 h. Then, the solvent was removed *in vacuo*. The residue was partially dissolved in dichloromethane (10mL), and the mixture was filtered through a pad of Celite®. The removal of the solvent gave the iodo gold NHC complex (0.053g,0.093mmol)

Yield: 93%

^{1}H-NMR (400MHz, DMSO-d_6): δ 7.40-7.34 (m, 5H, ***Ph ring***) 5.95 -5.75(m, 1H, ***OH group***); 5.18 -5.17 (m, 1H, OC***H***) 4.39-4.05(m, 2H, NC***H***$_2$); 3.91-3.81(s,3H, NC***H***$_3$)

^{13}C-NMR (100 MHz, DMSO): 182.92 (N***C***N) 141.28 *(ipso aromatic carbon*, **Ph-ring**), 128.47-125.78 (*aromatic carbons*, **Ph rings**) 117.54-116.62 (*backbone carbons*, N***C***=***C***N), 72.22(O***C***H), 56.41(N***C***H$_2$), 36.84(N***C***H$_3$)

MALDI-ToF (m/z): 739.06311 Da attributable to a bis-carbene structure $[C_{24}H_{24}AuCl_4N_4O_2]^+$

4.4.20 Synthesis of hexafluorophosphate 4,5-dichloro-[*N*-(methyl)-*N'*(2-hydroxy phenyl)ethyl-imidazolyden]gold(I) (AuL2-PF$_6$)

A solution of AuL2 (0.050g, 0.1 mmol, 1.0 eq) and silver hexafluorophosphate (0.030 g ,0.12mmol, 1.2eq) in acetonitrile (10mL) was stirred for 6 h. Thene, the mixture was filtered, and the solvent was removed under reduced pressure. The hexafluorophosphate gold NHC (0.030 g,0.05mmol) was obtained as grey powder.

Yield: 50%

^{1}H-NMR (400MHz, DMSO-d_6): δ 7.40-7.29 (m, 5H, ***Ph ring***) 4.99 (m, 1H, OC***H***) 4.33-4.30(m, 2H, NC***H***$_2$); 3.80(s,3H, NC***H***$_3$)

^{13}C-NMR (100 MHz, DMSO-d_6): δ 183.82 (N***C***N) 142.14 *(ipso aromatic carbon*, **Ph-ring**), 129.29-126.88 (*aromatic carbons*, **Ph rings**) 118.78-118.51 (*backbone carbons* N***C***=***C***N), 72.33(O***C***H), 57.63(N***C***H$_2$), 37.80(N***C***H$_3$)

^{31}P-NMR (162.60 MHz; DMSO): 193.93 (septuplet)

^{19}F-NMR (377.35 MHz, DMSO): 70.10 (duplet)

4.4.21 Synthesis of phenylacetylide 4,5-dichloro-[*N*-(methyl)-*N'*(2-hydroxy phenyl)ethyl-imidazolyden]gold(I) (AuL2CCPh)

A solution of phenylacetylene (0.010g, 0.1 mmol, 1.0 eq) and NEt$_3$ (0.060g ,0.6mmol, 6.0eq) in acetonitrile (10 mL) was stirred for 2 h. Then, it was added AuL2 (0.050g, 0.1 mmol, 1.0 eq), and the mixture was stirred for other 8h. The complex (0.045g ,0.08mmol) was obtained by filtration of the reaction mixture.

Yield: 80%

^{1}H NMR (400MHz, DMSO-d_6): δ 7.42-7.27 (m, 10H, ***Ph rings***) 5.97(m, 1H, ***OH group***); 5.17 (m, 1H, OC***H***) 4.27-4.26(m, 2H, NC***H***$_2$); 3.82(s,3H, NC***H***$_3$)

^{13}C-NMR (100 MHz, DMSO): δ 186.9$_5$ (N***C***N) 141.3$_9$ (*ipso aromatic carbon*, **Ph-ring**), 131.2$_4$-125.8$_5$ (*aromatic carbons*, **Ph rings,** Au***C***≡C-Ph) 117.4$_7$-116.5$_6$ (*backbone carbons* N***C***=***C***N,), 104.0$_3$ (AuC≡***C***-Ph) 72.3$_6$(O***C***H), 56.2$_7$(N***C***H$_2$), 36.7$_8$(N***C***H$_3$).

4.5 General Procedure for A^3 (aldehyde, amine, alkyne) coupling reaction promoted by M-NHC complexes

Under an inert atmosphere, in a 10 mL Schlenk tube equipped with a magnetic stirring bar, were added aldehyde (1.00 mmol), piperidine (1.2 mmol), phenylacetylene (1.5 mmol), 2-Bromo mesitylene as internal standard (1.00 mmol) and the NHC metal complex (3% mol). The reaction mixture was stirred for 6h at 80 °C. Later, the mixture was cooled to room temperature and was added a 1:1 solution of diethyl ether and dichloromethane. The organic phase dried on $MgSO_4$ and filtered. The yield of the propargylamine was evaluated by the integration of the singlet signal of the internal standard at 6.89 ppm and the hydrogen(s) of the product, in α position to nitrogen atom of the propargylic amine. The complete characterization of the coupling products is reported in the literature [130].

***N*-(3-phenyl-2-propynyl) piperidine**

^{1}H NMR (300 MHz, CD_2Cl_2): δ 7.42 (m, 2H, C*HAr*), 7.30 (m, 3H, C*HAr*), 3.43 (s, 2H, NC*H*$_2$), 2.53 (t, 4H, NC*H*$_2$CH$_2$), 1.60 (m, 4H, NCH$_2$C*H*$_2$), 1.43 (m, 2H, NCH$_2$CH$_2$C*H*$_2$).

^{13}C NMR (75 MHz, $CDCl_3$): δ 131.6, 128.1, 127.3 (3·s, 5C, *Car*),123.5 (s, 1C, *Car*), 85.1 (s, 1C, C=*C*-Ph), 84.9 (s, 1C, *C*=C-Ph), 53.3 (s,2C, NCH$_2$CH$_2$), 48.3 (s, 1C, NCH), 26.1 (s, 2C, NCH$_2$CH$_2$), 24.0 (s, 1C, NCH$_2$CH$_2$CH$_2$).

1-(1-cyclohexyl-3-phenyl-2propynyl)

^{1}H NMR (300 MHz, CD_2Cl_2): δ 7.42 (m, 2H, C*HAr*), 7.32 (m, 3H, C*HAr*), 3.11 (d, 1H, NC*H*), 2.64 (m, 2H), 2.33 (m, 2H), 2.07 (m, 2H), 1.86 (m, 2H), 1.67 (m, 6H), 1.56 (m, 2H), 1.43 (m, 3H), 1.10 (m, 2H).

^{13}C NMR (75 MHz, CD_2Cl_2): δ 132.0, 128.8, 128.2 (3·s, 5C, *Car*), 124.3 (s, 1C, *Car*), 88.4 (s, 1C, C=*C*-Ph), 86.4 (s, 1C, *C*=C-Ph), 64.8 (s, 1C, NCH), 51.2 (s, 2C, NCH$_2$CH$_2$), 40.1, 31.9, 30.8, 27.3 (4·s, 6C, Cyclohexyl), 26.6 (s, 2C, NCH$_2$CH$_2$CH$_2$), 25.3 (s, 1C, NCH$_2$CH$_2$CH$_2$).

***N*-(1,3-diphenyl-2-propynyl)piperdine**

^{1}H NMR (300 MHz, CD_2Cl_2): δ 7.89, 7.57, 7.50, 7.31, 7.24, 7.18(m, 10H, C*Har*), 4.79 (s, 1H, NC*H*), 2.59 (s, 4H, NC*H*$_2$CH$_2$CH$_2$), 1.62 (m, 4H, NCH$_2$C*H*$_2$CH$_2$), 1.49 (m, 2H, NCH$_2$CH$_2$C*H*$_2$).

^{13}C NMR (75 MHz, $CDCl_3$): 138.6, 131.8, 128.5, 128.2, 128.0, 127.7, 123.3 (8·s, 12C, *Car*), 87.5 (s, 1C, C=*C*-Ph), 86.1(s, 1C,*C*=C-Ph), 62.4 (s, 1C, NC*H*), 50.5 (s, 2C, NCH$_2$CH$_2$), 26.2 (s, 2C, NCH$_2$CH$_2$CH$_2$), 24.3 (NCH$_2$CH$_2$CH$_2$).

4.6 General Procedure for hydroamination reaction promoted by Au-NHC complex

In a Schlenk tube, under nitrogen atmosphere, were placed arylamine (1.0 mmol), the alkyne (1.5 mmol), AuNHC complex (1% mol), $AgSbF_6$ (2% mol), and 1.0 mL of the solvent. The

reaction flask was placed in oil bath, at 80°C and the mixture was stirred for sixteen hours. Afterward, the solvent was removed under reduced pressure, and at crude oil was added the dibromo methane, as internal standard (1.00 mmol). The yields of imine were determined by ^{1}H-NMR spectroscopy, after the dilution of the sample with $CDCl_3$.
All the hydroamination product were characterized in literature except for 4f, 4j (see Table 9, Chapter 4). 4a, 4c, 4g, 4h, 4i, 4l [202], 4b[207], 4d[208], 4e[209], 4k[210], 4m[211].

(E)-*N*-(4-nitrophenyl) -1-phenylethan-1-imine (4f)

^{1}H-NMR (300 MHz $CDCl_3$): δ 8.16-6.91(m, 9H, aromatic protons), 1.83 (s, 3H, CH_3).

(E)-*N*-(2,6-difluorophenyl)-1-phenylethan-1-imine (4f)

^{1}H-NMR (300 MHz $CDCl_3$): δ 7.96-7.01 (m, 8H, aromatic protons), 1.89 (s, 3H, CH_3).

4.7 Antibacterial Activity

The antibacterial activity of Ag and Au complexes (**AgL1**, **AgL2**, **AgL5**, **AgL6**, **AgL7**, **AgL1-OAc**, **AgL2-OAc**, **AgL7-OAc**) was valued by determining of minimal growth inhibitory concentrations (MIC), in accordance with the indications provided by Clinical and Laboratory Standards Institute (CLSI) [205]. All complexes were tested in the following concentrations: (0, 0.5, 1, 2, 4.5, 6.5, 7.5, 10, 15, 25, 40, 50, 75, 100, 150) μg/mL. The NHC-proligands (P-L1, P-L2, P-L5, P-L6, P-L7) were tested as experimental controls.
The bacteria were suspended in Luria-Bertini (LB) broth (tryptone, 10g/L; yeast extract 10 g/L; NaCl, 5g/L, pH=7) at density of $5 \cdot 10^5$ CFU/mL and incubated with each complex, at different concentrations, at 37°C, with constant stirring (250 rpm). After 24 h, the turbidity was used for the evaluation of the effect on the growth, measuring the optical density (OD) at 600 nm. The MIC was defined as the lowest concentration that did not change the turbidity of the sample respect to time 0. The MIC was replicated in three independent experiments, each in triplicate.

4.8 Antitumoral Activity

The *in vitro* anticancer activity of complexes was evaluated utilizing the MTT assay. The cells have been exposed to the target complexes (**AgL2**, **AgL5**, **AgL6**, **AgL7**, **AgL1-OAc**, **AgL2-OAc**, **AgL7-OAc**, **AuL2**, **AuL5**, **AuL6**, **AuL7**, **AuL1-OAc**, **AuL2-OAc**, **AuL7-OAc**), dissolved in DMSO at diverse concentrations (0.1, 1, 5, 10, 50, 100 and 200μM) for 72h. MTT (3-(4,5-dimethylthiazol-2-yl)-2,5-diphenyl tetrazolium bromide) was added at 37°C for 2h. The formazan crystals were dissolved in DMSO, and the optical density was quantified at 570nm using a microplate reader. All the measurements were performed in triplicate, and the results were shown as the percent (%) of basal. The IC_{50} values were determined using curve fitting GraphPad Prism 9 software (GraphPad Software, La Jolla, CA, USA) with nonlinear regression. The values represent the mean ± standard deviation (n=3)

Permissions

Figure 2:

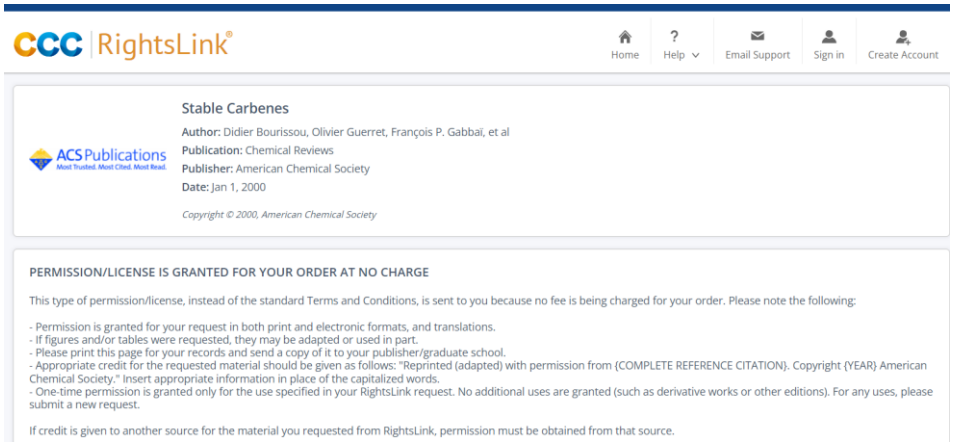

Figures 5,6,7

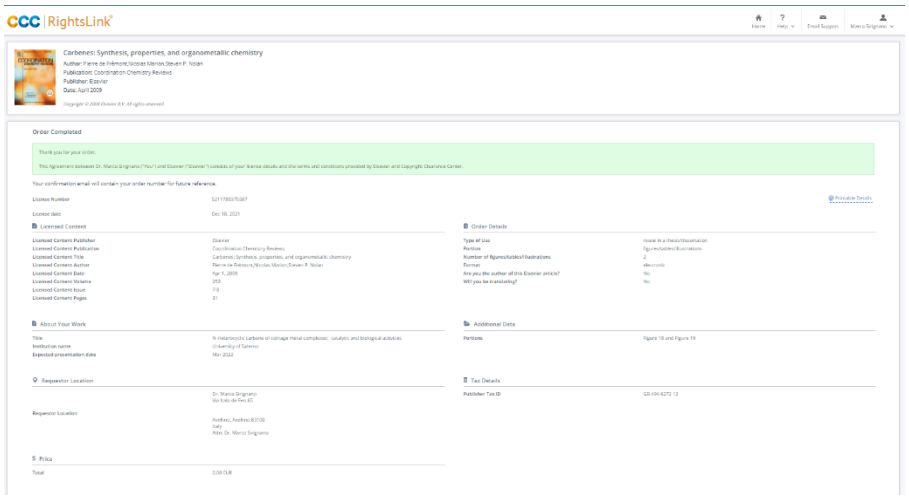

Scheme 1

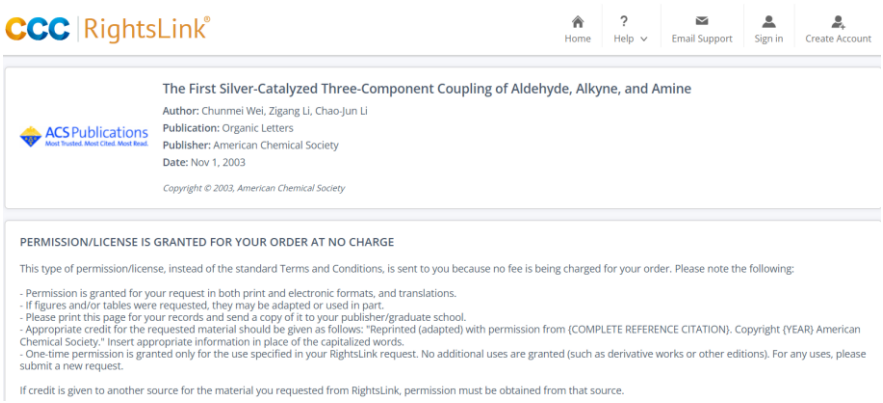

References

1. Bourissou, D.; Guerret, O.; Gabbaï, F.P.; Bertrand, G. Stable Carbenes. *Chem. Rev.* **2000**, *100*, 39–92, doi:10.1021/cr940472u.

2. Hahn, F.E.; Jahnke, M.C. Heterocyclic Carbenes: Synthesis and Coordination Chemistry. *Angew. Chem. Int. Ed.* **2008**, *47*, 3122–3172, doi:10.1002/anie.200703883.

3. Schuster, G.B. Structure and Reactivity of Carbenes Having Aryl Substituents. In *Advances in Physical Organic Chemistry*; Elsevier, 1986; Vol. 22, pp. 311–361 ISBN 978-0-12-033522-0.

4. Hoffmann, R.; Zeiss, G.D.; Van Dine, G.W. The Electronic Structure of Methylenes. *J. Am. Chem. Soc.* **1968**, *90*, 1485–1499, doi:10.1021/ja01008a017.

5. Harrison, J.F. Electronic Structure of Carbenes. I. Methylene, Fluoromethylene, and Difluoromethylene. *J. Am. Chem. Soc.* **1971**, *93*, 4112–4119, doi:10.1021/ja00746a003.

6. Bauschlicher, C.W.; Schaefer, H.F.; Bagus, P.S. Structure and Energetics of Simple Carbenes Methylene, Fluoromethylene, Chloromethylene, Bromomethylene, Difluoromethylene, and Dichloromethylene. *J. Am. Chem. Soc.* **1977**, *99*, 7106–7110, doi:10.1021/ja00464a002.

7. Harrison, J.F.; Liedtke, R.C.; Liebman, J.F. The Multiplicity of Substituted Acyclic Carbenes and Related Molecules. *J. Am. Chem. Soc.* **1979**, *101*, 7162–7168, doi:10.1021/ja00518a006.

8. Baird, N.C.; Taylor, K.F. Multiplicity of the Ground State and Magnitude of the T1-S0 Gap in Substituted Carbenes. *J. Am. Chem. Soc.* **1978**, *100*, 1333–1338, doi:10.1021/ja00473a001.

9. Pauling, L. The Structure of Singlet Carbene Molecules. *J. Chem. Soc. Chem. Commun.* **1980**, 688, doi:10.1039/c39800000688.

10. Schoeller, W.W. When Is a Singlet Carbene Linear? *J. Chem. Soc. Chem. Commun.* **1980**, 124, doi:10.1039/c39800000124.

11. Frontmatter. In *The Organometallic Chemistry of the Transition Metals*; John Wiley & Sons, Inc.: Hoboken, NJ, USA, 2005; pp. i–xiii ISBN 978-0-471-71876-5.

12. Fischer, E.O.; Maasböl, A. On the Existence of a Tungsten Carbonyl Carbene Complex. *Angew. Chem. Int. Ed. Engl.* **1964**, *3*, 580–581, doi:10.1002/anie.196405801.

13. Schrock, R.R. Alkylcarbene Complex of Tantalum by Intramolecular .Alpha.-Hydrogen Abstraction. *J. Am. Chem. Soc.* **1974**, *96*, 6796–6797, doi:10.1021/ja00828a061.

14. Tschugajeff, L.; Skanawy-Grigorjewa, M.; Posnjak, A.; Skanawy-Grigorjewa, M. Über Die Hydrazin-Carbylamin-Komplexe des Platins. *Z. Für Anorg. Allg. Chem.* **1925**, *148*, 37–42, doi:10.1002/zaac.19251480105.

15. Butler, W.M.; Parks, J. Chelative Addition of Hydrazines to Coordinated Isocyanides. The Structure of Chugaev's Red Salt. 7.

16. Stork, J.R.; Olmstead, M.M.; Balch, A.L. Effects of Pt···Pt Bonding, Anions, Solvate Molecules, and Hydrogen Bonding on the Self-Association of Chugaev's Cation, a Platinum Complex with a Chelating Carbene Ligand. *Inorg. Chem.* **2004**, *43*, 7508–7515, doi:10.1021/ic049226j.

17. Wanniarachchi, Y.A.; Slaughter, L.M. One-Step Assembly of a Chiral Palladium Bis(Acyclic Diaminocarbene) Complex and Its Unexpected Oxidation to a Bis(Amidine) Complex. *Chem. Commun.* **2007**, 3294, doi:10.1039/b703769d.

18. Taylor, T.E.; Hall, M.B. Theoretical Comparison between Nucleophilic and Electrophilic Transition Metal Carbenes Using Generalized Molecular Orbital and Configuration Interaction Methods. *J. Am. Chem. Soc.* **1984**, *106*, 1576–1584, doi:10.1021/ja00318a007.

19. Lappert, M.F. The Coordination Chemistry of Electron-Rich Alkenes (Enetetramines). *J. Organomet. Chem.* **1988**, *358*, 185–213, doi:10.1016/0022-328X(88)87079-7.

20. Arduengo, A.J.; Harlow, R.L.; Kline, M. A Stable Crystalline Carbene. *J. Am. Chem. Soc.* **1991**, *113*, 361–363, doi:10.1021/ja00001a054.

21. Wanzlick, H.; Esser, F.; Kleiner, H. Nucleophile Carben-Chemie, III. Neue Verbindungen vom Typ des Bis-[1.3-diphenyl-imidazolidinylidens-(2)]. *Chem. Ber.* **1963**, *96*, 1208–1212, doi:10.1002/cber.19630960505.

22. Wanzlick, H.-W.; Schönherr, H.-J. Direct Synthesis of a Mercury Salt-Carbene Complex. *Angew. Chem. Int. Ed. Engl.* **1968**, *7*, 141–142, doi:10.1002/anie.196801412.

23. Öfele, K. Pentacarbonyl(2,3-Diphenylcyclopropenylidene)-Chromium(0). *Angew. Chem. Int. Ed. Engl.* **1968**, *7*, 950–950, doi:10.1002/anie.196809501.

24. Hopkinson, M.N.; Richter, C.; Schedler, M.; Glorius, F. An Overview of N-Heterocyclic Carbenes. *Nature* **2014**, *510*, 485–496, doi:10.1038/nature13384.

25. Shi, S.; Nolan, S.P.; Szostak, M. Well-Defined Palladium(II)–NHC Precatalysts for Cross-Coupling Reactions of Amides and Esters by Selective N–C/O–C Cleavage. *Acc. Chem. Res.* **2018**, *51*, 2589–2599, doi:10.1021/acs.accounts.8b00410.

26. Monsigny, L.; Kajetanowicz, A.; Grela, K. Ruthenium Complexes Featuring Unsymmetrical N-Heterocyclic Carbene Ligands–Useful Olefin Metathesis Catalysts for Special Tasks. *Chem. Rec.* **2021**, tcr.202100126, doi:10.1002/tcr.202100126.

27. Cheng, L.-J.; Mankad, N.P. Copper-Catalyzed Carbonylative Coupling of Alkyl Halides. *Acc. Chem. Res.* **2021**, *54*, 2261–2274, doi:10.1021/acs.accounts.1c00115.

28. Jain, I.; Malik, P. N-Heterocyclic Carbene Complexes in Ring Opening Polymerization. *Eur. Polym. J.* **2021**, *150*, 110412, doi:10.1016/j.eurpolymj.2021.110412.

29. Huang, C.; Liu, J.; Huang, H.-H.; Ke, Z. Recent Progress in Electro- and Photo-Catalytic CO2 Reduction Using N-Heterocyclic Carbene Transition Metal Complexes. *Polyhedron* **2021**, *203*, 115147, doi:10.1016/j.poly.2021.115147.

30. Hahn, F.E.; Wittenbecher, L.; Boese, R.; Bläser, D. N,N′-Bis(2,2-Dimethylpropyl)Benzimidazolin-2-Ylidene: A Stable Nucleophilic Carbene Derived from Benzimidazole. *Chem. - Eur. J.* **1999**, *5*, 1931–1935, doi:10.1002/(SICI)1521-3765(19990604)5:6<1931::AID-CHEM1931>3.0.CO;2-M.

31. Gridnev, A.A.; Mihaltseva, I.M. Synthesis of 1-Alkylimidazoles. *Synth. Commun.* **1994**, *24*, 1547–1555, doi:10.1080/00397919408010155.

32. Herrmann, W.A. N-Heterocyclic Carbenes: A New Concept in Organometallic Catalysis. *Angew Chem Int Ed* **2002**, 20.

33. de Frémont, P.; Marion, N.; Nolan, S.P. Carbenes: Synthesis, Properties, and Organometallic Chemistry. *Coord. Chem. Rev.* **2009**, *253*, 862–892, doi:10.1016/j.ccr.2008.05.018.

34. A Patil, S.; P Hoagland, A.; A Patil, S.; Bugarin, A. *N* -Heterocyclic Carbene-Metal Complexes as Bio-Organometallic Antimicrobial and Anticancer Drugs, an Update (2015–2020). *Future Med. Chem.* **2020**, *12*, 2239–2275, doi:10.4155/fmc-2020-0175.

35. Mercs, L.; Albrecht, M. Beyond Catalysis: N-Heterocyclic Carbene Complexes as Components for Medicinal, Luminescent, and Functional Materials Applications. *Chem. Soc. Rev.* **2010**, *39*, 1903, doi:10.1039/b902238b.

36. Ott, I. Medicinal Chemistry of Metal N-Heterocyclic Carbene (NHC) Complexes. In *Inorganic and Organometallic Transition Metal Complexes with Biological Molecules and Living Cells*; Elsevier, 2017; pp. 147–179 ISBN 978-0-12-803814-7.

37. Wang, Y.; Chang, J.-P.; Xu, R.; Bai, S.; Wang, D.; Yang, G.-P.; Sun, L.-Y.; Li, P.; Han, Y.-F. N-Heterocyclic Carbenes and Their Precursors in Functionalised Porous Materials. *Chem. Soc. Rev.* **2021**, 10.1039.D1CS00296A, doi:10.1039/D1CS00296A.

38. Voloshkin, V.A.; Tzouras, N.V.; Nolan, S.P. Recent Advances in the Synthesis and Derivatization of N-Heterocyclic Carbene Metal Complexes. *Dalton Trans.* **2021**, *50*, 12058–12068, doi:10.1039/D1DT01847G.

39. Lee, M.-T.; Hu, C.-H. Density Functional Study of *N*- Heterocyclic and Diamino Carbene Complexes: Comparison with Phosphines. *Organometallics* **2004**, *23*, 976–983, doi:10.1021/om0341451.

40. Dorta, R.; Stevens, E.D.; Scott, N.M.; Costabile, C.; Cavallo, L.; Hoff, C.D.; Nolan, S.P. Steric and Electronic Properties of N-Heterocyclic Carbenes (NHC): A Detailed Study on Their Interaction with Ni(CO) $_4$. *J. Am. Chem. Soc.* **2005**, *127*, 2485–2495, doi:10.1021/ja0438821.

41. Trnka, T.M.; Grubbs, R.H. The Development of L $_2$ X $_2$ RuCHR Olefin Metathesis Catalysts: An Organometallic Success Story. *Acc. Chem. Res.* **2001**, *34*, 18–29, doi:10.1021/ar000114f.

42. Díez-González, S.; Nolan, S.P. Stereoelectronic Parameters Associated with N-Heterocyclic Carbene (NHC) Ligands: A Quest for Understanding. *Coord. Chem. Rev.* **2007**, *251*, 874–883, doi:10.1016/j.ccr.2006.10.004.

43. Jacobsen, H.; Correa, A.; Poater, A.; Costabile, C.; Cavallo, L. Understanding the M(NHC) (NHC=N-Heterocyclic Carbene) Bond. *Coord. Chem. Rev.* **2009**, *253*, 687–703, doi:10.1016/j.ccr.2008.06.006.

44. Wang, H.M.J.; Lin, I.J.B. Facile Synthesis of Silver(I)−Carbene Complexes. Useful Carbene Transfer Agents. *Organometallics* **1998**, *17*, 972–975, doi:10.1021/om9709704.

45. Collado, A.; Gomez-Suarez, A.; Martin, A.R.; Slawin, A.M.Z.; Nolan, S.P. Straightforward Synthesis of [Au(NHC)X] (NHC = N-Heterocyclic Carbene, X = Cl, Br, I) Complexes. **2013**, 3.

46. Visbal, R.; Laguna, A.; Gimeno, M.C. Simple and Efficient Synthesis of [MCI(NHC)] (M = Au, Ag) Complexes. **2013**, 3.

47. Martynova, E.A.; Tzouras, N.V.; Pisano, G.; Cazin, C.S.J.; Nolan, S.P. The '"Weak Base Route"' Leading to Transition Metal–N-Heterocyclic Carbene Complexes. **2021**, 21.

48. Russell, A.D.; Hugo, W.B. 7 Antimicrobial Activity and Action of Silver. In *Progress in Medicinal Chemistry*; Elsevier, 1994; Vol. 31, pp. 351–370 ISBN 978-0-444-81807-2.

49. Klasen, H.J. A Historical Review of the Use of Silver in the Treatment of Burns. II. Renewed Interest for Silver. *Burns* **2000**, *26*, 131–138, doi:10.1016/S0305-4179(99)00116-3.

50. Lansdown, A.B. A Review of the Use of Silver in Wound Care: Facts and Fallacies. *Br. J. Nurs.* **2004**, *13*, S6–S19, doi:10.12968/bjon.2004.13.Sup1.12535.

51. Melaiye, A.; Simons, R.S.; Milsted, A.; Pingitore, F.; Wesdemiotis, C.; Tessier, C.A.; Youngs, W.J. Formation of Water-Soluble Pincer Silver(I)−Carbene Complexes: A Novel Antimicrobial Agent. *J. Med. Chem.* **2004**, *47*, 973–977, doi:10.1021/jm030262m.

52. Melaiye, A.; Sun, Z.; Hindi, K.; Milsted, A.; Ely, D.; Reneker, D.H.; Tessier, C.A.; Youngs, W.J. Silver(I)−Imidazole Cyclophane *Gem* -Diol Complexes Encapsulated by Electrospun Tecophilic Nanofibers: Formation of Nanosilver Particles and Antimicrobial Activity. *J. Am. Chem. Soc.* **2005**, *127*, 2285–2291, doi:10.1021/ja040226s.

53. Kascatan-Nebioglu, A.; Melaiye, A.; Hindi, K.; Durmus, S.; Panzner, M.J.; Hogue, L.A.; Mallett, R.J.; Hovis, C.E.; Coughenour, M.; Crosby, S.D.; et al. Synthesis from Caffeine of a Mixed *N* -Heterocyclic Carbene−Silver Acetate Complex Active against Resistant Respiratory Pathogens. *J. Med. Chem.* **2006**, *49*, 6811–6818, doi:10.1021/jm060711t.

54. Hindi, K.M.; Siciliano, T.J.; Durmus, S.; Panzner, M.J.; Medvetz, D.A.; Reddy, D.V.; Hogue, L.A.; Hovis, C.E.; Hilliard, J.K.; Mallet, R.J.; et al. Synthesis, Stability, and Antimicrobial Studies of Electronically Tuned Silver Acetate *N* -Heterocyclic Carbenes. *J. Med. Chem.* **2008**, *51*, 1577–1583, doi:10.1021/jm0708679.

55. Panzner, M.J.; Deeraksa, A.; Smith, A.; Wright, B.D.; Hindi, K.M.; Kascatan-Nebioglu, A.; Torres, A.G.; Judy, B.M.; Hovis, C.E.; Hilliard, J.K.; et al. Synthesis and in Vitro Efficacy Studies of Silver Carbene Complexes on Biosafety Level 3 Bacteria. *Eur. J. Inorg. Chem.* **2009**, *2009*, 1739–1745, doi:10.1002/ejic.200801159.

56. Patil, S.; Dietrich, K.; Deally, A.; Gleeson, B.; Müller-Bunz, H.; Paradisi, F.; Tacke, M. Synthesis, Cytotoxicity and Antibacterial Studies of Novel Symmetrically and Nonsymmetrically 4-(Methoxycarbonyl)Benzyl-Substituted N-Heterocyclic Carbene-Silver Acetate Complexes. *Helv. Chim. Acta* **2010**, *93*, 2347–2364, doi:10.1002/hlca.201000310.

57. Patil, S.; Deally, A.; Gleeson, B.; Müller-Bunz, H.; Paradisi, F.; Tacke, M. Synthesis, Cytotoxicity and Antibacterial Studies of Symmetrically and Non-Symmetrically Benzyl- or p-Cyanobenzyl-Substituted N-Heterocyclic Carbene-Silver Complexes. *Appl. Organomet. Chem.* **2010**, *24*, 781–793, doi:10.1002/aoc.1702.

58. Patil, S.; Claffey, J.; Deally, A.; Hogan, M.; Gleeson, B.; Menéndez Méndez, L.M.; Müller-Bunz, H.; Paradisi, F.; Tacke, M. Synthesis, Cytotoxicity and Antibacterial Studies of *p* -Methoxybenzyl-Substituted and Benzyl-Substituted N-Heterocyclic Carbene–Silver Complexes. *Eur. J. Inorg. Chem.* **2010**, *2010*, 1020–1031, doi:10.1002/ejic.200900889.

59. Patil, S.; Deally, A.; Gleeson, B.; Müller-Bunz, H.; Paradisi, F.; Tacke, M. Novel Benzyl-Substituted N-Heterocyclic Carbene–Silver Acetate Complexes: Synthesis, Cytotoxicity and Antibacterial Studies. *Metallomics* **2011**, *3*, 74–88, doi:10.1039/C0MT00034E.

60. Hackenberg, F.; Lally, G.; Müller-Bunz, H.; Paradisi, F.; Quaglia, D.; Streciwilk, W.; Tacke, M. Novel Symmetrically P-Benzyl-Substituted 4,5-Diaryl-Imidazole N-Heterocyclic Carbene-Silver(I) Acetate Complexes – Synthesis and Biological Evaluation. *J. Organomet. Chem.* **2012**, *717*, 123–134, doi:10.1016/j.jorganchem.2012.07.006.

61. Patil, S.A.; Patil, S.A.; Patil, R.; Keri, R.S.; Budagumpi, S.; Balakrishna, G.R.; Tacke, M. *N* -Heterocyclic Carbene Metal Complexes as Bio-Organometallic Antimicrobial and Anticancer Drugs. *Future Med. Chem.* **2015**, *7*, 1305–1333, doi:10.4155/fmc.15.61.

62. Hussaini, S.Y.; Haque, R.A.; Razali, M.R. Recent Progress in Silver(I)-, Gold(I)/(III)- and Palladium(II)-N-Heterocyclic Carbene Complexes: A Review towards Biological Perspectives. *J. Organomet. Chem.* **2019**, *882*, 96–111, doi:10.1016/j.jorganchem.2019.01.003.

63. Berners-Price, S.J.; Johnson, R.K.; Giovenella, A.J.; Faucette, L.F.; Mirabelli, C.K.; Sadler, P.J. Antimicrobial and Anticancer Activity of Tetrahedral, Chelated, Diphosphine Silver(I) Complexes: Comparison with Copper and Gold. *J. Inorg. Biochem.* **1988**, *33*, 285–295, doi:10.1016/0162-0134(88)80007-2.

64. Liu, J.J.; Galettis, P.; Farr, A.; Maharaj, L.; Samarasinha, H.; McGechan, A.C.; Baguley, B.C.; Bowen, R.J.; Berners-Price, S.J.; McKeage, M.J. In Vitro Antitumour and Hepatotoxicity Profiles of Au(I) and Ag(I) Bidentate Pyridyl Phosphine Complexes and Relationships to Cellular Uptake. *J. Inorg. Biochem.* **2008**, *102*, 303–310, doi:10.1016/j.jinorgbio.2007.09.003.

65. Barnard, P.J.; Baker, M.V.; Berners-Price, S.J.; Day, D.A. Mitochondrial Permeability Transition Induced by Dinuclear Gold(I)–Carbene Complexes: Potential New Antimitochondrial Antitumour Agents. *J. Inorg. Biochem.* **2004**, *98*, 1642–1647, doi:10.1016/j.jinorgbio.2004.05.011.

66. Ray, S.; Mohan, R.; Singh, J.K.; Samantaray, M.K.; Shaikh, M.M.; Panda, D.; Ghosh, P. Anticancer and Antimicrobial Metallopharmaceutical Agents Based on Palladium, Gold, and Silver N-Heterocyclic Carbene Complexes. *J. Am. Chem. Soc.* **2007**, *129*, 15042–15053, doi:10.1021/ja075889z.

67. Medvetz, D.A.; Hindi, K.M.; Panzner, M.J.; Ditto, A.J.; Yun, Y.H.; Youngs, W.J. Anticancer Activity of Ag(I) N-Heterocyclic Carbene Complexes Derived from 4,5-Dichloro-1H-Imidazole. *Met.-Based Drugs* **2008**, *2008*, 1–7, doi:10.1155/2008/384010.

68. Patil, S.; Deally, A.; Hackenberg, F.; Kaps, L.; Müller-Bunz, H.; Schobert, R.; Tacke, M. Novel Benzyl- or 4-Cyanobenzyl-Substituted N-Heterocyclic (Bromo)(Carbene)Silver(I) and (Carbene)(Chloro)Gold(I) Complexes: Synthesis and Preliminary Cytotoxicity Studies. *Helv. Chim. Acta* **2011**, *94*, 1551–1562, doi:10.1002/hlca.201100107.

69. Teyssot, M.-L.; Jarrousse, A.-S.; Manin, M.; Chevry, A.; Roche, S.; Norre, F.; Beaudoin, C.; Morel, L.; Boyer, D.; Mahiou, R.; et al. Metal-NHC Complexes: A Survey of Anti-Cancer Properties. *Dalton Trans.* **2009**, 6894, doi:10.1039/b906308k.

70. Yaşar, Ş.; Köprülü, T.K.; Tekin, Ş.; Yaşar, S. Sulfonated *N* -heterocyclic Carbine-silver (I) Complexes: Synthesis, Characterisation and Biological Evaluation. *Appl. Organomet. Chem.* **2018**, *32*, doi:10.1002/aoc.4016.

71. Budagumpi, S.; Haque, R.A.; Endud, S.; Rehman, G.U.; Salman, A.W. Biologically Relevant Silver(I)–N-Heterocyclic Carbene Complexes: Synthesis, Structure, Intramolecular Interactions, and Applications. *Eur. J. Inorg. Chem.* **2013**, *2013*, 4367–4388, doi:10.1002/ejic.201300483.

72. Mohamed, H.A.; Khuphe, M.; Boardman, S.J.; Shepherd, S.; Phillips, R.M.; Thornton, P.D.; Willans, C.E. Polymer Encapsulation of Anticancer Silver–N-Heterocyclic Carbene Complexes. *RSC Adv.* **2018**, *8*, 10474–10477, doi:10.1039/C8RA00450A.

73. Ramírez, J.; Corberán, R.; Sanaú, M.; Peris, E.; Fernandez, E. Unprecedented Use of Silver(i) N-Heterocyclic Carbene Complexes for the Catalytic Preparation of 1,2-Bis(Boronate) Esters. *Chem. Commun.* **2005**, 3056, doi:10.1039/b503239c.

74. Iglesias-Sigüenza, J.; Ros, A.; Díez, E.; Magriz, A.; Vázquez, A.; Álvarez, E.; Fernández, R.; Lassaletta, J.M. C2-Symmetric S/C/S Ligands Based on N-Heterocyclic Carbenes: A New Ligand Architecture for Asymmetric Catalysis. *Dalton Trans.* **2009**, 8485, doi:10.1039/b910846g.

75. Johansson, M.J.; Gorin, D.J.; Staben, S.T.; Toste, F.D. Gold(I)-Catalyzed Stereoselective Olefin Cyclopropanation. *J. Am. Chem. Soc.* **2005**, *127*, 18002–18003, doi:10.1021/ja0552500.

76. Aktaş, A.; Celepci, D.B.; Gök, Y.; Aygün, M. 2-Hydroxyethyl-Substituted (NHC)Pd(II)PPh $_3$ Complexes: Synthesis, Characterization, Crystal Structure and Its Application on Sonogashira Cross-Coupling Reactions in Aqueous Media. *ChemistrySelect* **2018**, *3*, 10932–10937, doi:10.1002/slct.201802519.

77. Wang, Y.; Peng, F.; Zhang, H.; Shao, Z. Organocatalytic Synthesis of Terminal Propargylamine Derivatives by Tandem Amination-Alkynylation. *Synlett* **2009**, *2009*, 3287–3290, doi:10.1055/s-0029-1218354.

78. Peshkov, V.A.; Pereshivko, O.P.; Van der Eycken, E.V. A Walk around the A3-Coupling. *Chem. Soc. Rev.* **2012**, *41*, 3790, doi:10.1039/c2cs15356d.

79. Wei, C.; Li, Z.; Li, C.-J. The First Silver-Catalyzed Three-Component Coupling of Aldehyde, Alkyne, and Amine. *Org. Lett.* **2003**, *5*, 4473–4475, doi:10.1021/ol035781y.

80. Li, P.; Wang, L.; Zhang, Y.; Wang, M. Highly Efficient Three-Component (Aldehyde–Alkyne–Amine) Coupling Reactions Catalyzed by a Reusable PS-Supported NHC–Ag(I) under Solvent-Free Reaction Conditions. *Tetrahedron Lett.* **2008**, *49*, 6650–6654, doi:10.1016/j.tetlet.2008.09.026.

81. Li, Y.; Chen, X.; Song, Y.; Fang, L.; Zou, G. Well-Defined N-Heterocyclic Carbene Silver Halides of 1-Cyclohexyl-3-Arylmethylimidazolylidenes: Synthesis, Structure and Catalysis in A3-Reaction of Aldehydes, Amines and Alkynes. *Dalton Trans.* **2011**, *40*, 2046, doi:10.1039/c0dt01074j.

82. Cheng, C.-H.; Chen, D.-F.; Song, H.-B.; Tang, L.-F. Synthesis and Catalytic Activity of N-Heterocyclic Carbene Silver Complexes Derived from 1-[2-(Pyrazol-1-Yl)Phenyl]Imidazole. *J. Organomet. Chem.* **2013**, *726*, 1–8, doi:10.1016/j.jorganchem.2012.12.008.

83. Higby, G.J. Gold in Medicine: A Review of Its Use in the West before 1900. *Gold Bull.* **1982**, *15*, 130–140, doi:10.1007/BF03214618.

84. Parish, R.V. Gold in Medicine - Chrysotherapy. *Interdiscip. Sci. Rev.* **1992**, *17*, 221–228, doi:10.1179/isr.1992.17.3.221.

85. Merchant, B. Gold, the Noble Metal and the Paradoxes of Its Toxicology. *Biologicals* **1998**, *26*, 49–59, doi:10.1006/biol.1997.0123.

86. Berners-Price, S.J.; Filipovska, A. Gold Compounds as Therapeutic Agents for Human Diseases. *Metallomics* **2011**, *3*, 863, doi:10.1039/c1mt00062d.

87. Nobili, S.; Mini, E.; Landini, I.; Gabbiani, C.; Casini, A.; Messori, L. Gold Compounds as Anticancer Agents: Chemistry, Cellular Pharmacology, and Preclinical Studies: GOLD COMPOUNDS AS ANTICANCER AGENTS. *Med. Res. Rev.* **2010**, *30*, 550–580, doi:10.1002/med.20168.

88. Shaw, C.F. Gold-Based Therapeutic Agents. *Chem. Rev.* **1999**, *99*, 2589–2600, doi:10.1021/cr980431o.

89. Wenzel, M.; Casini, A. Mass Spectrometry as a Powerful Tool to Study Therapeutic Metallodrugs Speciation Mechanisms: Current Frontiers and Perspectives. *Coord. Chem. Rev.* **2017**, *352*, 432–460, doi:10.1016/j.ccr.2017.02.012.

90. Özdemir, İ.; Denizci, A.; Öztürk, H.T.; Çetinkaya, B. Synthetic and Antimicrobial Studies on New Gold(I) Complexes of Imidazolidin-2-Ylidenes. *Appl. Organomet. Chem.* **2004**, *18*, 318–322, doi:10.1002/aoc.668.

91. Özdemir, İ.; Temelli, N.; Günal, S.; Demir, S. Gold(I) Complexes of N-Heterocyclic Carbene Ligands Containing Benzimidazole: Synthesis and Antimicrobial Activity. *Molecules* **2010**, *15*, 2203–2210, doi:10.3390/molecules15042203.

92. Owings, J.P.; McNair, N.N.; Mui, Y.F.; Gustafsson, T.N.; Holmgren, A.; Contel, M.; Goldberg, J.B.; Mead, J.R. Auranofin and *N*- Heterocyclic Carbene Gold-Analogs Are Potent Inhibitors of the Bacteria *Helicobacter Pylori*. *FEMS Microbiol. Lett.* **2016**, *363*, fnw148, doi:10.1093/femsle/fnw148.

93. Mora, M.; Gimeno, M.C.; Visbal, R. Recent Advances in Gold–NHC Complexes with Biological Properties. *Chem. Soc. Rev.* **2019**, *48*, 447–462, doi:10.1039/C8CS00570B.

94. Wang, D.; Lippard, S.J. Cellular Processing of Platinum Anticancer Drugs. *Nat. Rev. Drug Discov.* **2005**, *4*, 307–320, doi:10.1038/nrd1691.

95. Berners-Price, S.J.; Sadler, P.J. Phosphines and Metal Phosphine Complexes: Relationship of Chemistry to Anticancer and Other Biological Activity. In *Bioinorganic Chemistry*; Structure and Bonding; Springer Berlin Heidelberg: Berlin, Heidelberg, 1988; Vol. 70, pp. 27–102 ISBN 978-3-540-50130-5.

96. Berners-Price, S.J.; Girard, G.R.; Hill, D.T.; Sutton, B.M.; Jarrett, P.S.; Faucette, L.F.; Johnson, R.K.; Mirabelli, C.K.; Sadler, P.J. Cytotoxicity and Antitumor Activity of Some Tetrahedral Bis(Diphosphino)Gold(I) Chelates. *J. Med. Chem.* **1990**, *33*, 1386–1392, doi:10.1021/jm00167a017.

97. Gromer, S.; Urig, S.; Becker, K. The Thioredoxin System?From Science to Clinic. *Med. Res. Rev.* **2004**, *24*, 40–89, doi:10.1002/med.10051.

98. Hickey, J.L.; Ruhayel, R.A.; Barnard, P.J.; Baker, M.V.; Berners-Price, S.J.; Filipovska, A. Mitochondria-Targeted Chemotherapeutics: The Rational Design of Gold(I) *N* -Heterocyclic Carbene Complexes That Are Selectively Toxic to Cancer Cells and Target Protein Selenols in Preference to Thiols. *J. Am. Chem. Soc.* **2008**, *130*, 12570–12571, doi:10.1021/ja804027j.

99. Pratesi, A.; Gabbiani, C.; Michelucci, E.; Ginanneschi, M.; Papini, A.M.; Rubbiani, R.; Ott, I.; Messori, L. Insights on the Mechanism of Thioredoxin Reductase Inhibition by Gold N-Heterocyclic Carbene Compounds Using the Synthetic Linear Selenocysteine Containing C-Terminal Peptide HTrxR(488-499): An ESI-MS Investigation. *J. Inorg. Biochem.* **2014**, *136*, 161–169, doi:10.1016/j.jinorgbio.2014.01.009.

100. Cheng, X.; Holenya, P.; Can, S.; Alborzinia, H.; Rubbiani, R.; Ott, I.; Wölfl, S. A TrxR Inhibiting Gold(I) NHC Complex Induces Apoptosis through ASK1-P38-MAPK Signaling in Pancreatic Cancer Cells. *Mol. Cancer* **2014**, *13*, 221, doi:10.1186/1476-4598-13-221.

101. Seliman, A.A.A.; Altaf, M.; Onawole, A.T.; Ahmad, S.; Ahmed, M.Y.; Al-Saadi, A.A.; Altuwaijri, S.; Bhatia, G.; Singh, J.; Isab, A.A. Synthesis, X-Ray Structures and Anticancer Activity of Gold(I)-Carbene Complexes with Selenones as Co-Ligands and Their Molecular Docking Studies with Thioredoxin Reductase. *J. Organomet. Chem.* **2017**, *848*, 175–183, doi:10.1016/j.jorganchem.2017.07.034.

102. Bertrand, B.; Stefan, L.; Pirrotta, M.; Monchaud, D.; Bodio, E.; Richard, P.; Le Gendre, P.; Warmerdam, E.; de Jager, M.H.; Groothuis, G.M.M.; et al. Caffeine-Based Gold(I) *N* -Heterocyclic Carbenes as Possible Anticancer Agents: Synthesis and Biological Properties. *Inorg. Chem.* **2014**, *53*, 2296–2303, doi:10.1021/ic403011h.

103. Karaca, Ö.; Scalcon, V.; Meier-Menches, S.M.; Bonsignore, R.; Brouwer, J.M.J.L.; Tonolo, F.; Folda, A.; Rigobello, M.P.; Kühn, F.E.; Casini, A. Characterization of Hydrophilic Gold(I) N-Heterocyclic Carbene (NHC) Complexes as Potent TrxR Inhibitors Using Biochemical and Mass Spectrometric Approaches. *Inorg. Chem.* **2017**, *56*, 14237–14250, doi:10.1021/acs.inorgchem.7b02345.

104. Hashmi, A.S.K. Gold-Catalyzed Organic Reactions. *Chem. Rev.* **2007**, *107*, 3180–3211, doi:10.1021/cr000436x.

105. Hashmi, A.S.K.; Hutchings, G.J. Gold Catalysis. *Angew. Chem. Int. Ed.* **2006**, *45*, 7896–7936, doi:10.1002/anie.200602454.

106. Ciriminna, R.; Falletta, E.; Della Pina, C.; Teles, J.H.; Pagliaro, M. Industrial Applications of Gold Catalysis. *Angew. Chem. Int. Ed.* **2016**, *55*, 14210–14217, doi:10.1002/anie.201604656.

107. Marion, N.; Nolan, S.P. N-Heterocyclic Carbenes in Gold Catalysis. *Chem. Soc. Rev.* **2008**, *37*, 1776, doi:10.1039/b711132k.

108. Schneider, S.K.; Herrmann, W.A.; Herdtweck, E. Synthesis of the First Gold(I) Carbene Complex with a Gold-Oxygen Bond— First Catalytic Application of Gold(I) Complexes BearingN-Heterocyclic Carbenes. *Z. Für Anorg. Allg. Chem.* **2003**, *629*, 2363–2370, doi:10.1002/zaac.200300247.

109. Gatto, M.; Del Zotto, A.; Segato, J.; Zuccaccia, D. Hydration of Alkynes Catalyzed by L–Au–X under Solvent- and Acid-Free Conditions: New Insights into an Efficient, General, and Green Methodology. *Organometallics* **2018**, *37*, 4685–4691, doi:10.1021/acs.organomet.8b00689.

110. Gatto, M.; Belanzoni, P.; Belpassi, L.; Biasiolo, L.; Del Zotto, A.; Tarantelli, F.; Zuccaccia, D. Solvent-, Silver-, and Acid-Free NHC-Au-X Catalyzed Hydration of Alkynes. The Pivotal Role of the Counterion. *ACS Catal.* **2016**, *6*, 7363–7376, doi:10.1021/acscatal.6b01626.

111. Gatto, M.; Baratta, W.; Belanzoni, P.; Belpassi, L.; Del Zotto, A.; Tarantelli, F.; Zuccaccia, D. Hydration and Alkoxylation of Alkynes Catalyzed by NHC–Au–OTf. *Green Chem.* **2018**, *20*, 2125–2134, doi:10.1039/C8GC00508G.

112. Biasiolo, L.; Del Zotto, A.; Zuccaccia, D. Toward Optimizing the Performance of Homogeneous L-Au-X Catalysts through Appropriate Matching of the Ligand (L) and Counterion (X^-). *Organometallics* **2015**, *34*, 1759–1765, doi:10.1021/acs.organomet.5b00308.

113. Fernández, G.A.; Chopa, A.B.; Silbestri, G.F. A Structure/Catalytic Activity Study of Gold(I)–NHC Complexes, as Well as Their Recyclability and Reusability, in the Hydration of Alkynes in Aqueous Medium. *Catal. Sci. Technol.* **2016**, *6*, 1921–1929, doi:10.1039/C5CY01278C.

114. Liu, X.-Y.; Ding, P.; Huang, J.-S.; Che, C.-M. Synthesis of Substituted 1,2-Dihydroquinolines and Quinolines from Aromatic Amines and Alkynes by Gold(I)-Catalyzed Tandem Hydroamination−Hydroarylation under Microwave-Assisted Conditions. *Org. Lett.* **2007**, *9*, 2645–2648, doi:10.1021/ol070814l.

115. Lavallo, V.; Frey, G.D.; Donnadieu, B.; Soleilhavoup, M.; Bertrand, G. Homogeneous Catalytic Hydroamination of Alkynes and Allenes with Ammonia. *Angew. Chem. Int. Ed.* **2008**, *47*, 5224–5228, doi:10.1002/anie.200801136.

116. Katari, M.; Rao, M.N.; Rajaraman, G.; Ghosh, P. Computational Insight into a Gold(I) N-Heterocyclic Carbene Mediated Alkyne Hydroamination Reaction. *Inorg. Chem.* **2012**, *51*, 5593–5604, doi:10.1021/ic2024605.

117. Dash, C.; Shaikh, M.M.; Butcher, R.J.; Ghosh, P. Highly Convenient Regioselective Intermolecular Hydroamination of Alkynes Yielding Ketimines Catalyzed by Gold(I) Complexes of 1,2,4-Triazole Based N-Heterocyclic Carbenes. *Inorg. Chem.* **2010**, *49*, 4972–4983, doi:10.1021/ic100087d.

118. Baron, M.; Battistel, E.; Tubaro, C.; Biffis, A.; Armelao, L.; Rancan, M.; Graiff, C. Single-Step Synthesis of Dinuclear Neutral Gold(I) Complexes with Bridging Di(N-Heterocyclic Carbene) Ligands and Their Catalytic Performance in Cross Coupling Reactions and Alkyne Hydroamination. *Organometallics* **2018**, *37*, 4213–4223, doi:10.1021/acs.organomet.8b00531.

119. Wei, C.; Li, C.-J. A Highly Efficient Three-Component Coupling of Aldehyde, Alkyne, and Amines via C−H Activation Catalyzed by Gold in Water. *J. Am. Chem. Soc.* **2003**, *125*, 9584–9585, doi:10.1021/ja0359299.

120. Price, G.A.; Brisdon, A.K.; Flower, K.R.; Pritchard, R.G.; Quayle, P. Solvent Effects in Gold-Catalysed A3-Coupling Reactions. *Tetrahedron Lett.* **2014**, *55*, 151–154, doi:10.1016/j.tetlet.2013.10.141.

121. Price, G.A.; Brisdon, A.K.; Randall, S.; Lewis, E.; Whittaker, D.M.; Pritchard, R.G.; Muryn, C.A.; Flower, K.R.; Quayle, P. Some Insights into the Gold-Catalysed A 3 -Coupling Reaction. *J. Organomet. Chem.* **2017**, *846*, 251–262, doi:10.1016/j.jorganchem.2017.06.019.

122. Torregrosa, R.; Pastor, I.M.; Yus, M. Solvent-Free Direct Regioselective Ring Opening of Epoxides with Imidazoles. *Tetrahedron* **2007**, *63*, 469–473, doi:10.1016/j.tet.2006.10.055.

123. Arnold, P.L.; Liddle, S.T. F-Block N-Heterocyclic Carbene Complexes. *Chem. Commun.* **2006**, 3959, doi:10.1039/b606829d.

124. Arnold, P.L.; Rodden, M.; Davis, K.M.; Scarisbrick, A.C.; Blake, A.J.; Wilson, C. Asymmetric Lithium(i) and Copper(Ii) Alkoxy-N-Heterocyclic Carbene Complexes; Crystallographic Characterisation and Lewis Acid CatalysisElectronic Supplementary Information (ESI) Available: Full Synthetic and Structural Details. See Http://Www.Rsc.Org/Suppdata/Cc/B4/B404614e/. *Chem. Commun.* **2004**, 1612, doi:10.1039/b404614e.

125. Scattolin, T.; Caligiuri, I.; Canovese, L.; Demitri, N.; Gambari, R.; Lampronti, I.; Rizzolio, F.; Santo, C.; Visentin, F. Synthesis of New Allyl Palladium Complexes Bearing Purine-Based NHC Ligands with Antiproliferative and Proapoptotic Activities on Human Ovarian Cancer Cell Lines. *Dalton Trans.* **2018**, *47*, 13616–13630, doi:10.1039/C8DT01831F.

126. Napoli, M.; Saturnino, C.; Cianciulli, E.I.; Varcamonti, M.; Zanfardino, A.; Tommonaro, G.; Longo, P. Silver(I) N-Heterocyclic Carbene Complexes: Synthesis, Characterization and Antibacterial Activity. *J. Organomet. Chem.* **2013**, *725*, 46–53, doi:10.1016/j.jorganchem.2012.10.040.

127. Mariconda, A.; Grisi, F.; Costabile, C.; Falcone, S.; Bertolasi, V.; Longo, P. Synthesis, Characterization and Catalytic Behaviour of a Palladium Complex Bearing a Hydroxy-Functionalized N-Heterocyclic Carbene Ligand. *New J Chem* **2014**, *38*, 762–769, doi:10.1039/C3NJ01281F.

128. Saturnino, C.; Barone, I.; Iacopetta, D.; Mariconda, A.; Sinicropi, M.S.; Rosano, C.; Campana, A.; Catalano, S.; Longo, P.; Andò, S. *N* -Heterocyclic Carbene Complexes of Silver and Gold as Novel Tools against Breast Cancer Progression. *Future Med. Chem.* **2016**, *8*, 2213–2229, doi:10.4155/fmc-2016-0160.

129. Iacopetta, D.; Mariconda, A.; Saturnino, C.; Caruso, A.; Palma, G.; Ceramella, J.; Muià, N.; Perri, M.; Sinicropi, M.S.; Caroleo, M.C.; et al. Novel Gold and Silver Carbene Complexes Exert Antitumor Effects Triggering the Reactive Oxygen Species Dependent Intrinsic Apoptotic Pathway. *ChemMedChem* **2017**, *12*, 2054–2065, doi:10.1002/cmdc.201700634.

130. Mariconda, A.; Sirignano, M.; Costabile, C.; Longo, P. New NHC- Silver and Gold Complexes Active in A3-Coupling (Aldehyde-Alkyne-Amine) Reaction. *Mol. Catal.* **2020**, *480*, 110570, doi:10.1016/j.mcat.2019.110570.

131. Bartoszewicz, A.; Marcos, R.; Sahoo, S.; Inge, A.K.; Zou, X.; Martín-Matute, B. A Highly Active Bifunctional Iridium Complex with an Alcohol/Alkoxide-Tethered N-Heterocyclic Carbene for Alkylation of Amines with Alcohols. *Chem. - Eur. J.* **2012**, *18*, 14510–14519, doi:10.1002/chem.201201845.

132. Costabile, C.; Mariconda, A.; Sirignano, M.; Crispini, A.; Scarpelli, F.; Longo, P. A Green Approach for A ^{3} -Coupling Reactions: An Experimental and Theoretical Study on NHC Silver and Gold Catalysts. *New J. Chem.* **2021**, *45*, 18509–18517, doi:10.1039/D1NJ03444H.

133. Erdemir, F.; Barut Celepci, D.; Aktaş, A.; Taslimi, P.; Gök, Y.; Karabıyık, H.; Gülçin, İ. 2-Hydroxyethyl Substituted NHC Precursors: Synthesis, Characterization, Crystal Structure and Carbonic Anhydrase, α-Glycosidase, Butyrylcholinesterase, and Acetylcholinesterase Inhibitory Properties. *J. Mol. Struct.* **2018**, *1155*, 797–806, doi:10.1016/j.molstruc.2017.11.079.

134. Yaşar, Ş.; Köprülü, T.K.; Tekin, Ş.; Yaşar, S. Synthesis, Characterisation and Cytotoxic Properties of N -Heterocyclic Carbene Silver(I) Complexes. *Inorganica Chim. Acta* **2018**, *479*, 17–23, doi:10.1016/j.ica.2018.04.035.

135. Bocchino, C.; Napoli, M.; Costabile, C.; Longo, P. Synthesis of Octahedral Zirconium Complex Bearing [NHC◎O] Ligands, and Its Behavior as Catalyst in the Polymerization of Olefins: Synthesis and Characterization of Zr Complex. *J. Polym. Sci. Part Polym. Chem.* **2011**, *49*, 862–870, doi:10.1002/pola.24495.

136. Sirignano, M.; Mariconda, A.; Vigliotta, G.; Ceramella, J.; Iacopetta, D.; Sinicropi, M.S.; Longo, P. Catalytic and Biological Activity of Silver and Gold Complexes Stabilized by NHC with Hydroxy Derivatives on Nitrogen Atoms. **2022**, 14.

137. Valdés, H.; Canseco-González, D.; Germán-Acacio, J.M.; Morales-Morales, D. Xanthine Based N-Heterocyclic Carbene (NHC) Complexes. *J. Organomet. Chem.* **2018**, *867*, 51–54, doi:10.1016/j.jorganchem.2018.01.008.

138. Hayes, J.M.; Viciano, M.; Peris, E.; Ujaque, G.; Lledós, A. Mechanism of Formation of Silver *N* -Heterocyclic Carbenes Using Silver Oxide: A Theoretical Study. *Organometallics* **2007**, *26*, 6170–6183, doi:10.1021/om700898d.

139. Mohamed, H.A.; Lake, B.R.M.; Laing, T.; Phillips, R.M.; Willans, C.E. Synthesis and Anticancer Activity of Silver(I)–N-Heterocyclic Carbene Complexes Derived from the Natural Xanthine Products Caffeine, Theophylline and Theobromine. *Dalton Trans.* **2015**, *44*, 7563–7569, doi:10.1039/C4DT03679D.

140. Atif, M.; Bhatti, H.N.; Haque, R.A.; Iqbal, M.A.; Ahamed Khadeer, M.B.; Majid, A.M.S.A. Synthesis, Structure, and Anticancer Activity of Symmetrical and Non-Symmetrical Silver(I)-N-Heterocyclic Carbene Complexes. *Appl. Biochem. Biotechnol.* **2020**, *191*, 1171–1189, doi:10.1007/s12010-019-03186-9.

141. Garrison, J.C.; Youngs, W.J. Ag(I) N-Heterocyclic Carbene Complexes: Synthesis, Structure, and Application. *Chem. Rev.* **2005**, *105*, 3978–4008, doi:10.1021/cr050004s.

142. Hashmi, A.S.K.; Yu, Y.; Rominger, F. Efficient One-Pot Synthesis of Unsymmetrical Gold(I) N-Heterocyclic Carbene Complexes and Their Use as Catalysts. *Organometallics* **2012**, *31*, 895–904, doi:10.1021/om2008919.

143. de Frémont, P.; Scott, N.M.; Stevens, E.D.; Nolan, S.P. Synthesis and Structural Characterization of *N* -Heterocyclic Carbene Gold(I) Complexes. *Organometallics* **2005**, *24*, 2411–2418, doi:10.1021/om050111c.

144. Zargaran, P.; Wurm, T.; Zahner, D.; Schießl, J.; Rudolph, M.; Rominger, F.; Hashmi, A.S.K. Front Cover Picture: A Structure-Based Activity Study of Highly Active Unsymmetrically Substituted NHC Gold(I) Catalysts (Adv. Synth. Catal. 1/2018). *Adv. Synth. Catal.* **2018**, *360*, 1–1, doi:10.1002/adsc.201701457.

145. Thallapally, P.K.; Nangia, A. A Cambridge Structural Database Analysis of the C–H···Cl Interaction: C–H···Cl– and C–H···Cl–M Often Behave as Hydrogen Bonds but C–H···Cl–C Is Generally a van Der Waals Interaction. *CrystEngComm* **2001**, *3*, 114–119, doi:10.1039/B102780H.

146. Adams, J.P.; Alder, C.M.; Andrews, I.; Bullion, A.M.; Campbell-Crawford, M.; Darcy, M.G.; Hayler, J.D.; Henderson, R.K.; Oare, C.A.; Pendrak, I.; et al. Development of GSK's Reagent Guides – Embedding Sustainability into Reagent Selection. *Green Chem.* **2013**, *15*, 1542, doi:10.1039/c3gc40225h.

147. Hong, B.-C.; Raja, A.; Sheth, V. Asymmetric Synthesis of Natural Products and Medicinal Drugs through One-Pot-Reaction Strategies. *Synthesis* **2015**, *47*, 3257–3285, doi:10.1055/s-0035-1560344.

148. Ardkhean, R.; Caputo, D.F.J.; Morrow, S.M.; Shi, H.; Xiong, Y.; Anderson, E.A. Cascade Polycyclizations in Natural Product Synthesis. *Chem. Soc. Rev.* **2016**, *45*, 1557–1569, doi:10.1039/C5CS00105F.

149. Hayashi, Y. Pot Economy and One-Pot Synthesis. *Chem. Sci.* **2016**, *7*, 866–880, doi:10.1039/C5SC02913A.

150. Anastas, P.; Eghbali, N. Green Chemistry: Principles and Practice. *Chem Soc Rev* **2010**, *39*, 301–312, doi:10.1039/B918763B.

151. Bienaymé, H.; Hulme, C.; Oddon, G.; Schmitt, P. Maximizing Synthetic Efficiency: Multi-Component Transformations Lead the Way. *Chem. - Eur. J.* **2000**, *6*, 3321–3329, doi:10.1002/1521-3765(20000915)6:18<3321::AID-CHEM3321>3.0.CO;2-A.

152. Ruijter, E.; Scheffelaar, R.; Orru, R.V.A. Multicomponent Reaction Design in the Quest for Molecular Complexity and Diversity. *Angew. Chem. Int. Ed.* **2011**, *50*, 6234–6246, doi:10.1002/anie.201006515.

153. *Multicomponent Reactions*; Zhu, J., Bienaymé, H., Eds.; Wiley-VCH: Weinheim, 2005; ISBN 978-3-527-30806-4.

154. *Multicomponent Reactions: Concepts and Applications for Design and Synthesis*; Herrera, R.P., Marques-Lopez, E., Eds.; John Wiley & Sons, Inc: Hoboken, New Jersey, 2015; ISBN 978-1-118-86397-8.

155. Touré, B.B.; Hall, D.G. Natural Product Synthesis Using Multicomponent Reaction Strategies. *Chem. Rev.* **2009**, *109*, 4439–4486, doi:10.1021/cr800296p.

156. Dömling, A.; Wang, W.; Wang, K. Chemistry and Biology Of Multicomponent Reactions. *Chem. Rev.* **2012**, *112*, 3083–3135, doi:10.1021/cr100233r.

157. Eckert, H. Diversity Oriented Syntheses of Conventional Heterocycles by Smart Multi Component Reactions (MCRs) of the Last Decade. *Molecules* **2012**, *17*, 1074–1102, doi:10.3390/molecules17011074.

158. McNally, J.J.; Youngman, M.A.; Dax, S.L. Mannich Reactions of Resin-Bound Substrates: 2. A Versatile Three-Component Solid-Phase Organic Synthesis Methodology. *Tetrahedron Lett.* **1998**, *39*, 967–970, doi:10.1016/S0040-4039(97)10716-X.

159. Dyatkin, A.B.; Rivero, R.A. The Solid Phase Synthesis of Complex Propargylamines Using the Combination of Sonogashira and Mannich Reactions. *Tetrahedron Lett.* **1998**, *39*, 3647–3650, doi:10.1016/S0040-4039(98)00639-X.

160. Langston, J.W.; Irwin, I.; Langston, E.B.; Forno, L.S. Pargyline Prevents MPTP-Induced Parkinsonism in Primates. *Science* **1984**, *225*, 1480–1482, doi:10.1126/science.6332378.

161. Birks, J.; Flicker, L. Selegiline for Alzheimer's Disease. *Cochrane Database Syst. Rev.* **2003**, doi:10.1002/14651858.CD000442.

162. Chen, J.J.; Swope, D.M. Clinical Pharmacology of Rasagiline: A Novel, Second-Generation Propargylamine for the Treatment of Parkinson Disease. *J. Clin. Pharmacol.* **2005**, *45*, 878–894, doi:10.1177/0091270005277935.

163. Baranyi, M.; Porceddu, P.F.; Gölöncsér, F.; Kulcsár, S.; Otrokocsi, L.; Kittel, Á.; Pinna, A.; Frau, L.; Huleatt, P.B.; Khoo, M.-L.; et al. Novel (Hetero)Arylalkenyl Propargylamine Compounds Are Protective in Toxin-Induced Models of Parkinson's Disease. *Mol. Neurodegener.* **2016**, *11*, 6, doi:10.1186/s13024-015-0067-y.

164. Bolea, I.; Gella, A.; Unzeta, M. Propargylamine-Derived Multitarget-Directed Ligands: Fighting Alzheimer's Disease with Monoamine Oxidase Inhibitors. *J. Neural Transm.* **2013**, *120*, 893–902, doi:10.1007/s00702-012-0948-y.

165. Cesura, A.M. Monoamine Oxidase B. In *xPharm: The Comprehensive Pharmacology Reference*; Elsevier, 2007; pp. 1–10 ISBN 978-0-08-055232-3.

166. He, Y.; Zhao, Y.; Wang, L.; Bohrer, L.R.; Pan, Y.; Wang, L.; Huang, H. LSD1 Promotes S-Phase Entry and Tumorigenesis via Chromatin Co-Occupation with E2F1 and Selective H3K9 Demethylation. *Oncogene* **2018**, *37*, 534–543, doi:10.1038/onc.2017.353.

167. Cereda, E.; Cilia, R.; Canesi, M.; Tesei, S.; Mariani, C.B.; Zecchinelli, A.L.; Pezzoli, G. Efficacy of Rasagiline and Selegiline in Parkinson's Disease: A Head-to-Head 3-Year Retrospective Case–Control Study. *J. Neurol.* **2017**, *264*, 1254–1263, doi:10.1007/s00415-017-8523-y.

168. Trost, B.M. Modern Alkyne Chemistry. 423.

169. Sarode, P.; Bahekar, S.; Chandak, H. Zn(OTf)2-Mediated Expeditious and Solvent-Free Synthesis of Propargylamines via C–H Activation of Phenylacetylene. *Synlett* **2016**, *27*, 2209–2212, doi:10.1055/s-0035-1562114.

170. Agrahari, B.; Layek, S.; Ganguly, R.; Pathak, D.D. Synthesis and Crystal Structures of Salen-Type Cu(II) and Ni(II) Schiff Base Complexes: Application in [3+2]-Cycloaddition and A ^{3} -Coupling Reactions. *New J. Chem.* **2018**, *42*, 13754–13762, doi:10.1039/C8NJ01718B.

171. Zeng, T.; Chen, W.-W.; Cirtiu, C.M.; Moores, A.; Song, G.; Li, C.-J. Fe3O4 Nanoparticles: A Robust and Magnetically Recoverable Catalyst for Three-Component Coupling of Aldehyde, Alkyne and Amine. *Green Chem.* **2010**, *12*, 570, doi:10.1039/b920000b.

172. Chen, W.-W.; Bi, H.-P.; Li, C.-J. The First Cobalt-Catalyzed Transformation of Alkynyl C-H Bond: Aldehyde-Alkyne-Amine (A^3) Coupling. *Synlett* **2010**, *2010*, 475–479, doi:10.1055/s-0029-1219173.

173. Abbiati, G.; Rossi, E. Silver and Gold-Catalyzed Multicomponent Reactions. *Beilstein J. Org. Chem.* **2014**, *10*, 481–513, doi:10.3762/bjoc.10.46.

174. Kılınçarslan, R.; Sadıç, N. Catalytic Activity of *N* -Heterocyclic Carbene Silver Complexes Derived from Imidazole Ligands. *Inorg. Nano-Met. Chem.* **2017**, *47*, 462–466, doi:10.1080/15533174.2016.1186054.

175. Scattolin, T.; Canovese, L.; Visentin, F.; Paganelli, S.; Canton, P.; Demitri, N. Synthesis of Novel Allyl Palladium Complexes Bearing Purine Based NHC and a Water Soluble Phosphine and Their Catalytic Activity in the Suzuki-Miyaura Coupling in Water. *Appl. Organomet. Chem.* **2018**, *32*, doi:10.1002/aoc.4034.

176. Szadkowska, A.; Staszko, S.; Zaorska, E.; Pawłowski, R. A Theophylline Based Copper N-Heterocyclic Carbene Complex: Synthesis and Activity Studies in Green Media. *RSC Adv.* **2016**, *6*, 44248–44253, doi:10.1039/C6RA06682H.

177. Mohammadi, E.; Movassagh, B. Polystyrene-Resin Supported N-Heterocyclic Carbene-Pd(II) Complex Based on Plant-Derived Theophylline: A Reusable and Effective Catalyst for the Suzuki-Miyaura Cross-Coupling Reaction of Arenediazonium Tetrafluoroborate Salts with Arylboronic Acids. *J. Organomet. Chem.* **2016**, *822*, 62–66, doi:10.1016/j.jorganchem.2016.08.017.

178. Baker, M.V.; Barnard, P.J.; Brayshaw, S.K.; Hickey, J.L.; Skelton, B.W.; White, A.H. Synthetic, Structural and Spectroscopic Studies of (Pseudo)Halo(1,3-Di-Tert-Butylimidazol-2-Ylidine)Gold Complexes. *Dalton Trans.* **2005**, 37, doi:10.1039/b412540a.

179. de Frémont, P.; Marion, N.; Nolan, S.P. Cationic NHC–Gold(I) Complexes: Synthesis, Isolation, and Catalytic Activity. *J. Organomet. Chem.* **2009**, *694*, 551–560, doi:10.1016/j.jorganchem.2008.10.047.

180. Scattolin, T.; Tzouras, N.V.; Falivene, L.; Cavallo, L.; Nolan, S.P. Using Sodium Acetate for the Synthesis of [Au(NHC)X] Complexes. *Dalton Trans.* **2020**, *49*, 9694–9700, doi:10.1039/D0DT02240C.

181. Herrero-Gómez, E.; Nieto-Oberhuber, C.; López, S.; Benet-Buchholz, J.; Echavarren, A.M. Cationic H1/H2-Gold(I) Complexes of Simple Arenes. *Angew. Chem. Int. Ed.* **2006**, *45*, 5455–5459, doi:10.1002/anie.200601688.

182. Müller, T.E.; Hultzsch, K.C.; Yus, M.; Foubelo, F.; Tada, M. Hydroamination: Direct Addition of Amines to Alkenes and Alkynes. *Chem. Rev.* **2008**, *108*, 3795–3892, doi:10.1021/cr0306788.

183. Casnati, A.; Voronov, A.; Ferrari, D.G.; Mancuso, R.; Gabriele, B.; Motti, E.; Della Ca', N. PdI2 as a Simple and Efficient Catalyst for the Hydroamination of Arylacetylenes with Anilines. *Catalysts* **2020**, *10*, 176, doi:10.3390/catal10020176.

184. Huang, L.; Arndt, M.; Gooßen, K.; Heydt, H.; Gooßen, L.J. Late Transition Metal-Catalyzed Hydroamination and Hydroamidation. *Chem. Rev.* **2015**, *115*, 2596–2697, doi:10.1021/cr300389u.

185. Patel, M.; Saunthwal, R.K.; Verma, A.K. Base-Mediated Hydroamination of Alkynes. *Acc. Chem. Res.* **2017**, *50*, 240–254, doi:10.1021/acs.accounts.6b00449.

186. Haggin, J. Chemists Seek Greater Recognition for Catalysis: ▪ Catalysis Society Meeting Mulls over International Efforts to Increase Funding, Gain Direction for the Discipline. *Chem. Eng. News Arch.* **1993**, *71*, 23–27, doi:10.1021/cen-v071n022.p023.

187. Straub, T.; Haskel, A.; Neyroud, T.G.; Kapon, M.; Botoshansky, M.; Eisen, M.S. Intermolecular Hydroamination of Terminal Alkynes Catalyzed by Organoactinide Complexes. Scope and Mechanistic Studies. *Organometallics* **2001**, *20*, 5017–5035, doi:10.1021/om010434i.

188. Chen, J.; Lu, Z. Asymmetric Hydrofunctionalization of Minimally Functionalized Alkenes *via* Earth Abundant Transition Metal Catalysis. *Org. Chem. Front.* **2018**, *5*, 260–272, doi:10.1039/C7QO00613F.

189. Griffin, S.E.; Pacheco, J.; Schafer, L.L. Reversible C–N Bond Formation in the Zirconium-Catalyzed Intermolecular Hydroamination of 2-Vinylpyridine. *Organometallics* **2019**, *38*, 1011–1016, doi:10.1021/acs.organomet.8b00904.

190. Eedugurala, N.; Hovey, M.; Ho, H.-A.; Jana, B.; Lampland, N.L.; Ellern, A.; Sadow, A.D. Cyclopentadienyl-Bis(Oxazoline) Magnesium and Zirconium Complexes in Aminoalkene Hydroaminations. *Organometallics* **2015**, *34*, 5566–5575, doi:10.1021/acs.organomet.5b00771.

191. Reznichenko, A.L.; Nguyen, H.N.; Hultzsch, K.C. Asymmetric Intermolecular Hydroamination of Unactivated Alkenes with Simple Amines. *Angew. Chem. Int. Ed.* **2010**, *49*, 8984–8987, doi:10.1002/anie.201004570.

192. Hong, S.; Marks, T.J. Organolanthanide-Catalyzed Hydroamination. *Acc. Chem. Res.* **2004**, *37*, 673–686, doi:10.1021/ar040051r.

193. Ryu, J.-S.; Li, G.Y.; Marks, T.J. Organolathanide-Catalyzed Regioselective Intermolecular Hydroamination of Alkenes, Alkynes, Vinylarenes, Di- and Trivinylarenes, and Methylenecyclopropanes. Scope and Mechanistic Comparison to Intramolecular Cyclohydroaminations. *J. Am. Chem. Soc.* **2003**, *125*, 12584–12605, doi:10.1021/ja035867m.

194. 김현석; 이필호 Intramolecular Hydroaminations of Aminoalkynes Catalyzed by Yttrium Complexes and Aminoallenes Catalyzed by Zirconium Complexes. *Bull. Korean Chem. Soc.* **2007**, *28*, 1127–1134, doi:10.5012/BKCS.2007.28.7.1127.

195. Yahata, K.; Kaneko, Y.; Akai, S. Cobalt-Catalyzed Intermolecular Markovnikov Hydroamination of Nonactivated Olefins: N^2-Selective Alkylation of Benzotriazole. *Org. Lett.* **2020**, *22*, 598–603, doi:10.1021/acs.orglett.9b04375.

196. Yang, X.-H.; Lu, A.; Dong, V.M. Intermolecular Hydroamination of 1,3-Dienes To Generate Homoallylic Amines. *J. Am. Chem. Soc.* **2017**, *139*, 14049–14052, doi:10.1021/jacs.7b09188.

197. Gurak, J.A.; Yang, K.S.; Liu, Z.; Engle, K.M. Directed, Regiocontrolled Hydroamination of Unactivated Alkenes via Protodepalladation. *J. Am. Chem. Soc.* **2016**, *138*, 5805–5808, doi:10.1021/jacs.6b02718.

198. Sevov, C.S.; Zhou, J. (Steve); Hartwig, J.F. Iridium-Catalyzed, Intermolecular Hydroamination of Unactivated Alkenes with Indoles. *J. Am. Chem. Soc.* **2014**, *136*, 3200–3207, doi:10.1021/ja412116d.

199. Nuevo, D.; Poyatos, M.; Peris, E. A Dinuclear Au(I) Complex with a Pyrene-Di-N-Heterocyclic Carbene Linker: Supramolecular and Catalytic Studies. *Organometallics* **2018**, *37*, 3407–3411, doi:10.1021/acs.organomet.8b00087.

200. E. Müller, T.; Pleier, A.-K. Intramolecular Hydroamination of Alkynes Catalysed by Late Transition Metals. *J. Chem. Soc. Dalton Trans.* **1999**, 583, doi:10.1039/a808938h.

201. Dentoni Litta, A.; Buonerba, A.; Casu, A.; Falqui, A.; Capacchione, C.; Franconetti, A.; Garcia, H.; Grassi, A. Highly Efficient Hydroamination of Phenylacetylenes with Anilines Catalysed by Gold Nanoparticles Embedded in Nanoporous Polymer Matrix: Insight into the Reaction Mechanism by Kinetic and DFT Investigations. *J. Catal.* **2021**, *400*, 71–82, doi:10.1016/j.jcat.2021.05.024.

202. Kumar, A.; Singh, C.; Tinnermann, H.; Huynh, H.V. Gold(I) and Gold(III) Complexes of Expanded-Ring N-Heterocyclic Carbenes: Structure, Reactivity, and Catalytic Applications. *Organometallics* **2020**, *39*, 172–181, doi:10.1021/acs.organomet.9b00718.

203. Ibáñez, S.; Poyatos, M.; Peris, E. A D_{3h}-Symmetry Hexaazatriphenylene-Tris-N-Heterocyclic Carbene Ligand and Its Coordination to Iridium and Gold: Preliminary Catalytic Studies. *Chem. Commun.* **2017**, *53*, 3733–3736, doi:10.1039/C7CC00525C.

204. Hussaini, S.Y.; Haque, R.A.; Razali, M.R. Recent Progress in Silver(I)-, Gold(I)/(III)- and Palladium(II)-N-Heterocyclic Carbene Complexes: A Review towards Biological Perspectives. *J. Organomet. Chem.* **2019**, *882*, 96–111, doi:10.1016/j.jorganchem.2019.01.003.

205. Weinstein, M.P.; Patel, J.B. *Methods for Dilution Antimicrobial Susceptibility Tests for Bacteria That Grow Aerobically: M07-A11*; Documents / Clinical and Laboratory Standards Institute; 11. edition.; Committee for Clinical Laboratory Standards: Wayne, PA, 2018; ISBN 978-1-56238-836-2.

206. Iacopetta, D.; Rosano, C.; Sirignano, M.; Mariconda, A.; Ceramella, J.; Ponassi, M.; Saturnino, C.; Sinicropi, M.S.; Longo, P. Is the Way to Fight Cancer Paved with Gold? Metal-Based Carbene Complexes with Multiple and Fascinating Biological Features. *Pharmaceuticals* **2020**, *13*, 91, doi:10.3390/ph13050091.

207. Peeters, A.; Valvekens, P.; Ameloot, R.; Sankar, G.; Kirschhock, C.E.A.; De Vos, D.E. Zn–Co Double Metal Cyanides as Heterogeneous Catalysts for Hydroamination: A Structure–Activity Relationship. *ACS Catal.* **2013**, *3*, 597–607, doi:10.1021/cs300805z.

208. Chen, D.; Wang, Y.; Klankermayer, J. Enantioselective Hydrogenation with Chiral Frustrated Lewis Pairs. *Angew. Chem. Int. Ed.* **2010**, *49*, 9475–9478, doi:10.1002/anie.201004525.

209. Wang, Z.; Ye, X.; Wei, S.; Wu, P.; Zhang, A.; Sun, J. A Highly Enantioselective Lewis Basic Organocatalyst for Reduction of *N*-Aryl Imines with Unprecedented Substrate Spectrum. *Org. Lett.* **2006**, *8*, 999–1001, doi:10.1021/ol060112g.

210. Venkat Reddy, C.R.; Urgaonkar, S.; Verkade, J.G. A Highly Effective Catalyst System for the Pd-Catalyzed Amination of Vinyl Bromides and Chlorides. *Org. Lett.* **2005**, *7*, 4427–4430, doi:10.1021/ol051612x.

211. Anderson, L.L.; Arnold, J.; Bergman, R.G. Catalytic Hydroamination of Alkynes and Norbornene with Neutral and Cationic Tantalum Imido Complexes. *Org. Lett.* **2004**, *6*, 2519–2522, doi:10.1021/ol0492851.

Acknowledgments

Scrivere i ringraziamenti non è mai stato facile. In questi mesi, li ho immaginati così tante volte da restare deluso in ogni occasione. Non so bene il motivo di tale smania. Immagino che sia perché tutti crediamo che quello che facciamo sia importante, che le persone pendano dalle nostre parole, che diano importanza a ciò che pensiamo e che capiscano quanto, loro, siano preziosi per noi.
Oggi si è 'chiuso un cerchio', aperto nel lontano ottobre 2011, ed è giusto ringraziare le persone che hanno arricchito il mio percorso e hanno contribuito al raggiungimento di questo obiettivo.
Il primo ringraziamento va ai miei genitori, **Flora** e **Pellegrino**; il mio porto sicuro. Nonostante questi tre anni si siano stati segnati da perdite fondamentali, periodi di dolore e inutile sofferenza, Loro non mi hanno mai fatto mancare il sostegno e l'aiuto prezioso. Grazie infinite!
Questo lavoro di tesi è dedicato a **Claudia**, la mia ragazza. In questi anni mi hai sempre sostenuto nei momenti più duri, e hai gioito nei giorni migliori e al raggiungimenti degli obiettivi. Grazie per il tuo supporto e per il tuo essere barricadiera nel difendere i miei sogni.
Non esistono parole sufficienti per esprimere la gratitudine e la rinconoscenza al **Professore Pasquale Longo,** tutor accademico e guida. In questi tre anni di dottorato, ha contribuito ad arrichhire il mio bagaliaglio culturale, raccontando esperienze passate con gli annessi trucchi del mestiere, contagiandomi, sempre, con la Sua preparazione, professionalità e il Suo fondamentale ottimismo.
Ringrazio la **Professoressa Annaluisa Mariconda**, che è e sarà, sempre, una fonte di ispirazione per la Sua bravura, il Suo stakanovismo e la Sua competenza. Il Marco ,chimico, deve molto ai Suoi pregevolissimi consigli.
In questi anni di dottorato ho avuto la fortuna di conoscere tante persone, che hanno contribuito ad arricchire le conoscenze, nei vari *brainstorming*/inciuci. La fortuna più grande è stata quella di aver avuto la possibilità di condividere la vita laboratoriale con due splendide amiche e colleghe: **Rubina** e **Simona**. Il bene nei loro confronti 'viaggia di pari passo' con la stima che provo. Grazie per le bellissime giornate trascorse, i consigli professionali, gli scazzi e il nostro capirci con un semplice sguardo. Sono felicissimo e onorato di essere un vostro compagno di squadra.
Voglio ringraziare il mio caro amico,collega dottorando **Salvatore I**. La nostra amicizia di lunga data si è arricchita di tante esperienze vissute da dottorandi. Gli auguro il meglio per Lui, per la Sua neonata e la Sua compagna Denise.
Un ringraziamento va a **Gaetano** e **Massimo**, colleghi chimici che ho avuto il piacere di conoscere in questi tre anni dottorato. Ogni confronto è stato arricchente e coinvolgente.
L'esperienza del dottorato mi ha offerto tanti onori. Vedere stampato il mio nome ad un *paper*, viaggiare e conoscere altri colleghi chimici, nelle varie sedi congressuali, sono solo alcuni degli episodi accaduti che ho avuto il piacere di vivere e che mai dimenticherò. L'onore più importante, però, è stato quello di interpretare il ruolo di tutor di laboratorio. Cercare di sviluppare l'autorevolezza, che consentisse di far crescere umanamente e professionalmente i vari tirocinanti, è stata l'esperienza più formativa. Ringrazio tutti i tesisti che si sono succeduti in questi tre anni,

perché da ognuno di Loro, ho avuto la possibilità di poter imparare e 'toccare con mano' di quanto la Scienza sia democratica.

Un ringraziamento va ai colleghi e tirocinanti del Lab 2, compagni di (dis)avventure, di reazioni chimiche andate malissimo, e di giornate dedicate a lavare la vetreria risalente a Lavoisier. Voglio ringraziare nello specifico **Vissia**, **Salvatore**, **Federica**, **Francesca**, e tanti altri ancora. Con voi ho vissuto momenti di ilarità, scambi arricchenti e lunghe file ai distributori.

Un ringraziamento va agli amici di sempre che mi hanno sostenuto, chi più chi meno, duranti questi tre anni di formazione.